

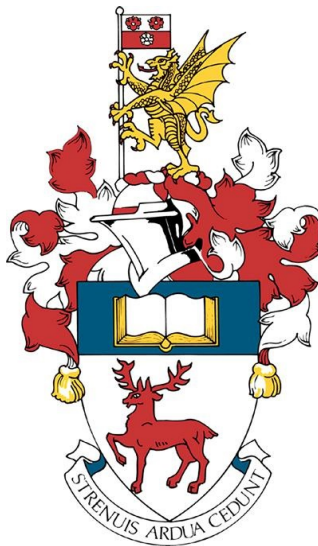
**University of Southampton**  
Faculty of Engineering and Physical Sciences  
Engineering Sciences

# **Vehicle-to-Grid for Road-to-Rail Energy Exchange:**

Using aggregated electric vehicles to provide large-scale energy  
storage support for electric rail systems

**Hannes Krueger**

A thesis submitted for the degree of  
Doctor of Philosophy



September 2020





## ABSTRACT

Vehicle-to-Grid (V2G) describes an energy storage concept in which the built-in battery packs of parked electric vehicles (EVs) are aggregated and connected to bi-directional chargers to provide various services to the electric power grid (such as frequency regulation or load balancing). Applications of this type of energy storage can vary widely in scale and purpose. This project explores a novel application for V2G in which the aggregated storage potential of parked EVs is used to support nearby electric rail infrastructure. Connected battery packs can be discharged, thereby providing traction power to accelerating electric trains, or charged to accept power from the regenerative braking of arriving trains. The latter is of particular value for low voltage, direct current (DC) rail systems which typically do not support regeneration into the grid.

This novel concept is referred to as Road-to-Rail Energy Exchange (R2REE). It represents a large-scale energy storage application in which power demands can change rapidly by several megawatts, thus requiring fast and dynamic aggregator control, capable of managing hundreds of connected EVs. This is achieved by separating aggregator control into several smaller, independently operational tasks and by exploiting the predictable and repetitive power demand patterns of timetabled rail traffic. A novel modular high-level aggregator control structure is presented that addresses these challenges of R2REE through dynamic, real-time aggregator operation along with suitable communications and data management strategies.

Furthermore, a novel method of event-based V2G scheduling is proposed that is applicable in deterministic systems where the network provides or receives electricity in reoccurring and predictable patterns or 'events'. Within the scope of this project, an event represents either the arrival of an electric train at a station (a train of known type provides power from regenerative braking to be dissipated over EV population) or a train's departure (where power is drawn from parked EVs to support train acceleration).

The proposed scheduling method consists of three algorithm layers, differentiating between predictive scheduling for in-event periods, smart charging for out-of-event periods and reactive scheduling for ongoing adjustments in real-time to account for uncertainty.

Making use of this purpose-built aggregator control strategy, communications scheme and scheduling method the R2REE concept is explored, based on a real 750 V DC-powered third-rail train line in Merseyside, England and a simulated EV population. Each simulation presented covers a full day of real-time V2G network operation with rail power demands based on an actual train schedule. The size of the connected EV population, the maximum charging/discharging rates per EV and the overall power made available through a shared power grid connection vary between simulations.

This project further explores a method of accounting for charging preferences of EV owners in the scheduling process. This is achieved using a scoring system to assess the potential of each EV to be either charged or discharged prior to the scheduling process, thus reducing the negative impact of additional complexity on the responsiveness of the system. This novel scoring system allows the user of an EV to select between four different ‘charging modes’ to determine if and how the EV can participate in the V2G operation. User inputs are made via a touchscreen user interface developed for a hardware prototype of an on-board EV communication system which is fully compatible with the V2G aggregator control presented.



## CONTENTS

<i>List of Tables</i> . . . . .	9
<i>List of Figures</i> . . . . .	14
<i>Declaration of Authorship</i> . . . . .	16
<i>Acknowledgements</i> . . . . .	19
<i>Acronyms</i> . . . . .	22
<i>1. Introduction</i> . . . . .	24
1.1 Project Overview . . . . .	24
1.2 Project Novelty and Publications . . . . .	28
<i>2. Literature Review</i> . . . . .	30
2.1 Emergence of electro-mobility and the need for energy storage . .	30
2.2 Vehicle-to-Grid distributed energy storage . . . . .	34
2.2.1 V2G Applications . . . . .	36
2.2.2 User Acceptance of V2G . . . . .	39
2.3 Economic Considerations of V2G . . . . .	40
2.3.1 Case studies and projects on V2G economics . . . . .	43
2.4 Communications and Control . . . . .	47
2.5 Communication Standards and Protocols . . . . .	55
2.6 Aggregator control literature and projects . . . . .	57
<i>3. Vehicle-to-Grid Aggregator Control</i> . . . . .	63
3.1 Modular high-level aggregator control structure . . . . .	63
3.2 Data Collection . . . . .	69

---

3.3	Schedule Implementation . . . . .	75
3.4	V2G Scheduling . . . . .	78
3.4.1	Pre-scheduling EV suitability assessment . . . . .	80
3.4.2	Multi-layer event-based V2G scheduling . . . . .	82
3.4.3	Predictive scheduling for in-event periods, first layer . . . .	85
3.4.4	Reactive scheduling for schedule refinement, second layer .	89
3.4.5	Scheduling for non-event periods (smart charging), third layer	91
3.4.6	Interaction between predictive and reactive scheduling layers	92
3.5	EV communication system prototype . . . . .	100
3.6	EV Simulator . . . . .	104
4.	<i>Road-to-Rail Energy Exchange</i> . . . . .	110
4.1	V2G as support for Rail systems . . . . .	110
4.2	Train Station Power Demand Model . . . . .	113
4.3	EV Population Model . . . . .	122
4.4	R2REE Simulations . . . . .	126
4.4.1	Size of EV population . . . . .	128
4.4.2	Maximum EV charging rates . . . . .	132
4.4.3	Grid connection limit . . . . .	134
5.	<i>EV Owner Control Over V2G Scheduling</i> . . . . .	140
5.1	Charging Modes . . . . .	141
5.2	EV communication system user interface . . . . .	142
5.3	Integration into existing scoring system . . . . .	146
5.4	SQL triggers . . . . .	149
5.5	R2REE simulations with enabled EV owner charging preferences .	152
5.5.1	Control EV and scenario definitions . . . . .	153
5.5.2	Simulation results . . . . .	154
6.	<i>Conclusions</i> . . . . .	165
6.1	Vehicle-to-Grid Aggregator Control . . . . .	166
6.2	Road-to-Rail Energy Exchange . . . . .	170
6.3	EV Owner Control Over V2G Scheduling . . . . .	173
6.4	Summary and further work . . . . .	174

<i>Appendix</i>	177
<i>A1.SQL Database Table Definitions . . . . .</i>	179
<i>A2.Aggregator Control Code Repository . . . . .</i>	182
<i>A3.Communication Benchmark . . . . .</i>	188
<i>A4.Train Schedule . . . . .</i>	190
<i>A5.Full Simulation Results For Chapter 4 . . . . .</i>	192
<i>A6.Full Simulation Results For Chapter 5 . . . . .</i>	215
<i>Bibliography . . . . .</i>	258

## LIST OF TABLES

1.1	Project novelty and associated publications . . . . .	29
3.1	Execution times for predictive scheduling algorithm for varying number of connected EVs (over 1,000 scheduling cycles) . . . . .	95
3.2	EV model specifications used for EV simulator, compiled using ev-database.uk as well as stated sources. . . . .	106
4.1	Excerpt of train timetable, period of interest: 07:00 to 07:30 . . .	120
4.2	Control EV configurations valid for all simulations discussed in this chapter. . . . .	126
4.3	Comparison of Control EV battery pack SOC at departure time for EV populations of varying sizes . . . . .	132
4.4	Comparison of Control EV battery pack SOC at departure time for different global charging rate limits . . . . .	135
4.5	Comparison of Control EV battery pack SOC at departure time for different grid connection limits . . . . .	139
5.1	Scenario definitions . . . . .	153
5.2	User charging preferences of Control EVs . . . . .	154
5.3	Comparison between scenarios I and IV, SOC (in %) of EVs at 18:00	155
5.4	Comparison between scenarios II and V, SOC (in %) of Control EVs at 18:00 . . . . .	160
5.5	Comparison between scenarios III and VI, time at which each EV is considered fully charged . . . . .	162

**Note:** this list only contains tables from the main body of this document (tables in the appendices are not listed).

## LIST OF FIGURES

1.1	Modular aggregator control structure for Road-to-Rail Energy Exchange using multiple scheduling modules. . . . .	25
1.2	V2G for support of local electric rail systems, system overview and power flows . . . . .	26
1.3	EV user interface screen capture . . . . .	27
2.1	Global EV rolling stock (including PHEVs) according to the International Energy Agency . . . . .	31
2.2	Global EV sales (including PHEVs) and forecast according to the International Energy Agency . . . . .	32
2.3	Fees and compensations paid between the three parties in a V2G network . . . . .	41
2.4	Visualisation of using IEC 61850 and ISO/IEC 15118 for V2G applications . . . . .	56
3.1	Modular aggregator control structure, one module per task - first-order modularisation . . . . .	65
3.2	Modular aggregator control structure, multiple modules per task - second-order modularisation . . . . .	66
3.3	Task sequencing of aggregator control in a multi algorithm structure	67
3.4	Modular aggregator control structure for Road-to-Rail Energy Exchange using multiple scheduling modules. . . . .	69
3.5	Flow diagram of the data collection module responsible for regularly updating EV data in the 'Vehicles' table in the SQL database.	72
3.6	Flow diagram of the schedule implementation module responsible for implementing charging & discharging instructions from the 'Schedule' table in the SQL database. . . . .	77



---

3.7	(a) V2G for support of local electric rail systems, system overview and power flows; (b) Rail system power demand over one hour. . .	79
3.8	Modular aggregator control structure using multiple independent scheduling modules. . . . .	82
3.9	Combined effects to two stacked 'counter-events' on the rail station power demand . . . . .	84
3.10	Visualisation of in-event (blue) and out-of-event (green) periods for a sequence of events (left to right: single train accelerating, single train braking, train accelerating while another is braking). .	85
3.11	Three layer scheduling, top-level control routine: node $\alpha$ leads to Figure 3.12, node $\beta$ to Figure 3.13 and node $\gamma$ to Figure 3.14 . . .	86
3.12	Predictive scheduling layer flow diagram . . . . .	87
3.13	Reactive scheduling layer flow diagram . . . . .	90
3.14	Smart charging scheduling layer flow diagram . . . . .	91
3.15	Simulated V2G network response to two counter-active events (one train departing at 0 seconds, one train arriving at 30 seconds) using predictive scheduling only . . . . .	94
3.16	Simulated V2G network response to two counter-active events (one train departing at 0 seconds, one train arriving at 30 seconds) using reactive scheduling only . . . . .	96
3.17	Simulated V2G network response to two counter-active events (one train departing at 0 seconds, one train arriving at 30 seconds with sudden unpredicted braking) using both predictive and reactive scheduling . . . . .	99
3.18	EV communication system with user interface . . . . .	100
3.19	EV communication system components . . . . .	101
3.20	Communication trials between Arduino Mega and BMS using synchronous serial communication . . . . .	103
3.21	Charging profile for Tesla Model S 90D, charging power (kW) against SOC (%) . . . . .	107
3.22	Assumed charging profile for idealised EVs, % of maximum charging power against SOC (%) . . . . .	108

4.1	Powerflow in a V2G network used for train brake energy recovery in a third rail powered rail system . . . . .	111
4.2	R2REE: Vehicle-to-Grid schematic supporting local rail system . .	112
4.3	Third rail system in electrified rail track . . . . .	113
4.4	Section of Merseyrail system modelled in case-study . . . . .	114
4.5	Aerial view of Hoylake train station and surroundings . . . . .	115
4.6	Assumed speed profile of simulated train . . . . .	116
4.7	Train traction power demand during acceleration and regenerative braking power output during deceleration . . . . .	117
4.8	Assumed traction power demand for train departure event . . . .	118
4.9	Assumed regenerative braking power from train arrival event . . .	119
4.10	Train arrivals and departures during the model day per hour . . .	120
4.11	Rail system power demand over period of interest . . . . .	121
4.12	R2REE, system overview and power flows . . . . .	122
4.13	Assumed car park occupancy rate over model day . . . . .	123
4.14	Assumed car park occupancy rate and number of train arrival/de- parture events over 24 simulation period . . . . .	124
4.15	Assumed maximum charging rate against SOC for simulated EV population . . . . .	125
4.16	Total power provision potential of EV populations of varying size over 24 hours. . . . .	128
4.17	Total power absorption potential of EV populations of varying size over 24 hours. . . . .	129
4.18	Changes in SOC over time of the three control EVs within EV populations of varying size. . . . .	131
4.19	Total power absorption potential of the connected EV population with varying global charging limits over 24 hours. . . . .	133
4.20	Changes in SOC over time of the three control EVs within the connected EV population with varying global charging limits over 24 hours. . . . .	134
4.21	Total power absorption potential of the connected EV population with varying global charging limits over 24 hours. . . . .	135

4.22	Changes in SOC over time of the three control EVs within the connected EV population with varying global charging limits over 24 hours. . . . .	136
4.23	Total power absorption potential of 100 EVs at varying grid connection limits over 24 hours. . . . .	137
4.24	Changes in SOC over time of the three control EVs within an EV population of 100 EVs at varying grid connection limits over 24 hours. . . . .	138
5.1	EV owner user interface, screen elements . . . . .	143
5.2	EV owner user interface, charging mode description on info page .	143
5.3	EV owner user interface, charging mode 1 selected (no inputs needed)	144
5.4	EV owner user interface, charging mode 2 selected (target SOC provided) . . . . .	144
5.5	EV owner user interface, charging mode 3 selected (no inputs needed)	145
5.6	EV owner user interface, charging mode 4 selected (target SOC and targed date/time provided) . . . . .	145
5.7	EV owner user interface, target SOC selection . . . . .	145
5.8	EV owner user interface, target date/time selection . . . . .	145
5.9	Scenario I: changes in SOC for all control EVs while connected . .	155
5.10	Scenario IV: changes in SOC for all control EVs while connected, user charging preferences disabled . . . . .	155
5.11	Comparison: EV A SOC over time in scenarios I and IV . . . . .	156
5.12	Scenario I: EV A effective charging rate over time . . . . .	156
5.13	Scenario IV: EV A effective charging rate over time . . . . .	156
5.14	Comparison: EV B SOC over time in scenarios I and IV . . . . .	158
5.15	Scenario I: EV B effective charging rate over time . . . . .	158
5.16	Scenario IV: EV B effective charging rate over time . . . . .	158
5.17	Scenario II: changes in SOC for all control EVs while connected .	159
5.18	Scenario V: changes in SOC for all control EVs while connected, user charging preferences disabled . . . . .	159
5.19	Comparison: EVs C and E, SOC over time in scenario II . . . . .	160
5.20	Scenario II: EV C effective charging rate over time . . . . .	161
5.21	Scenario II: EV E effective charging rate over time . . . . .	161

5.22	Scenario III: changes in SOC for all control EVs while connected .	161
5.23	Scenario VI: changes in SOC for all control EVs while connected, user charging preferences disabled . . . . .	161
5.24	Comparison of scenarios I, II and III: total power absorption po- tential of the aggregated EV population over time . . . . .	162
5.25	Comparison of scenarios IV, V and VI: total power absorption potential of the aggregated EV population over time . . . . .	162
5.26	Total power provision potential of aggregated EV populations over 24 hours, Scenarios I to VI . . . . .	163

**Note:** this list only contains figures from the main body of this document (figures in the appendices are not listed).



## DECLARATION OF AUTHORSHIP

I, Hannes Krueger, declare that this thesis entitled "***Vehicle-to-Grid for Road-to-Rail Energy Exchange: Using aggregated electric vehicles to provide large-scale energy storage support for electric rail systems***" and the work presented in it are my own and has been generated by me as the result of my original research.

I confirm that:

1. This work was done wholly or mainly while in candidature for a research degree at this University;
2. Where any part of this thesis has previously been submitted for a degree or any other qualification at this University or any other institution, this has been clearly stated;
3. Where I have consulted the published work of others, this is always clearly attributed;
4. Where I have quoted from the work of others, the source is always given. With the exception of such quotations, this thesis is entirely my own work;
5. I have acknowledged all main sources of help;
6. Where the thesis is based on work done by myself jointly with others, I have made clear exactly what was done by others and what I have contributed myself;

---

7. Parts of this work have been published as:

- Krueger, H., Cruden, A. (2018). Modular strategy for aggregator control and data exchange in large scale Vehicle-to-Grid (V2G) applications, *Energy Procedia: 3<sup>rd</sup> Annual Conference in Energy Storage and Its Applications* [1]
- Krueger, H., Cruden, A. (2020). Multi-layer event-based Vehicle-to-Grid (V2G) scheduling with short term predictive capability within a modular aggregator control structure, *IEEE Transactions in Vehicular Technology* [2]
- Krueger, H., Cruden, A. (2020). Integration of electric vehicle user charging preferences into Vehicle-to-Grid (V2G) aggregator controls, *Energy Reports: 4<sup>th</sup> Annual Conference in Energy Storage and Its Applications* [3]
- Krueger, H., Fletcher, D., Cruden, A. (2020). Vehicle-to-Grid (V2G) as line-side energy storage for support of DC-powered electric railway systems, *Journal of Rail Transport Planning and Management* (submitted on 11.09.2020 and under review, manuscript number: JRTPM-D-20-00029)

Signed: ..... Date: .....





## ACKNOWLEDGEMENTS

During the seemingly endless hours spent on this project, I have received the support of several people I must mention here. The completion of this thesis would not have been possible without their help.

First and foremost, I want to thank **Professor Andrew Cruden** who, as my supervisor, helped to shape this project from the very beginning.

*Thank you for your patience. Your contributions are too numerous to list and your advice was always welcome. Help was never further away than a knock on your office door.*

I also want to extend my gratitude to **Professor David Fletcher** who introduced me to his work on electric rail systems, willingly shared his findings and co-authored my latest paper.

*So much of my work was built upon your data. Thank you for your comprehensive advice and creative input in the many way-past-bedtime email exchanges.*

I am also grateful to **Sharon Brown** who, as CDT Centre Manager, handled much of the tedious administrative work required, particularly during the first half of this project.

*Dealing with bureaucracy at university can be tiresome – even more so when two universities are involved. Thank you for the countless instances of last-minute problem solving!*

Thanks to **Andy Westerman** who supported many of the practical aspects of this project.

*From quick advice on soldering to purchasing equipment, no task too big or small, I could always count on your help. Thank you!*

Finally, my thanks go out to all my peers in the Energy Storage CDT from both Sheffield and Southampton.

*You made the time spent on this project so much more bearable - both, during and after office hours. Best of luck to those of you who have yet to conclude their projects.*



## ACRONYMS

AC	Alternating Current
API	Application Programming Interface
BMS	Battery Management System
CAN	Controller Area Network
CPU	Central Processing Unit
CW	Charge Weighting
DC	Direct Current
DCW	Discharge Weighting
DOI	Digital Object Identifier
DSO	Distribution System Operator
EU	European Union
EVs	Electric Vehicles
G2V	Grid-to-Vehicle
GPS	Global Positioning System
ICE	Internal Combustion Engine
ID	Identification
IEA	International Energy Agency
IP	Internet Protocol address

---

IT . . . . .	Information Technology
OBD . . . . .	On-Board Diagnostics
PHEVs . . . . .	Plug-in Hybrid Electric Vehicles
PLC . . . . .	Power Line Communications
PV . . . . .	Photovoltaics
R2REE . . . . .	Road-to-Rail Energy Exchange
RAM . . . . .	Random Access Memory
REST . . . . .	REpresentational State Transfer
SDS . . . . .	Sustainable Development Scenario
SOC . . . . .	State of Charge
SPI . . . . .	Serial Peripheral Interface
SQL . . . . .	Structured Query Language
TfL . . . . .	Transport for London
TSO . . . . .	Transmission System Operator
UART . . . . .	Universal Asynchronous Receiver/Transmitter
V2B . . . . .	Vehicle-to-Building
V2G . . . . .	Vehicle-to-Grid
V2H . . . . .	Vehicle-to-Home
V2R . . . . .	Vehicle-to-Rail
V2V . . . . .	Vehicle-to-Vehicle
VIN . . . . .	Vehicle Identification Number

## 1. INTRODUCTION

### **Vehicle-to-Grid for Road-to-Rail Energy Exchange:**

Using aggregated electric vehicles to provide large-scale energy storage support for electric rail systems

#### *1.1 Project Overview*

Global efforts in combating climate change and pollution through the reduction of fossil fuel usage have led to increased transport electrification in recent years – this affects personal transportation through the uptake in Electric Vehicles (EVs) as well as mass transportation through, among others, increased railway electrification. In both areas, upgrades to the underlying electric power supply infrastructure are inevitable to meet increased electricity demands.

This challenge on the demand side of our electricity systems is accompanied by significant changes on the supply side which undergoes a shift towards renewable electricity generation. Thus, increased electricity consumption from electromobility coincides with increased intermittency in the electricity supply. Mitigating issues surrounding electricity supply intermittency typically involves the usage of energy storage technologies.

Vehicle-to-Grid (V2G) is an energy storage concept in which the battery packs of parked EVs are aggregated and charged or discharged to provide a variety of grid services. Power flows in a V2G network are managed through an aggregator that arbitrates between the needs of EVs and the electric power grid. This project is concerned with a novel large scale V2G application in which the energy storage potential of aggregated EV batteries is used to support nearby electrified rail infrastructure - a concept referred to as Road-to-Rail Energy Exchange

(R2REE).

As with any V2G application, aggregator control is the key challenge in this project – many of the concepts presented are applicable, not only to the titular R2REE concept but to any large-scale V2G applications (with potentially thousands of EVs on the same network). EV management, communication and scheduling, although often underappreciated in current literature, are major challenges in a large scale V2G application. Yet, many energy storage applications require quick and dynamic network responses to changing power demands. In R2REE, power demands from the rail system may change by megawatts within just a few seconds.

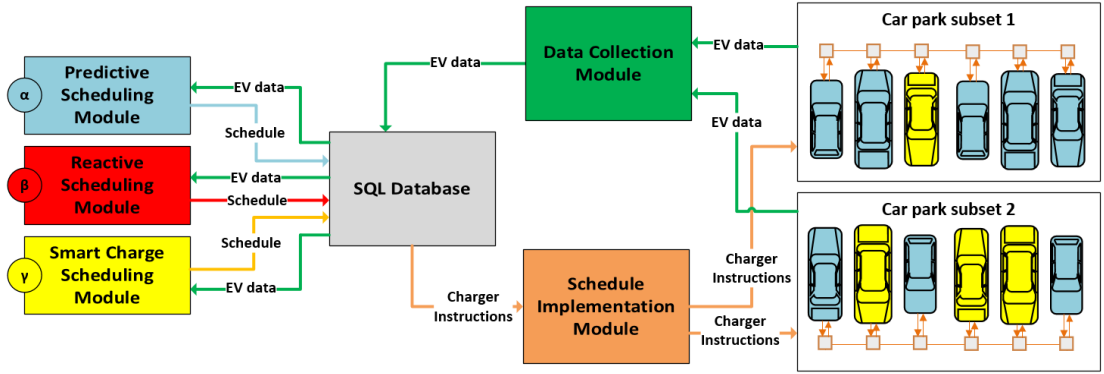


Figure 1.1: Modular aggregator control structure for Road-to-Rail Energy Exchange using multiple scheduling modules.

This project presents the benefits of separating aggregator control algorithms in a V2G network into several modules accessing a mutual database. A novel modular aggregator control structure, as shown in Figure 1.1 is proposed to improve system responsiveness and versatility. This involves splitting up the fundamental tasks of V2G aggregator control – data collection, scheduling and schedule implementation – into separate processes (here referred to as first-order modularisation) and integrate these processes with a suitable communications and data management system.

The modular control structure further allows for each task to be shared between multiple processes (referred to as second-order modularisation) – a characteristic that is particularly valuable for scheduling within R2REE (the process by which charging/discharging decisions for individual EVs are taken).

A novel method for multi-layered event-based scheduling uses multiple scheduling processes - or layers - to combine predictive scheduling (in which changing power demands are anticipated in advance and planned for) with a reactive scheduling approach (in which a V2G network reacts to changes as they occur). The predictive portion of this method exploits reoccurring and predictable power demand patterns, defined as events.

An example of such events are the traction power demands of accelerating electric trains - thus the usefulness of this approach for R2REE. This scheduling strategy is shown to be compatible with the proposed modular high-level aggregator control structure. It consists of three algorithm layers, differentiating between predictive scheduling for in-event periods (while an event is ongoing, e.g. during train departures), smart charging for non-event periods (i.e. when no rail traffic occurs) and reactive scheduling to account for uncertainty (e.g. an unexpected brake manoeuvre of the train invalidates the predicted power demand).

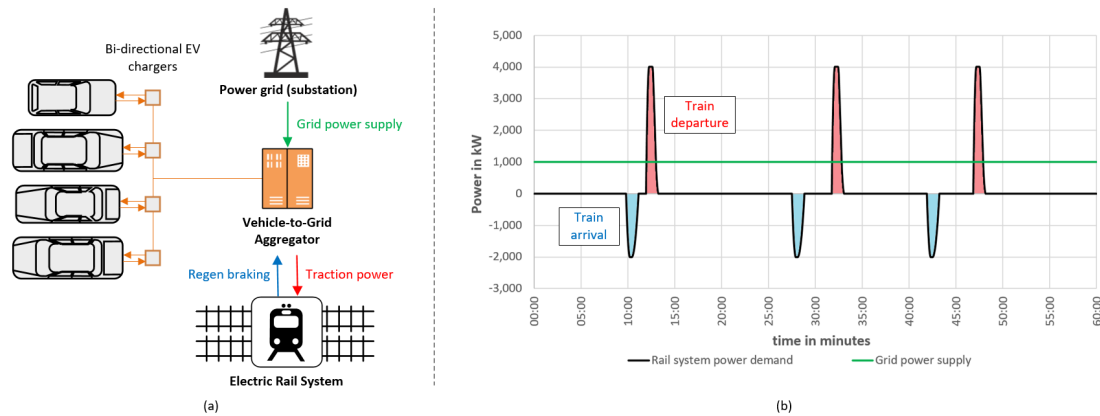


Figure 1.2: (a) V2G for support of local electric rail systems, system overview and power flows: EV population acts as buffer between the grid connection and the fluctuating rail system power demands; (b) Rail system power demand over one hour: traction power drawn for train acceleration - positive/red, power supplied from regenerative braking - negative/blue.

While using the aggregator control strategy introduced above to oversee a simulated EV population, the R2REE concept is explored. This novel V2G application (see Figure 1.2) is proposed to reduce local peak power demand stresses on the power grid arising from electrified rail traffic and to enable brake energy recovery. An existing low-voltage (750 V) Direct Current (DC) powered third-rail system



(traction power is supplied through a third rail along the tracks) in Merseyside, England serves as a case study.

The operation of a V2G network is simulated in real-time for a 24-hour period of V2G supported rail traffic from the view of a single train station with nearby V2G enabled car park. Three main factors determining the performance of such a V2G system were identified and examined: the EV population size, the EV charging rates and the power made available to the whole system through the shared power grid connection.

The simulations found that EV populations between 50 and 100 EVs can be sufficient to fully absorb power from, and thereby enable, brake energy recovery on the rail system. However, this is highly conditional on the EV connection times and charging rates (an EV population capable of fully absorbing an electric train's regenerated brake energy in the morning may no longer be capable of doing so in the afternoon).

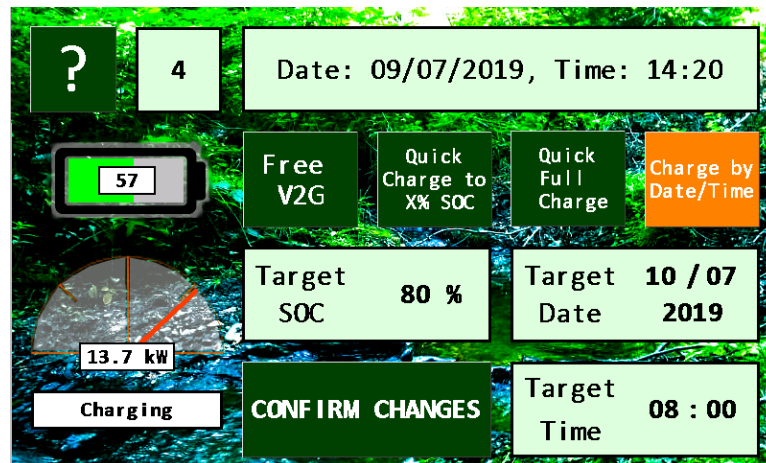


Figure 1.3: EV user interface screen capture: the user may choose between four different charging modes; here, the user has set a date and time by which a target State of Charge (SOC) of 80 % should be reached.

The last major topic covered in this thesis adds more depth to the scheduling process by granting the owners of EVs a degree of control over V2G scheduling. ‘Range anxiety’ is believed to be a major factor holding back the EV market as many drivers consider range limitations as a major disadvantage of EVs over more traditional vehicles with an internal combustion engine. Enabling V2G has the

potential to worsen this perception as connected EVs may actually lose charge over short periods. A method is proposed that allows owners to state charging preferences via an EV on-board user interface as shown in Figure 1.3.

The inclusion of user charging preferences adds constraints on the scheduling process and increases computational complexity. Taking these preferences into account and weighing them against the often conflicting needs of the power grid without negatively affecting system responsiveness is a challenge to be overcome. The impact of added complexity on the execution time of the scheduling process is addressed by resolving user inputs prior to the actual scheduling.

The ability of each EV to either charge or discharge is being assigned a weighting factor while taking into account user inputs and the current state of the battery pack. This weighting system, along with the options available to EV owners will be presented. This computationally efficient method of capturing charging preference is suitable for other V2G applications than just R2REE.

## *1.2 Project Novelty and Publications*

Work on this project has led to a number of novel contributions and publications as listed in Table 1.1, including the thesis location of the description and evidence in support of each claim of novelty.

Novel Contribution	Location in Thesis	Associated Publication
Formulation of a novel modular V2G aggregator control strategy separating data collection, scheduling and schedule implementation into distinct processes based around a single mutual database.	Chapter 3: Vehicle-to-Grid Aggregator control, in particular sections 3.1: Modular high-level aggregator control structure, 3.2: Data collection and 3.3: Schedule implementation	“Modular strategy for aggregator control and data exchange in large scale Vehicle-to-Grid (V2G) applications”, <i>Energy Procedia: 3<sup>rd</sup> Annual Conference in Energy Storage and Its Applications</i> [1]
Novel method of event-based predictive V2G scheduling suitable for dynamic aggregator control in large scale car park-based V2G applications with reoccurring power demand profiles.	Chapter 3: Vehicle-to-Grid Aggregator control, in particular section 3.4 on V2G Scheduling	”Multi-layer event-based Vehicle-to-Grid (V2G) scheduling with short term predictive capability within a modular aggregator control structure”, <i>IEEE Transactions on Vehicular Technology</i> [2]
Method of accounting for charging preferences expressed by EV owners/users in the previously mentioned event-based predictive V2G scheduling.	Chapter 3, section 3.5: EV communication system prototype; Chapter 5: EV owner control over V2G Scheduling	”Integration of electric vehicle user charging preferences into Vehicle-to-Grid aggregator controls”, <i>Energy Reports: 4<sup>th</sup> Annual Conference in Energy Storage and Its Applications</i> [3]
Novel application of V2G as line-side energy store for electrically powered rail transport systems - Road-to-Rail Energy Exchange (R2REE).	Chapter 4: Road-to-Rail Energy Exchange	”Vehicle-to-Grid (V2G) as line-side energy storage for support of DC-powered electric railway systems”, <i>Journal of Rail Transport Planning and Management (submitted on 11.09.2020 and under review, manuscript number: JRTPM-D-20-00029)</i>

Table 1.1: Project novelty and associated publications

## 2. LITERATURE REVIEW

### 2.1 *Emergence of electro-mobility and the need for energy storage*

The transportation sector is responsible for much of the global energy consumption - within member countries of the International Energy Agency (IEA), which includes all of North America, most of Europe, Australia, New Zealand, Japan and South Korea, transport accounts for about 36 % of all energy consumption as of 2017 [4]. Most of this energy consumption (about 21 % of the total can be attributed to passenger cars and about 10 % through road-bound freight transport. It is therefore unsurprising that global ambitions to reduce the dependence on fossil fuels are largely aimed towards transportation.

Fossil fuel savings in transport may be achieved through 1) improved efficiency of vehicles using Internal Combustion Engine (ICE), 2) shifting individual transportation to mass transportation (i.e. public transport instead of private passenger vehicles), 3) the usage of cleaner alternative fuels (i.e. biofuels, hydrogen, etc.) and 4) – most relevant on the topic of V2G – transport electrification [5]. The electrification of transport further aids decarbonisation efforts [6] - in particular when renewables have a high penetration in the electricity generation [7], it can help improve air quality (especially in urban environments) [8] and increase energy security [9].

Electro-mobility is, therefore, being pursued worldwide – thus far with noticeable success in Asia [5][9], Europe [8][10] and North America [6][7] but with first steps also undertaken in Latin America [11] and parts of Africa [12]. Governments around the globe are pushing policies aimed at increasing EV uptake (although against consistent calls for further financing and political support [10]).

One noteworthy international initiative is the so-called ‘EV30@30’ campaign. The stated objective is to reach a 30 % share of EVs in vehicle sales by 2030 in all participating countries (Canada, China, Finland, France, India, Japan, Mexico,

the Netherlands, Norway and Sweden) [13]. The campaign does not specify how this is achieved in each country and includes no strict commitments or penalties for failure to achieve the objective. It is, however, a clear statement of intent against which success can be measured and that can inform government policy on transport electrification. The UK joined the EV30@30 initiative in 2018 [14] and as recent as March 2020 has extended subsidies to support the uptake of EVs [15].

The global pursuit of increased electro-mobility along with improvements in battery technology have led to significant increases in the number of EVs in recent years (see Figure 2.1). According to the International Energy Agency, the global EV fleet grew by 2 million in 2018 alone, exceeding 5.1 million (these numbers include Plug-in Hybrid Electric Vehicles (PHEVs) [16]. About half of this growth can be attributed to EV sales in China and about a fifth each for the European market and the US. As of 2018, the countries with the highest market shares of EV sales were Norway with 46 % (thus easily achieving its EV30@30 target already), Iceland with 17 % and Sweden with 8 % [16].

Electric car deployment in selected countries, 2013-2018

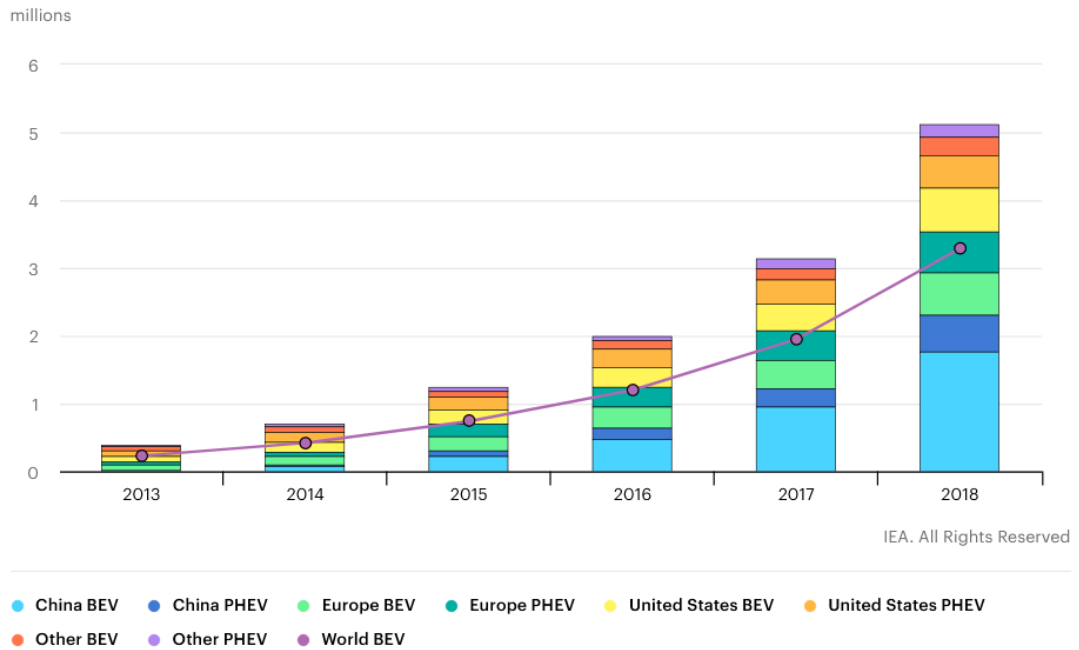


Figure 2.1: Global EV rolling stock (including PHEVs) according to the International Energy Agency, figure taken from [17]

While the IEA has not yet released its final analysis for the 2019 calendar year, global EV sales (again including PHEVs) are estimated to have reached about 2.26 million units according to ‘EV volumes’, a website dedicated to tracking the development of global EV markets [18] (by contrast, total global car sales are estimated to about 75 million units in 2019 [19]). If correct, this number would suggest a year-on-year growth in EV sales of around 10 % which indicates a significant slowdown compared to previous years (see Figure 2.1). This slowdown seems to stem predominantly from stagnation on the Chinese and US EV markets in 2019 [18].

Longterm forecasts predict that the trend of rising EV sales is set to continue. Looking yet again at the IEA, it predicts the share of EVs in global passenger car stock to rise from 0.6 % in 2018 to 14.5 % in 2030 (see Figure 2.2). This forecast assumes adherence to the IEA Sustainable Development Scenario (SDS) which describes pathways for all energy-related sectors to achieve global climate change goals - in particular, the Paris climate change agreement [20]. Unlike most other sectors, the IEA judges the uptake of EVs as ‘on track’ with the SDS [21] (as of 2018).

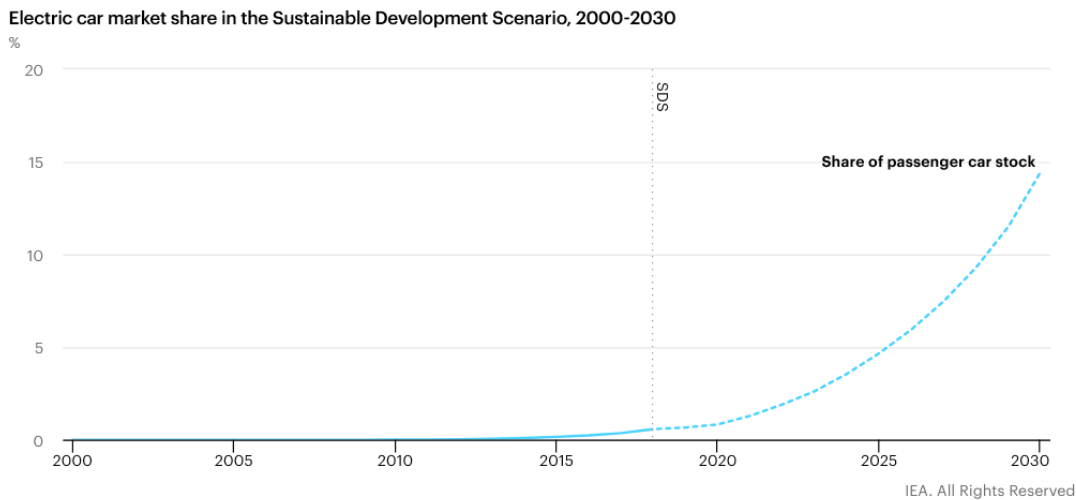


Figure 2.2: Global EV sales (including PHEVs) and forecast according to the International Energy Agency, figure taken from [22]

This forecast seems to align with expectations in the automotive industry as evidenced by heavy investments in EV technology in recent years. With industry ‘heavy-weights’ such as Ford [23], Toyota [23], Jaguar Land Rover [24], Volkswagen [23][25], BMW [26], Nissan [23] and Porsche [27] all committed to shifting

their vehicle portfolio away from ICE vehicles towards EVs. The drive towards electro-mobility even sparks seemingly unlikely alliances between supposed rivals as evidenced by the recent announcement of a collaboration between Jaguar Land Rover and BMW to develop EV technologies [24] (arguably as both companies lag behind the Japanese competition with regards to EVs).

It should be noted that at the time of writing it is not clear how the relatively new and unusual circumstances of the COVID-19 pandemic will affect the uptake of EVs in 2020 and beyond. Given the general downturn in global economic activity, factory closures, low demand and supply-line issues (such as lithium supplies [28]) for at least the first half of 2020 it is plausible, if not likely, that year-on-year growth of the global EV fleet will be well below the projections or even negative. Should this be the case, it remains to be seen if this will be a one-off event or lead to a lasting trend reversal of growing EV numbers.

However, the pandemic's economic impact similarly affects the production and sales of 'traditional' ICE vehicles due to factory closures and lower demands [29]. Thus, it is plausible that the growth of EV sales relative to ICE vehicles will continue at pace. Assuming no significant changes in policy regarding transport electrification or the reversal of investments in relevant industries, the author remains optimistic that the shift towards electric vehicles will continue regardless. In either case, the working assumption for the remainder of this thesis is a greater abundance of EVs on our roads in the not too distant future.

Of course, ongoing transport electrification is not limited to road vehicles but can equally be observed in rail transportation. Rail transport accounts for about 4 % of the total energy consumption within IEA member states [4]; significantly less than road transport (about 31 %). Differences in the degree of rail electrification between countries are stark. In China about three-quarters of Chinese rail is electrified [30] while only about 1 % of tracks in the USA are electrified [31]. Many European countries and the European Union (EU) itself push for more electric rail systems to reduce carbon emission and battle air pollution [32][33]. The UK in particular aims to completely replace diesel locomotives by 2040 [32][34].

Railway electrification typically implies having electrically driven trains powered by either overhead transmission lines or third-rail (see chapter 4) and fourth-rail systems. Thus, it not only includes replacing the locomotives but also building the infrastructure to continuously power electric rail vehicles. However, there are some proposals for trains with on-board battery energy storage [35] to reduce the

dependence on power infrastructure along the track.

Apart from the need for additional infrastructure, transport electrification also poses challenges to the existing power grid. While generally regarded as a positive development, an ever-increasing number of EVs and PHEVs risks overwhelming local distribution networks [36]. Shifting individual transportation away from fossil fuel combustion increases the electricity demand for EV battery charging and creates power demand peaks if charging is not managed effectively. The risk of overloading substations is particularly severe when peak demand from EV charging coincides with the megawatt level power demands of electric rail vehicles [37].

It should also be noted that transport electrification is not the only considerable transformation of our electricity systems but is accompanied by shifts towards renewable electricity generation. As such, increased electricity consumption from electro-mobility happens to coincide with increased intermittency in the electricity supply. To mitigate issues with supply intermittency, energy storage technologies are generally accepted as absolute necessity [38].

Another route to avoid overwhelming the grid is demand-side management. With regards to EVs, this implies the avoidance of uncontrolled ‘dumb charging’. Instead, charging can be controlled by limiting charging rates and/or delaying charging to off-peak periods. This approach of ‘smart charging’ has been widely explored over the years and is already commonly used [39][40][41].

Smart charging generally treats EVs as a burden to the power grid which has to be constrained. However, an increase in EV rolling stock also leads to a larger number and higher total capacity of EV batteries ‘on the road’. Considering that most vehicles are parked for most of their lifetime (about 95 % [42]) a lot of potentially useful battery capacity may be sitting idle. Making use of this capacity could turn EVs from a burdensome load into useful energy storage for the grid – which is the core idea of the V2G concept.

## 2.2 *Vehicle-to-Grid distributed energy storage*

V2G is an energy storage concept that uses the aggregated batteries within parked EVs as an energy store for the power grid [43]. It treats the EVs’ battery packs as distributed grid-based battery energy storage. Power flows are managed by the so-called aggregator, which arbitrates between the needs of EVs and the grid. The



aggregator decides when and at what rate individual EV battery packs are being charged or discharged in a process usually referred to as scheduling [44].

V2G is a multidisciplinary field of research concerned with the power grid, communication networks, transportation systems and urban infrastructure [45]. Exact definitions of what constitutes V2G vary but in general, the concept requires the control of energy flow between the power grid and grid-connected EVs. One major difference between definitions of V2G is whether energy flows can be unidirectional [46][47] (i.e. controlled charging of EVs) or have to be strictly bidirectional (controlled charging and discharging of EVs).

The description of unidirectional V2G (even referred to as V1G [47]) has only a few examples in literature and seems to be outdated terminology. It is however quite prominent on the English Wikipedia page on 'Vehicle-to-Grid' (and has been for years). The latter may be of little to no relevance to researchers in the field but is a main source of information for the general public.

Unidirectional V2G would certainly be easier to implement than the bidirectional counterpart but the potential to provide grid services is obviously limited to EV batteries receiving power from the grid (at periods of low power demand) or simply not charging (when the power demand on the grid is high). While unidirectional V2G can be advantageous to the power grid and has some potential for monetisation for vehicle owners [46] it arguably falls under the umbrella of 'smart charging'. Thus, the definition used for V2G in this work strictly implies bidirectional power transfers between EVs and the power grid, which appears to be in line with the vast majority of literature in the field [48][49][50][43][51].

Another piece of V2G related terminology to be clarified is the (slightly more common) distinction between V2G and Grid-to-Vehicle (G2V). Some authors in the field make a distinction between V2G and G2V to denote the direction of power flow with the same system being either in V2G mode when EVs are discharged or G2V moded when EVs are charged [52][53][54][55]. While this distinction can be a useful shorthand in certain discussions, it will not be employed in this work to avoid confusion wherever the term V2G is used.

The essential element at the centre of any V2G network is the so-called aggregator. The aggregator groups several EVs together and acts as the intermediary between EVs and the power grid (more precisely the locally operating Distribution System Operator (DSO) or, assuming the V2G network is large enough the Transmission System Operator (TSO) [56]). For a number of EVs (typically parked on the same

car park) charging and discharging would be managed through the aggregator in accordance with the DSO or TSO [57].

Definitions for aggregator vary in the literature depending on context and it is not always clear if the term refers to the power infrastructure grouping the EVs together, the control logic making charging/discharging decisions or the economic entity trading electricity/grid services. However, these definitions are not mutually exclusive and an aggregator may roughly be described as anything needed to manage power flows and arbitrate between the needs of EVs and the grid. Thus, all three definitions may apply where relevant.

Another aspect in which V2G literature appears to be split is the inclusion of PHEVs. There is no inherent reason why PHEVs could not be used in a V2G application – however, their battery packs typically have much lower capacities and charging rates than ‘pure’ (i.e. non-hybrid) EVs. Thus the potential value of PHEVs for any grid services is significantly lower – usually, but not always, excluding PHEVs from consideration.

Within this work, PHEVs are not included in any analysis (any simulations in chapter 4 and chapter 5 are based on ‘pure’ EVs, see section 3.6). However, any of the findings regarding aggregator control presented in chapter 3 could be equally applied to a V2G network with a population of connected PHEVs. Some of the references used throughout this thesis may have included PHEVs in their analysis/models – this will be pointed out only where relevant for context.

### 2.2.1 V2G Applications

V2G has been proposed for various applications in literature. A V2G network acts as a distributed grid-based battery energy store offering a high power density and high energy density but with additional complications such as a varying capacity and potential limitations on the minimum SOC of the EV batteries. A V2G network could serve many different purposes and perform various grid services:

- Act as (pseudo) spinning reserve [53]: Spinning reserve describes extra generating capacity available and already connected to the grid (i.e. generators already running, but not at full power). V2G could serve the same purpose although it is not generating electrical power but releases energy stored already (hence ‘pseudo’).

- Improve load factors and balance loads through peak shaving or valley filling [52]: A reduction in peak power demand may decrease the need for power utilities, thus reducing costs (even if the total electricity consumption is unchanged).
- Provide backup power in cases of power outages [52][58]: The V2G network could potentially power single buildings or whole communities during short outages (or just core-infrastructure over longer periods).
- Buffer the intermittency of renewable energy sources [52]: This could allow the integration of more renewables in the power grid and reduce the need for gas turbine power plants (as demand response), ultimately reducing emissions (as long as battery degradation is not excessive [59]).
- Provide frequency regulation [52][60][61]: Closing gaps between power generation and demand help to maintain the grid frequency at 50 Hz (in most parts of the world) or 60 Hz (in North America and parts of Asia) [62].
- While doing any or all of the above, generating revenue (multiple potential revenue streams to be discussed in section 2.3).

The above examples are all rather common grid services that are widely discussed in the literature – not just with regards to V2G but also energy storage in general. Most publications on V2G assume one or more of the above applications (thus, these applications will re-emerge throughout the rest of this review). There are, however, several examples of highly specialised ‘niche’ applications for V2G. One of which - R2REE – as the topic of this thesis will be discussed in detail in section 4.1 and throughout later chapters.

In other examples, V2G has been proposed to help to make small islands energy self-sufficient [63] or as a tool for triad avoidance [64][65] for large-scale electricity consumers. The latter application is very UK specific as ‘triads’ (three half-hour periods of the highest power demand in a year [66]) are used by National Grid to determine the charges for industrial and commercial power consumers. Shifting the electricity consumption away from such a triad period (time of occurrence unknown beforehand) can significantly lower electricity costs for a large business – even if the total electricity consumption has not changed (leading some to criticise the whole concept of triad-based billing [67]).

Some proposed applications employ the general idea behind V2G on a smaller scale. Vehicle-to-Building (V2B) and Vehicle-to-Home (V2H) are energy storage concepts in which EVs are connected to the electrical grid of individual buildings [68]. Just as in V2G, EVs are charged and discharged (supplying electricity to the building) with regard to the building's energy demand. V2B and V2H are usually not concerned with grid services but are aimed to change a building's power demand profile to reduce electricity costs or make more efficient use of local renewable energy sources (for example solar panels on the roof of the same building). Further, the EVs can potentially power the building during power outages [58]. As these concepts may reduce a building's electricity consumption at times of peak demand, they may also be indirectly beneficial to the power grid if widely implemented.

V2H is being developed by Nissan for example, using a smart home-based bidirectional charging station connecting a single Nissan Leaf to a typical family house [69]. An interesting example of V2B is the 'EV-elocity' demonstrator project which aimed at using 100 EVs to support the power demands of an airport [70]. Unfortunately, at the time of writing the project progress is unclear as its funding body currently lists the project's status as 'on-hold'. However, the idea of using the V2G concept at an airport has also been mentioned with reference to London Heathrow in an article hailing potential environmental benefits while admitting that economic benefits are 'uncertain' [71].

For the airport, this concept supposedly offers increased energy security and end the reliance on diesel generators to keep Information Technology (IT) systems, lighting etc. running during outages. Interestingly, the same article implies that "Airports, train stations or workplace car parks could really support the transition to a low-carbon electricity network" – one of the very few mentions of V2G in the context of rail systems although without any further detail on the topic.

Several ongoing V2G projects are focused on commercial EV fleets. The project titled 'Integrated Energy Systems for Commercial Vehicles' [72] is a feasibility study for using V2G in commercial fleets. As the project abstract points out, commercial vehicles are particularly well-suited for V2G as they congregate at depots, follow duty cycles scheduled in advance, typically possess larger battery packs than passenger vehicles and are owned by businesses able to assess the trade-offs of V2G revenue and costs associated with reduced battery life [72].

Another ongoing project titled 'Bus2Grid' investigates using V2G with 30 electric buses at London bus depots [73]. While the project description does not give any details on the buses used, it seems likely that this refers to Transport for London's fleet of BYD ADL Enviro200EV (single deck) and BYD ADL Enviro400EV (double deck) busses [74] [75]. These buses have purely electric drivetrains with 330 kWh battery packs and dual plug 2x40kW Alternating Current (AC) charging [76][77].

### 2.2.2 User Acceptance of V2G

Unlike with commercial fleets, when relying on privately owned EVs V2G faces the issue of encouraging user participation [78]. While owners/managers of commercial fleets may be expected to objectively decide for or against V2G participation purely on economic merits, EV-owning consumers may take issue with other rather subjective factors. For example, the loss of control over the EV charging process or the struggle to accept an increased rate of battery degradation from V2G participation.

Social factors, however, are sparsely covered in V2G literature. Sovacool et al. found that the topics of social acceptance, consumer behaviour or consumer information were represented in less than 3 % of V2G literature – despite the social acceptance of V2G technologies being paramount for a successful rollout of V2G [79]. The social acceptance and perception are also important for electro-mobility itself as the electrification of individual transportation is widely considered to be hampered by 'range anxiety' – the perceived inferiority of EVs to traditional ICE vehicles in terms of driving range [80][81]. A survey from 2012 of drivers in the US found that range limitations were named as 'biggest concern' regarding EV adoption by 33 % of participants followed by cost with 27 % [82][79].

Although this survey is somewhat dated, this description of public perception is in line with personal experiences of discussing electro-mobility with members of the public – even as both, range and cost of EVs has improved significantly over recent years. In many cases, EVs are already cheaper to own and maintain than ICE vehicles over 5 years of ownership [83] (as low maintenance cost and electricity prices compensate for a higher initial purchase price of an EV).

As range anxiety remains, it is not unreasonable to assume that it could negatively affect the acceptance of V2G technologies. EV users may fear a loss of control over the charging process of their EVs and the EV batteries may actually lose

charge over short periods. While of course purely anecdotal evidence, the author is frequently confronted with questions such as ‘What if my car’s battery is empty when I return?’ when explaining the concept of V2G to a layman audience.

As a relatively new technology V2G is still rather unknown not only to the general public but even to those working in the transport and electricity sector; even among those aware, it is often conflated with smart charging [84]. The acceptance of smart charging among EV users is quite high with up to 95 % being happy to use smart charging if it reduces their electricity bills [85]. It is unclear if V2G could achieve an equally high acceptance. The concept of smart charging and potential cost savings through off-peak charging at lower electricity tariffs is relatively easy to grasp. V2G is a more complex proposition and comes with the (at least perceived) risk of a decrease in EV battery SOC.

A study undertaken by Parsons et al. [86] found that EV drivers are hesitant to enter into binding V2G contracts, desire flexibility in car usage and lack awareness of the times that their cars are parked. One suggestion made to address this hesitation is to eliminate strict contract requirements in favour of more convenient, flexible ‘pay-as-you-go’ services [86]. As discussed in chapter 5, this work addresses similar issues by providing EV drivers with flexibility via means of user control over the V2G usage of their vehicles.

Allowing users to state charging preferences for the aggregator to abide by is a possible approach to increased V2G acceptance and, by extension, V2G participation. This can be done using simple user interfaces providing a range of charging options either remotely via smartphone apps or on-board ‘infotainment’ systems (multi-media devices used for entertainment, climate control, navigation, etc.) [87].

V2G participation by EV owners may also be encouraged through ‘gamification’ to make V2G more accessible to the public. V2G gamification, i.e. the integration of competitions, games and virtual rewards is the subject of an ongoing project [88][89] with yet unknown outcome.

### 2.3 *Economic Considerations of V2G*

As for most new technologies, successful and far-reaching implementation of V2G depends greatly on its potential economic benefits. Building and maintaining the infrastructure necessary for widespread V2G adoption is costly and so is

potentially accelerated EV battery degradation from V2G participation [68][90]. In a strongly simplified V2G network, there are three parties, each with their own financial interests: the **grid operator**, the **aggregator** and the **EV owner(s)**. A visualisation of how fees and compensations might be transferred between the parties can be seen in Figure 2.3.

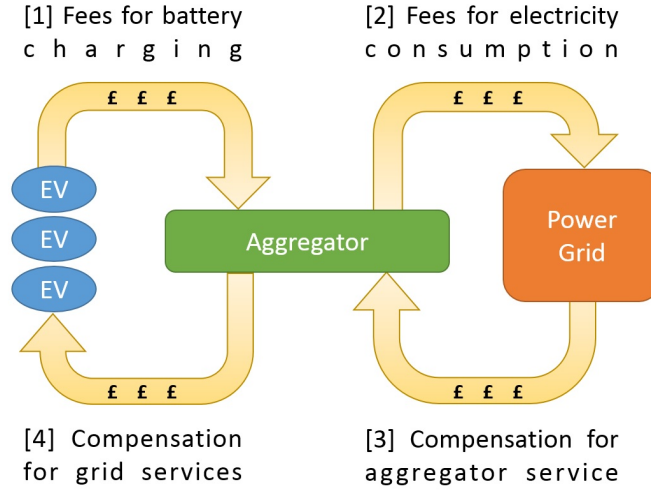


Figure 2.3: Fees and compensations paid between the three parties in a V2G network

The **grid operator**, depending on the current situation, either sells electricity to or purchases grid services from the aggregator. Purchasing grid services might simply mean buying electricity back from the aggregator when needed but could also include charges just for the availability of grid services regardless the actual usage (i.e. as insurance against outages/imbalance). For example, the grid operator may pay a fixed monthly fee to the aggregator to ensure that a certain capacity is available as a spinning reserve for the grid at any given time [54]. Thus the grid operator serves as both, a supplier (of electricity) and a customer (of grid services).

The **aggregator** which, from an economical view may be defined as "an entity that assembles customers into a buying group for the purchase of a commodity service such as electricity [91]" acts as a broker between the grid operator and EV owners and, in most cases, also seeks to generate profits from V2G participation. For EV battery charging the aggregator may pass on electricity costs to the EV owners but can also charge additional fees for charger usage. For performing grid services, the aggregator receives compensations which may be shared with the EV owners.

There are several ways in which EVs might be grouped by aggregators. The simplest example to consider is a single car park with a fixed number of spaces managed by a single aggregator. Here the aggregator might be the car park owner/operator, or a business renting the car park to make profits from V2G services [57]. Participating in a market as an aggregator is challenging due to a high level of uncertainty - the available battery capacity is constantly changing with the number, the SOC and connection time of EV batteries.

To ensure the profitability of aggregator projects, reliable predictions of the behaviour of EV owners are needed. Statistical data might be used to predict EV owner behaviour, which is influenced by social and economic aspects [92]. Depending on where V2G is employed, difficulty and accuracy of such predictions vary. The situation in a public car park near a shopping centre is likely to be more variable than in a coach operator's parking space (where coaches usually have strict driving schedules). Hence, an aggregator might manage a fixed fleet of EVs (coaches, lorries, taxis, etc.) from the same owner rather than public parking areas (several examples of V2G usage with commercial EV fleets are discussed below).

**EV owners** provide the EV battery capacity to be used for grid services during the parking time. As the counterpart to the grid operator, they similarly act as both a customer (of electricity for EV charging purposes) and as providers of grid services. The main costs for EV owners are due to battery degradation (which is a major financial risk [93][51]) and should be fully covered by the compensations received – ideally including profits for EV owners - to encourage V2G participation. Further, the EV owner requires the EV to be operational (battery charged to a certain SOC) when leaving the parking space, which may limit the grid services that can be performed.

The potential economic benefits of V2G for each of the three parties depend on electricity market conditions at the time, EV charging strategies and vehicle aggregation [52]. There are numerous studies on the economic viability of V2G. However, these studies are so diverse in terms of underlying market conditions (i.e. a grid service that is profitable in the US may or may not be profitable in European markets) and the assumptions made (i.e. fixed and predictable charging schedules, constant ambient temperature, etc.), that too often, the results cannot be meaningfully compared with one another.



There are case studies of both, profitable and unprofitable V2G scenarios (a selection of which are discussed below) but it seems too early to make a general judgement on the economic viability of V2G as there is still a high degree of uncertainty over the future cost developments (e.g. cost of EVs and charging hardware) as well as the compensation paid for grid services going forward.

As discussed in the previous section, one central concern of V2G is the encouragement of EV owners to participate – which is also (although not exclusively) an economic concern for owners of EVs. Just covering their cost of V2G participation may be considered insufficient and it is widely believed that a significant yearly per-vehicle profit is needed to persuade EV owners to take part.

While some individuals may happily participate for non-profit reasons if, for example, environmental benefits are perceived as a ‘greater good’ – the apparent underlying assumption in the relevant literature is that EV owners require financial incentives to participate. Without fair pricing mechanisms, EV users may avoid V2G services. Finding such mechanisms is however difficult as aggregators are unaware of individual user preferences [94] (this problem is addressed in chapter 5). It should be noted that financial incentives may not be limited to direct payments for V2G services but could also take the form of free parking [95] (valuable especially in urban environments) or discounted EV-charging.

Further, it should be noted that costs from V2G participation for EV owners may not be limited to increased battery degradation. It is possible that V2G-related cost already occurs when purchasing an EV if V2G-enabled models are more expensive than models capable of charging only (the opposite might also be true should policymakers decide to subsidise V2G). While there is no indication of the EV market developing in either direction this could significantly impact the economic case of V2G for EV owners.

### 2.3.1 Case studies and projects on V2G economics

One 2013 case study for Ontario, Canada assumed that EVs are being paid feed-in-tariffs similar to the local feed-in-tariffs for renewable energies for providing peak power provision [96]. While the study could identify scenarios, in which yearly profits could be achieved under such feed-in-tariffs (around \$50-60 per vehicle per year, to be shared between aggregator and EV owner), the study’s author believes these would be too low to encourage V2G participation. A further problem with such feed-in-tariffs is that the energy is merely stored in EVs and

not generated. Hence, it may not be seen as justified by some to pay similar tariffs to electricity generation, even though storing energy can be equally useful.

A 2017 study also looking into using privately owned EVs for peak reduction (this time in the United States) similarly showed that V2G can generate profits (ranging between \$129 and \$342 per vehicle per year) [51]. While higher than the previous example, the author's of this study, too, have doubts that this provides sufficient incentives for EV owner participation. Profits are, however, increased slightly in scenarios in which a carbon dioxide tax is introduced into electricity prices (up to \$30 per vehicle per year for currently common carbon pricing – which may increase in the future).

The rather recent ‘Vehicle to Grid Britain (V2GB)’ project (concluded in 2019), as the name implies, focused its feasibility analysis of V2G for domestic customers on the UK energy market [97]. It, rather unsurprisingly, identified plug-in rates (i.e. the fraction of time that an EV is connected to the bi-direction charger) as a major driver of profitability. While the average plug-in rate of participants was rather low at around 30 %, for those participants with 75 % plus plug-in-rates annual revenues above £400 could be achieved – four times that of the average participant (based mainly on frequency regulation through a 7 kW bi-directional charger). However, costs for a V2G charger are significant (predictions range from £650 to £1150 one-off cost for a 7 kW charger) [97], so only committed EV users with high plug-in rates will experience net revenues. From a macroeconomic perspective, the project concludes that V2G could help save £200 million in upgrade costs in the distribution network between 2020 and 2030 compared to completely unmanaged EV charging [97].

Revenues from V2H systems in the UK were also found to be ‘modest’ according to the ‘Home As a Virtual Energy Network’ or ‘HAVEN’ project (also 2019). It concluded that a single EV added to a home energy network could generate about £100 annual revenue/savings through day-ahead electricity price optimisation (compared to unmanaged charging). Consumers with Photovoltaics (PV) installations *and* other energy storage solutions that allow for electricity shifting with the EV could see around £70 of additional annual revenue by maximising the self-consumption of PV generation. An EV on its own was found to increase PV self-consumption to a very limited degree as EVs are typically not connected during peak PV generation [98]. Consumers matching these criteria may be relatively rare and even for them revenue increases/savings from V2H seem quite

low (undoubtedly, at least in parts, due to limited efficiency of PV generation in the UK).

Another study published in late 2015 investigated the potential costs of electric school buses in Philadelphia, USA [99] (including cost compensation via V2G usage for frequency regulation). The study compared the overall costs relative to traditional diesel buses and found a net increase in costs of \$7,200 per seat. While the higher costs are mostly associated with the generally higher capital costs of EVs, the authors interestingly emphasise significantly lowered V2G profits due to cold ambient temperatures. It was assumed that the fleet participates in frequency regulation services and while the prices for this service spiked during very cold weather, the V2G performance of the EV batteries was low. This indicates that weather and climate are important factors to consider when assessing V2G profitability.

There are several other studies focussing on EV fleets which are interesting from an economic viewpoint as aggregator and fleet owner may coincide instead of being separate parties with differing financial interests. One other example examined the economic and environmental benefits of electric delivery trucks being used in V2G frequency regulation (in the US) [100]. This study found significant additional revenue and emission savings from participating in V2G with a centralised fleet (around 30 vehicles). It was assumed that delivery trucks are parked 10 to 12 hours per day and that driving schedules were known. Further, it was noted by the authors that the prices for frequency regulation vary strongly depending on time and location and that even range-extended electric vehicles with small batteries are also useful for frequency regulation. The authors also mention the possibility of cost reduction for fleet owners participating in V2G through a reduction in carbon tax (as participation indirectly helps mitigating greenhouse gas emissions).

An example of a UK-based project with a focus on commercial EV fleets is ‘Vehicle-To-Grid Oxford (V2GO)’ demonstrator project. It is still ongoing at the time of writing (project outcomes unknown) and investigates potential business models of V2G services for UK fleet operators [101]. With an anticipated 100 EVs in real-world V2G trials [102], this is one of the largest V2G demonstrator projects. Given its scale, this project will surely provide some valuable insights – unfortunately, the specifics of the project are rather ambiguous so far: “The V2GO project has four main aims: Demonstrate the benefits of EV adoption and

value of V2G and Smart Charging for fleet operators; Compare and assess the benefits of EV adoption and V2G against existing operating systems and practices; Understand how modifications to the fleet operation or charging patterns could help to optimise overall value; Provide real-world experience of V2G and the technology to trial participants and stakeholders [103].”

The ‘E-FLEX’ project, another UK-based V2G project involving 200 EVs served as a demonstrator for a ‘functioning V2G market’ [104]. It found that while “the true commercial benefits of the technology are yet to be comprehensively proven, [...] V2G could represent a strong accelerating factor in the uptake of EVs and the achievement of ambitious cost - and carbon emission - cutting targets”. Seemingly, the economic case for V2G (at least under current market conditions) has not been conclusive.

While there is still controversial discussion on the economic viability of V2G technologies, most authors appear to agree that (at least for now) frequency regulation is the most profitable grid service [60][97][99][100] for V2G. Overreliance on this grid service, however, is a risky proposition as compensations are volatile and may fall quickly if a successful uptake of V2G along with other energy storage alternatives saturates the market [105]. In none of the studies found, it was considered how a large-scale implementation of V2G (or the simultaneous rollout of other energy storage technologies) might affect the prices paid on the market for frequency regulation. Only in case of the V2GB project do the authors warn of a potential saturation of the market as EV numbers increase [97] (although without concrete predictions on the matter).

Further, the economic benefits for certain parties to participate in V2G may not come from direct payments, but through avoiding other costs (i.e. a reduction of carbon tax [51][100] for fleet owners, discounted charging or free parking for individual EV owners). Finally, it might also be worth discussing if V2G technologies strictly have to be profitable on their own. The argument could be made that the environmental benefits and the public need for a reliable electricity supply despite increased intermittency from renewable energy sources justify some degree of public financing of V2G (and/or other energy storage technologies).

## 2.4 Communications and Control

Communications is a major challenge in V2G systems – partially due to a lack of standardisation on the EV market (although as will be discussed later, some early attempts on standardising some aspects of V2G communication exist). V2G operation requires the exchange of information between three distinct parties: the grid-side (in the form of TSO or DSO), the aggregator and the EVs. With multiple EVs present, there is not just a single stream of information to be managed, but multiple streams of – potentially simultaneous – data exchange on the V2G network. The frequency of data exchange, communication routes and type-/amount of information required may differ significantly depending on the V2G application. Yet, some general observation can be made depending on the parties communicating.

### **Grid operator-to-aggregator communication**

This type of communication may be the least challenging as it follows techniques and conventions already in place on the electricity market in which the V2G network operates. In practice, this means that grid operator-to-aggregator communication in a V2G network follows that between the grid operator and power stations or energy storage facilities. While these standards are country-specific they are typically well regulated and based on matured technologies.

In the UK, any system connected to the transmission system has to comply with regulations set by national grid (National Electricity Transmission System Security and Quality of Supply Standard NETS SQSS) [106]. Depending on the scale of an aggregator, it might be connected to the transmission system, or a local distribution system (i.e. a collector substation). In either case, the communication between the aggregator and the TSO or DSO requires the exchange of real-time (e.g. frequency), static (e.g. voltage limits) as well as technical data [107].

Aggregators are likely designed to operate as autonomous systems without the need for regular intervention by human operators. Autonomous power systems commonly use control and communications systems called Supervisory Control And Data Acquisition (SCADA) [108]. These systems could be implemented to inform the aggregator and handle communication with the TSO or DSO using a dedicated communications network or encrypted internet connections.

### **Aggregator-to-vehicle communication**

This branch of communication is potentially the most challenging one. This is due to the varying amount of connected battery capacity, the potentially high number of EVs on the network, a variety of different EV models, need for standardisation of communication between EV manufacturers, safety concerns and even legal issues regarding privacy protection of EV owners. There are several degrees of communication depth (in terms of the type of information transferred), which might be chosen:

#### *1. No active information exchange*

In the simplest case, aggregator and EVs do not actively exchange any information. Instead, the aggregator could simply try to draw as much electricity as needed from a connected, unidentified, EV unless an on-board system in the EV prevents this. This way no communication system is required, but it comes with several disadvantages. Firstly, there is no certainty for the aggregator on how much capacity and power is available on the network. It might be possible to predict the capacity available based on statistical and empirical models (i.e. the number of parked vehicles known, the fraction of connected EVs known, average SOC and total capacity estimated), but this could only lead to rough estimates.

Further, no communication between aggregator and EVs makes collecting billing information difficult as an additional system would be required to identify EVs (or rather their owners) and store usage data. Finally, the degree of uncertainty over the connected energy capacity and potential power output prevents the aggregator from optimising its profitability.

A major advantage of this approach is the lack of potential privacy or data protection violations as no sensitive data is collected. As this method is likely to lead to ineffective utilisation of V2G enabled EVs, it is barely considered in the relevant literature. It is usually assumed that at a minimum, an aggregator would need to know how much and at what rate electricity could be drawn from a parked vehicle.

#### *2. Unique vehicle ID*

To enable a simple automatic system to track payments to be made from (i.e. charging fees) or to (i.e. compensation for V2G participation) the EV owners there needs to a system to identify each EV on the network and track the elec-

tricity flow into or from the vehicle. Such an Identification (ID) might be chosen to be permanently associated with a specific EV similar to the frame number of any street-legal vehicle or might change regularly similar to the way a computer's Internet Protocol address (IP) changes every time a new internet connection is set up.

The former makes tracking of EVs charging schedules easier, while the latter enables better privacy protection for EV owners. Changing IDs, just like changing IP addresses requires a register to allow identifying an EV for billing (similar to registers kept temporarily by internet providers [109]).

Permanent or not, vehicle IDs might be set up to be a seemingly random and anonymised string of numbers and letters or are chosen to contain some basic information about the vehicle (e.g. make and model, battery capacity, etc.). Following the latter, one might use a digital version of the Vehicle Identification Number (VIN) already in place as the ID. The 17 digit VIN code is unique to each vehicle (specifically the frame) and contains information on the vehicle manufacturer, model and year of manufacture [110] but no private information about the vehicle owner.

This information is kept at national registers. Such a register or database in which vehicle IDs can be linked to the vehicle owners and their payment details would also need to be available for billing purposes in a V2G network. It is also possible to use multiple (procedurally generated) vehicle ID's, which could improve privacy and safety [111]. Any system chosen for vehicle identification has major implications for privacy, data protection and security aspects and may face legal challenges in different countries.

Within this work, (simulated) EVs are assigned a unique but temporary ID upon connecting to the network (see chapter 3). This ID, a simple integer value, is assigned within the database by auto-increment. It only serves the purpose of identifying an EV until it disconnects (should the same EV re-connect later it will be assigned a new unique ID). A billing system, which would require identifying EV owners, is not implemented within this work.

### 3. EV technical information

Unlike in most other energy storage technologies, the energy capacity and potential power output of a V2G network vary depending on the number and type of connected EVs. In order to optimise and plan for the provision of grid ser-

vices it generally assumed that the aggregator knows these parameters - or at the very least - has fairly accurate estimates available. For this, the aggregator needs information about the current EV population, for example how many EVs are connected, how much capacity each EV provides as well as the SOC of each connected EV.

Thus a system is required that allows EVs to share information on the battery pack with the aggregator. However, there is no single agreed approach on how such a system would operate. What type of communication technology is used? How are messages between aggregator and EV structured? How often does this information need to be updated?

As will be shown later, such communications related considerations are usually not considered in the literature on V2G scheduling or specific V2G applications where the underlying assumption typically seems to be that the aggregator has perfect knowledge on the EV population at any time. In this work, by contrast, the aggregator control system presented (see chapter 3) includes a communications scheme suitable for and addressing specific challenges of the R2REE application (see chapter 4 and [2]).

#### *4. Future EV usage, EV user charging preferences*

To achieve a high degree of predictability for the aggregator, EVs would not only provide information on the current state of its battery but also on how the EV will be used in the future. Such information could contain the time at which the vehicle is expected to depart as well as the SOC which the battery is required to have at that time. This level of information would allow the aggregator to make full use of connected EVs for V2G services while ensuring that EVs are sufficiently charged when the drivers return.

On the downside, EV owners might not be willing to share this level of information or do not want to make predictions on their return. Further, for EVs to share information on future usage there must be a system in place which allows drivers to express their preferences. Within this work, such a system is integrated into the aggregator control along with a suitable user interface (see chapter 5).

### **Vehicle-to-driver communication**

With regards to V2G, this branch of communication serves two purposes: informing the EV driver about the state of the battery and/or allowing the driver to influence charging/V2G usage of the EV. The former is already featured in any



commercially available EV, typically through displays showing the battery SOC or an estimate of the remaining driving range. An interface to allow the latter, however, is not yet universally implemented.

In its simplest form, such an interface might be chosen to be a simple on/off switch enabling or disallowing V2G participation. In order to maximise participation in V2G and with its potential profits for EV owners and aggregators, more sophisticated systems would have to be applied. One approach might be to allow the driver to set a minimum SOC to which the batteries might be discharged along with a default value, which is applied if no selection was made. This gives drivers some control of the vehicle range which might limit the EV's V2G usage while being parked.

Ideally, drivers can even input the time of their next journey along with the range (or SOC) that is required by that point. This again might be used with a default setting (i.e. battery must be fully charged every morning by 8 am) for driver convenience. When designing more sophisticated user interfaces care must be taken to maintain user convenience. If the interface is too complicated to use or hidden within a plethora of other vehicle settings, drivers may not bother to use such systems and simply opt-out of V2G usage.

Such interfaces may be implemented into already existing hardware. Most modern EVs are already equipped not only with displays showing detailed information on the current battery state but advanced multi-media devices or 'infotainment' systems [87] - often using touchscreen displays. Newer systems even possess internet connectivity and may be interfaced with smartphone devices to share vehicle information or even control certain features, such as heating, remotely [112]. Where such systems are already in place, the addition of an interface allowing drivers to control V2G charging/discharging may only be a matter of a software update.

However, the difficulty remains that such systems do not yet follow a single design standard. EV manufacturers may use different systems even within their own product portfolio and certain infotainment features may not be part of the base models but expensive options that are chosen only by a subset of customers. Thus a V2G control interface designed for one EV may not be compatible with others.

As an example of how this could cause problems in V2G systems, some current EV models such as the BMW i3 [113] give drivers the option to limit the maximum

charging rates that the vehicle accepts for certain hours of the day (allowing EV owners to make use of off-peak electricity prices). These limitations, however, are not communicated to the charging station (or by extension an aggregator) and thus could not be taken into account in the scheduling process – the EV will simply not accept charging rates exceeding the set limit.

To avoid the risk of immediately fracturing the (not yet existing) V2G market via incompatible systems, attempts should be made to bring together various EV manufacturers and standardise on-board control systems – in particular any features linked to charging.

Another risk arises from adding even more driver controls to already complex systems that might overwhelm drivers. Tesla EVs, for example, are popular with many ‘tech-savvy’ consumers for including a rather comical amount of settings into their central multi-media systems (e.g. controlling mirrors, seats, doors etc. from the main screen). It is not unreasonable to assume that simply adding another page of settings for V2G controls may go unnoticed by many drivers who may not make use of the options given.

### **Telematics, On-board data logging**

Communications and controls in V2G applications require appropriate data acquisition on the EV side (measurements of SOC, battery temperature, voltages, etc.). Instead of adding dedicated systems for V2G related data acquisition to EVs, already existing hardware might be used. The general term telematics refers to any telecommunication and information processing technologies. Nowadays it nearly exclusively refers to automobile communication applications [114]. Telematics can be used for navigation, safety (e.g. automated calls for emergency services when an accident is detected), entertainment (e.g. internet access in a vehicle) [115] or usage-based motor insurance billing (currently requires dedicated telematics devices retrofitted into vehicles) [116]. It can be employed with various wireless technologies like IEEE 802.11 Wi-Fi, cellular communication or satellite-based technologies [117].

Telematics also includes vehicular On-Board Diagnostics (OBD). For EVs, it is very likely that OBD systems already collect most, if not all, data required for V2G applications. Most modern vehicles are equipped with a so-called OBD-II bus, which can be used to access data from the OBD system (legally required for all cars sold in the US, but also very common in the EU and other markets). This data bus could potentially be used for V2G applications (although the bus is

typically located inside the vehicles and another access point might be required). The Nissan Leaf's OBD-II bus can be read using (*unofficial*) programs such as 'LeafSpyPro', revealing a wide range of information about the vehicle and the battery (SOC, voltages of each cell pair in the battery pack, temperature readings) [118]. Similar Information can be retrieved via the OBD-II bus of a Toyota Prius (including the plug-in version) [119][120].

However, just as many other aspects regarding EVs, OBD in general and the OBD-II bus, in particular, is lacking standardisation. OBD-II is not designed for EVs, but for any vehicle and may or may not be used to communicate battery data. Tesla EVs are also equipped with OBD-II buses, but only transmit the minimum information required by law. For detailed diagnostics, Tesla uses its own dedicated system with a Controller Area Network (CAN) bus used exclusively by this manufacturer [121][122]. So, while the already existing OBD systems in modern EVs could be very useful for V2G, a system commonly used by all manufacturers has yet to be agreed upon (and potentially be enforced via regulation).

### **Vehicle-to-Vehicle communication**

Vehicle-to-Vehicle (V2V) communication is an advancing field of technologies using short-distance communication between road vehicles. It has potential applications in road surveillance [123], traffic control through 'smart' traffic lights [124], driver assistance (i.e. warnings of traffic jams, automated braking, etc.) [125] and some concepts of autonomous vehicles.

While V2V is still in its infancy, it shares many of the challenges of V2G communication. While it is in no way a pre-requisite for V2G, both technologies could use the same, shared, communication hardware. Unsurprisingly, V2V communication is generally assumed to be wireless and for many safety-related applications speed and reliability of the wireless information exchange is crucial.

### **Privacy and safety concerns**

Depending on the level of information shared within the V2G network, privacy preservation can be a serious issue with social and even legal implications. This is especially true when consumer-owned EVs are used for V2G applications. Assuming the highest level of information shared between EVs and aggregators (vehicle IDs, battery information and EV usage information), EV owners are required to share private information, which potentially allows profiling the daily schedules

of individuals. This sharing of information comes with certain risks (real or perceived) that could negatively affect the willingness of EV owners to participate in V2G.

Privacy preservation can be divided into anonymity (i.e. an EV cannot be identified), unlinkability (i.e. EV and owner cannot be linked), undetectability (i.e. it cannot be determined if a certain vehicle ID exists or not), unobservability (i.e. it cannot be determined what action an EV performs) and pseudonymity (i.e. an EV uses a pseudonym ID for certain actions) [126][127]. Obviously, full privacy preservation cannot be guaranteed in a V2G network (EVs have to be identified and linked to their owners for billing, based on charging and discharging actions performed).

To ensure at least some level of privacy preservation, the network should be set up in a way in which no single database and no single line of communication holds all the available data (for example, the billing process only needs to know payment information and services performed, but no technical information about the EV used). In V2G networks, privacy preservation is very challenging as EVs frequently change locations and join or depart the networks. This makes it easier for attackers to go unnoticed infiltrating the system using fake IDs [127] (for example IDs of EVs that are not in the same network anymore where the dual usage of such IDs cannot be detected).

Communication in V2G networks is not only required to be reliable but must also be reasonably secure against external attacks. Such attacks can have very different, but generally malicious intentions. Concerning private information shared by EV owners (i.e. anticipated EV journeys), this information might be used to conclude the wealth and daily schedules of EV owners. This could potentially be used to plan frauds, burglaries or vehicle thefts. When it comes to monetisation of V2G participation, attacks on the communications network may also aim at identity theft and fraud to redirect payments towards the attacker. Finally, attacks may be aimed at disrupting charging infrastructure as an act of vandalism or potentially even economic terrorism (i.e. interfering with charging schedules may leave several EVs discharged and practically immobilised).

Depending on the type of communication used within a V2G network, data security might be more or less difficult to achieve. Wireless communication is generally riskier than wired communication and using the internet or cloud-based services for communication exchange is riskier than using a localised dedicated system.

Further, the less information that is being shared and stored the lower the risk of misuse. Encryption may be necessary at any stage to minimise the risk of attacks although it also increases computational costs. Of course, such safety concerns are not unique to V2G networks. Any type of energy infrastructure must have its communication network protected from potential attacks.

## 2.5 *Communication Standards and Protocols*

As previously mentioned, a potential rollout of V2G is made difficult by lacking standardisation in certain areas. There are, however, some noteworthy attempts on addressing this issue. While some V2G specific standards may still have to be defined, where already existing technologies are utilised, V2G networks are, in effect, bound to comply with already existing standards. This may cover communication and charging hardware, safety equipment or communication protocols. A communications protocol can be defined as a set of rules for analogue or digital telecommunication. This includes signalling, error handling, syntax and other aspects that need to be implemented in software and hardware to allow a standardised way of communication between different devices [128][129].

For communication between aggregator and DSO/TSO, the standard IEC 61850 [130] is proposed [131]. This (global) standard is already employed for communication and control within substations (DSO to TSO communication) and is not specifically designed for V2G purposes. However, the interaction between an aggregator and the DSO/TSO is similar to that between a substation and the TSO. IEC 61850 is typically implemented using wired Ethernet or serial connections as well as Power Line Communications (PLC) (using active power lines to transmit signals) [132] and with a degree of redundancy to improve system reliability [133]. While rarely used, this standard also allows wireless communication methods, including IEEE 802.11 Wi-Fi [134]. IEC 61850 was developed focussing on automated substation control, protection and monitoring [135] making it suitable for autonomous aggregator controls.

A standard often proposed for communication between charging stations and EVs is ISO/IEC 15118 [137][138][139][131] (see Figure 2.4). In contrast to the standard discussed before, this one is specifically designed for V2G applications. It should be noted that ISO/IEC 15118 is not yet finalised and still open to the inclusion of new developments [140]. Being designed for V2G, this standard has a couple of interesting features: it allows for AC and DC charging, allows wireless

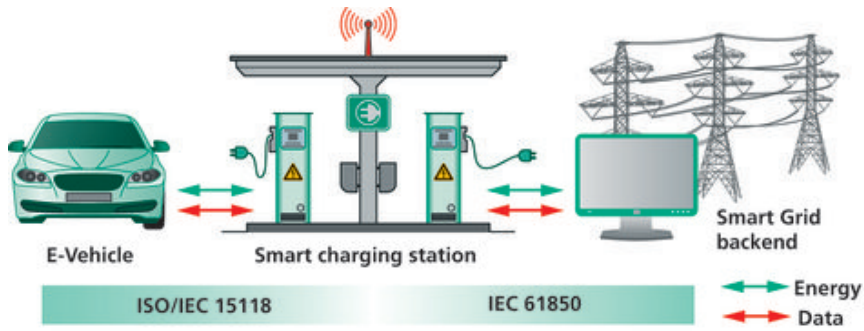


Figure 2.4: Visualisation of using IEC 61850 and ISO/IEC 15118 for V2G applications, figure taken from [136]

charging, accounts for the communication of customer requirements (although methods of vehicle to driver communication are not specified) [141]. Additionally, it incorporates vehicle authentication, automatic time-delayed charging and billing models (bidirectional billing) [136].

In particular, the ‘Plug & Charge’ aspect should be highlighted – the idea is that upon plugging the charging cable into an EV, the charging station can automatically identify the EV and link it to the corresponding billing information without the need for any interaction with the driver. This makes many older systems relying on payment cards, logins to online accounts or RFID chips to identify EVs obsolete [142]. Such driver convenience features are useful when relying on driver inputs elsewhere (see chapter 5) as drivers are more likely to make use of optional features when the charging process is less burdensome.

Despite being used as base-line in some technical papers on smart charging [143] and wireless V2G communications using Wi-Fi [144] as well as some V2G demonstrator systems by the Fraunhofer Institute for Embedded Systems and Communication Technologies [140] ISO/IEC 15118 is still lacking commercial applications. Thus it is unknown if it will be widely adopted by industry and EV manufacturers. ISO/IEC 15118 allows different communication technologies being used: PLC, which uses electrical wiring to carry data and alternating current simultaneously [141][132]; Wi-Fi, which creates medium-range wireless connections and cellular communication as used by mobile devices [132].

While this standard has been consulted in the early stages of this project, the aggregator control system structure developed (see chapter 3) does not strictly

adhere to it for aggregator-to-EV communication. For most of the duration of this project, only the draft stage version of ISO/IEC 15118 was available and was insufficient in detail to guide the system design [139]. The current version from mid-2019 [137] provides more detail and might be incorporated into the system described in chapter 3. Nonetheless, on a hardware-level (i.e. the choice of Ethernet and Wi-Fi as communication routes) ISO/IEC 15118 is in agreement with the work presented in this thesis.

Both standards, IEC 61850 and ISO/IEC 15118 include Wi-Fi as a potential route of wireless communication. Wi-Fi uses the IEEE 802.11 family of communication protocols [134] compatible with many consumer products like smartphones and tablet PCs [145]. It is often proposed for wireless communication between EV and aggregator [127][146]. Wi-Fi is a widely used and tested technology that offers fast and direct communication between numerous devices, although at a limited range.

Any communication standard or protocol has certain vulnerabilities and 'loop-holes' which may be used by attackers for malicious purposes [127]. The security of communication protocols can be enhanced using additional security protocols to fix certain vulnerabilities. These might be integrated into communication protocols (by packaging and encrypting information before transmission), or by monitoring and securing the network from unauthorised access (which is difficult in a network with a high number of participants). A security protocol proposed for V2G is the so-called PRAC (Privacy via Randomized Anonymous Credentials) which aims to provide anonymity and untraceability of EVs when authenticating to an aggregator [147]. This serves to protect EV owners against attacks such as identity theft, which could reduce fears regarding V2G participation.

## 2.6 *Aggregator control literature and projects*

As discussed in the earlier sections, V2G has been proposed as an energy storage solution for a variety of grid services at different scales (with regards to the size of the connected EV population). Each grid service may pose different challenges with regards to aggregator control or scheduling processes. The R2REE application discussed in this work represents a large-scale V2G application (potentially hundreds of connected EVs) that still requires quick system responsiveness (up to a few seconds, see chapter 3) as rail-system power demands can change rapidly.

In this section different V2G aggregator control and scheduling strategies are explored. Controlling the charging or discharging of individual EVs in a V2G network gets increasingly difficult with an increasing number of connected EVs. V2G scheduling must ensure that the network meets the demands of the power grid while also distributing power over the EV population. Scheduling may be an optimisation problem aimed at, for example, minimising carbon emissions [148] or minimising charging costs/maximising profits [149][150].

In the relevant literature, there is typically some overlap between the topics of V2G scheduling and so-called ‘unit commitment’. Unit commitment describes the mathematical process in which power-generating units (i.e. generators) are scheduled to reduce operation costs. The individual generators connected to the power grid are ‘committed’ to generate a specific amount of power for a certain period for the whole grid to maintain balance [151]. As V2G enabled EVs have to undergo a similar process (although simultaneously being a load while charging) unit commitment algorithms and V2G scheduling algorithms often share many characteristics. Scheduling can be challenging due to the complexity and sheer quantity of data that has to be analysed to determine how much electricity each EV receives [152]. As this directly affects battery degradation and financial compensation for each EV, V2G scheduling is also a matter of fairness in spreading both risk and reward across the EVs on the network (and their owners).

Due to the variety in grid services and scale of EV population, the requirements towards overall system responsiveness (i.e. how quickly a V2G network adapts to changes in power demand or EV population) also varies. In [153] V2G is being proposed for load shifting with scheduling taking place for a whole day ahead using hourly time intervals. The paper lays out a rather complex scheduling strategy including multiple optimisation variables to reduce overall costs in the system. It is only similar to the scheduling strategy described in this thesis insofar that it relies on power demand predictions to determine the V2G schedule (i.e. the set of charging instruction for the EV population) in advance. It is, however, operating on a completely different temporal resolution of 1-hour intervals (in contrast to 1-second time steps used in the predictive scheduling layer developed for R2REE, see section 3.4). Thus, the computational complexity of the scheduling rule set in this paper (and by extension its impact on the responsiveness of the V2G network) is not a concern.



Similarly, in [154] a decentralised V2G dispatch strategy where schedules are determined at the beginning of every 30 minute time interval is proposed. This is in contrast to the centralised approach used in this project. [155] proposes the usage of V2G for aggregator profit maximisation during peak load shaving while lowering the cost of EV charging to the customer. The model used includes factors such as battery degradation and battery replacement costs and uses 30 minute time intervals for scheduling. Again, a rather complex scheduling strategy is used, presumably at great computational complexity per time interval.

The maximisation of aggregator profits is also the aim of [156], which is using a 5-minute resolution. In [157] the aim is to minimise the charging cost of EVs in a rather large distributed population of up to 400 EVs (similar in scale to this project) but again at a very rough temporal resolution of 1 hour time intervals. Similarly aimed at minimising the charging costs of individual EVs is the work presented in [158] where 10-minute timesteps were identified as the best compromise between precision and computational cost. While a detailed analysis of computational cost is not provided, this is the first example where computational cost is even considered by the authors.

In [94] EV users are offered a variety of contracts when connecting to a V2G network stating how much energy will be available for charging, how much will be drawn from the EV for V2G as well as the charging costs and compensation for V2G participation. Such an approach gives a lot of control to the EV user but adds significant complexity and constraints to the scheduling process. In all the examples above, system responsiveness is not a major consideration as changes in power demand are gradual and a delay of a few seconds while computing a complex charging schedule would not significantly affect the system performance.

[159] proposes a cloud-based solution (i.e. remote scheduling via the internet) that uses machine learning to optimise V2G schedules for charging costs and EV battery degradation. This paper is rather theoretical and does not seem intended for real-time aggregator control. While not discussed, one might assume that remote control via the internet introduces minor communication delays (which may not be problematic, depending on the grid services provided) and *could* negatively impact system reliability.

‘Upside Energy’ is also developing a cloud-based platform, claimed to be able to manage the demand side response of over a hundred thousand devices (includ-

ing battery storage systems, EV charging points, uninterruptible power supplies (UPS) as well as heating and cooling systems) through 'advanced algorithms' and 'artificial intelligence' [160]. While detailed information on how exactly this is achieved or how well the system performs cannot be obtained at the time of writing, 'Upside Energy' is involved in several V2G projects already mentioned in earlier sections (V2Street [161], HAVEN [98] and V2GO [102]) – presumably making use of said cloud-based platform.

The 'Vehicle-to-Grid Intelligent control' or 'VIGIL' project focuses on the development of a robust communications and control platform for a large number of EVs (unfortunately unspecified) [162]. As it involves a full communication network, including with Distribution Network Operator (DNO) and Distribution System Operator (DSO) and real-time control of bidirectional V2G power flows the project must have faced very similar challenges to those addressed in this thesis. However, even though there is evidence of the recent 'successful' project completion [163] [164] [165] (May 2020) at the time of writing, no information can be found that allows any meaningful comparison between the VIGIL communications and control platform and the strategies presented in this thesis.

In [166] a V2G network is used to provide frequency regulation in a power grid with integrated renewable electricity generation while minimising costs. An EV population of 1,000 EVs was simulated, but execution times for decision-making processes have not been reported. Similarly in [167] a V2G network also provides frequency regulation but the focus lies on fairness criteria in the treatment of different EVs (fair distribution of power within the EV population). Again, execution times have not been reported. The response times required for frequency regulation can vary widely between 'milliseconds' up to 20 minutes [168], whereas primary frequency response requires energy storage systems to deliver rated power within 10 seconds [169] (similar to the system response times required for R2REE, see chapter 4). Such system response times of a few seconds or even on a sub-second time-scale can be achieved with a V2G network, however, several challenges need to be addressed [2] including:

- the size of the connected EV population on the network
- the changing aggregated energy storage potential (connected capacity, power available, SOC of EV battery packs)
- predictability of EV availability and power grid demands

- the necessity to charge EVs over time (constraining scheduling process)
- aggregator-to-EV communication delays (exacerbated by the need for encryption to address security and privacy concerns [170])
- complexity of underlying scheduling rules

In this work, these challenges are addressed via a multi-layered V2G scheduling approach that combines predictive scheduling (charge and discharge decisions are taken ahead of predictable changes in the power demand) for system responsiveness with reactive scheduling (decisions are taken in reaction to changes in power demand) to account for uncertainty/inaccuracies in the power demand predictions (see section 3.4). Uncertainty is a major challenge of a purely predictive scheduling approach whereas a purely reactive scheduling approach leads to a lag in system response.

When combining both approaches, rather than addressing uncertainties through complex stochastic programming (modelling/optimisation involving probabilities [44]), the predictive scheduling layer can ignore uncertainties and assume perfect knowledge on the EV population and the power demand. The reactive scheduling element can then account for uncertainties and refine the schedule over time (the better the initial predictive scheduling, the less interference is needed from the reactive scheduling element).

Further, unlike the scheduling strategies in existing literature (which typically just assume that accurate and up-to-date information of the state of connected EV population is readily available at the point of scheduling), the scheduling strategy presented in this thesis is fully embedded into a communication network that covers the data acquisition from individual EVs as well as the implementation of charging schedules (see chapter 3).

A rather promising development in the field of V2G has been a small number of UK-based V2G demonstration projects which are seemingly crossing the line from fundamental research towards innovation. While still far from a mass roll-out there are some early indicators for a ‘marketable’ degree of maturity in V2G technologies.

While conducting an overarching V2G market study Cenex lists 40 ongoing European V2G projects as of mid-2018 [101]. Most of these projects have already been mentioned and are either marked as ‘feasibility studies’, ‘R&D only’ or are rather small in scale and ambition. The notable exceptions, large-scale V2G

demonstrator projects shall be mentioned here. It should be noted, however, that all of these projects are still ongoing so project outcomes are not yet publically available.

The first of which, ‘PowerLoop’ [171] is a large-scale domestic V2G demonstrator project involving 135 V2G units according to [101]). It is most notable here as ‘PowerLoop’ is already offering leasing packages for Nissan Leaf EVs with V2G chargers to be purchased by consumers in the UK.

Even larger in scale is the Nissan-led ‘e4Future’ project [172] with an anticipated 1,000 V2G units [101]. This project is described as ”a large-scale V2G demonstrator, deployed in groups and controlled by an innovative aggregator platform stacking multiple services that supports a more efficient electricity system and decreases ownership costs to vehicle users. [173]” It explores using EV fleets to provide grid services such as frequency response, arbitrage, distribution services or time-shifting for energy users [173].

Finally, the ‘Sciurus’ project has the same anticipated scale of 1,000 EVs [101]. In this case, however, it focuses on domestic V2G installations to test the commercial proposition of V2G for grid balancing. EV owners interact with the system via a smartphone app and the EV population consists of Nissan Leaf EVs only [174][175].

Noteworthy in the three projects above (and in fact many other projects/papers mentioned in this chapter) is the heavy involvement of Nissan, in particular the Nissan Leaf, which seems to be the ‘go-to’ EV model for any authors discussing V2G (including the publications associated with this thesis). There are multiple reasons for this: Nissan is undoubtedly among the most successful EV manufacturers and the Leaf is one of the most common pure EVs. The Leaf is rather average in both price and battery capacity and thus serves as a good example for a ‘typical’ EV. Further, Nissan itself is investing in V2H/V2G related R&D (as partner in many of the projects mentioned here [69][172][174]).

Nissan has a strong manufacturing presence in its home market Japan, and in the UK – both countries are involved heavily in V2G research. There might be a risk of V2G becoming too closely associated, if not dependent, on a single manufacturer. Perhaps, authors/researchers should be encouraged to broaden their analysis to include a wider range of EV models and thus widen the appeal of V2G.

### 3. VEHICLE-TO-GRID AGGREGATOR CONTROL

At the centre of any V2G application is the aggregator, which manages all power flows and arbitrates between the needs of connected EVs and the power grid [61]. The control strategies employed by the aggregator can be highly different depending on the V2G application, e.g. a control strategy aimed at frequency control may lead to completely different results from a strategy aimed at an increased utilisation of nearby renewables. Further, the scale of the connected EV population can also affect aggregator control strategies – the sequencing of tasks and data management is more challenging for thousands of EVs than for just a handful. Thus, there is no single correct approach to V2G aggregator control.

Nonetheless, many of the concepts presented in this chapter are applicable to various V2G applications. The modular high-level aggregator control structure presented here was designed with large EV populations (hundreds of connected EVs) in mind. While it is perfectly capable of managing just a few EVs, some of its design aspects might be redundant in such cases. Any challenges specific to Road-to-Rail Energy Exchange, in particular rapidly changing power demands on a megawatt-scale are fully reflected within the scheduling portion of this chapter (see section 3.4). The findings of all other parts in this chapter are equally valid for other large scale V2G applications.

#### 3.1 *Modular high-level aggregator control structure*

The nature of V2G differs from most other energy storage technologies in the sense that storage capacity, as well as the power that the system can provide, varies dynamically with the number and status of the EVs connected. Depending on the application of V2G its energy storage potential might also be very difficult to predict as individual EVs may connect or disconnect from the network at any time. This is particularly the case if V2G is implemented in a public setting (as is

the case for R2REE), rather than in a limited strongly controlled environment (i.e. managing a commercial vehicle fleet with known driving schedules [72][73]).

Due to the degree of unpredictability of V2G, any aggregator control must be dynamic enough to quickly adjust to any changes in power grid demands or the availability of EV batteries. Further, aggregator control is a problem of scale. An aggregator might manage just a handful of EVs (i.e. a small local car park), or thousands of them (i.e. spread over a city). Ideally, the same aggregator control strategy could be employed for either case, rather than creating a completely new solution for every application. An ideal aggregator control might be expected to be:

- **Dynamic:** The system can quickly adapt to changes in both the EV population and the power grid.
- **Scalable:** The system can manage a wide range in numbers of connected EVs.
- **Robust:** A faulty communication route (i.e. to a single EV with malfunctioning hardware) does not “break” the whole system.
- **Computationally efficient:** The execution and sequencing of tasks is optimised to ensure low computational costs.
- **Compatible:** All parts of the V2G network comply with common hardware and software standards to ensure inter-compatibility.

Aggregator control, in the most general sense, involves three tasks: 1) data collection - collecting relevant information on connected EVs and the state of the power grid, 2) V2G scheduling - making charging and discharging decisions for each connected EV, and 3) schedule implementation – instructing EV charging hardware on schedules and, if applicable, monitoring the correct execution. All tasks are interdependent and are generally to be completed in sequence. The latter may encourage the design of a single aggregator control algorithm to fulfil every task in a single loop.

However, having a single linear process responsible for all tasks creates a number of problems. As data collection, scheduling and implementation have to happen in sequence, any delay or fault at an early stage would create a cascade of delays or other issues throughout the whole process.

For a V2G network, this may mean that, for example, a faulty (or just slow) communication between the aggregator and a single EV delays data collection for the whole car park as well as subsequent scheduling and implementation of charging/discharging decisions. For a small number of EVs on the network, such problems might not be substantial as each stage of the aggregator control requires little computational resources. On a larger scale, however, delays and faults (even if fixed quickly) can add up, significantly reducing responsiveness and robustness of the V2G network.

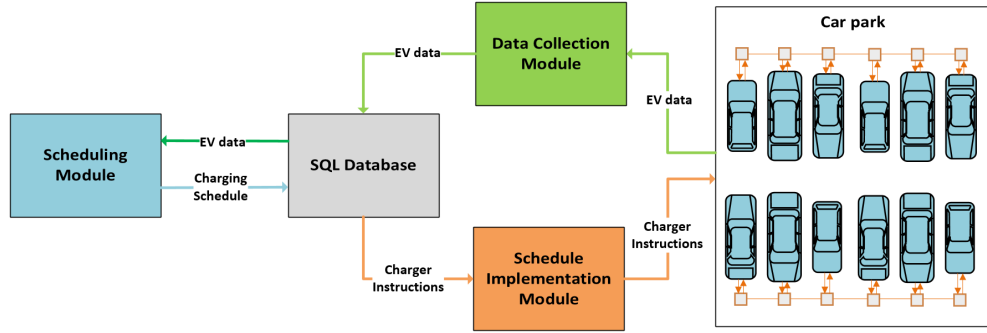


Figure 3.1: Modular aggregator control structure, one module per task - first-order modularisation

Aiming for dynamic and robust, yet scalable aggregator control, these issues can be approached by splitting up the three tasks into separate processes. Each task of the aggregator control is an ongoing recurring process. Any data collected needs to be regularly updated and schedules need to be adjusted and re-implemented. Splitting up processes allows them to reiterate independently from each other should one of them be delayed. Further, it allows distribution of the total workload over multiple processors, making the up-scaling of aggregator control easier.

Going even further and adopting an approach where these separate processes consist of interchangeable modules (see Figure 3.1) can significantly simplify V2G implementation for different grid services (e.g. frequency control vs. congestion management) or different environments (e.g. public car park vs. electric bus fleet). For example, the same 'data collection module' and 'schedule implementation module' might be compatible with different 'scheduling modules' (aimed at providing different grid services) that can be swapped as required. This separation of the fundamental aggregator control tasks is referred to as *first-order modularisation* in following discussions.

It is further possible that multiple modules are used for the same task as shown in Figure 3.2. These might be two instances of the same module sharing the workload for one task over multiple processors or modules using a different set of rules for the same task. In Figure 3.2, data collection is handled by two separate instances of the data collection module, each managing just a subset of the connected EVs. Assuming that the subsets are about equal in size and the two instances are run on separate machines, the time taken for updating all EV information is effectively halved. The same approach could be taken using multiple schedule implementation modules.

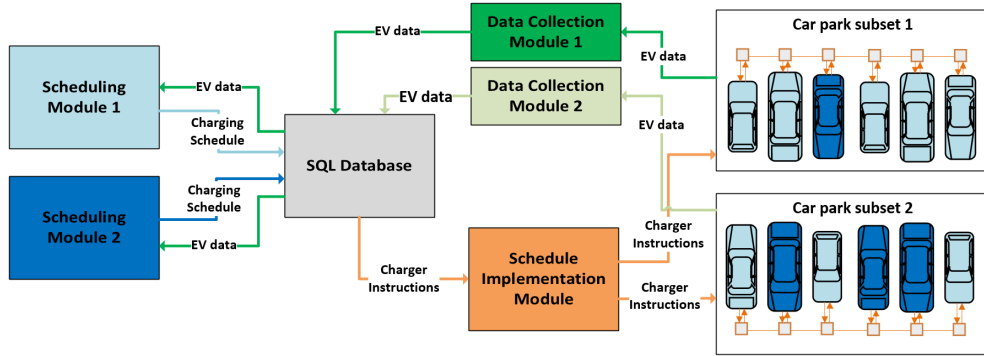


Figure 3.2: Modular aggregator control structure, multiple modules per task - second-order modularisation

Also, as shown in Figure 3.2, two separate and potentially different scheduling modules could be used on the same V2G network to provide two different grid services using two subsets of the connected EV population. For example, the bulk of connected EVs might be used to provide peak shaving services (requiring mainly energy capacity), whereas some EVs with nearly full battery packs could be used for frequency regulation services (requiring mainly power and quick system responsiveness) under a different scheduling regime. The usage of aggregator control modularisation can thereby drastically increase the versatility of a V2G network. This splitting of a single aggregator control task is hereafter referred to as *second-order modularisation*.

As will be discussed in the following sections, both first- and second-order modularisation require careful algorithm design to address new challenges such as task sequencing and data exchange between modules. One major challenge of this modular approach is to ensure inter-compatibility between various modules. In this project, this is achieved by developing each module around a mutual data



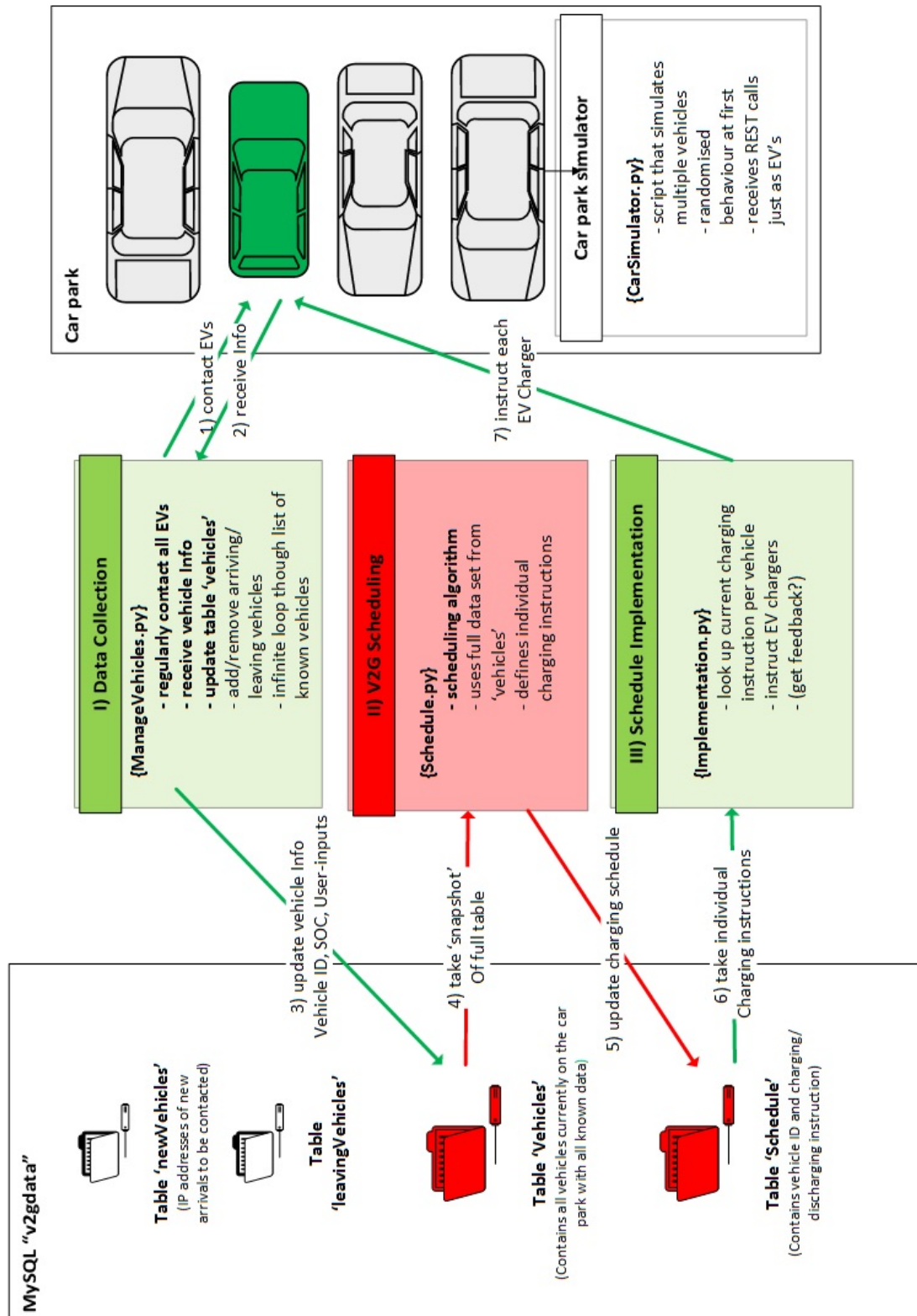


Figure 3.3: Task sequencing of aggregator control in a multi algorithm structure

storage rather than relying on direct communication between modules (which could also lead to one module 'waiting' for another). For this purpose, a shared database is used, which can be accessed and manipulated independently by each module.

However, the various modules can only be regarded as operating semi-independently due to the underlying sequencing; implementing a schedule requires the schedule to be finalised and accessible which in turn requires information from the data collection. A breakdown of the sequencing in the aggregator control is shown in Figure 3.3. As is shown in this figure, the only interaction between modules is via the mutual database. While the database is also used for data logging, its main purpose is to hold up-to-date information on all EVs currently connected to the network as well as the latest schedule information.

Hence, the database contains two main tables (other auxiliary tables exist and will be mentioned where applicable): the table 'Vehicles' contains the latest available data for each EV (one dataset each) and the table 'Schedule' contains any outstanding charging/discharging instructions. How these tables are used by the various modules is explained in the following sections. The variable definitions for each table are shown in appendix Appendix A1.

The database management system used is MySQL which is open-source, but widely used for commercial and academic purposes [176]. As the name implies, it is based on Structured Query Language (SQL). Importantly, it allows for simultaneous access by multiple computers on the same network. Thus, aggregator control is not confined to a single machine and multiple modules may run on different computers.

In summary, within this project, a modular high-level aggregator control structure is used. The fundamental tasks of the V2G aggregator (data collection, scheduling and schedule implementation) are separated via first-order modularisation. The structure further allows for multiple modules per task, defined here as second-order modularisation. Modules only communicate indirectly by accessing and manipulating a shared database. All of these design aspects could be implemented for any V2G application, but are particularly useful for managing large EV populations (especially workload sharing via second-order modularisation).

To explore the specific V2G application of Road-to-Rail Energy Exchange, the control structure shown in Figure 3.4 is used in later discussions. As shown in

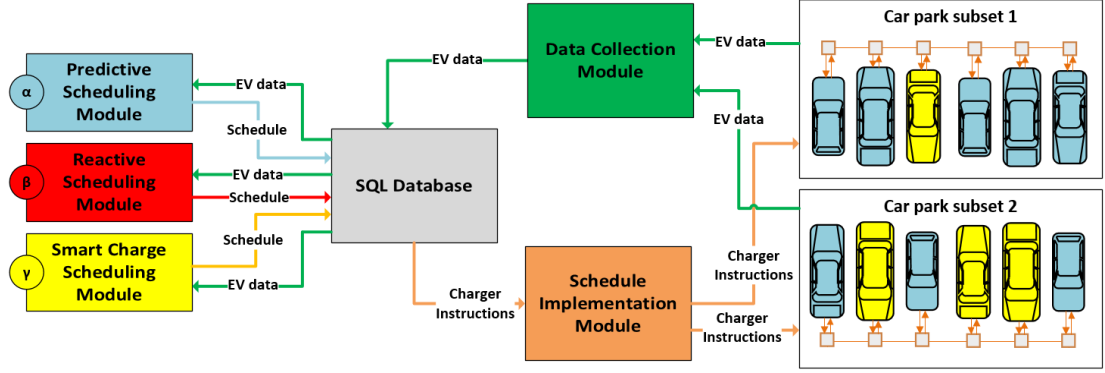


Figure 3.4: Modular aggregator control structure for Road-to-Rail Energy Exchange using multiple scheduling modules.

the figure, first-order modularisation is fully employed, but second-order modularisation is exclusive to the task of scheduling. Here, a total of three scheduling modules are featured - these do not only share the workload, but each employs entirely different scheduling rules (discussed in detail in section 3.4). Second-order modularisation for data collection and schedule implementation was found not to be necessary for the moderate size of EV populations considered in the case study in chapter 4 (up to 100 connected EVs).

### 3.2 Data Collection

The first module of the aggregator control algorithms developed in this project is responsible for monitoring the EV population that is connected to the aggregator. This means collecting data from individual vehicles and regularly updating the database. The EVs under monitoring may represent those parked in a single car park (as is assumed in chapter 4), a vehicle fleet owned by a company or even a number of EVs parked in different locations (e.g. spread out over a city). It should be noted that the location of the vehicles is not relevant for the discussion in this chapter as long as a vehicle is within the same network.

*The annotated python code for the EV monitoring algorithm can be found in appendix section A2.1.*

The scheduling routines discussed later require EV data to assess the state of each EV and to determine how each EV should be charged or discharged. This information is sourced and entered into the database following the routine in

Figure 3.5. Upon initialisation, the algorithm connects to the SQL database and opens a table called 'Vehicles' using read/write access with auto-commit (as the algorithm makes frequent changes to the table). The table 'Vehicles' contains information on every known EV currently within the network (one dataset per EV). This information includes a vehicle ID, the IP address of the EVs communication system, the battery pack capacity, the battery pack SOC, the vehicle location, charging preferences (as discussed in chapter 5) as well as the current charging/discharging instruction.

The 'Vehicles' table exists independently from the monitoring algorithm, so no data is lost when the algorithm is delayed, disrupted or shut down. The table can also be read and altered by multiple processes simultaneously. Not only does this allow for multiple instances of the monitoring algorithm simultaneously overseeing subsets of the EV population, but it is also essential for independent access by the scheduling modules. This table only contains the latest EV data - as soon as new data is available, older datasets are overwritten. While some datasets might be older for some EVs than for others (EVs are contacted sequentially), during scheduling it is assumed that any information in the database is accurate and up-to-date at the point of scheduling. The dataset for each EV on the V2G network contains the following parameters:

- **EV ID:** A unique unsigned integer value (using internal auto-increment function in SQL database) used to identify connected EVs.
- **Name:** Name of the EV (typically make & model) as string value. Not essential to the aggregator operation but simplifies later analysis.
- **IP address:** Unique IP address of the charging hardware corresponding to each EV. It is assumed that each EV has its own network connected charger (either on-board or external).
- **Capacity:** EV battery pack capacity (in kWh) as an unsigned float value.
- **SOC:** EV battery pack SOC (in %) as an unsigned float value.
- **Charging rate:** Current charging rate of this EV (in kW) as a signed float value. A negative value represents discharging of the EV battery pack.
- **Maximum charging rate:** Assumed current maximum charging rate for this EV (in kW) as an unsigned float value. The value depends on the EV's battery pack (and may change with SOC, see section 3.6) and the charging

hardware. The lower limit shall apply.

- **Maximum discharging rate:** Assumed current maximum discharging rate for this EV (in kW) as an unsigned float value. Again, the value depends on the EV's battery pack and charging hardware. The lower limit applies.
- **Event status:** Binary value to signal if this EV is currently assigned to provide grid services for an event (as described in section 3.4). A value of 1 means the EV is assigned to an event (limiting its usage for other scheduling operations). A value of 0 means the EV is not currently used for grid services and can be assigned freely during scheduling.
- **Mode:** Charging mode selected by EV user (see chapter 5) as unsigned integer. Default value is 0 (no selection made).
- **Target SOC:** Target SOC selected by EV user (in %) as an unsigned float value. Default value is 100 %.
- **Target Date/Time:** Date and time by which the target SOC shall be reached according to user selection in datetime format (YYYY-MM-DD HH:MM:SS). Default value is 0000-00-00 00:00:00.
- **Location:** EV location as string. No fixed format, but typically contains latitude, longitude and altitude coordinates sourced via Global Positioning System (GPS). Empty by default.
- **Charge Weighting (CW)\*:** An unsigned float value quantifying the EV's suitability to receive power (the higher the value, the higher the chance of this EV to be allocated to charging) - see section 3.4, Equation 3.1. Value is zero when SOC is 100 % and thus an EV cannot be charged further. Derived from other parameters and calculated within the SQL database.
- **Discharge Weighting (DCW)\*:** An unsigned float value quantifying the EV's suitability to deliver power (the higher the value, the higher the chance of this EV to be allocated to discharging) - see section 3.4, Equation 3.2. Value is zero when SOC is zero and thus an EV cannot be discharged further. Derived from other parameters and calculated within the SQL database.

After connecting to the database, the monitoring algorithm first checks for any new EVs on the network. This could be done by scanning the network for new IP

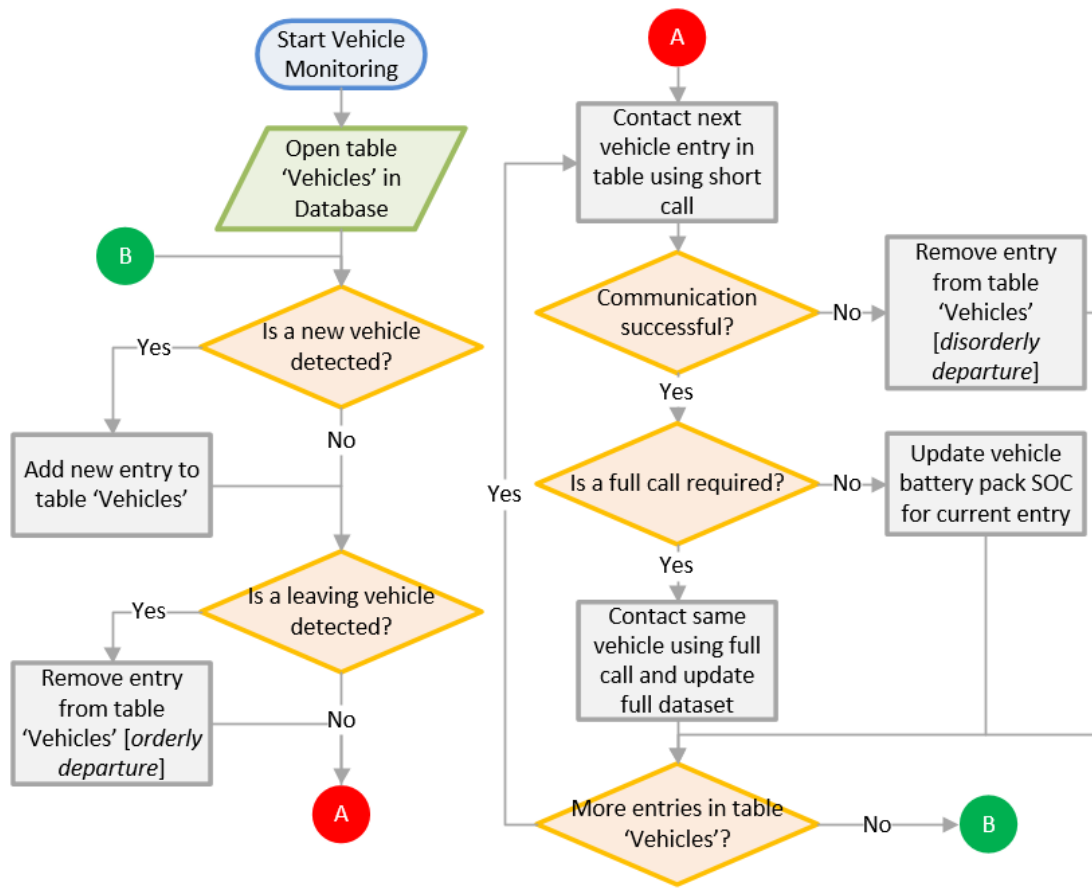


Figure 3.5: Flow diagram of the data collection module responsible for regularly updating EV data in the 'Vehicles' table in the SQL database.

addresses(\*) belonging to newly connected devices on the network. Assuming that the network is used exclusively for the purpose of V2G aggregator control and that only EVs connect to the network, any new IP address must belong to an EV. In a public setting, however, it is likely that an existing network (particularly when using Wi-Fi) would be shared with other devices (e.g. smartphones, laptops, etc.) for multimedia purposes. In such cases, a mechanism would need to be implemented to check if the newly detected IP belongs to an EV.

*\*Note: This initial check for new EVs functions slightly different for this project. The author made use of the university's campus-wide computer network for all inter-aggregator and aggregator-to-EV communication (via both car park and Wi-Fi). Looking up IP addresses on this network is not possible without admin privileges. As a regular user, the author could fully utilise the network, but any IP*

*addresses had to be sourced differently. This was remedied by using an additional table in the SQL database. This table named 'newVehicles' contains only new IP addresses. These were either entered manually for the hardware prototype (see section 3.5) or directly by the simulated EVs (see section 3.6). The downside of this approach is that each (simulated) EV had to be granted access to the SQL database to self-register. For security reasons alone, this would be totally unfeasible in a real V2G network with public access. However, within the scope of this project, this slight flaw is deemed acceptable and does not justify the extra cost of creating a dedicated network.*

If a new IP address is found by the monitoring algorithm, it is contacted and the full dataset of available information is requested (using a 'full information call' as described below). The new vehicle is assigned a unique ID (for simplicity a simple integer value incrementing by one for every new vehicle) and the dataset is added to the 'Vehicles' table. After checking for new arrivals, the monitoring algorithm similarly checks if a vehicle is leaving the network. It is assumed that a vehicle leaving the network (i.e. before disconnecting the charger) informs the aggregator. The entry of the leaving vehicle is then removed from the table 'Vehicles'. This 'orderly departure' is assumed to be the norm during operation.

In contrast, the algorithm also accounts for cases of 'disorderly departures'. This occurs when communication attempts between aggregator and an individual EV fail. Failing communication (i.e. no response or unrecognisable response to any of the monitoring algorithm's requests) triggers a number of retries and eventually the removal of the vehicle from the table 'Vehicles' as well as the shutdown of the corresponding vehicle charger (if applicable).

For simplicity, any failure to communicate successfully between EV and aggregator is treated equally regardless of the reason for failure. However, for commercial applications, a more refined approach should be used to identify and react appropriately to different causes of failed communication (a short-term loss of Wi-Fi connectivity might be a regular occurrence). Within the scope of this research, the current handling of communication failure is sufficient and mainly serves to maintain the stability of the monitoring algorithm during the long 24 hour simulations described in chapter 4. Such failures are rare and usually caused by events like a loose cable in the prototype communication hardware (see section 3.5).

After checking for new EV arrivals or departures, the monitoring algorithm begins sequentially contacting all known EVs and requesting the most recent vehi-

cle information. Aggregator-to-EV communication happens via either Ethernet or Wi-Fi connection using the REST Application Programming Interface (API) [177][178] (see section 2.4). It is set up in a master-slave configuration: the 'slave' (i.e the EV) never initiates communication, but only responds to requests by the 'master' (i.e. the aggregator). Thus, the aggregator is in full control of any communication timing and sequencing, independent of size and makeup of the connected EV population. There are three different types of information requests specifically defined for this work:

**1) All information call:** This call requests the full set of information available with annotations. It is used for debugging purposes only as the annotations are not required for aggregator-to-EV communication. The size of the response varies slightly depending on the current status of an EV but is usually around 200 bytes.

- The call takes the form: */[IP address]/info/all*
- Example request: */10.9.133.131/info/all*
- Example response (202 bytes): *"Name: Cobra; Capacity: 50; SOC: 50.00; Charging Value: 0.00; Mode: 4; Target SOC: 80; Target Date: 2019-06-24; Target Time: 12:00:00; Location: 5056.0796N, 123.5799W, 21.90; Date/Time: 23.06.2019, 13:11"*

**2) Full information call:** This call requests the full set of information available, but without annotations (reducing network traffic). The order in which information is transmitted never changes and is identical to the call above. Only, the current date and time information is not transmitted here. For efficiency, it is assumed that date and time information are in sync between the aggregator and the EVs (hence redundant). The response to this call typically has a size of around 75 bytes (over 60 % shorter than the previous call).

- The call takes the following form: */[IP address]/info/full*
- Example request: */10.9.133.131/info/full*
- Example response (74 bytes): *"Cobra;50;50.00;0.00;4;80;2019-06-24 12:00:00;5056.0796N, 123.5799W, 21.90"*



**3) Short information call:** This call leads to a response carrying only two pieces of information. One is the vehicles SOC (which changes constantly), the other one is a boolean value (True or False) indicating if any other vehicle information has changed since the last full information call (the charging rate or any user inputs regarding charging preferences). This call is used the most by the monitoring algorithm as the resulting network traffic is the lowest with a typical response size of just 10 or 11 bytes (85 % reduction over the full information call).

- The call takes the following form: *[IP address]/info/short*
- Example request: */10.9.133.131/info/short*
- Example response (11 bytes): *"False;50.00"*

The first time that an EV is contacted in each loop, only the 'short information call' is used. This allows updating the EV's frequently changing battery pack SOC. If the EV's response contains the boolean 'False', the algorithm knows that no other parameters of the vehicle information have changed since the last update. In case the EV response reads 'True', the monitoring algorithm knows that a full information call is required to update the full dataset held on this EV. After a vehicle entry in the database is updated, the algorithm proceeds to contact the next EV in the table (sorted by the assigned vehicle ID in ascending order).

Once every dataset is updated, the algorithm reiterates the main loop, checking for arriving and leaving vehicles then updating all EV information again. It should be noted that this algorithm does not have an end state of any sort, but repeats until shut down manually. The time taken for each loop strongly depends on the number of EVs on the network.

### 3.3 Schedule Implementation

This module of the aggregator control algorithm is used to implement any decisions taken during the scheduling. This algorithm is structured similarly to that used for data collection, although the data-flow direction is reversed. It uses information already in the SQL database as inputs and transmits it to EVs on the network.

*The annotated python code for the schedule implementation algorithm can be found in appendix section A2.2.*

Upon initialisation of this algorithm (see Figure 3.6), it connects to the SQL database and opens the table 'Schedule' (read access only). The schedule is a list of charging instructions, or orders, that are fed into the SQL database by the scheduling module(s) (see section 3.4). Each order represents the instruction to change the charging rate of a specific EV (or rather a specific IP address) to a given kW value at a given time. The SQL table 'Schedule' contains all orders in the format outlined below.

- **Order ID:** A unique integer value (using internal auto-increment database function) used to identify orders should the schedule be subject to revisions.
- **Execution time:** Time at which this order is to be implemented in the datetime format. It is assumed that all devices on the network are synced following the universal coordinated time (UTC) time standard.
- **IP address:** Unique IP address of the EV/charging hardware to receive the order.
- **Charging rate:** Anticipated charging rate (in kW) as a signed float value. A negative value represents an instruction to discharge the EV battery pack at the given rate.
- **Order status:** Data string used for schedule implementation/revision. If empty, this order is not yet due for execution and could be revised/cancelled if necessary. If 'queued', this order has already been loaded by the (or one of multiple) implementation module(s) and is about to be executed - this order cannot be altered to avoid contradictory instructions and race errors (changing algorithm behaviour depending on the order in which sub-routines are executed [179]). If 'cancelled', this order was revised by subsequent scheduling and will not be executed.

Entries in the 'Schedule' table may have execution times that lie up to a few minutes in the future (see predictive scheduling in section 3.4) and may still be subject to revision. To allow for such revisions by the scheduling module(s), the implementation algorithm only loads and queues orders with an execution time no further than 3 seconds in the future (this value might be adjusted for other applications, but 3 seconds was found to be sufficient to ensure timely implementation but not too long to constrain schedule revisions). Unfulfilled orders with execution times in the past are loaded regardless (and consequently implemented with delay). Such orders might exist if the scheduling process has

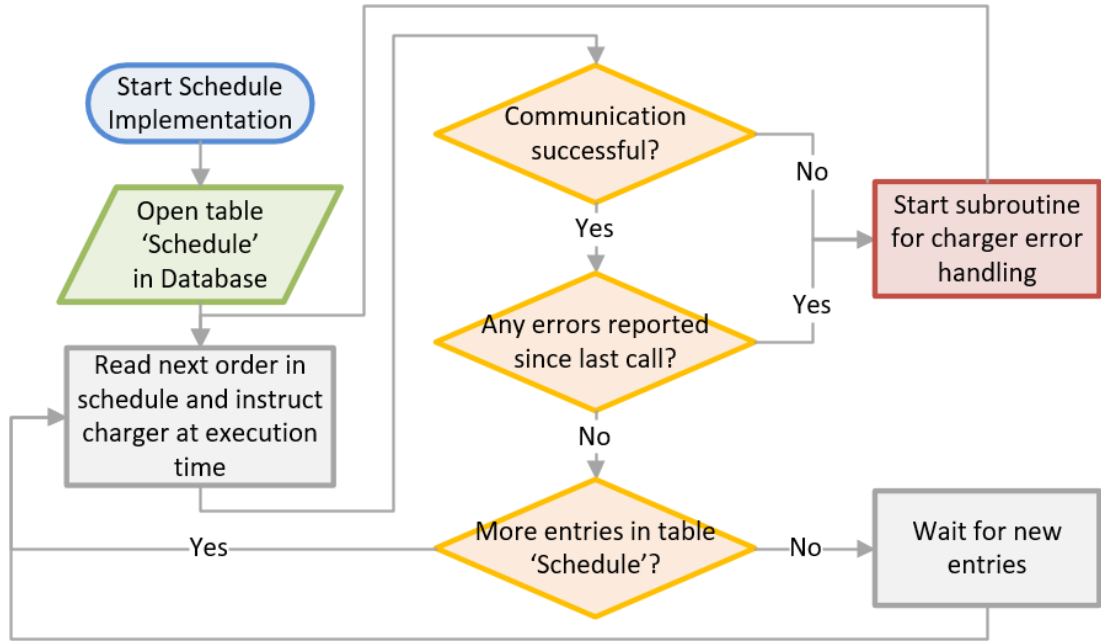


Figure 3.6: Flow diagram of the schedule implementation module responsible for implementing charging & discharging instructions from the 'Schedule' table in the SQL database.

been delayed or took too long to execute for any reason. While this should not happen during normal operation, this handling of outdated orders aids the robustness of the aggregator control (implementing an order too late is assumed to be better than not implementing it).

Queued orders are being processed once the execution time is reached or exceeded. Again, aggregator-to-EV communication uses either Ethernet or Wi-Fi connections and the REST API in a master-slave configuration. The implementation algorithm contacts the IP addresses of the EVs/charging hardware associated with each order using a charge REST request. These requests are in the format: */[IP address]/charge/[start or stop charging]/[charging power in kW]*. Three example REST requests are shown below. The EV communication prototype (see section 3.5), as well as any EVs simulated in this project (see section 3.6) respond to any charging requests as shown, the response format has no relevance for the schedule implementation.

1) Example REST request to start charging an EV with the local IP address of 10.9.133.131 at a rate of 10 kW:

- Example request: */10.9.133.131/charge/1/10*
- Example response (37 bytes) *"charging activated, level set to 10 kW"*

2) Example REST request to start discharging the same EV at a rate of 7.5 kW:

- Example request: */10.9.133.131/charge/1/-7.5*
- Example response (39 bytes) *"charging activated, level set to -7.5 kW"*

3) Example REST request to stop charging the same EV:

- Example request: */10.9.133.131/charge/0/00*
- Example response (20 bytes) *"charging deactivated"*

### 3.4 V2G Scheduling

V2G scheduling describes the process by which the aggregator in a V2G network creates the schedule - i.e. the list of charging decisions for each connected EV (the format of the schedule has been defined in the previous section). Usually, V2G scheduling algorithms have to consider two sides: the power grid and the EV population being managed. The requirements of both sides need to be satisfied to perform a given grid service and simultaneously ensure EVs are sufficiently charged for mobility purposes.

The Road-to-Rail Energy Exchange concept explored in this project (see Figure 3.7) is different as a third party - the rail system - has to be considered as well. Thus, the aggregator needs to arbitrate between three distinct parties:

1. **EVs owners:** the EVs being parked locally and connected to the charging infrastructure are generally expected to receive net power while being parked and leave with a higher SOC than on arrival. This has to be the default assumption unless charging preferences stated by the EV owner (see chapter 5) allow deviation from this rule (possible if there is sufficient financial incentive for EV owners to participate, see section 2.3). V2G scheduling

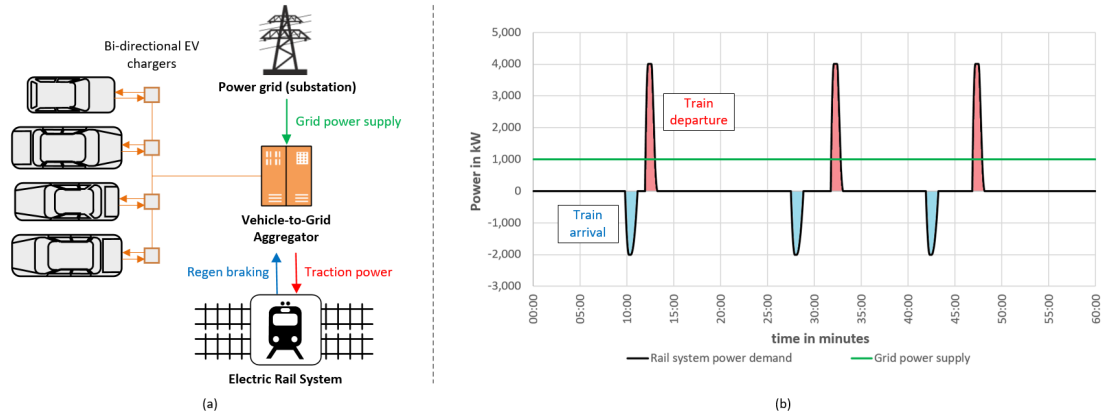


Figure 3.7: (a) V2G for support of local electric rail systems, system overview and power flows: EV population acts as buffer between the grid connection and the fluctuating rail system power demands to ensure steady power flow from the grid; (b) Rail system power demand over one hour (3 trains arriving/departing sequentially, varying dwell time): traction power drawn for train acceleration - positive/red, power supplied from regenerative braking - negative/blue.

should ensure that connected EVs, over time, receive more energy than they supply.

2. **Rail system:** the rail system has a highly variable power demand with many peaks as well as periods of low demand. As a resting electric train starts to accelerate, the traction power demand surges to a few megawatts in a matter of seconds (see chapter 4). If brake energy recovery is used, the opposite is true and a power surplus (also on a megawatt-scale) quickly has to be dissipated upon train arrival.
3. **Power grid:** the grid provides power to both, the EV population and the rail system. As the grid has to constantly balance power supply and demand (to maintain a steady grid frequency of around 50 Hz) fluctuations in power demand should be avoided. Hence, it is beneficial to decouple the variable power demands of the rail system from the power grid by using the V2G network as a buffer.

### 3.4.1 Pre-scheduling EV suitability assessment

For V2G scheduling, the aggregator has to assess which of the connected EVs are suitable to either receive or supply power as electric trains are arriving or leaving the station respectively. Not all EVs may be treated equally, as some are more useful to the aggregator than others - this is assessed using the EV data from the SQL database.

This project uses a scoring system in which each EV is assigned two weighting parameters: The first, the Charge Weighting (CW) quantifies, from an aggregator point of view, the EVs suitability to receive power (the higher the value, the higher the chance of this EV to be allocated to charging). The second parameter, the Discharge Weighting (DCW) quantifies its suitability to deliver power (the higher the value, the higher the chance of this EV to be allocated to discharging).

When power has to be fed into the car park, EVs are particularly useful to the aggregator when:

- Battery pack SOC is low: meaning the EV can store a lot of energy (relative to its overall capacity) and the need to charge the EV is high. Hence, a low SOC results in a high CW.
- Battery pack capacity is high: meaning the EV can store a lot of energy overall and could be charged for a long period of time. Hence, high capacity results in a high CW.
- Maximum charging rate is high: meaning the EV can accept a relatively high share of the power being fed into the car park. Hence, a high maximum charging rate results in a high CW.

Similarly, when power has to be supplied by the car park, EVs are particularly useful to the aggregator when:

- Battery pack SOC is high: meaning the EV can provide a lot of energy (relative to its overall capacity) and the need to charge the EV is relatively low. Hence, a high SOC results in a high DCW.
- Battery pack capacity is high: meaning the EV can provide a lot of energy overall and could be discharged for a long period of time. Hence, high capacity results in a high DCW.
- Maximum discharging rate is high: meaning the EV can provide a relatively

high share of the power required. Hence, a high maximum discharging rate results in a high DCW.

Additional factors determining the usefulness of an EV to the aggregator may exist and the underlying functions used to evaluate CW and DCW can be very different depending on the specific application. In chapter 5 CW and DCW further depend on charging preferences of EV owners. However, for the base case scheduling process, only the three factors above are taken into account and carry equal weight.

It should be noted, that both weightings, CW and DCW, scale with capacity and maximum charge/discharge rate. As the aggregator treats EVs as energy storage, this is to be expected as both, high capacity and high power are generally positive characteristics in most energy storage applications. In practice, a high capacity EV with high charge/discharge rates is more useful for V2G applications than a low capacity PHEV with lower charge/discharge rates. For the scope of this chapter CW and DCW are defined as:

$$CW = (100 - SOC) * \frac{Capacity}{Base\ Capacity} * \frac{Max\ Charging\ Rate}{Base\ Power\ Rating} \quad (3.1)$$

$$DCW = SOC * \frac{Capacity}{Base\ Capacity} * \frac{Max\ Discharging\ Rate}{Base\ Power\ Rating} \quad (3.2)$$

Base Capacity and Base Power Rating are chosen to be 1 kWh and 1 kW respectively. CW and DCW are used by the scheduling modules to determine which EVs are given priority when assigning them for charging or discharging. Thus, the absolute values of CW and DCW are of little importance, and only meaningful when compared with those of other EVs on the network. Within the aggregator control, the determination of CW and DCW is implemented using SQL triggers within the database (see section 5.4). An SQL trigger is a pre-defined stored procedure in an SQL database that is executed automatically when a relevant dataset is manipulated. The trigger condition might be the insertion of a new data entry, the deletion of an existing entry or an update to an existing entry.

In this case, the SQL database is set up to update CW and DCW whenever the corresponding EV dataset is updated by the data collection module. The main advantage of calculating this within the database, rather than during the

actual scheduling process is a reduction in computational complexity of the time-sensitive scheduling process. Instead, the often idling computational resources of the database server are used.

### 3.4.2 Multi-layer event-based V2G scheduling

As was shown in chapter 2, V2G scheduling can happen in a reactive fashion, where the aggregator simply reacts to changes in power demand or the EV population after they occur, or it may be approached by trying to predict these changes beforehand and preparing a suitable network response. Both approaches have disadvantages: A purely reactive scheduling approach always leads to a lag in system response, while predictive scheduling is prone to suboptimal decision-making due to uncertainty.

In R2REE, the rapid multi-megawatt spikes in power demand for train arrival or departure require a fast system response, ideally on a sub-second level - yet, coordinating large EV populations takes time, making a purely reactive scheduling approach difficult. A predictive scheduling approach might be feasible as the timing and magnitude of the rail system's power demand are predictable due to a timetabled train operation and ongoing tracking. However, a purely predictive scheduling approach relies on the accuracy of its predictive capabilities and lacks the ability to adjust to unforeseen developments. Some uncertainty within the EV population (e.g. one in a few hundred connected EVs suddenly disconnecting) may be insignificant due to scale, but uncertainty on the rail side (e.g. a sudden unexpected braking manoeuvre) could threaten system stability.

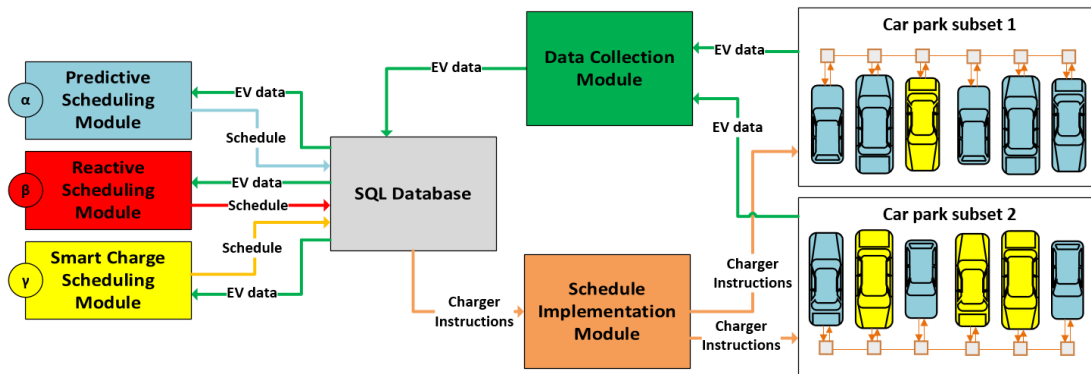


Figure 3.8: Modular aggregator control structure using multiple independent scheduling modules.



To mitigate the disadvantages of each approach, predictive and reactive scheduling are used alongside each other in this project. When combined, the predictive scheduling element can ignore uncertainties and assume perfect knowledge on the connected EV population (rather than using complex stochastic programming involving modelling/optimisation of uncertainties and probabilities). The reactive scheduling element can then account for uncertainties and refine the schedule over time (the better the initial predictive scheduling, the less interference is needed from the reactive scheduling element). This combined approach is realised by using multiple scheduling algorithm layers within the modular aggregator control structure (shown in Figure 3.8).

The predictive element makes use of the repetitive nature of the rail system power demands. Departures or arrivals of trains with known type and speed pattern can be regarded as reoccurring events. Such patterns on the power demand side can be exploited to enable dynamic fast-response V2G scheduling using multi-layer event-based scheduling.

Within this project, an event is defined as either the arrival or the departure of a single electric train at a train station (train type and speed pattern are known). The underlying assumption is that two similar events, for example, two identical trains accelerating at the same rate will result in similar power demands over time - irrespective of when each event takes place. It is further assumed, that each event has a known beginning and end time when predictive scheduling takes place (i.e. the time at which a train moves out of the V2G network's range and into the next track section supplied by another substation).

Multiple events may take place simultaneously so the power demands may stack or, partially, cancel each other out (as exploited where dwell-time optimisation is employed [180]). For further discussion, two events are defined as 'co-active' when either, both require power flow from the EV car park (i.e. both departing trains) or both require power flow into the car park (i.e. both arriving trains). In contrast, two events are defined as 'counter-active' when one event has a positive power demand and the other one a negative power demand (i.e. one train departing, one train arriving).

The power demand profile of any event depends heavily on the train type and the speed pattern (see chapter 4). For the discussion in this chapter, the highly simplified power demand curves shown in Figure 3.9 are used. On a typical rail system, we can expect busy periods with many train arrival or departure

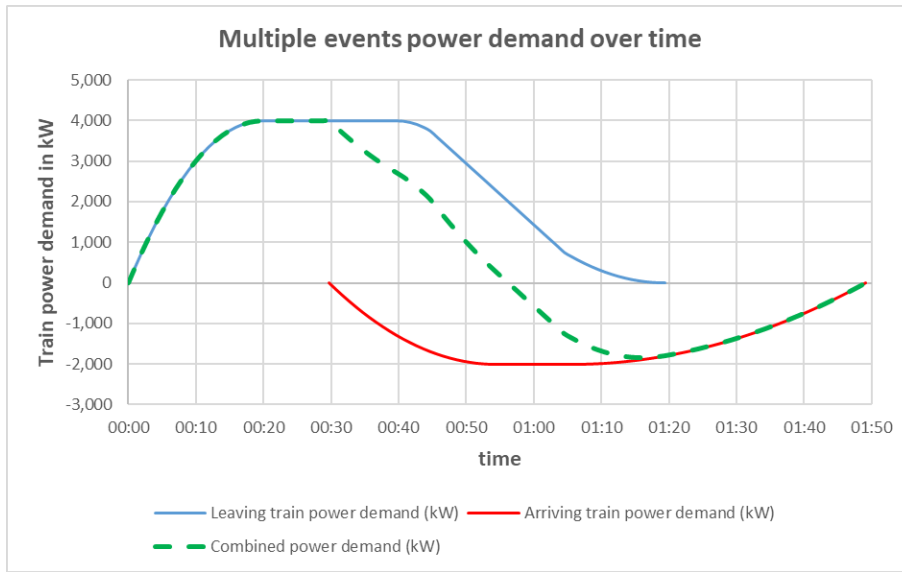


Figure 3.9: Combined effects to two stacked 'counter-events' on the rail station power demand

events as well as calmer ones in which no events take place. To account for this, the multi-layer scheduling approach can differentiate between in-event periods (during which an event is ongoing) and non-event periods where no events are happening and different scheduling rules may apply, see Figure 3.10.

The predictive element is only relevant during in-event periods, although the corresponding scheduling layer is executed shortly before an event occurs. To account for any uncertainties, a separate reactive scheduling layer is active at all times to fix any mismatch between the anticipated and the actual aggregated power flow between EV population and rail system. During non-event periods, there are no power demands from the rail system. Hence the aggregator can use this time purely to charge connected EVs. For this purpose, a separate scheduling layer for smart charging is employed.

These three layers are presented in the following subsections. The overarching control over how and when these layers are engaged follows the routine shown in Figure 3.11. For simplification, all the following discussion assumes that all connected EVs are forced to participate in the V2G operation (i.e. no opt-outs allowed).

*The annotated python code for each scheduling layer can be found in appendices*

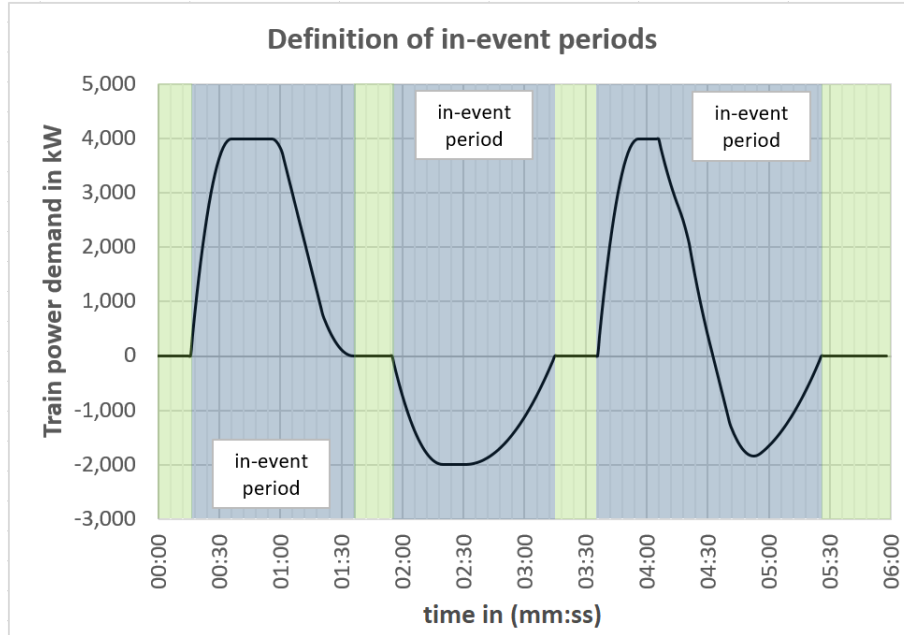


Figure 3.10: Visualisation of in-event (blue) and out-of-event (green) periods for a sequence of events (left to right: single train accelerating, single train braking, train accelerating while another is braking).

section A2.3, section A2.4 and section A2.5.

### 3.4.3 Predictive scheduling for in-event periods, first layer

The first scheduling layer is responsible for managing the V2G network's response to events occurring in the near future (i.e. in a few seconds). It creates the schedule for the whole duration of an anticipated event before its occurrence. This layer can be initialised once the starting time of the event is known. For this purpose, the algorithm (see Figure 3.12) regularly checks the train schedule in the database for any entries within the next 10 seconds. This value was chosen as it is 1) long enough to allow scheduling and subsequent schedule implementation (see Table 3.1) and 2) not so long as to expect any major delays on rail network (typical timescale between a train closing its doors and its actual departure). It is important to note that this train schedule is not identical to the fixed, published train schedules that show anticipated departure times. These cannot be relied upon as delays and changes to train schedules are still a source of uncertainty. Instead the entries on train departure and arrival times in the database must be updated regularly and be up-to-date at the point of scheduling.

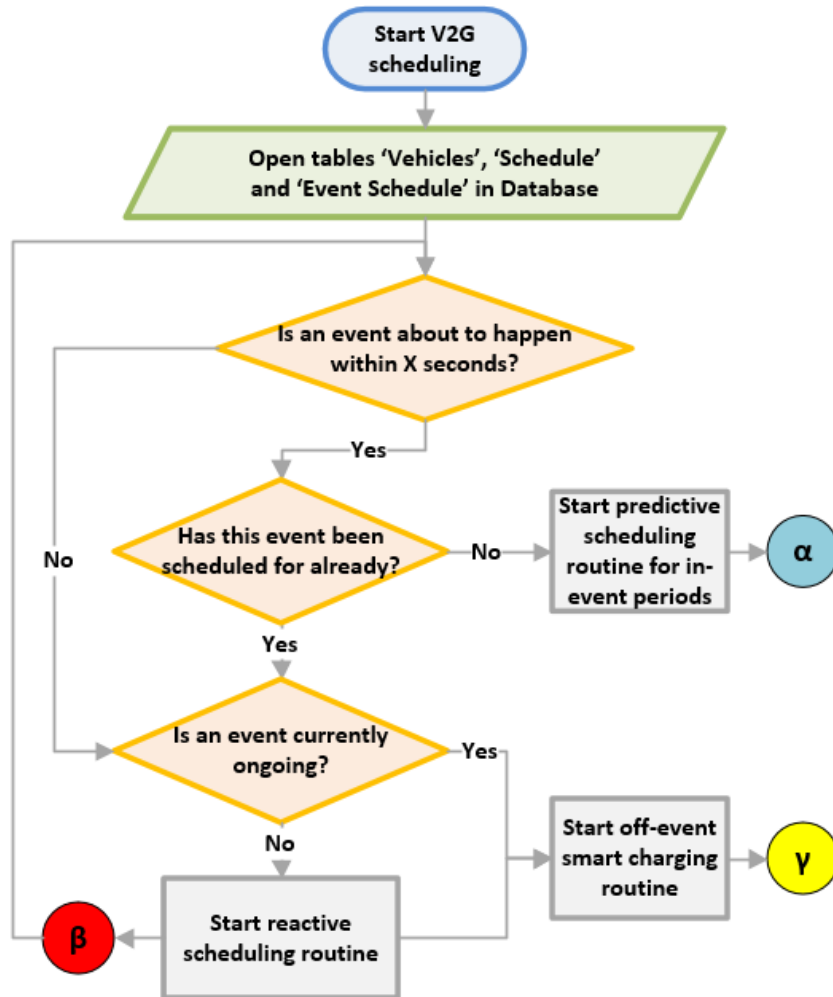


Figure 3.11: Three layer scheduling, top-level control routine: node  $\alpha$  leads to Figure 3.12, node  $\beta$  to Figure 3.13 and node  $\gamma$  to Figure 3.14

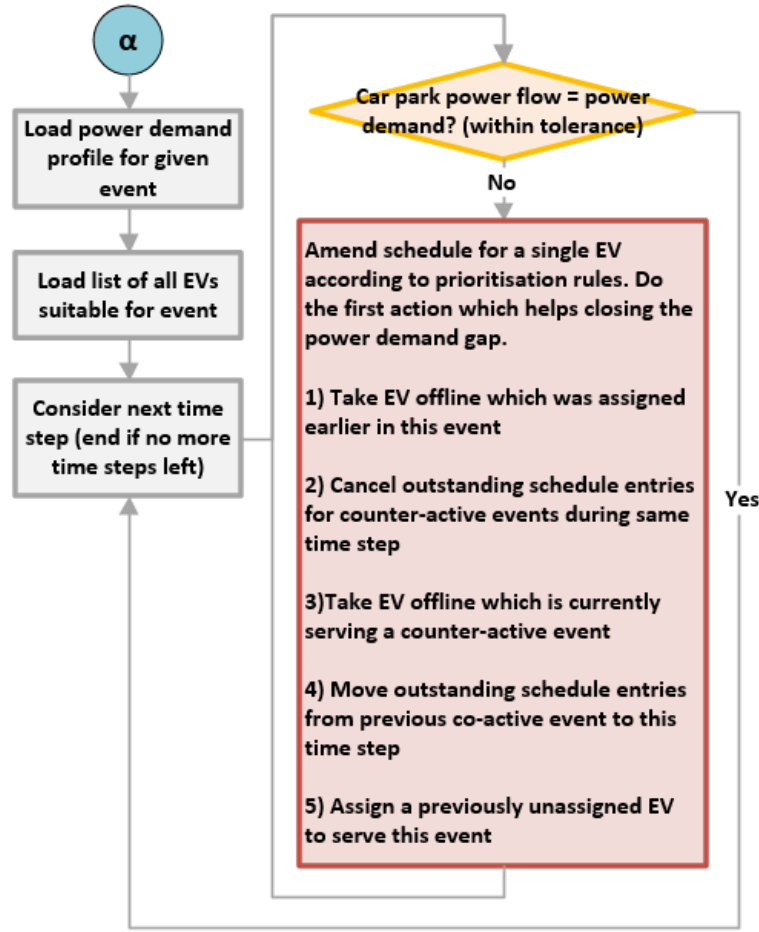


Figure 3.12: Predictive scheduling layer flow diagram

Within this work it is assumed that railway signalling systems and tracking of trains ensure predictive capability in the short term (the position of trains on the rail network is continuously monitored). While this is not always the case yet, positional tracking is commonly used as part of Positive Train Control (PTC) systems [181] and might utilise GPS (Global Positioning System) [182][183] or alternative systems such as the Galileo satellite navigation system [182]. Consequently, departure/arrival times are assumed to be known at least 10 seconds beforehand, which is when this algorithm is initialised.

For example, if a train of known type is delayed and expected to depart at 12:05:30 ( $t$ ) the scheduling algorithm identifies the event and initiates scheduling at 12:05:20 ( $t-10s$ ) - this is still true if said train was originally scheduled to

depart at 12:00:00 as long as the expected departure time has been updated in time.

Once an event is identified to begin within 10 seconds, the algorithm loads the corresponding power demand profile (power demand versus time) into memory. This demand profile depends on train type and speed profile but is pre-determined (based on the assumption of repetitive events) and hard-coded into the algorithm. Next, all relevant EV data is obtained from the network-wide mutual SQL database (IP address, maximum charge/discharge rate, current charge/discharge rate, CW/DCW). For train departure events, EV data is sorted by DCW from high to low so that the most suitable EVs are assigned first. Similarly, for train arrival events EV data is sorted by CW from high to low - EVs with a CW of zero (signalling full battery) are completely ignored.

Next the algorithm iterates through each time step in the power demand curve. The temporal resolution is a major factor determining computational complexity of this layer as it determines how often the main loop shown in Figure 3.12 is executed. This project uses one second time steps. Shorter time steps could be used for more refined scheduling, but at the expense of increased computational cost.

Assuming only one event is happening at the time of execution, the algorithm will sequentially assign EVs to charge/discharge at maximum rate (to reduce the number of EVs per timestep and hence the necessary communication attempts) in order to match the change in power demand between each time step. Further, assigned EVs are marked as 'busy' in the mutual database (set 'Event Status' to 1) to prevent conflicting instructions being given by another scheduling algorithm. As the event comes to an end and power demands decrease, these EVs are set to return to their previous charge/discharge rates. As a result, for each EV being used in an event two new charging instructions are added to the schedule table.

In more complicated cases where multiple events overlap, this scheduling layer also has to consider previous schedule entries. Each event is being scheduled without consideration of future events. Consequently, schedule entries from a previous event that is still ongoing may contradict and interfere with the event currently being scheduled. The predictive scheduling layer is designed to correct previous schedule entries if applicable before assigning new EVs. This avoids situations where a subset of the EV population is being discharged to support a

departing train while another subset is simultaneously being charged to accept power from an arriving train.

Thus any available actions to minimise the mismatch between power demand and power flow from the EV car park are prioritised in the following order:

1. Take any EVs offline (return to pre-event charging rate) that were assigned in this event. This is the top priority to ensure that every EV assignment is reversed as the event comes to an end.
2. Cancel any outstanding charge/discharge orders scheduled for this time step to serve counter-event. This revision of a previous schedule prevents conflicting charging instructions from being executed in the future. Only possible for an order not yet queued by the implementation module(s).
3. Take any EVs offline that are already charging/discharging at this time step to serve counter-event. This schedule revision moves forward the execution time of an already planned order to end an EV assignment.
4. Move orders from any previous co-active event forward/backward in time. This revision leads to an already planned EV assignment to be executed earlier or cancelled later. Only the extra time period of the EV's assignment is counted towards the current event.
5. Assign an EV that is not currently serving any event to charge/discharge at maximum rate. Only when no useful revisions of previous scheduling decisions are available are additional EVs being assigned.
6. If there is still a power gap, the current population of EVs cannot fully serve the event as not enough suitable EVs are available. Previous assignments are still valid and the scheduling algorithm will still try to meet demands as far as possible for subsequent time steps.

#### 3.4.4 *Reactive scheduling for schedule refinement, second layer*

The second scheduling layer is a reactive one continuously implementing minor corrections in real-time to ensure the power flow into/out of the EV car park matches the rails system's power demand (within a given tolerance, here a value of 5 kW is being used as tolerance). The corresponding algorithm routine is shown in Figure 3.13. Corrections may be necessary due to uncertainty at the time of the predictive schedule creation (e.g. EV data may be outdated, an EV

might have unexpectedly disconnected in the meantime, the power demand may differ from the initial predictions, etc.).

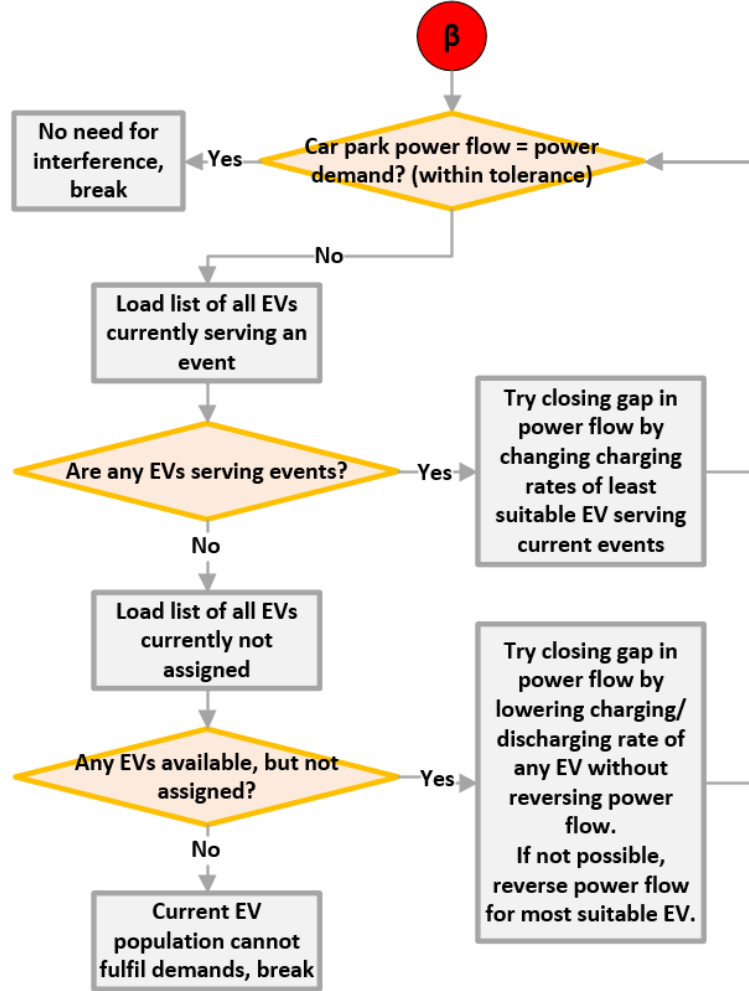


Figure 3.13: Reactive scheduling layer flow diagram

In contrast to the first layer, the second one does not follow fixed time steps, but instead loops continuously (the temporal resolution does not determine execution times but rather depends on them). Further, this layer is capable of assigning charging rates other than an EVs respective maximum charging or discharging rate at the time of scheduling (if a lower rate for a single EV is enough to close the gap between power demand and supply). This gives it the ability for finer adjustments to the power flow into and out of the EV population. Revisions to the existing charging schedule or new charging instructions are fed into the database to be executed by the implementation module.



As was the case in the first layer, the size of the EV population impacts computational complexity through the size of the dataset being manipulated. However, any schedule revision only takes place if the mismatch between car park power flow and application power demand exceeds the stated tolerance (see Figure 3.13). It follows that computational complexity of this second layer is dependent on the accuracy of the preceding predictive scheduling. If the predicted power demand in the previous layer matches the actual power demand (and no active EVs have suddenly disconnected since) the reactive layer will not interfere (hence, no need for further communication with database to load EV data or manipulate the existing schedule).

#### 3.4.5 Scheduling for non-event periods (smart charging), third layer

The third scheduling layer applies a different set of rules outside of events. Depending on the V2G application these rules may differ. Considering the electric rail support, this layer is used as a smart charging scheduler. This is necessary as the rules of the other scheduling layers inevitably lead to a situation where, on average, more power is drawn from the EV population during events than is supplied to the EVs (arriving trains are expected to supply significantly less energy from regenerative braking than they require for acceleration - around a third of the traction energy according to [184]). However, the aggregator is responsible for ensuring EVs are sufficiently charged for mobility purposes and must (at least over time) receive a net charge.

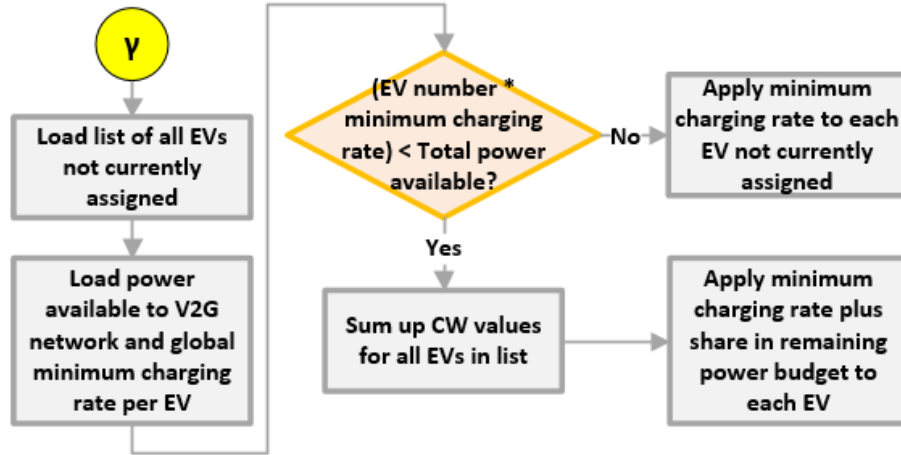


Figure 3.14: Smart charging scheduling layer flow diagram

A flow diagram describing the smart charging algorithm routine is shown in Figure

3.14. This layer requires two additional parameters (both of which may change throughout the day): a minimum charging rate per EV and an optimal total power flow from the grid (the power drawn by the EV car park plus train station through a shared grid connection). Both values are obtained from the database and have to be chosen based on car park size and V2G application. Ideally, the minimum charging rate on its own is sufficient to ensure EVs are being charged over time.

The algorithm is designed to make full use of the power available to the EV car park. Individual EVs are assigned the minimum charging rate plus a share of the remaining power available that is proportional to each EV's CW value (up to the maximum charging rate of each EV). The higher the CW, the more power is being allocated. The computational cost of this algorithm depends mainly on the size of the connected EV population. As decisions are based on the pre-assigned CW scores of EVs no in-depth analysis of EVs is required.

As this layer operates in non-event periods where system wide power flows only change gradually and system responsiveness is less significant, computational cost are not a major concern. Therefore alternative, more complex smart charging algorithms may be employed instead (taking into account additional factors such as EV battery degradation [154][159] or fairness criteria[167]).

#### *3.4.6 Interaction between predictive and reactive scheduling layers*

In order to analyse the behaviour of the scheduling algorithms presented, the same combination of events (e.g. a train departure followed by a train arrival 30 seconds later) are scheduled and simulated using A) only predictive scheduling and B) only reactive scheduling. Finally, the same event combination (altered with a braking manoeuvre unknown to the predictive layer) is being scheduled for using C) combined predictive and reactive scheduling.

The scheduling algorithms have been tested using two desktop PCs connected to the same computer network via Ethernet connection. The computer network is not a dedicated one so traffic outside of the authors' control can have a minor impact on the results reported. All aggregator control algorithms (data collection, scheduling, schedule implementation) were handled on a machine equipped with an Intel Core i5-2400 Central Processing Unit (CPU) (4x3.1 GHz) and 4 gigabyte DDR3 Random Access Memory (RAM). The memory usage was carefully monitored to ensure algorithm execution is not 'bottlenecked' and slowed

down by a lack of memory (typically around 70 % of memory was in use during operation).

The EV population was simulated on another machine equipped with an Intel Core i5-4590 CPU (4x3.3 GHz) and 16 gigabyte DDR3 RAM. Available memory is the major restriction for the number of EVs that can be simulated (typically around 90 to 95 % of the available RAM is reserved while simulating 1,000 EVs).

Each simulated EV has a unique IP address and network port combination so that aggregator-to-EV communication via the REST API realistically mirrors the communication delays that could be expected on a network with a real EV population. It was found that data collection (requesting information from an EV, receiving information and storing it in the database) as well as schedule implementation (retrieving charging instructions from the database, submitting instructions to EV charger and receiving confirmation) each take about 15 milliseconds per EV using an Ethernet connection (see Appendix A3).

### **Predictive scheduling only**

Initially, only the predictive scheduling layer is being tested (i.e. the reactive layer is not enabled). The predictive layer is set up to begin scheduling 10 seconds before an event begins and to create the schedule for the whole duration of an event in 1 second time steps. The execution times for this layer (time passed between the program initialisation and the schedule for a single event being fully passed onto the database) vary significantly with the number of EVs on the network (see Table 3.1).

The relationship between execution time and number of EVs on the network is non-linear as for each time step the algorithm stops when a solution is reached or no more EVs are available. This means that for a low number of EVs, the scheduling process may be fast, but the power demand may not have been met. Similarly, for a large number of EVs, solutions might be reached with less EVs than available and the execution times only increase as more EV data had been loaded into memory from the database.

It should be noted that even the longest execution time reported in Table 3.1 with 1.82 seconds remains well below the 10 seconds made available to the algorithm before the beginning of the event. Thus the predictive scheduling could take place closer to the beginning of an event (which might lead to less uncertainty

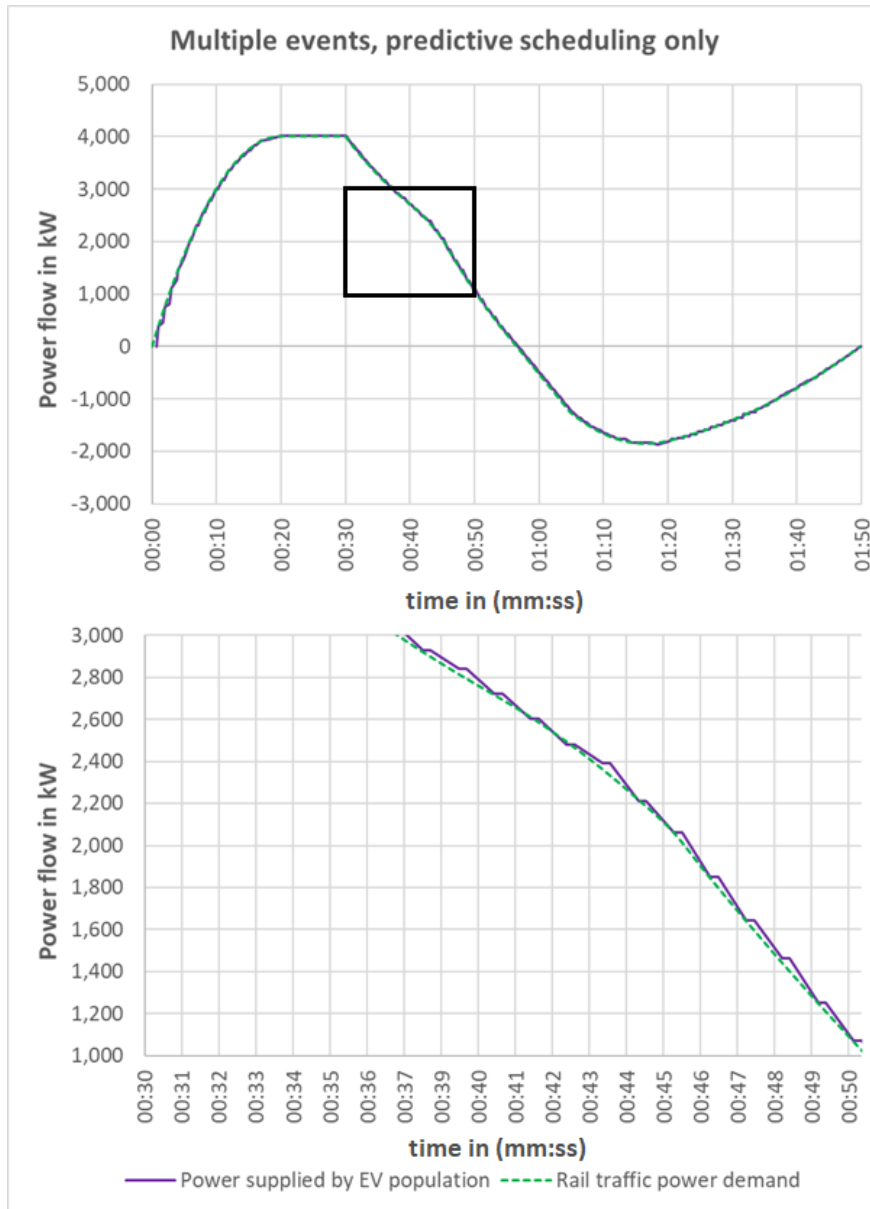


Figure 3.15: Simulated V2G network response to two counter-active events (one train departing at 0 seconds, one train arriving at 30 seconds) using predictive scheduling only

at the point of scheduling) or the time available could be used for more complex scheduling (smaller time steps, more complex scheduling rules, smaller increments in charging rates assigned per EV, etc.).

Number of EVs	Min. time (s)	Average time (s)	Max. time (s)
50	0.007	0.034	0.496
100	0.011	0.353	0.765
200	0.147	0.527	0.844
500	0.328	0.649	1.141
1000	0.469	0.837	1.820

*Table 3.1:* Execution times for predictive scheduling algorithm for varying number of connected EVs (over 1,000 scheduling cycles)

Figure 3.15 shows the V2G network response to the two counter-active events for a connected EV population of 500 simulated EVs. The rail traffic power demand over time represents an input to the scheduling process. The network response is represented by the sum of all individual EV power flows over time. This sum changes whenever a new charging/discharging instruction is being sent to an EV by the schedule implementation modules (i.e. when the V2G aggregator is taking action in response to a change in power demand).

For the purely predictive scheduling approach, the simulations show that the power supplied by the EV population closely matches the rail power demand and without significant delay. Delays are being avoided here as the schedule has been entered into the database and made available to the schedule implementation algorithm well in advance (10 seconds minus execution time for scheduling). Minor mismatches in power supply and demand exist due to the predictive layer's limitation of assigning EVs at maximum charging or discharging rate.

However, it must be noted that the predictive scheduling only followed the predicted power demand curves defined for departing or arriving trains. Any noise or deviation from these predictions on the power system have not been part of the simulation, thus the initial prediction was in fact a perfect one within this simulation (deviation in power demand from the initial prediction will be addressed when combining predictive and reactive scheduling below).

### **Reactive scheduling only**

Similar to the previous test, the reactive scheduling layer has been tested by scheduling for the same event combination while the predictive layer has been disabled. The results are shown in Figure 3.16 (an identical simulated EV population of 500 EVs has been used). The figure shows that the V2G network

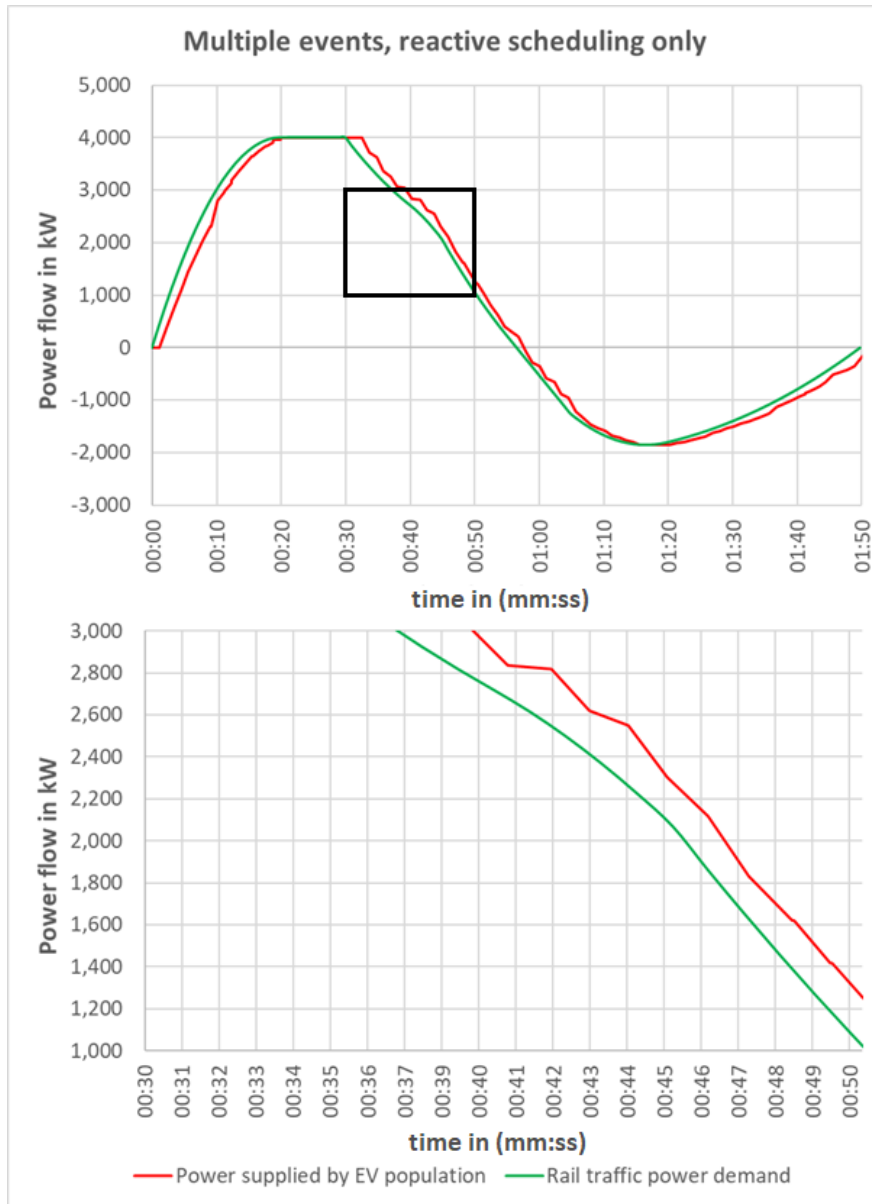


Figure 3.16: Simulated V2G network response to two counter-active events (one train departing at 0 seconds, one train arriving at 30 seconds) using reactive scheduling only

response is following the power demand of the rail traffic, but that the response is continuously lagging behind by between 1 and 2.5 seconds. This lag is only in parts due to the actual schedule creation and primarily caused by communication delays within the network.

The execution times of the reactive scheduling layer were found to vary between about 47 and 187 milliseconds with an average execution time of 73 milliseconds (measured over 10,000 scheduling cycles, in-event periods only with 500 connected EVs). On average, 48 milliseconds of this time (between 31 and 140 milliseconds) was required just to determine the difference in power flow from the EV population and the power demand from the rail application. This information is sourced from the SQL database and delays are therefore due to database communication, database-internal computation and sequencing of SQL queries (as other algorithms simultaneously access the same database).

In each cycle the algorithm made between 1 and 21 changes to the schedule – on average 12.88 schedule changes per cycle. These new schedule entries in the database have to be processed by the implementation module and communicated to the EV chargers. At around 15 milliseconds per EV, implementing 13 schedule entries is expected to take about 195 milliseconds. The last source of delay in system response is the time taken to detect the effects of any changes in power flow within the EV population. The power flow data relied upon for scheduling originates from the data collection module which updates EV data sequentially. For a population of 500 EVs it was found that, on average, 3.04 seconds pass before all EVs have been checked. This delay is highly situational depending on when an EV is being contacted. Thus, any schedule change made may not be accounted for in subsequent scheduling cycles for a few seconds.

### **Combined scheduling with predictive and reactive scheduling layer**

In the next test both the reactive and predictive scheduling layers are enabled. Again, the algorithms are determining the V2G network's response to a departing train followed by an arriving train 30 seconds later. To show the ability of this combined scheduling approach to adjust to uncertainty, the rail traffic power demand has been altered to differ from the predicted power demand curves.

As shown in Figure 3.17, the simulation now features a drop in the power provided from brake energy recovery of the arriving train from 1 minute and 17 seconds onwards. This could present a situation in which a train engages its mechanical brakes for an emergency stop, drastically reducing brake energy recovery. As this drop was unknown to the predictive scheduling layer, the initial schedule for charging/discharging the population of 500 EVs has been identical to the previous one (thus created at the same computational cost). This initial schedule has then been adjusted by the reactive layer once a mismatch above the 5 kW tolerance

between power supply and demand has been detected.

Figure 3.17 shows that the V2G network's response closely matches the power demand without any significant delay until the unpredictable braking manoeuvre, followed by a relatively consistent delay in network response of about 1 second as the reactive scheduling layer makes ongoing adjustments. Thus, the system responsiveness has been improved as long as the initial prediction closely matches the actual power demand. Yet, the ability to account for uncertainty has been maintained by the reactive scheduling layer.



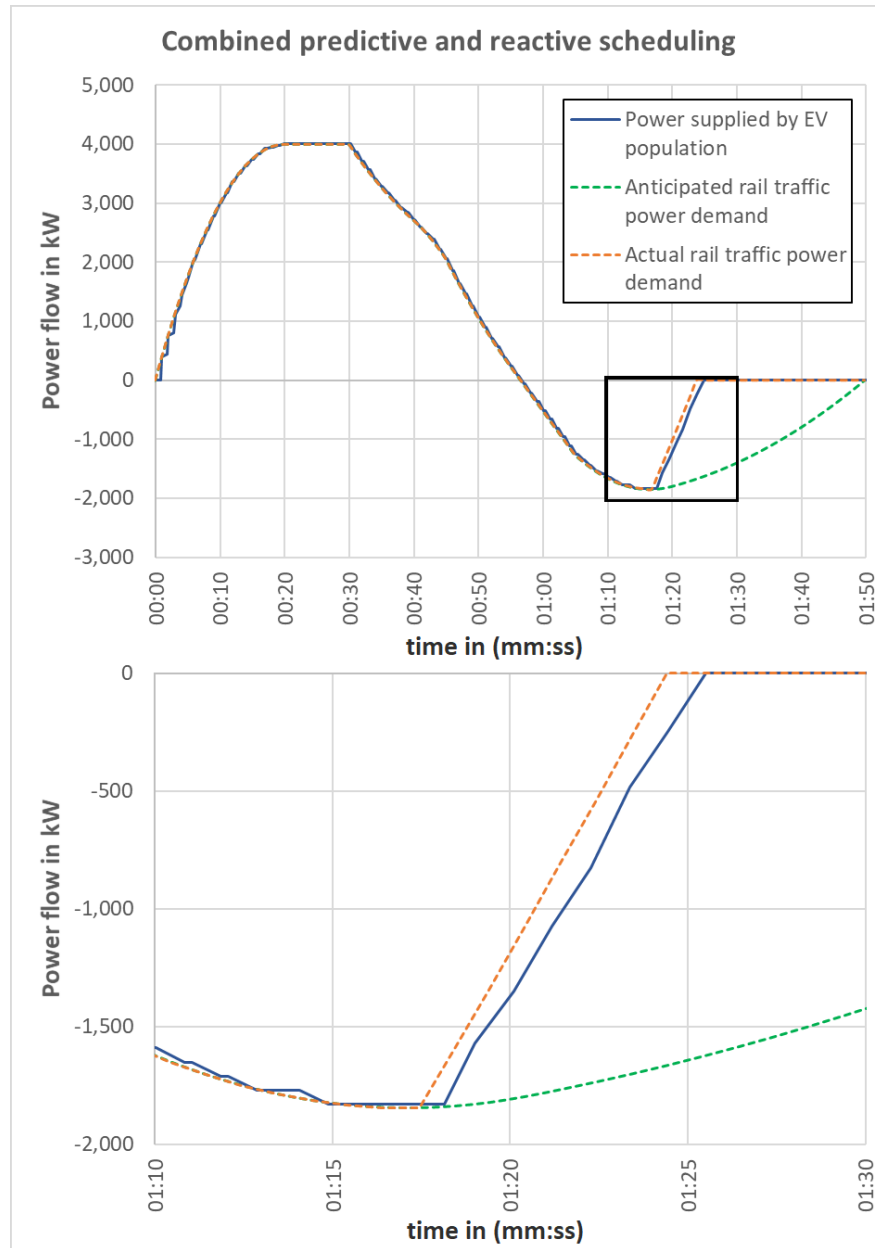


Figure 3.17: Simulated V2G network response to two counter-active events (one train departing at 0 seconds, one train arriving at 30 seconds with sudden unpredicted braking) using both predictive and reactive scheduling

### 3.5 EV communication system prototype

For this project, a prototype communication system has been developed as a proof-of-concept to represent a single EV in any aggregator-to-EV communication. The system was designed to connect to an existing computer network (Ethernet or Wi-Fi) to receive orders from, or transmit EV data to the aggregator via REST API (in line with the REST calls defined in section 3.2 and section 3.3). The device, shown in Figure 3.18 further features a touchscreen display to run the user-interface developed for EV user charging preferences (see chapter 5).

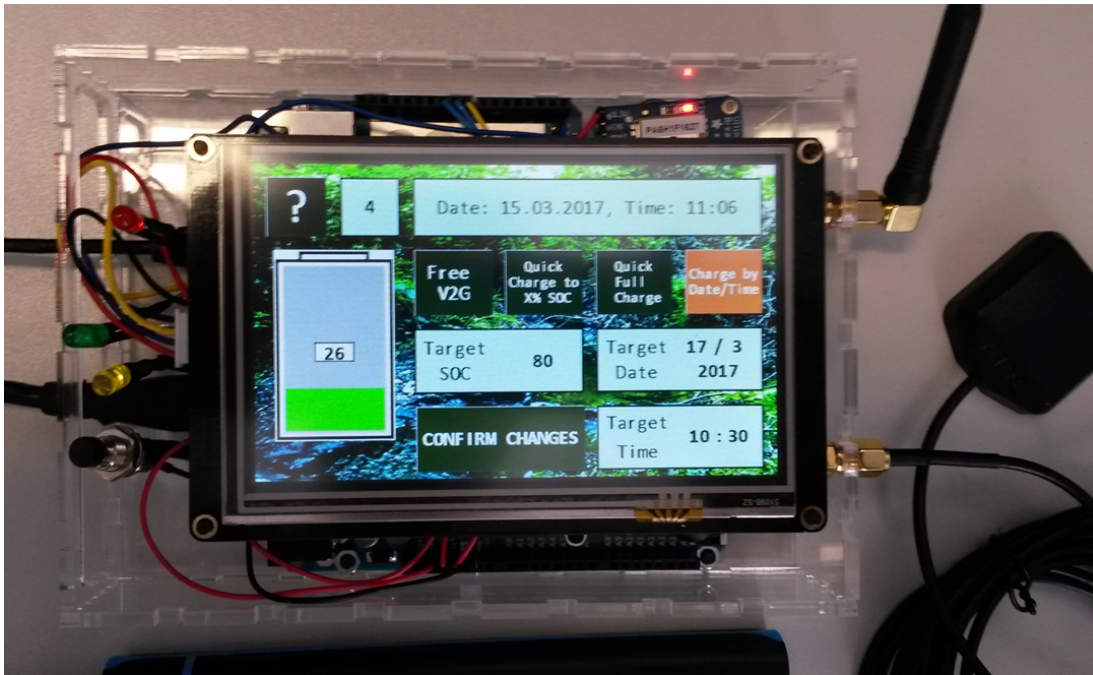


Figure 3.18: EV communication system with user interface

By default, the system uses the university's on-campus Wi-Fi network 'eduroam'. This is a network with multiple access points, which supports a large number of users simultaneously connected to the network. Hence, it is similar to the type of Wi-Fi network that would likely be employed in a large scale V2G environment (assuming that Wi-Fi is the chosen method of communication).

In this location (other locations *may* differ), 'eduroam' uses 'WPA2-enterprise' encryption (each user has a unique ID and an own encryption key [185]) as well as 'PEAP' (Protected Extensible Authentication Protocol [186]) authentication (the process with which the network decides which devices it allows access to).

The encryption method used by 'eduroam' would suit the application for V2G as every EV communicating with the aggregator could use its own, unique, encryption key (lowering the risk of data theft or other criminal abuse of a V2G data network).

The communication system consists of four main components (see Figure 3.19). The core of the system is an Arduino Mega Micro-controller board [187], which is used to exchange and collect data from all the other components. This board was chosen as its processor supports four asynchronous serial connections (Universal Asynchronous Receiver/Transmitter (UART) 0 to 3) and one synchronous serial connection (Serial Peripheral Interface (SPI)) operating simultaneously. Three of the asynchronous connections (UART 1, 2 and 3) are already required to communicate with the other components within the communication system. The fourth (UART 0) by default is used for the USB interface to program the board, but can also be used as another communication line (for example to an EV's battery management system).

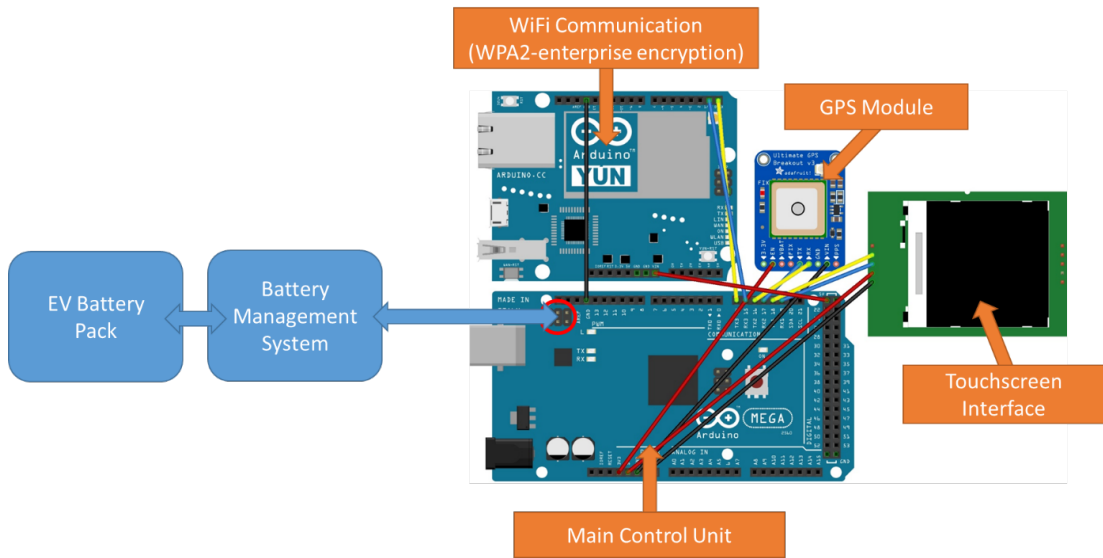


Figure 3.19: EV communication system components

A second component is used for the Wi-Fi connectivity of this system. This is done using another microcontroller board: the Arduino Tian [188]. The Tian has two processor structure in which, one processor (the SAMD21G18) runs 'sketches' (as algorithms on Arduinos are usually called), while the other one (the Atheros AR9342) runs a Linux based operating system, called Linino OS [189]. This first

processor is used for a range of Arduino models and hence compatible with most libraries available for Arduino programming. The second processor's operating system is required to connect the system to 'eduroam' as the WPA2-enterprise encryption used is handled by the operating system. Unfortunately, this adds another processor and with it, more complexity to the communication system. The Tian exchanges relevant data with the Arduino Mega via asynchronous serial communication (UART 3).

Ideally, there would be a single microcontroller board for both, Wi-Fi connectivity and serial communications with other components in this device. Unfortunately, no board within the Arduino range available at the time could provide the ability to use WPA2-enterprise encrypted Wi-Fi while still having a sufficient number of serial connectors. Yet, using the Arduino range was chosen as its open-source concept provided relative ease of programming. For the communication systems of actual commercial electric vehicles, clearly more potent hardware should be used. However, as a proof-of-concept, the double microcontroller setup is sufficient.

A third component is an 'Adafruit Ultimate GPS Breakout' module [190]. This module provides the system with time, date and location data via asynchronous serial connection with the Arduino Mega (UART 2). This module has been equipped with an external antenna as well as a battery that prevents it from losing the current location, date and time if the power supply from the Arduino Mega is disrupted (re-calibration after a hard reset can take several minutes depending on weather conditions).

The user interface was developed using a 7" Nextion Touchscreen Display [191] - the fourth component - and the corresponding Nextion Editor Software [192]. This display is equipped with its own microprocessor and only exchanges relevant data with the Arduino Mega via an asynchronous serial connection (UART 1). Thus, it does not need to be controlled 'pixel by pixel' by the Arduinos and has little negative impact on the system's speed and responsiveness.

The complete communication system is programmed to behave as such: On start-up, the system tries to establish a Wi-Fi connection with 'eduroam' (trying again indefinitely, if unsuccessful). The IP address assigned is shown on the display so that the system can be registered with the aggregator control (see chapter 3). *[This step would not be necessary when having full control over the network as any newly connected device could be registered automatically.]* The Arduino Mega

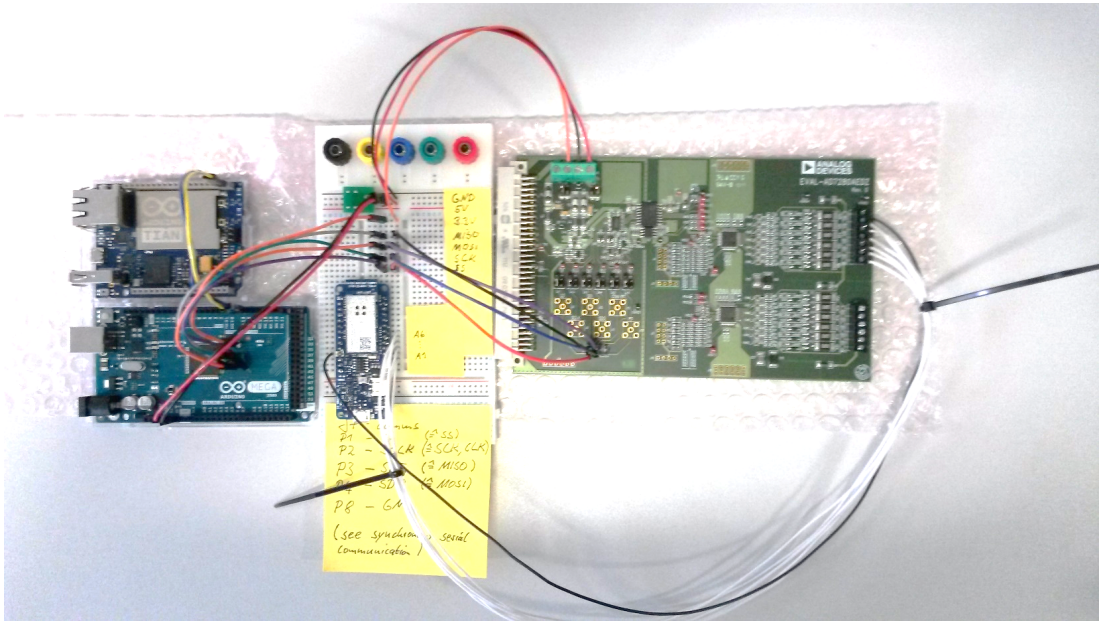


Figure 3.20: Communication trials between Arduino Mega and BMS using synchronous serial communication

is regularly collecting updated data from the user-interface and the GPS module while waiting ('listening') for commands from the network. These commands come in the form of REpresentational State Transfer (REST) calls [193] used by the aggregator to either request information from the EV (section 3.2) or instruct the EV to charge/discharge at a certain rate (section 3.3).

The system has not been connected to an actual EV battery pack as this would be outside the scope of this project. It was, however, successfully trialled to interface with a Battery Management System (BMS) using synchronous serial communication. The BMS\* used is an 'Analog Devices EVAL-AD734AEDZ Lithium Ion Battery Monitoring System' [194]. This board can monitor up to 6 lithium-Ion cells with inputs for both voltage and temperature and can be used for cell balancing (\*although further circuitry would be required for that, which is a likely reason the board is not called Battery Management System by its manufacturer). As this BMS had no batteries connected, it has not been used to provide any data in this project.

The EV communication prototype behaviour was programmed to simulate a real EV connected to the V2G network. It responds to information and charging REST calls in the manner described in section 3.2 and section 3.3. It is set up

to simulate a battery pack capacity of 50 kWh and an initial SOC of 50 % (after every reset). When receiving an instruction to charge or discharge, it continuously adjusts the SOC over time in line with the given charging/discharging rate (assuming an efficiency of 90 % both ways). Self-discharge of the battery pack over time is not simulated as the system was usually only used for a few hours at a time. EV user charging preferences (see chapter 5) are not selected by default (i.e. charging mode 0 at start-up), but can be input manually via the touchscreen interface.

*The C-based source codes for the Arduino Mega and the Arduino Tian can be found in appendices section A2.6 and section A2.7. Code for the touchscreen interface can be found in appendix section A2.8*

### 3.6 EV Simulator

To test the aggregator control strategy presented in this chapter and to investigate its usage for Road-to-Rail Energy Exchange (see chapter 4) a large number of (virtual) EVs are required to model a substantial EV car park. As it is obviously not feasible to build tens if not hundreds of the EV communication systems presented in section 3.5, an EV simulation algorithm was developed. This algorithm is not part of the aggregator control but is used to create a realistic testing environment for it. It is designed to behave just as the EV communication system prototype by responding to REST calls (info or charging calls) in the same manner as a single EV would. Unlike the real system, the simulator runs from a stationary desktop PC (connected to the same computer network as the machine(s) running the aggregator control), pretending to be a number of EVs.

To simulate multiple EVs on a single machine, multiple instances of this algorithm can be run simultaneously. However, as each PC usually only features one IP address when connected to a network, this address would be insufficient to uniquely identify individual simulated EVs. To account for this not only the machine's IP address but also a network port needs to be specified. The latter should be uniquely assigned to each instance of the simulator on a machine.

For example, a PC with IP address 123.123.12.12 may run a hundred instances of the EV simulator with unique IP addresses 123.123.12.12:5000, 123.123.12.12:5001, ..., 123.123.12.12:5099. Whenever the aggregator is contacting an instance of the

EV simulator it has to use a unique IP address/Network port combination so that each communication attempt is a realistic representation of that between an aggregator and a real communication system – even though the aggregator keeps communicating to the same stationary machine. For the aggregator, this means that IP addresses may also include network ports. This is fully compatible with the SQL database as well as the REST calls used during data collection and schedule implementation previously presented. Thus no further action is needed to adjust the actual aggregator control.

When initialising an EV simulation, a random vehicle model is chosen from a pre-determined list of EVs currently commercially available. This list contains twenty EV models, each with the same chance of being chosen (see Table 3.2 [195]). The simulation then uses the model name, the battery pack capacity as well as the maximum charging and discharging rates of the randomly chosen EV. It also creates random values for the initial battery pack SOC, the user inputs regarding charging preferences (see chapter 5) as well as the vehicle location data. This random data is used whenever the aggregator requests information. It should be noted that a 'seeded' random number generator is used, meaning that any random selection can be reproduced by initialising a simulation with the same 'seed' as input. This allows re-running a simulation with the exact same initial conditions when needed (see section 4.3).

After initialisation, the algorithm connects to the aggregator's SQL database to register it's IP address and network port in the 'newVehicles' table\*. *\*Note: As was explained in section 3.2, this registration step is only necessary due to a lack of admin privileges over the network that was used for this project. Otherwise, the aggregator could easily look-up the IP addresses of any newly connected device. In any real-life implementation of V2G this step would not only be unnecessary but highly unadvisable – for security reasons alone, should EVs not be able to access the aggregator's database! As EV access to the database effectively equates to 'public' access the risk of malicious misuse such as SQL-injection [202][203][204] or 'denial of service' attacks [205] is rather high.*

Once initialised, the simulation algorithm regularly updates the battery pack SOC according to any charging instructions it has received from the aggregator. To reduce the processing resources required per simulator instance, the SOC is updated every time a REST call is received. The simulator algorithm then evaluates how the SOC would have changed in the time passed since the last

Electric Vehicle Model	Capacity (kWh)	Max charging rate (kW)	Drivetrain power (kW)
Audi e-tron 55 quattro [196]	95	150	300
BMW i3	33.2	50	125
BMW i3 (2019) [113]	42.2	50	128
Hyundai Ioniq [197]	30.5	70	88
Jaguar i-Pace [198]	90	100	294
Kia Soul	33	100	81
Nissan e-NV200 [199]	40	50	80
Nissan Leaf	30	50	80
Nissan Leaf (2019) [200]	40	50	112
Renault Kangoo Z.E.	33	7.4	44
Renault ZOE Q90	41	43	65
Renault ZOE R90	41	22	68
Smart Fortwo Electric Drive	17.6	22	60
Tesla Model 3	75	80	150
Tesla Model S 100D	100	120	311
Tesla Model S 75D	75	120	245
Tesla Model X 100D	100	120	311
Tesla Model X 75D	75	120	245
Volkswagen e-Up	18.7	50	60
VW e-Golf [201]	35.8	40	100

Table 3.2: EV model specifications used for EV simulator, compiled using ev-database.uk as well as stated sources.



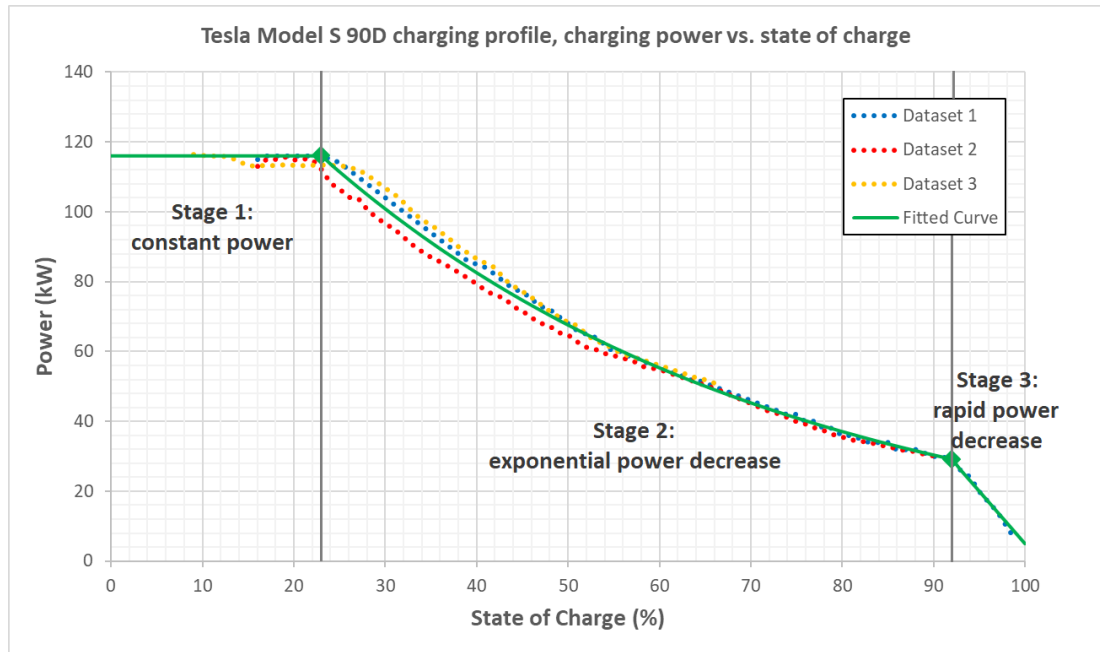


Figure 3.21: Charging profile for Tesla Model S 90D, charging power (kW) against SOC (%) [206]

call at the current charging/discharging rate. Just like the EV communication system, a 90 % efficiency is assumed for charging and discharging.

Further, the EV simulator algorithm accounts for changes in the maximum charging rate that an EV can accept depending on the current SOC. Ideally, this would be assessed separately for each EV model simulated, but suitable data is very hard to come by. Instead, this issue is significantly simplified within this project, by assuming the same charging power to SOC relationship for all EVs. A suitable dataset was found for a Tesla Model S 90D (the previous version to the Model S 100D that features in Table 3.2). This EV has a battery pack capacity of 90 kWh and a stated maximum charging power 120 kW.

Tom Bryden, a previous CDT in Energy Storage and its Applications student, analysed the charging behaviour of this vehicle using datasets uploaded to the Tesla forum by owners of said EV model [206]. In the datasets, the EVs were charged through the Tesla supercharger (charging rate up to 150 kW) - the charging profiles are shown in Figure 3.21. While these datasets are not perfect (they originate from private individuals, effects of temperature and battery state of health have not been accounted for), an approximate relationship between the

maximum charging rate of these EVs and the battery pack SOC is apparent. Within this project, it is assumed that all EV models show similar behaviour and hence the charging profile shown in Figure 3.22 (based on the fitted curved in [206]) is used for the EV simulator algorithm.

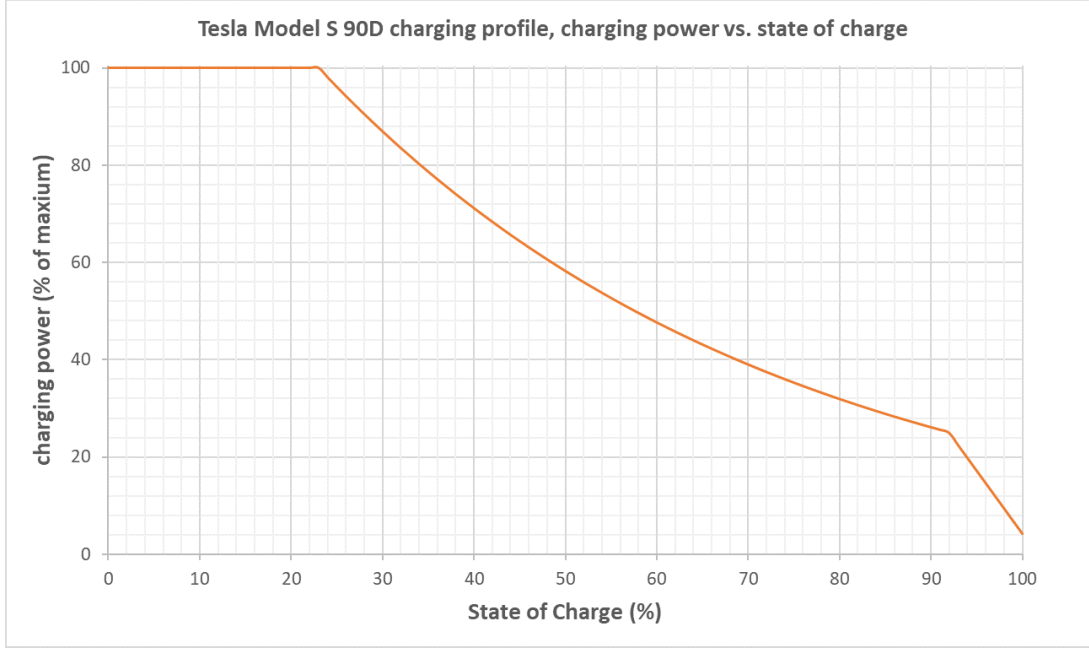


Figure 3.22: Assumed charging profile for idealised EVs, % of maximum charging power against SOC (%)

The machine used for these EV simulations is equipped with 16 GB RAM memory, which is the major limiting factor. Due to a large number of EV simulator instances, but the low processing load for each instance (it only reacts when being contacted), the EV simulation is very memory intensive, but not processor intensive. This machine has been used to reliably simulate the communication between aggregator and up to 1,000 EVs. From about 1,100 simulated EVs and upwards the system was found to be prone to serious delays and crashes (only the EV simulations, NOT the aggregator control). Multiple PCs could be employed for the simulation of even larger EV populations. However, as will become apparent in the following chapters, this is not necessary within the scope of this project.

While this simulation algorithm is very useful to create large numbers of EVs for the aggregator to communicate with, it is based on random number generation

---

and does not allow for full control over the initial conditions of the simulated EV. For any analysis focussing on an individual EV, a second version of the simulation algorithm was created.

This controlled version is initialised using user inputs (in the code's preamble) for EV battery pack parameters, initial SOC and user charging preferences. Further, this version is logging SOC data and charging rates as well as every command that was received from the aggregator. This allows for deeper analysis into how decisions by the aggregator affect individual EVs. A downside to this data logging is the associated computational cost, making it unfeasible to use the controlled version as default to simulate hundreds of EVs. This version has mainly been used during simulations in chapter 5 where a number of 'control EVs' were analysed as part of a larger, mostly randomised EV population.

*The annotated python code for the EV simulator algorithms can be found in appendices section A2.9 and section A2.10.*

## 4. ROAD-TO-RAIL ENERGY EXCHANGE

Road-to-Rail Energy Exchange (R2REE) describes a novel V2G application in which the energy storage potential of aggregated EV batteries is used to support nearby electrified rail infrastructure. As such it addresses the issues tied to transport electrification on two fronts; the uptake of EVs in personal transportation and the power demands of electrically powered trains for mass transportation. In both areas, this electrification increases demand stresses on the electric power grid and must be accompanied by upgrades to the underlying power supply infrastructure.

### 4.1 *V2G as support for Rail systems*

A car park based V2G network can act as a buffer between rail system and power grid by supplying traction power for electric trains (thus reducing peak demand stresses on the power grid) and absorb energy from regenerative braking of electric trains. For new rail electrification projects reduced power demand peaks might reduce network upgrade requirements. Further, it could lower upgrade requirements for new EV charging infrastructure (assuming an EV car park can share the connection with the electrified rail infrastructure).

As a specific application of V2G, one might choose to follow the ‘V2X’ naming convention predominant in related literature (such as V2H, V2B, V2V and others, see chapter 2) and describe the concept as Vehicle-to-Rail (V2R). However, this terminology is already established in logistics representing supply chains involving both road and rail transport [207][208]. Thus, to avoid confusion this terminology will not be used within this work.

In R2REE, as electric trains accelerate (causing a spike in power demand for traction power) the connected EV population (or parts thereof) are discharged, feeding into the rail system and reducing the load on the local substation (see Figure 4.1). As arriving trains decelerate using regenerative braking, the result-

ing spike in power from the rail system is fed into the V2G network. Both these operations reduce fluctuations in the power demand experienced by the substation. In periods without rail traffic, the EV population can draw power from the shared grid connection for battery charging, thereby maintaining a steady power flow from the grid.

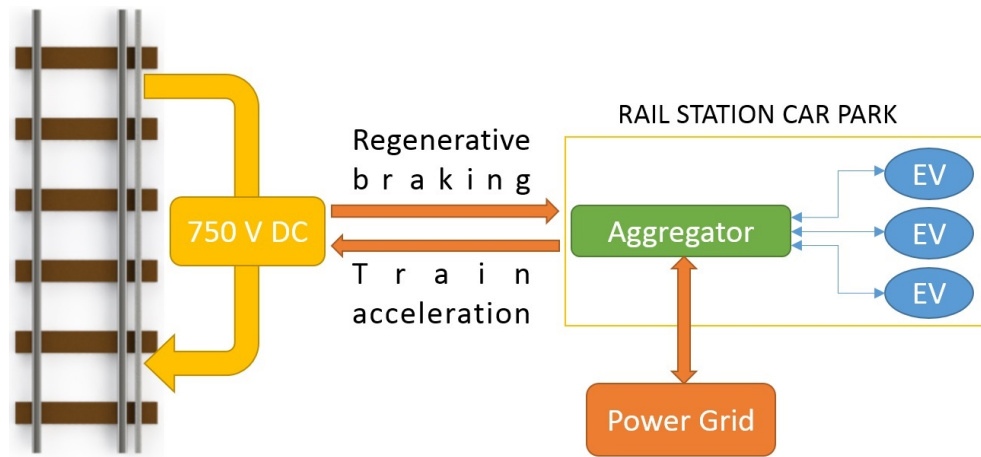


Figure 4.1: Powerflow in a V2G network used for train brake energy recovery in a third rail powered rail system

Accepting power from regenerative braking is especially beneficial in rail networks which typically cannot support it. For rail systems with AC power supplies (typically operating at about 25 kV), electricity from regenerative braking can usually be fed back into the power grid without major transmission losses. DC networks, however, typically operate at much lower voltages (about 650-1500 V) significantly lowering the efficiency of power transmission.

Thus, regeneration of power from brake energy recovery into the grid is not a common feature of DC-powered networks. Consequently, DC-powered rail networks, whether using third rail, fourth rail or overhead catenary DC power supply, may greatly benefit from energy storage in general, and R2REE in particular, from enabling regenerative braking where it has not been feasible before.

Unlike approaches such as dwell time optimisation [180], in which power from regenerative braking of one train is immediately absorbed as traction power by another, the usage of energy storage does not interfere with train schedules. Various types of energy storage, such as batteries, supercapacitors or flywheels have been proposed either on-board or along track lines to accept power from regen-

erative braking for later use during acceleration [209][210]. R2REE could serve the same purpose - with the advantage of using batteries that are already in use and awaiting charging.

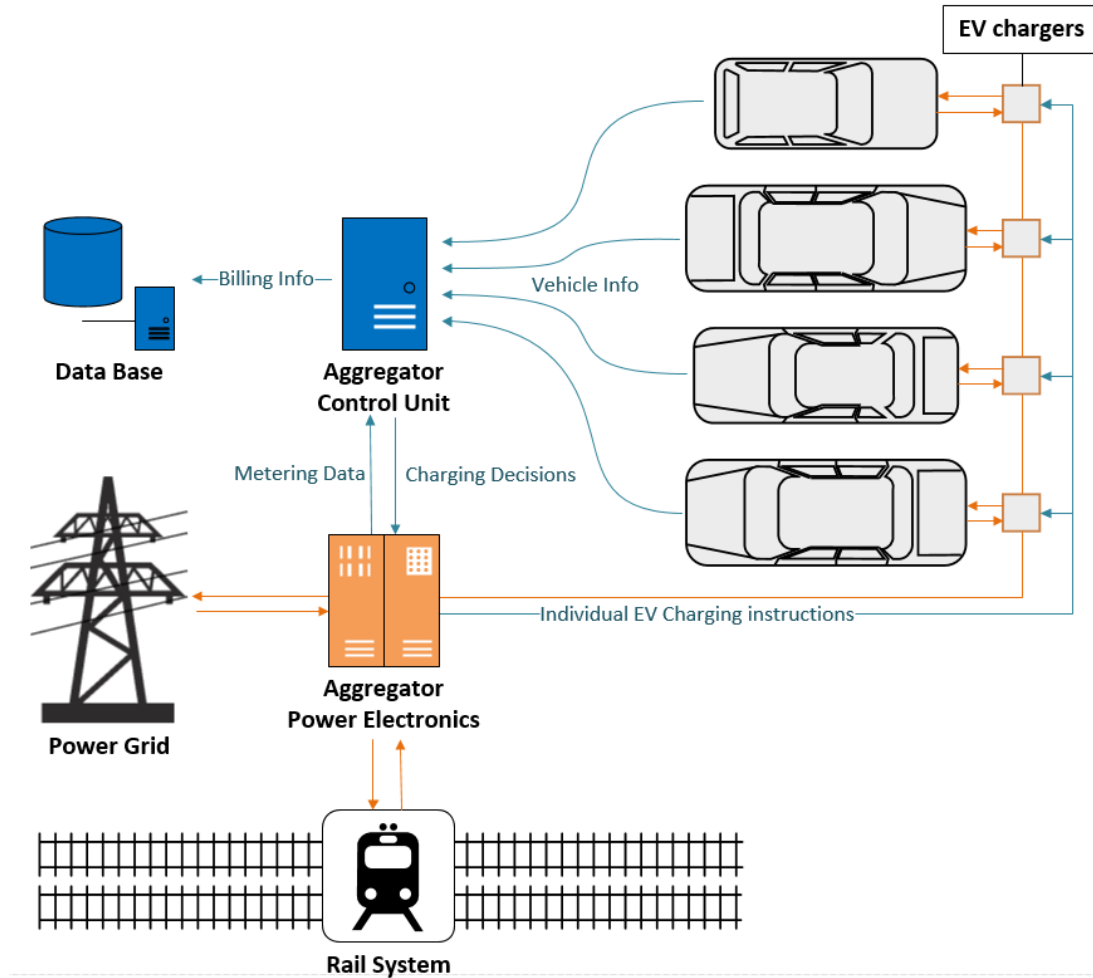


Figure 4.2: R2REE: Vehicle-to-Grid schematic supporting local rail system

An existing low-voltage (750 V) DC-powered third-rail system in Merseyside, England serves as a case study in this work - supported by a V2G network modelled after the findings in the previous chapter, see Figure 4.2. Of the electrified railways in the UK, about two thirds (by length) use a 25 kV, 50 Hz AC overhead supply system (63.7 % in 2003) [211]. This type of electricity supply was also set as the standard for future railway electrification projects. The second widely used system (others exist, but are rarely used nowadays) with about one-third of the electrified railways (36.04 % in 2003) is the use of 660/750 V DC third-rail

systems [211]. In these systems, the train's electricity is supplied via mechanical contact between the train's power supply system and an additional rail parallel to the two rails used for travelling (see Figure 4.3).

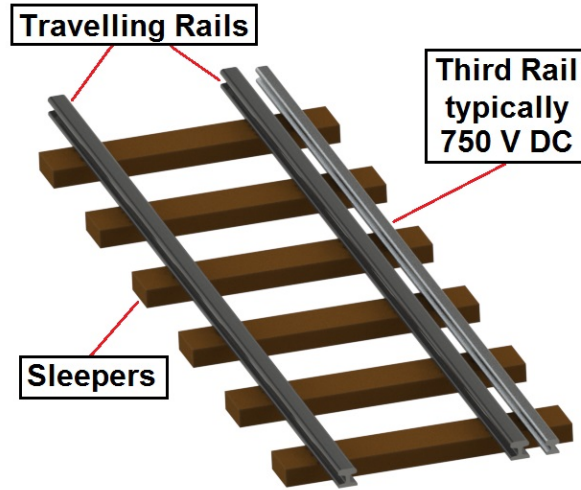


Figure 4.3: Third rail system in electrified rail track

Third rail systems are associated with safety risks and friction losses [212] and hence are often regarded as inferior compared to 25 kV overhead supply. However, the existing third rail infrastructure is likely to be used for decades to come so should not be excluded from consideration for brake energy recovery. As third rail is commonly used in the most populated areas in and around London, it also accounts for a large fraction of UK rail traffic by passenger numbers and number of train starts/stops [211].

## 4.2 Train Station Power Demand Model

To explore the practicality of the R2REE the 24-hour operation of the proposed system is simulated using the rail power demand model presented in this section along with the EV population model in section 4.3. The aggregator control scheme described in chapter 3 and in particular, the predictive scheduling approach presented in section 3.4 requires the power demand model to be defined as a sequence of predictable and repetitive 'events'.

For R2REE each event represents either a departure (requiring traction power) or the arrival (surplus power from regenerative braking) of a train of known type.

While the aggregator control was developed for real-time operation and only requires to know event starting times a few seconds prior, a full 24-hour fixed event schedule is created so that any simulations discussed henceforth assume an identical power demand profile throughout the day. In the case of R2REE, this event schedule represents a list of all train arrivals and departures.

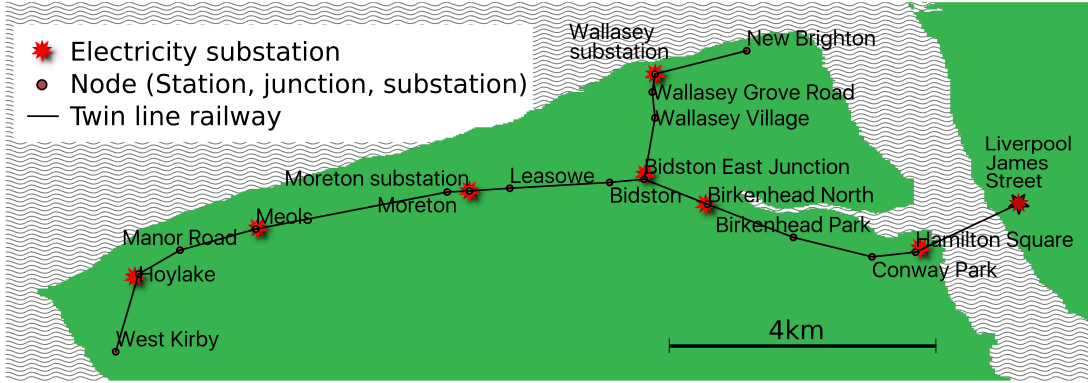


Figure 4.4: Section of Merseyrail system modelled in case-study, figure taken from [213]

The rail power demand model defined in this project uses the 750 V third-rail powered DC 'Merseyrail' rail network [215] operating in Merseyside, England as a case study. In particular, the train station in Hoylake (near Liverpool) along the 'Wirral Line' was chosen (see Figure 4.4). Hoylake train station is interesting as it allows for several simplifying assumptions during modelling and analysis:

- The train station is in close proximity to the single substation powering this section of the rail network (see Figure 4.5), thus removing the need to analyse interactions between multiple substations or transmission losses.
- A public car park belonging to the station is also nearby (less than 50 meters away). This car park could be equipped with bi-directional chargers as outlined in section 4.3.
- The train station has two tracks and only serves this one line (both directions).
- Merseyrail only operates British Rail Class 507 and Class 508 trains on the 'Wirral Line' - both of which can be regarded as identical in terms of traction power demands and are thus treated as a single type of train within this work.



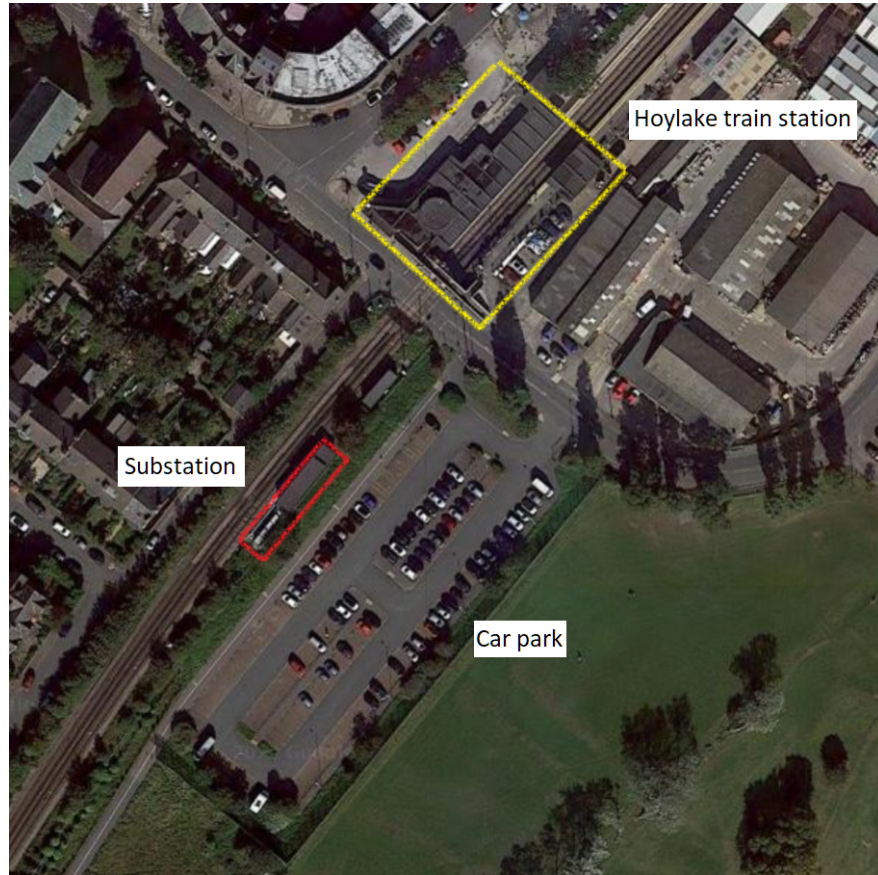


Figure 4.5: Aerial view of Hoylake train station and surroundings: train station, car park and substation in close proximity, image taken from [214]

- The Merseyrail network does not currently utilise regenerative braking and could therefore potentially gain from enabling it through the introduction of energy storage technologies.

*Note: the findings presented in this section are based in large parts on work undertaken by Professor David Fletcher (Department of Mechanical Engineering, University of Sheffield) who created a comprehensive model of the electrical system of the Merseyrail 'Wirral Line' [213]. The author acknowledges this contribution and is grateful for the cooperation with Professor Fletcher throughout this project.*

The power consumption of trains moving along the whole Wirral line has been modelled in detail and validated in [213]. This model describes the traction power



Figure 4.6: Assumed speed profile of simulated train

requirements of trains moving on the rail network as well as the resulting power draw experienced by substations along the line. Unlike the real rail system, the model also allows for the inclusion of regenerative braking. Parts of this existing model forms the basis of this work: to construct the 'event' definitions needed here, the power demand profile (as experienced by the substation, including theoretical regenerative braking) of a single train accelerating from a standstill at 'West Kirby' train station and stopping at Hoylake is used.

West Kirby is the next stop after Hoylake and thus the end of the Wirral line (see Figure 4.4). The track section Hoylake-West Kirby is single-ended and thus fully powered by the substation at Hoylake. The speed profile of a train journey from West Kirby to Hoylake can be seen in Figure 4.6 (this speed profile was created from GPS data recorded while travelling on the real train line [213]). The resulting power demand experienced by the substation during this journey is shown in Figure 4.7 (no other trains were using the relevant track sections at the time, negative demand represents power from regenerative braking).

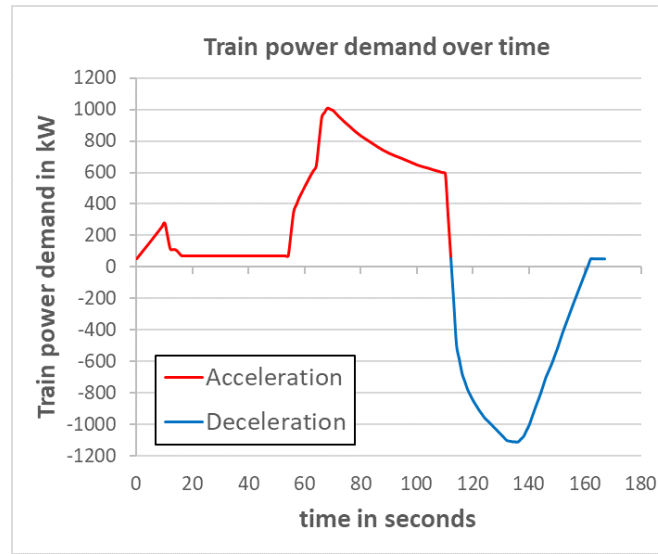


Figure 4.7: Train traction power demand during acceleration and regenerative braking power output during deceleration

This power demand profile for the journey was 'deconstructed' into two distinct 'events' for trains leaving from or arriving at Hoylake station:

1. the train departure event (acceleration from standstill to travelling speed, traction power required, see Figure 4.8)
2. the arrival event (deceleration from travelling speed to standstill, energy from regenerative braking needs to be dissipated , see Figure 4.9).

This assumes that the speed profile of a train leaving West Kirby is the same as a train leaving Hoylake (in either direction) and the speed profile of a train arriving from 'Manor Road' (next stop from Hoylake eastward) is identical to the arrival from West Kirby. The departure event can be verified by comparing it to the findings in [215], Figure 7 in which the current drawn from the substation in Hoylake were measured under a similar train journey (not simulated as in [213]).

These two event definitions were used by the V2G scheduling algorithms (see section 3.4) as the only two event types in any simulations discussed below. The same approach could be employed for more complex rail systems, such as any large urban rail station with a dozen or more platforms. However, this would require defining a large number of 'events' to represent the various train lines, train

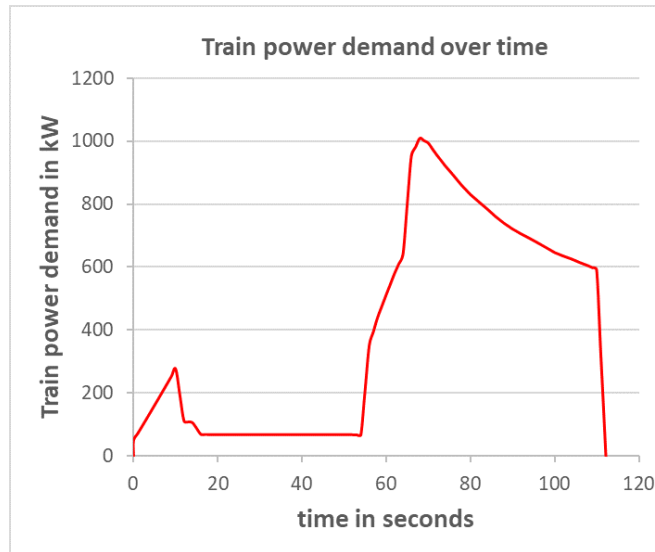


Figure 4.8: Assumed traction power demand for train departure event

types and resulting differences in speed profiles and power demands. It should be noted that the aggregator control presented in chapter 3 could accommodate any number of train arrival or departure events.

To construct a 24-hour rail system power demand profile for Hoylake train station these events were matched with each departure on the Hoylake train schedule [216] (both directions, for weekdays, see Appendix A4). The timetable used was valid for December 2019 to May 2020, a rather unremarkable period that can be assumed to represent a typical timetable for the line (no construction works or other planned disruptions in this period). It was assumed that each train departs perfectly on time (as scheduled in the public timetable) and arrives at the station (coming to a full stop) exactly 60 seconds before the scheduled departure. It was further assumed that no rail traffic occurs that is not marked on the public schedule (neither stopping at nor ‘passing through’ Hoylake).

The resulting 24-hour power demand model features 117 of each train departures and arrivals (see Figure 4.10). It can be seen that the frequency at which trains arrive or depart changes drastically throughout the day with little activity during night times, a ramp-up in activity during the morning hours, followed by a period of steady high-level activity before the eventual decline in the late evening.

This pattern indicates when rail system power demands are most likely to cause strain on the local power grid. As will be discussed in the next section, this

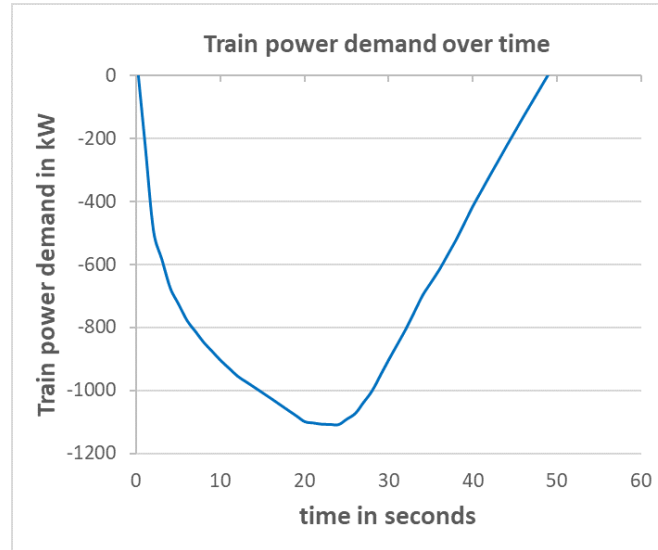


Figure 4.9: Assumed regenerative braking power from train arrival event

distribution of activity throughout the day on the rail system is not dissimilar from the assumed availability of EVs on the nearby public car park.

Summing up the durations of departure or arrival events offers some initial insights into potential R2REE usage: For about 3.6 hours (about 15 % of the day) the rail system requires traction power for acceleration while regenerative braking could generate power for about 1.5 hours per day (roughly 6 %) – during these times the rail system could benefit from a connected V2G network. The rest of the day – about 18.9 hours – no rail traffic is present (EVs on the V2G network could charge freely during these periods).

Each train departure event has an energy consumption of roughly 46 MJ or 12.7 kWh. Over 24 hours, this adds up to about 5,382 MJ or 1,486 kWh. Similarly, each arrival event could regenerate 35 MJ or 9.7 kWh, adding up to about 4,095 MJ or 1,135 kWh per day.

If this regenerative braking energy could be fully ‘saved’, the accumulative energy savings would be equivalent to the electricity consumption of about 115 UK households (based on an average per household electricity consumption of about 3,600 kWh per year, as of 2018 [217]). At a typical electricity price of 15p per kWh, this is equivalent to savings of about £62,000 annually in electricity costs.

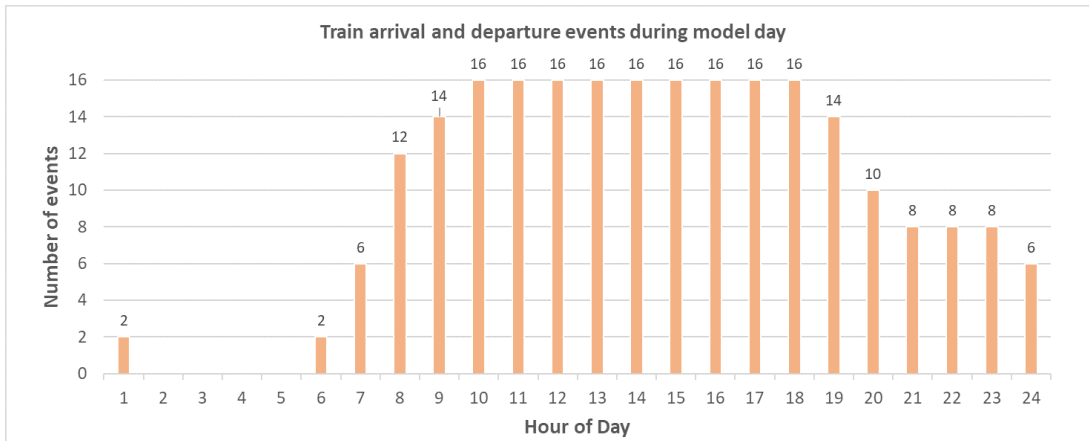


Figure 4.10: Train arrivals and departures during the model day per hour

Time	Destination	Platform
07:09:00	Liverpool	1
07:22:00	West Kirby	2
07:24:00	Liverpool	1

Table 4.1: Excerpt of train timetable, period of interest: 07:00 to 07:30

Considering a short example period of the full 24-hour rail power demand model reveals the nature of power peaks on the rail system: The train timetable excerpt shown in Table 4.1 translates to rail system power demand shown in Figure 4.11 and Figure 4.12 (each departure in the timetable is accompanied by an arrival event ending 60 seconds beforehand). Most trains timetabled arrive or depart without any overlap with other trains' departures or arrivals, thus most power peaks can be clearly identified and attributed to one event.

There are however periods in which two events overlap and, at least partially, 'cancel out' – in Figure 4.11 this can be seen where the arrival of the third train overlaps the departure of the second train. In this rail system with only two tracks and just one train line serving both directions, such overlaps are very limited and may only occur between one arrival and one departure event. Two simultaneous arrivals or departures, in which peaks may 'stack' are not plausible here during normal operation (both trains would have to travel on the same track with little distance in between).

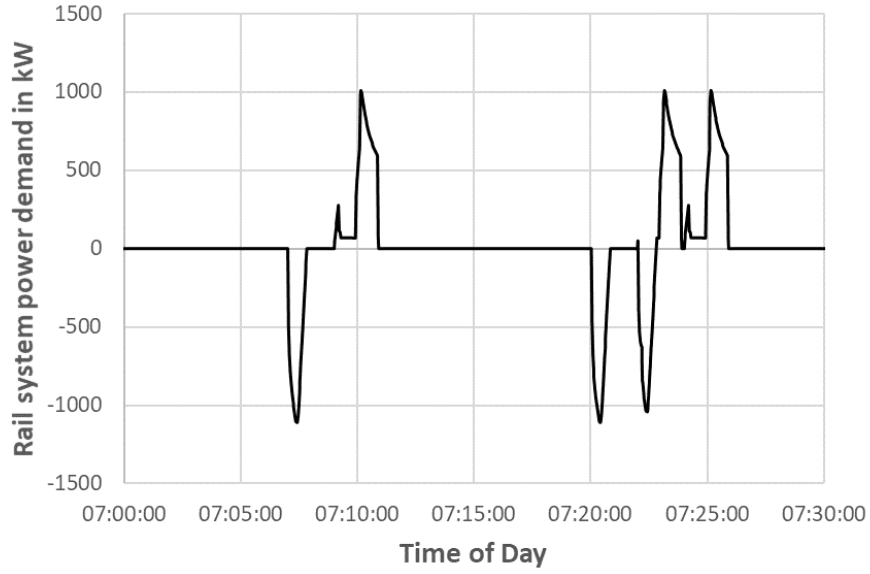


Figure 4.11: Rail system power demand over period of interest

Thus, the maximum power expected to be drawn from the V2G network for traction power is limited to the peak value in the departure event (1,009 kW - hereafter referred to as ‘traction power threshold’). Similarly, the maximum power expected to be fed from the rail system into the V2G network is limited to the peak in the arrival event (1,109 kW – hereafter referred to as ‘regenerative braking threshold’).

It should be noted that the 24-hour rail power demand model is not passed onto the V2G aggregator control as a full-day dataset of ‘power demand over time’ but instead as an event schedule via the SQL database (see section 3.4). Thus it takes the form of a list containing only the starting time and type (here, only departures or arrivals) of events. As the V2G aggregator control operates in real-time, each event is resolved individually as the time of day approaches the starting time of a listed event (10 seconds prior).

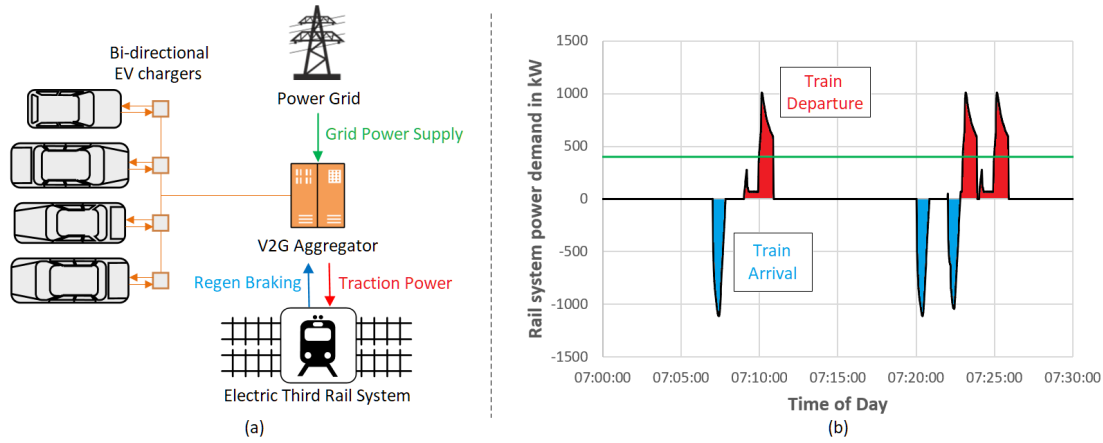


Figure 4.12: (a) system overview and power flows: aggregated EV population acts as buffer between the grid connection and the fluctuating rail system power demands to ensure steady power flow from the grid; (b) rail system power demand during period of interest: traction power drawn for train acceleration - positive/red, power supplied from regenerative braking - negative/blue, power supplied from the power grid - green (would have to follow peaks/troughs without V2G buffer).

### 4.3 EV Population Model

The EV population in the proposed V2G system is modelled as a group of parked EVs situated in the same car park near the train station. Each EV in the population is assumed to be connected to a bi-directional charger. Non-participation of any connected EVs in V2G operation is not considered in this chapter - every EV on the network is assumed to allow discharging through the aggregator (the possibility for EV users to opt out of V2G operation is considered in chapter 5).

The Hoylake train station has 670 parking spaces available nearby – it is assumed that a fraction of these spaces can be equipped with bi-directional EV chargers and only this portion of parking spaces is considered in the further discussion. The number of EV chargers varies between the simulations in section 4.4 - depending on the scenario, either 50, 75 or 100 of parking spaces are assumed to be equipped with EV chargers respectively.

In the simulations discussed later, the EV population is represented by multiple instances of the EV simulation algorithm (see section 3.6) being run on a server other than the machine running the aggregator control (so that realistic commu-



nication via the network is taking place between aggregator and the simulated EVs, see chapter 3).

To model a car park in line with the train station model described in section 4.2, the number of EV's connected to the network at any time over 24 hours needs to be determined. For the server running the EV simulation algorithm, this means determining when to initiate a new instance of a car simulation (i.e. a new EV connects to the network) and when to end an instance (an EV leaves the network). To achieve this it is assumed that the car park has a variable occupancy rate (the percentage of parking spaces in use) over the simulation period where 0 % occupancy represents no connected EVs and 100 % represents the all available EV chargers being in use by V2G enabled EVs.

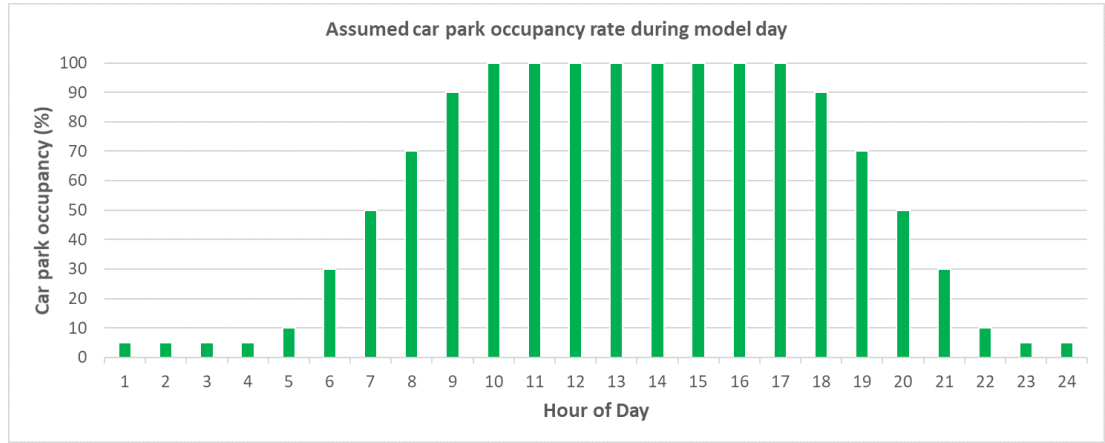


Figure 4.13: Assumed car park occupancy rate over model day

This assumed occupancy rate over the 24-hour simulation period is shown in Figure 4.13 and is based on data provided by Transport for London (TfL) about car park usage at the London underground [218] (which unfortunately does not cover a full day). It is assumed that a car park at a train station is being used similarly (although the example train station is situated in a commuter area rather than an urban environment).

The data provided by TfL only covers the ramp-up in occupation in the mornings (6 to 9 am) and the decrease in the evenings (4 to 7 pm) on a weekday. Thus further assumptions were needed for a full 24-hour car park occupancy rate. Night-time occupancy was assumed to be very low at 5 % and day-time occupancy between the morning ramp up and the evening decline was assumed to reach maximum occupancy of 100 %.

When compared with the event occurrence on the rail system (see Figure 4.14), it can be noted that periods of high car park occupancy generally coincide with periods of frequent rail traffic. However, as the frequency of rail events does not impact the peak power demands expected, the V2G network's ability to support the rail system is severely limited during the early and late hours of the day.

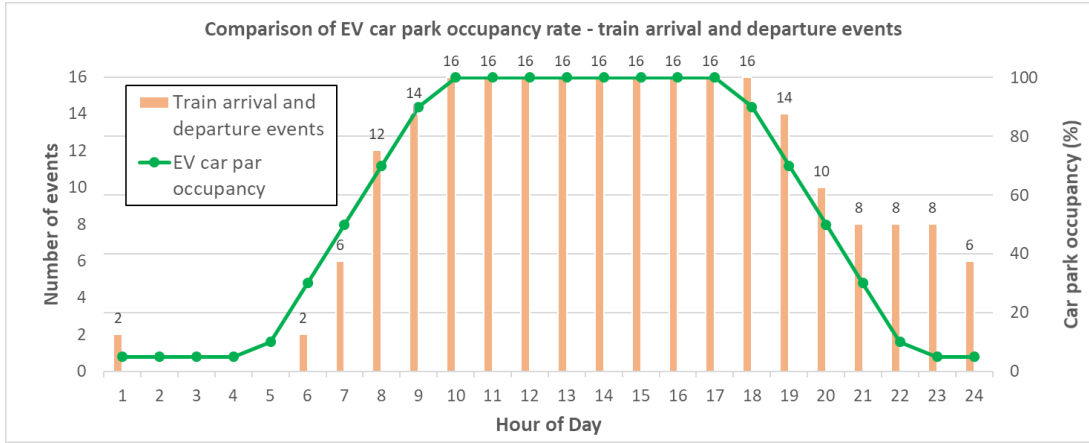


Figure 4.14: Assumed car park occupancy rate and number of train arrival/departure events over 24 simulation period

To simulate the car park behaviour the server is tracking the occupancy rate throughout the day, assuming that the number of EVs increases or decreases linearly between the hourly levels specified in Figure 4.13. Whenever another EV is required to meet the model occupancy rate, the server initiates another EV simulation. When too many EVs are simulated, the server ends an already running instance of the EV simulator. Instances are ended in the same order they are initialised (the first EV to connect is also the first to leave). While this is not realistic behaviour, it significantly simplifies the model. The total size of the car park (the number of spaces equipped with EV chargers) is variable and determined before launching the server to allow simulating any number of EVs.

This EV population model is deemed sufficient as long as the behaviour of individual EVs (i.e. arrival and departure times, initial SOC, etc.) is not an important part of the analysis. Potential inaccuracies within the analysis could arise from the uncontrolled length-of-stay of individual EVs (a real EV population may contain several short-stay and long-stay EVs connected to the network). Within the model adopted, this has an averaging effect wherein all simulated EVs within

the population end up being connected to the V2G network for similar periods. However, given the general lack of reliable data on EV user behaviour (which could serve as a basis for more detailed and more realistic model), this potential source of inaccuracy is to be accepted within the scope of this work.

Each instance of the EV simulation algorithm is initialised using a seeded random number generator to determine its initial conditions (see section 3.6). This means that characteristics of the simulated EVs are not being controlled directly; however, initialising an EV simulator instance using the same 'seed' for random number generation results in the exact same initial conditions. This can be used to re-create an identical, although random, EV population. In this work, the seed of each EV simulator instance is coupled to the overall size of the car park. Thus, any simulation based on the same overall EV population size uses an identical EV population.

To simplify the analysis in section 4.4, all simulated EVs have the same battery pack specifications, mirroring those of the Nissan Leaf (unless stated otherwise). Using the specifications of the 2019 Nissan Leaf model, simulated EVs are assumed to have a 40 kWh capacity battery with a charging rate of up to 50 kW [200]. It is important to note that this charging rate is only achievable while the battery pack state-of-charge (SOC) is relatively low. The maximum charging rate of each EV depends on the battery pack SOC at the time. Figure 4.15 shows the assumed relationship between the maximum charging rate and SOC. This relationship was adapted from the findings in [206].

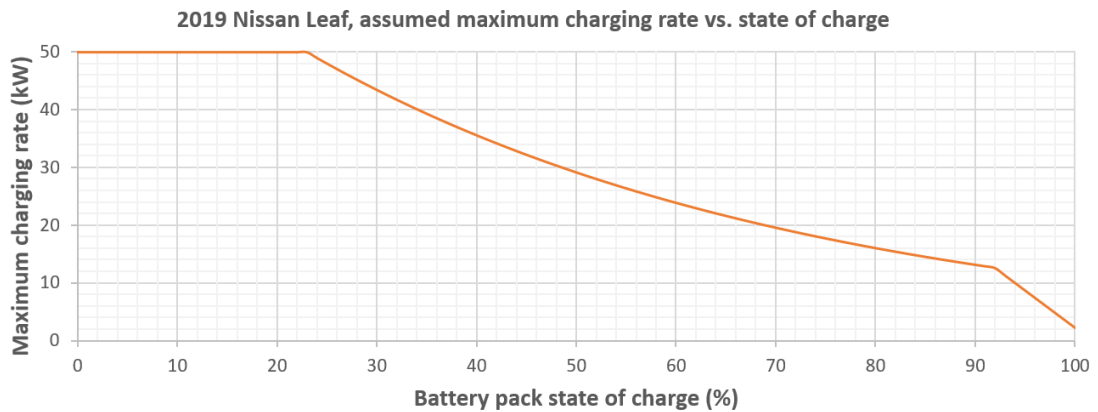


Figure 4.15: Assumed maximum charging rate against SOC for simulated EV population

<b>Control EV Name</b>	<b>Initial SOC</b>	<b>Connection Time</b>	<b>Disconnection Time</b>
EV A	50 %	08:00:00	16:00:00
EV B	30 %	09:00:00	17:00:00
EV C	70 %	10:00:00	18:00:00

Table 4.2: Control EV configurations valid for all simulations discussed in this chapter.

While the maximum discharging rate of the Nissan Leaf battery pack is unknown, the drive train power of this EV is stated as 112 kW. Thus, it is reasonable to assume that the battery pack can be discharged at least at this rate, irrespective of the battery pack SOC. This discharging rate exceeds any of the assumed charging/discharging rate limits of the bi-directional EV chargers (also up to 50 kW, see section 4.4).

To analyse the effects of V2G scheduling on individual EVs, the random ‘bulk’ EV population can be accompanied by a small number of controlled EV simulation instances (see section 3.6). These use a slightly different version of the EV simulation algorithm that a) logs the EV’s SOC over time as well as any commands received from the aggregator and b) is initialised as a specific EV model with a specified initial SOC. The ‘Control EVs’ used in this chapter (also Nissan Leaf spec) are defined in Table 4.2.

#### 4.4 R2REE Simulations

V2G aggregation within this work assumes that all EVs are connected to identical bi-directional EV chargers (assumed to have the same power rating in both directions - either 20 kW, 35 kW or 50 kW) and that both charging and discharging of EVs have an efficiency of 90%. The V2G network is assumed to use the same substation as the rail system as its shared power grid connection (see Figure 4.12). The aggregator attempts to maintain the power flow from this substation at a constant level – the grid connection limit - following the event-based multi-layer scheduling approach outlined in section 3.4.

Connected EVs are constantly monitored and assessed in terms of suitability for receiving or supplying power using the CW and DCW weighting in subsection 3.4.1. For train departure events (EVs are discharged to provide traction power), the aggregator prioritises EVs with high battery capacity, high maxi-

imum discharging rate and high SOC. For arrivals (EVs charge to absorb power from regenerative braking), EVs with high capacity, high maximum charge rate and low SOC are prioritised. All EVs are assumed able to charge or discharge without any hardware or software restrictions (no V2G opt-outs or other EV user control as discussed in chapter 5).

The scheduling strategy differentiates between 'in-event' periods (i.e. times of power transfer between the EV population and the rail system) and periods without rail traffic. When no rail traffic occurs the EV population makes use of the shared grid connection for smart charging where each EV receives a minimum of 1 kW plus a share of the remaining available power corresponding to its ranking (see subsection 3.4.5).

During events, the aggregator assigns EVs sequentially to charge/discharge at the maximum possible rate until the power drawn from the substation matches the pre-determined grid connection limit. The degree to which the V2G network can decouple the power demands of the rail system from grid connection mainly depends on the following three parameters: the EV population size, the global charging rate limit (the maximum charging rates supported by the EV chargers) and the anticipated grid connection limit.

The power demands from the rail system are assumed to be fixed - failure by the V2G network to serve train events does not result in feedback, affecting the rail system model. Should the connected EV population and the substation not be able to supply sufficient traction power for a train departure under the grid connection limit, the aggregator draws excess power from the grid regardless, but train acceleration is not affected. Similarly, if the EV connection cannot fully absorb power from regenerative braking during a train arrival event, train deceleration is not affected.

Three main factors determining the performance of R2REE were identified and are individually examined through multiple simulations: the EV population size, the EV charging rates and the power made available to the whole system through the shared power grid connection.

*Full simulation results for every scenario discussed below can be found in appendix Appendix A5.*

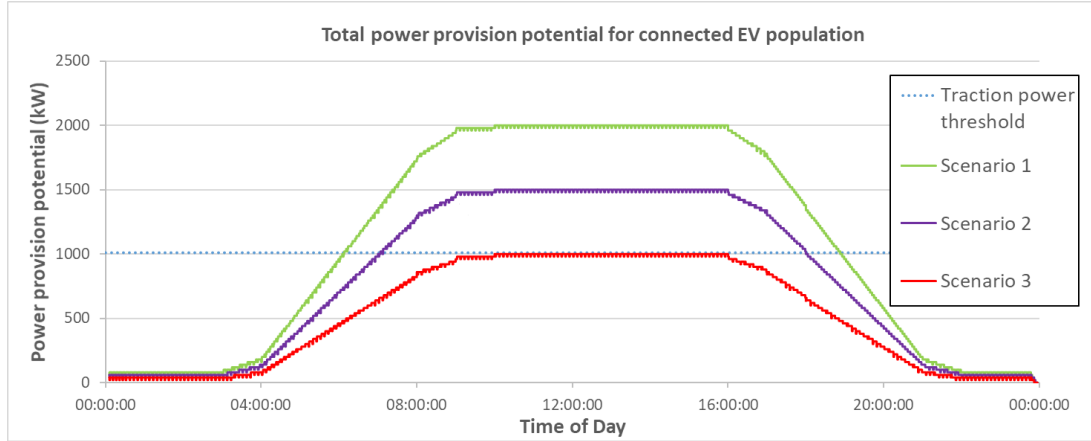


Figure 4.16: Total power provision potential of EV populations of varying size over 24 hours.

#### 4.4.1 Size of EV population

The first major factor influencing the performance of the proposed V2G system is the size of the connected EV population (i.e. the number of EVs connected). To investigate this, the 24-hour system operation was simulated using EV populations of up to 100, 75 and 50 EVs (recall that all EVs here are modelled after the Nissan Leaf, see section 3.6) respectively while the global charging rate limit (the maximum charging and discharging rate supported by all bi-directional chargers) and the grid connection limit remained constant at 20 kW and 200 kW respectively. The latter two parameters will be altered in subsequent simulations.

- Scenario A: 100 EVs
- Scenario B: 75 EVs
- Scenario C: 50 EVs

Figure 4.16 shows the potential aggregated power output from the V2G network over time in each of the 3 Scenarios (i.e. the sum of the maximum rate at which all EV can be discharged). As the global discharging limit of 20 kW is well below the possible power output of any simulated EVs (the Nissan Leaf has a nominal drive train power of 112 kW, at no time is any of the EVs fully discharged), the aggregated potential power output of the system is equal to 20 kW times the number of EVs connected at any time.

The V2G network is considered capable of fully powering a train departure event whenever the power provision potential exceeds the threshold of 1,009 kW (i.e. the peak power demand of the train departure event). As seen in Figure 4.16, in scenarios A and B the system exceeds this threshold from about 06:00 to 19:00 (a period covering 95 of the 117 daily train departures, or roughly 81 %) and 07:00 to 18:00 (covering 85 departures, or about 73 %) - during these periods, train traction power could be provided entirely from discharging the connected EV population, completely eliminating any power demand peak by the local power grid.

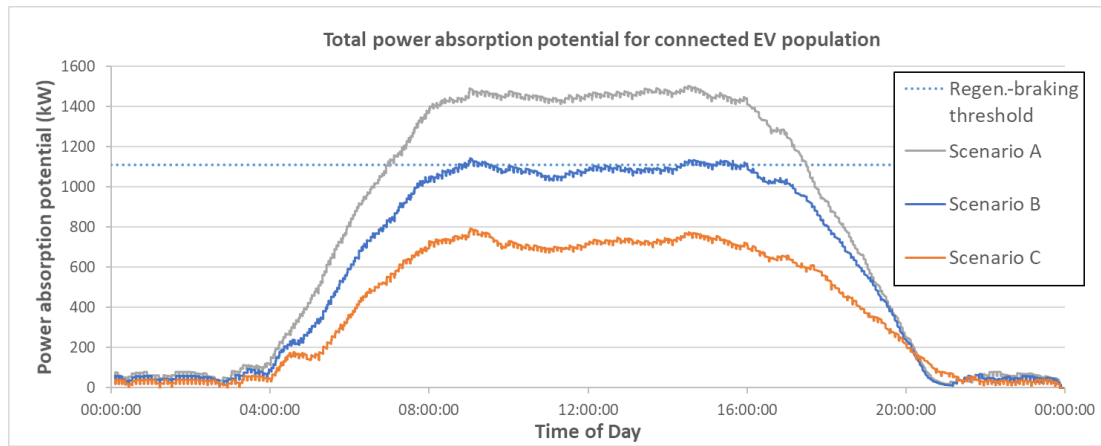


Figure 4.17: Total power absorption potential of EV populations of varying size over 24 hours.

Figure 4.17 shows the V2G network's potential for receiving power over time (i.e. the sum of all EVs maximum charging rate at any point in time, limited to the global charging limit of 20 kW). For each EV the maximum charging power that can be received is dependent on its current SOC as per Figure 4.15 (and may fall way short of the 20 kW supported by the EV chargers in these scenarios).

For the V2G network to be capable of fully absorbing power from regenerative braking on the rail system, the aggregated power absorption potential has to exceed the threshold of 1,109 kW (i.e. the peak of output of the rail system during a train arrival event). As seen in Figure 4.17, this threshold is not reached at any point in scenario C (EV population up to 50 EVs) and only during short periods during scenario B (up to 75 EVs). Only in scenario A (up to 100 EVs) is the V2G network capable of fully absorbing regenerative braking power for an extended period (about 7:00 to 18:00, covering 85 of the 117 train arrivals, or roughly 73 %).

Comparing figures 4.16 and 4.17 it should be noted that whenever the power absorption potential of an EV population exceeds the threshold to fully absorb power from a train's regenerative braking, the power provision potential also exceeds the threshold for fully providing traction power. Recalling that 1) the regenerative braking threshold is of a larger magnitude than the traction power threshold and that 2) for each EV the maximum discharging rate is always equal to or greater than the maximum charging rate, it follows that, within this work, any EV population capable of fully absorbing regenerative braking energy from an arrival event is also capable of fully providing traction power for a departure event. Hence any further analysis below will exclude the power provision potential of EV populations.

One rather obvious conclusion from this system-wide analysis is that R2REE performs better (or covers more train departure/arrivals) the larger the size of the connected EV population. This is of course expected and true for most, if not all, V2G applications - the availability of EVs however, is not a controlled design variable, but depends on future developments regarding EV ownership amongst the general public and the behaviour of EV users (e.g. will EV users bother to connect to the network while parked?).

Another issue regarding EV availability is its distribution throughout the day. Even when the busiest periods on the rail system are well covered by available EVs, trains in the early and late hours still rely mainly on traction power from



the power grid.

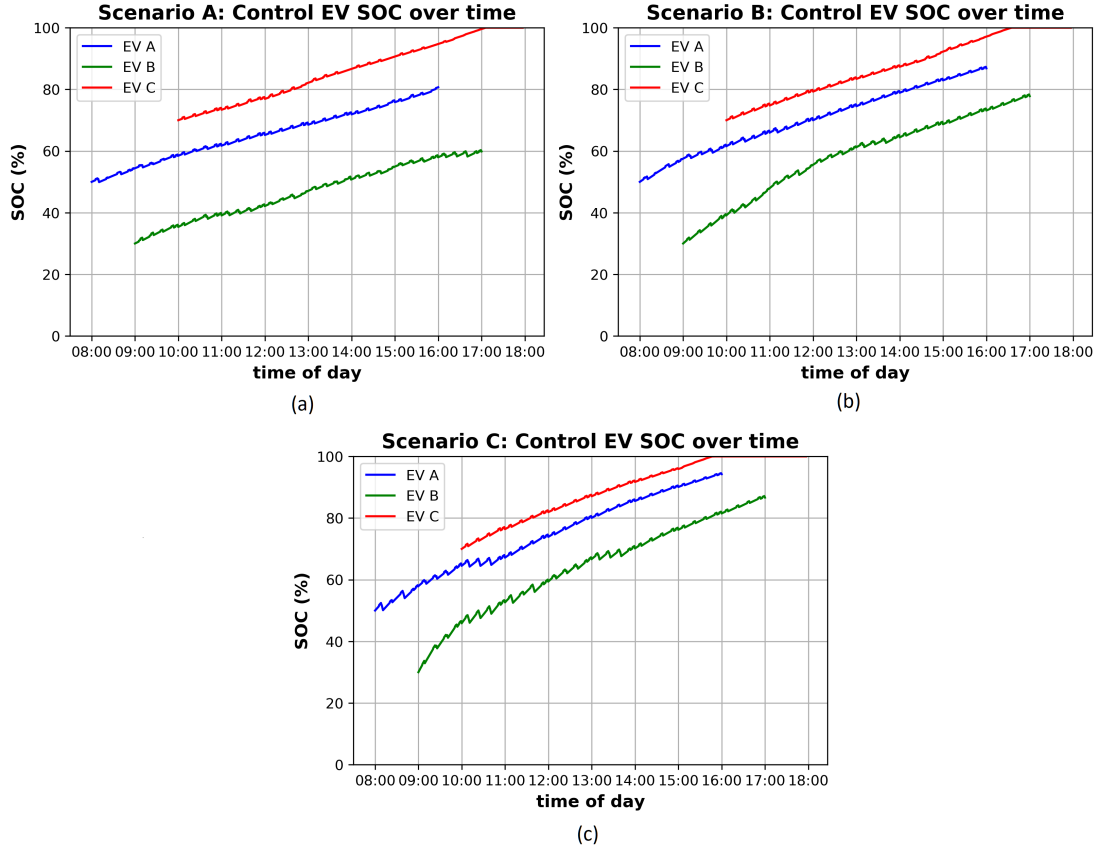


Figure 4.18: Changes in SOC over time of the three control EVs within EV populations of varying size: (a) 100 EVs, (b) 75 EVs, (c) 50 EVs.

Nonetheless, for long periods of the day, covering most train arrivals and departures R2REE would reduce peak demand stresses on the local power grid and enable brake energy recovery. As EVs are charged from the rail systems existing power grid connection, it would also reduce upgrade requirements for new EV charging infrastructure (which would require its own grid connection otherwise).

If the availability of EVs could be reliably expanded in the early and late hours - for example by expanding the V2G network to include EVs parked overnight in nearby residential areas - R2REE *may* also lower grid connection upgrade requirements for any new rail electrification projects (i.e. a rail system that would usually require a substation capable of providing more than a megawatt

Control EV	SOC at departure (Scenario A)	SOC at departure (Scenario B)	SOC at departure (Scenario C)
EV A	81 %	87 %	93 %
EV B	60 %	78 %	86 %
EV C	100 % (at ~17:00)	100 % (at ~16:30)	100 % (at ~15:45)

Table 4.3: Comparison of Control EV battery pack SOC at departure time for EV populations of varying sizes

may instead be powered through a grid connection rated at half a megawatt). This is however a rather risky proposition to rely upon.

Figure 4.18 shows how the SOC develops over time for the three control EVs in each scenario, indicating the V2G network’s ability to serve the purpose of charging connected EVs over time. Table 4.3 below shows the final SOC values for each control EV. In any of the three scenarios, each control EV significantly gained in SOC. As expected, given that the grid connection limit was fixed at 200 kW for all three scenarios (limiting how much power can be shared between EVs during smart charging periods), the SOC gains per EV are higher at lower EV population sizes.

#### 4.4.2 Maximum EV charging rates

The next factor influencing system performance is the system-wide maximum charging rate of connected EVs. Each EV has an individual maximum charging rate at any given time (depending mainly on its’ SOC, see Figure 4.15), but is also subject to the maximum charging rates supported by the bi-directional chargers that each EV is connected to.

In this analysis, the latter is assumed to be constant and equal for each EV (i.e. each EV is connected to identical bi-directional chargers) and referred to as the global charging rate limit (per EV). Similar to the previous analysis, the 24-hour system operation was simulated multiple times while varying the global charging rate limit between 50 kW, 35 kW and 20 kW respectively. The EV population size was 75 EVs and the grid connection limit was 200 kW for each simulation.

- Scenario D: 50 kW global charging rate limit
- Scenario E: 35 kW global charging rate limit

- Scenario B: 20 kW global charging rate limit (same scenario as in previous discussion)

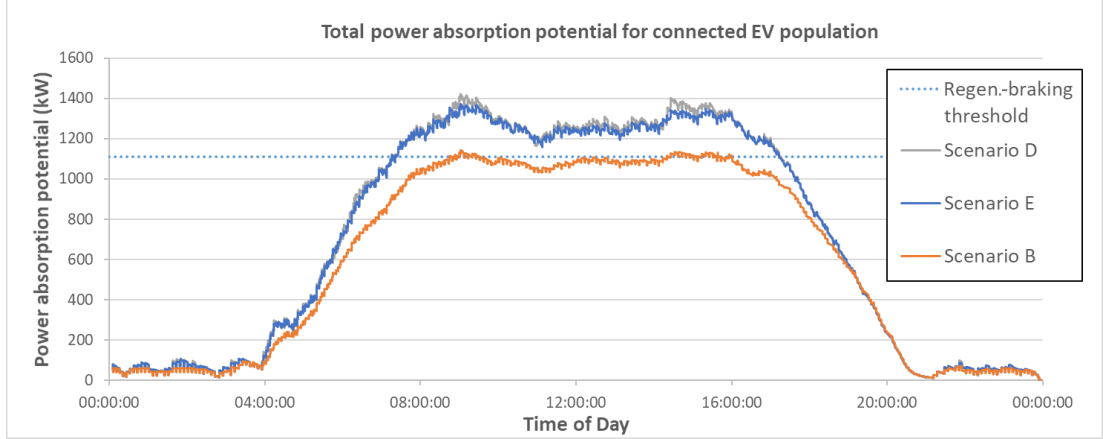


Figure 4.19: Total power absorption potential of the connected EV population with varying global charging limits over 24 hours.

As seen in Figure 4.19. The difference in power absorption potential between scenarios D and E is fairly insignificant. This is due to the maximum charging rates of individual EVs dropping below the global charging rate limit as SOC increases (i.e. EVs can only utilise higher global limits while the SOC is low). The power absorption potential in scenario B is clearly lower and only meets the threshold sporadically. However, the impact of the global charging limit on the power absorption potential appears to be only moderate suggesting that even lower-end charging hardware may be sufficient for this V2G application.

Analogous to the previous discussion, Figure 4.20 shows the changes in SOC over time and Table 4.4 shows the final SOC for the three control EVs. Comparing the three scenarios, it can be seen that changing the global charging rate limit had very little impact on the control EVs.

This can be attributed to the short duration of train arrival and departure events – EV charging and discharging rates approaching the global limit only occur close to peak power regeneration or peak power demand on the rail system. During periods of no rail traffic (nearly 80 % of the day) EV charging rates are typically well below the global limit.

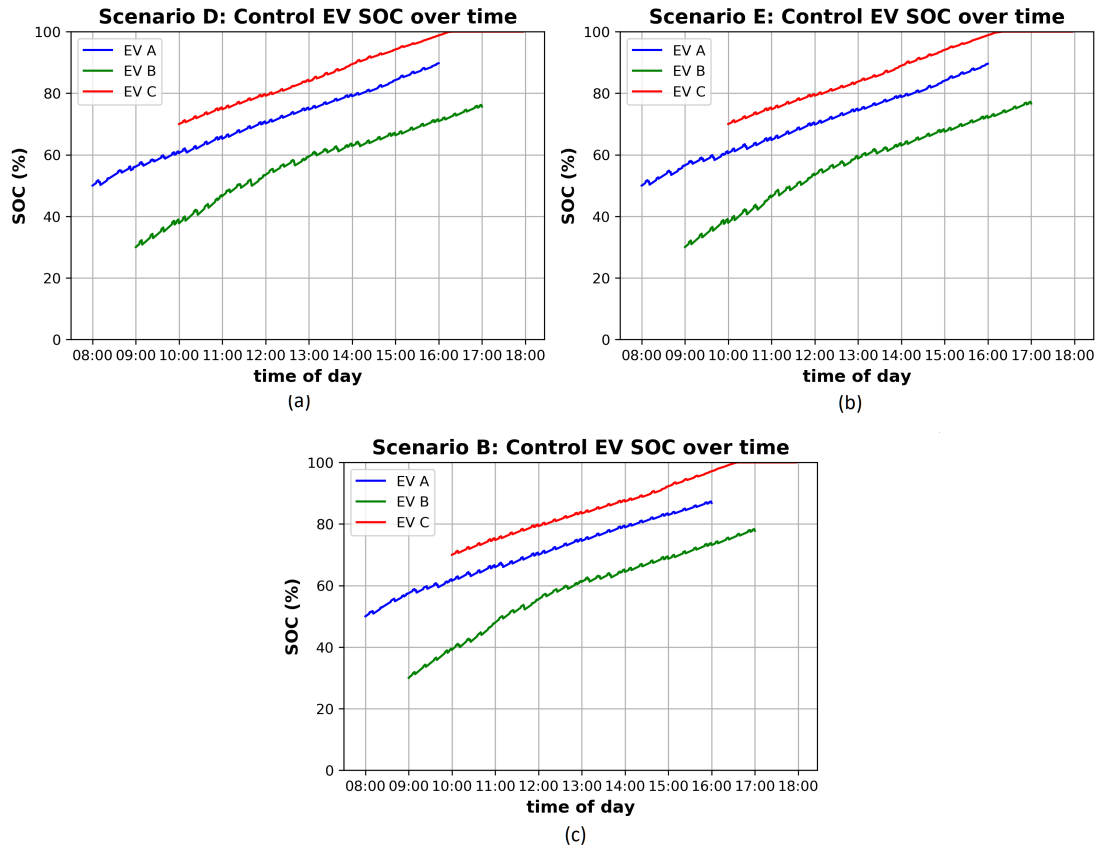


Figure 4.20: Changes in SOC over time of the three control EVs within the connected EV population with varying global charging limits over 24 hours.

#### 4.4.3 Grid connection limit

The last factor influencing system performance to be examined in this work is the power made available to the whole system (rail and EVs) via the shared grid connection. For an initial assessment of how this influences the R2REE network, the previous set of scenarios, in which global charging limits were varied between simulations, is repeated, but instead of the 200 kW grid connection limit from before, 300 kW is now made available.

- Scenario F: 50 kW global charging rate limit
- Scenario G: 35 kW global charging rate limit
- Scenario H: 20 kW global charging rate limit

Control EV	SOC at departure (Scenario D)	SOC at departure (Scenario E)	SOC at departure (Scenario B)
EV A	88 %	88 %	86 %
EV B	76 %	77 %	78 %
EV C	100 % (at ~16:10)	100 % (at ~16:10)	100 % (at ~16:30)

Table 4.4: Comparison of Control EV battery pack SOC at departure time for different global charging rate limits

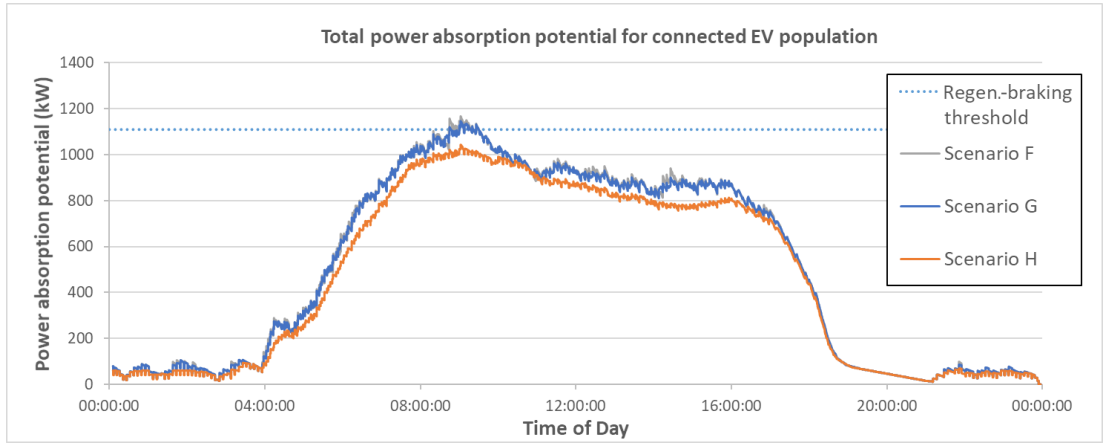


Figure 4.21: Total power absorption potential of the connected EV population with varying global charging limits over 24 hours.

Comparing the resulting power absorption potentials for these scenarios (Figure 4.21) with the previous results in (Figure 4.19) reveals that the V2G network significantly underperforms in the new set of scenarios - despite featuring the same EV population size with identical initial conditions. The power absorption potential reaches a peak at around 09:00 (about the time at which the car park first reaches its peak occupancy) and continues to drop afterwards despite the number of connected EVs remaining steady until about 16:00.

From SOC developments of the control EVs in Figure 4.22 it becomes apparent that 1) as before, the differences in global charging rates makes little difference between scenarios and 2) that EVs were charged significantly faster than in the previous set of simulations.

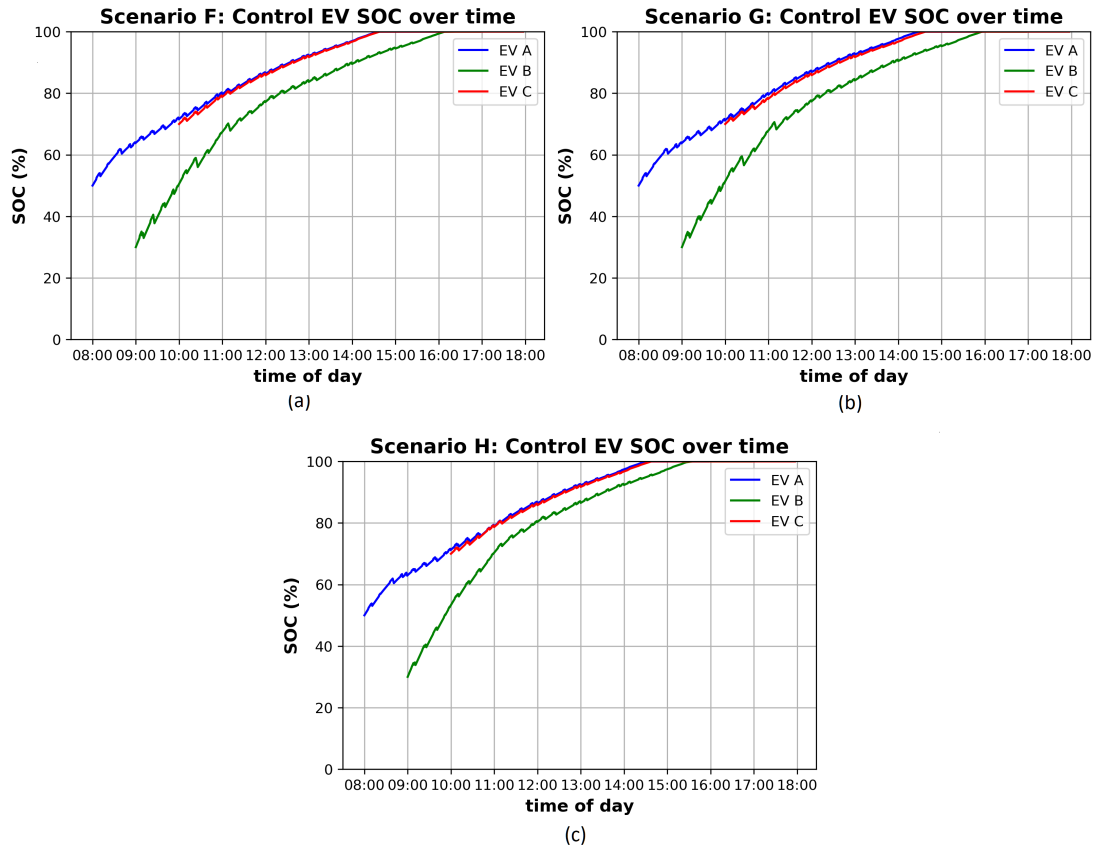


Figure 4.22: Changes in SOC over time of the three control EVs within the connected EV population with varying global charging limits over 24 hours.

To further examine this behaviour in more detail, the 24-hour system operation was simulated several times while varying the grid connection limit between 200, 300, 400 and 500 kW respectively. EV population size was kept constant between simulations at 100 EVs and the global charging limit per EV was set to 20 kW.

- Scenario A: 200 kW grid connection limit (same scenario as in previous discussion)
- Scenario I: 300 kW grid connection limit
- Scenario J: 400 kW grid connection limit
- Scenario K: 500 kW grid connection limit

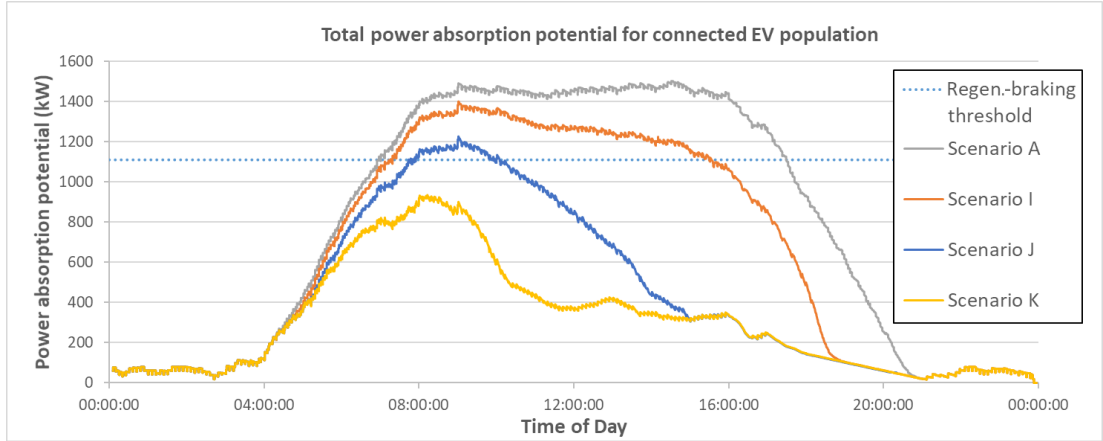


Figure 4.23: Total power absorption potential of 100 EVs at varying grid connection limits over 24 hours.

As can be seen in Figure 4.23, increasing the grid connection limit significantly impedes on the ability of the aggregated EV population to absorb power from the rail system. It should be noted that this impact on the power absorption potential is more pronounced in the afternoon/evening than in the early hours of the day. As the rail system's power demand remains unaltered between scenarios, any increases in the power made available to the system leads to increased EV charging rates and thus faster gains in SOC for connected EVs. However, recall from Figure 4.15 that the maximum charging rate for individual EVs decreases as the SOC increases. Consequently, the power absorption potential of the aggregated EV population declines not only when some EV batteries are fully charged, but as they approach higher SOC levels.

Examining SOC developments of the control EVs in Figure 4.24 as well as Table 4.5 confirms the previous observations. As expected, the controls EVs are charging faster as the grid connection limit increases. In scenario K, with the highest simulated grid connection limit of 500 kW, all three control EVs are already fully charged well before midday. While fully charged EVs can no longer absorb power from the rail system's regenerative braking, they are still useful to supply traction power during train departure events.

In summary, this chapter has introduced a novel V2G application in which aggregated parked EVs are charged and discharged to support nearby DC-powered rail systems. Three main factors determining the performance of R2REE were identified: the EV population size, the EV charging rates and the power made

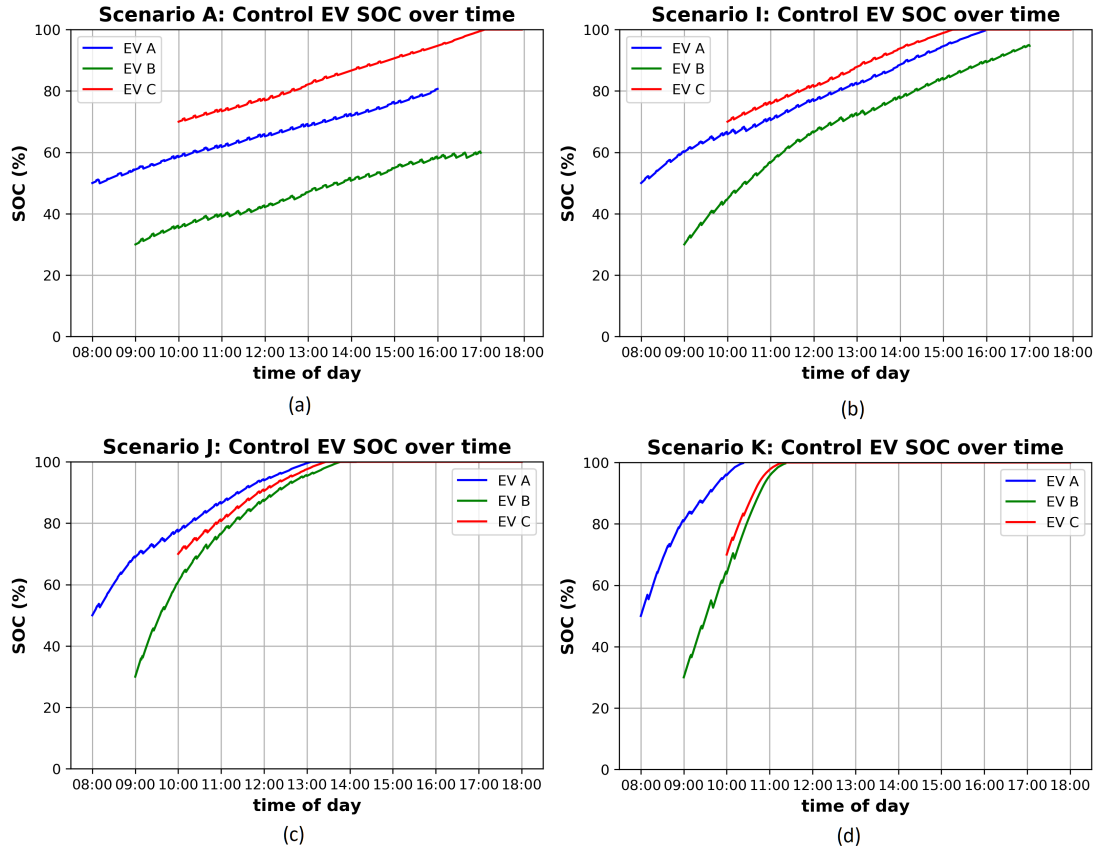


Figure 4.24: Changes in SOC over time of the three control EVs within an EV population of 100 EVs at varying grid connection limits over 24 hours.

available to the whole system through the shared power grid connection.

Unsurprisingly, the V2G network performs better with larger EV populations although the limited availability of EVs in the early and late hours of the day is major issue impeding on both power provision and power absorption potential. Rail traffic in the early morning and late evening/night cannot be fully supported with an EV population as modelled within this work. Potential solutions may be an expansion of the EV population (rather than focusing on one central car park, the aggregator may also oversee nearby residential/commercial parking lots with EVs parked overnight) or treating R2REE as temporary support of the rail system (perhaps as part of a hybrid energy storage solution).

It was found that individual EV charging rates, in particular, the diminishing maximum charging rates associated with increases in SOC, have a more signif-



Control EV	SOC at departure (Scenario A)	SOC at departure (Scenario I)	SOC at departure (Scenario J)	SOC at departure (Scenario K)
EV A	81 %	100 % (at ~15:50)	100 % (at ~13:00)	100 % (at ~10:20)
EV B	60 %	94 %	100 % (at ~13:40)	100 % (at ~11:20)
EV C	100 % (at ~17:10)	100 % (at ~15:15)	100 % (at ~13:20)	100 % (at ~11:15)

Table 4.5: Comparison of Control EV battery pack SOC at departure time for different grid connection limits

ificant impact on the performance of R2REE than the global (i.e. system-wide) charging rate limits of the bi-directional chargers. The V2G network’s aggregate power absorption potential (determining its ability to absorb power from the rail system’s regenerative braking) decreases as EVs are reaching higher SOC levels. Therefore, a large fraction of low SOC EVs within the EV population is more beneficial to R2REE than having highly rated EV chargers.

The grid connection limit was found to be a very delicate issue as relatively minor adjustments can cripple the V2G system by charging EVs ‘too quickly’ to support regenerative braking. By contrast, the network’s power provision potential (determining its ability to provide traction power for train acceleration) is not negatively affected by higher grid connection limits - thus maintaining significant peak power reduction as long as enough EVs are connected.

## 5. EV OWNER CONTROL OVER V2G SCHEDULING

In the work presented thus far, all EVs have been regarded as fully available for V2G usage while connected to the network. Consequently, connected EVs were assessed purely by the state of the battery pack to inform the scheduling process (see section 3.4). Individual usage scenarios for each EV were not considered leading to sub-optimal utilisation of the connected EV population. Some EVs may be parked for days and do not require to be charged quickly. Other EVs may not be available for discharging as owners need to continue their journey as soon as possible. These shortcomings are addressed in this chapter.

This chapter discusses a novel method of capturing, assessing and accounting for EV user charging preferences in the scheduling process - providing EV users with a degree of control over the V2G usage of their vehicles. This method is built upon and fully compatible with the aggregator control strategy presented in chapter 3. The introduction of EV user preferences puts further constraints on the aggregator but potentially increases the social acceptance of V2G (and thereby EV owner participation) and aids the effective utilisation of individual EVs for grid services. The challenge of maintaining system responsiveness despite the increased computational complexity is addressed by assessing EVs prior to the scheduling process and using the (often idle) resources of the SQL database server. The method is explored in the context of the R2REE model (see chapter 4) but is equally suitable to other V2G applications.

## 5.1 Charging Modes

Range limitations are often mentioned as a major disadvantage of electric vehicles over more ‘traditional’ ICE vehicles. While the argument can be made that limited range is often a perceived, rather than an actual problem for the majority of drivers (see chapter 2), so-called ‘range anxiety’ appears to be one of the reasons for a slow and lacklustre electrification of personal transport [80][81].

As V2G applications involve discharging the battery packs of parked EVs, it is not unreasonable to assume that range anxiety could have a negative effect on the acceptance of V2G technologies (which rely heavily on EV owner participation). EV users may fear a loss of control over the charging process of their EV batteries, which may actually lose charge over short periods due to V2G participation.

While purely anecdotal evidence, comments along the lines of ‘What if I come back to my car and the battery is empty?’ are a common first reaction when introducing laymen to the concept of V2G. Such scepticism towards the technology might be addressed by granting EV owners some control over the usage of their vehicles via some form of control interface.

In its simplest form, this could be a switch within each EV giving users a binary choice of participating in V2G or not. However, such simplicity would offer little benefit to either the EV user or the V2G network. For more complex inputs and more refined EV owner control one might utilise existing user interfaces that are already present in most modern vehicles (see section 2.4).

In this project, users can state charging preferences by selecting one of the available ‘charging modes’ via a simple EV on-board touch-screen user interface (see section 5.2). The charging modes offer range between the two extreme positions of ‘no preference’ (i.e. not limiting V2G usage of an EV beyond any system-wide scheduling rules) to fully opting out of V2G usage (i.e. allowing EVs to be charged only).

Consequently, the choices of individual EV owners have the potential to severely constrain the V2G aggregator and its ability to supply grid services. This, again, highlights the necessity of sufficient financial incentives to EV owners to participate in V2G (see section 2.3) as well as ‘fairness criteria’ [167] when allocating power within the connected EV population (see chapter 2). As these are complex and highly debated fields of research in their own right, such considerations exceed the scope of this project. Thus, the focus lies on the technical implementation of

owner charging preferences in the rest of this chapter.

The available charging modes should not only reflect a binary choice of either accepting V2G usage or opting out completely but should offer options conditional on user defined targets in between. In this work, the following four charging modes have been defined. The EV user can select any charging mode for the vehicle and, if applicable, specify charging targets (target SOC and target date/time).

- 'Free V2G mode' [Mode 1]: The user expresses no preference. Thus, the aggregator can schedule charging and discharging of this particular EV freely (subject only to system-wide scheduling rules). This charging mode is the most beneficial to the aggregator as it applies no further constraints to the usage of this EV.
- 'Quick charge to X % SOC' [Mode 2]: The user expects the EV battery pack to be charged as quickly as possible to a given target SOC. Thus, any discharging is prohibited until the target SOC is met. Afterwards, the EV is available for bi-directional power flow (but must not be discharged below the target SOC).
- 'Quick charge to full' [Mode 3]: The user expects the EV battery pack to be fully charged as quickly as possible while prohibiting any discharging. This effectively removes this EV from V2G usage.
- 'Charge by date/time' [Mode 4]: The user inputs a target date and time by which the EV battery pack should be charged to a given SOC. The EV can be charged or discharged at any time, as long as the target is met.

While additional charging modes with further user inputs and restrictions to the aggregator are feasible (i.e. limiting charging/discharging rates, taking into account electricity prices, etc.), the four modes above should cover the needs of most EV owners and thus form the basis of any following discussion/analysis.

## 5.2 EV communication system user interface

Based on the charging modes presented above, a user interface has been designed that is compatible with the hardware prototype of an EV communication system discussed in the third chapter (see section 3.5). The prototype developed for this

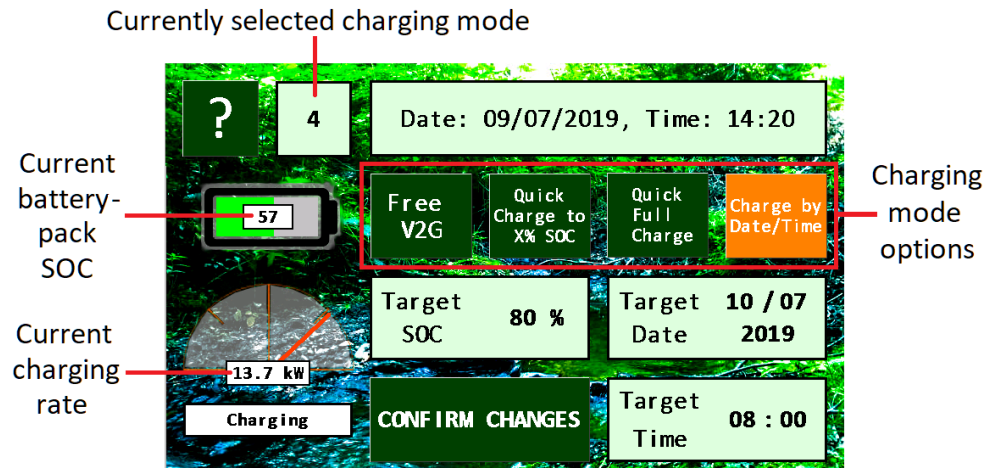


Figure 5.1: EV owner user interface, screen elements

project is equipped with a 7" Nextion Touchscreen Display [191]. This screen was programmed to display the purpose-built user interface.

The 'home screen' of the interface, containing the most relevant information and the current mode selection can be seen in Figure 5.1, with the description page explaining the four charging modes to the EV user shown in Figure 5.2. The interface was created using the proprietary Nextion Editor Software [192].

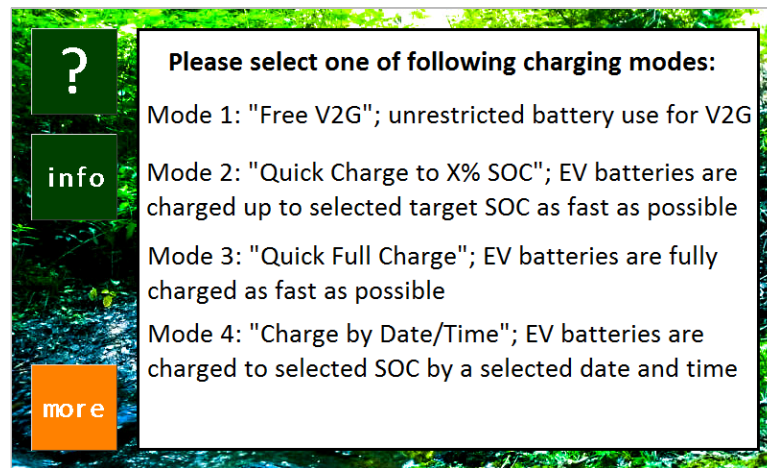


Figure 5.2: EV owner user interface, charging mode description on info page

Like the hardware prototype that it was designed for, the user interface as shown is a rather simple proof-of-concept. Similar interfaces (as well as the EV communication system itself) may be implemented in commercially available EVs as

part of the on-board ‘infotainment’ systems (i.e. multi-media devices used for entertainment, climate control, navigation, etc.). Such systems are commonly available in modern vehicles, and many of which even possess the Wi-Fi capabilities that would be required for EV-to-aggregator communication [87].

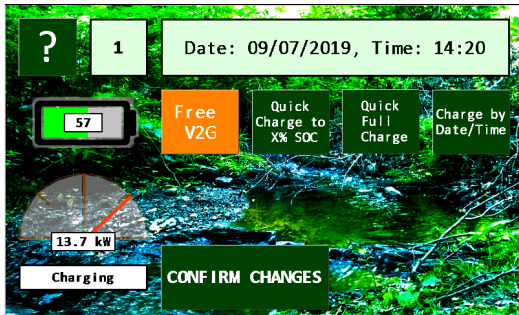


Figure 5.3: EV owner user interface, charging mode 1 selected (no inputs needed)

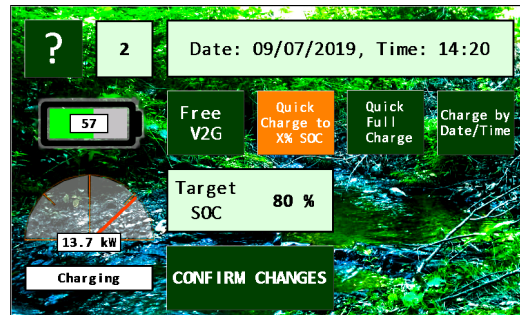


Figure 5.4: EV owner user interface, charging mode 2 selected (target SOC provided)

For any commercial implementation, such an interface should be designed to be easy to understand as well as easy to reach for the average EV owner (i.e. not ‘buried’ within a plethora of other vehicle settings). To address the former, it should be noted that the charging mode definitions as stated are intended for usage within the aggregator control. These modes might be presented differently to the end user.

For example, it is common practice in modern vehicles (either electric or using internal combustion engines) to display an estimate of the remaining range of the vehicle somewhere prominent within the central console. Thus, it may be beneficial to convert SOC targets to range targets, which may be easier to understand - or simply more relevant - to the end user. Consequently, the user input for mode 2 in a commercial EV might be the minimum remaining range required. And mode 4 might be defined by users inputting information on the next journey (i.e. picking a destination on the map and a departure time).

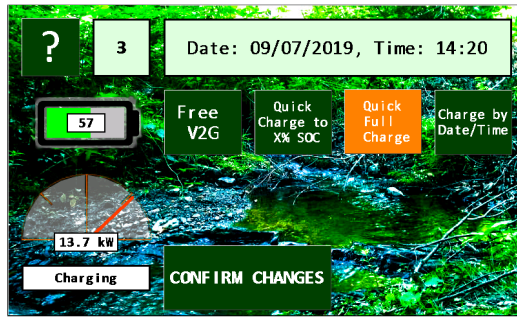


Figure 5.5: EV owner user interface, charging mode 3 selected (no inputs needed)

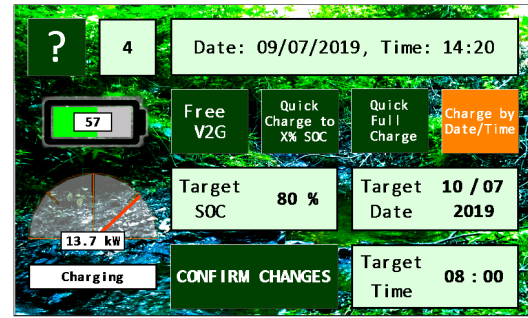


Figure 5.6: EV owner user interface, charging mode 4 selected (target SOC and target date/time provided)

Determining the remaining range of any vehicle (electric or otherwise) is a fairly complex problem in itself and requires information on the driving style and the terrain to be driven on to be accurate. Often such systems estimate the leftover range by assuming the power (or fuel-) consumption of the vehicle will follow the previous averages [219] (potentially with a safety margin so as to not overestimate the range).

While such matters of product design could have an impact on the acceptance and usage of V2G for end users, these are not essential for this project and therefore not included. Similarly, 'convenience features' such as a default selection (i.e. for commuters with the same regular journeys) are not included in the interface created for this project.

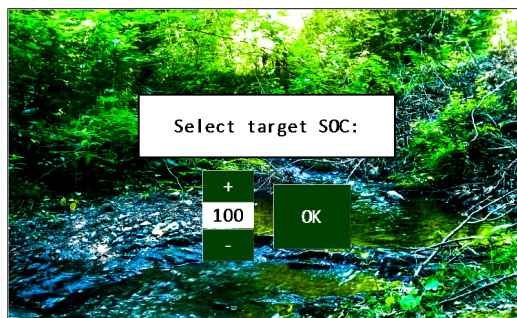


Figure 5.7: EV owner user interface, target SOC selection

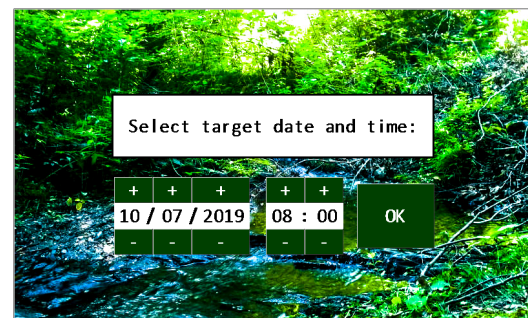


Figure 5.8: EV owner user interface, target date/time selection

In the simplified interface shown, the user can select one of the four pre-defined charging modes from the main screen. Depending on the mode selected, additional windows for the selection of a target SOC and/or target date/time open up (see Figure 5.3 to Figure 5.8).

Once the charging mode selection is confirmed (by touching the ‘confirm’ button), the touch screen (which has its own micro-controller, see section 3.5) transmits the mode selection and selected targets to the Arduino Mega micro-controller board at the centre of the hardware prototype. From that moment the EV communication system will respond to any ‘full information call’ by the aggregator (see section 3.2) with the updated dataset, including the new charging mode selection.

### 5.3 Integration into existing scoring system

Following the definition of charging modes and their integration into the aggregator’s data stream via the user interface/EV communication system, this section discusses how to account for the expressed wishes of EV owners in the scheduling process. From chapter 3 (in particular subsection 3.4.1) recall that the EV assessment happens prior to scheduling (to minimise the impact on system responsiveness) via a scoring system that determines a Charge Weighting (CW) and a Discharge Weighting (DCW) for each EV. CW and DCW were introduced as a measure of the capability of each EV to receive or supply power respectively. CW and DCW were defined as:

$$CW = (100 - SOC) * \frac{Capacity}{Base Capacity} * \frac{Max Charging Rate}{Base Power Rating} \quad (3.1)$$

$$DCW = SOC * \frac{Capacity}{Base Capacity} * \frac{Max Discharging Rate}{Base Power Rating} \quad (3.2)$$

Base Capacity and Base Power Rating are chosen to be 1 kWh and 1 kW respectively (simplifying implementation in database, see section 5.4). These two equations - from here on referred to as the ‘base equations’ - have so far been applied to any EV and depend purely on EV battery pack parameters. The scheduling method defined in chapter 3 prioritises EVs with high CW or DCW values for charging or discharging; this will still be the case after accounting for EV owner



charging preferences. As will be outlined below, the base equations are still used in the updated scoring system but will be subject to certain conditions.

It should be noted that the absolute values of CW and DCW are in themselves meaningless and only serve the purpose of directly comparing multiple EVs in the same population. Further, as was mentioned in chapter 3, equations 3.1 and 3.2 may not be suitable for V2G applications that require to take into account additional parameters (i.e. electricity prices, grid frequency, etc.). Thus the base equations may change if the methods presented in this chapter are to be applied to other V2G applications.

In the updated scoring system the base equations are applied conditionally to each of the four charging modes. Mode 1, the 'Free V2G mode' is the simplest to implement as the aggregator is essentially unconstrained in the usage of this particular EV and only applies global (i.e. system-wide) scheduling rules. Therefore, the CW and DCW for mode 1 follow the base equations 3.1 and 3.2 at all times.

$$CW_{Mode1} = (100 - SOC) * \frac{Capacity}{Base\ Capacity} * \frac{Max\ Charging\ Rate}{Base\ Power\ Rating} \quad (5.1)$$

$$DCW_{Mode1} = SOC * \frac{Capacity}{Base\ Capacity} * \frac{Max\ Discharging\ Rate}{Base\ Power\ Rating} \quad (5.2)$$

For mode 2 ('Quick charge to X % SOC') the usage of base equations is dependent on the current SOC of the EV battery pack as well as the target SOC specified by the EV owner. Assuming that EVs operating under mode 2 are not prioritised while charging but are only exempt from being discharged, the CW follows the base equation at all times. By contrast, the EV usage for discharging under mode 2 is prohibited while the battery pack SOC is below the specified target. Thus, the value for DCW is conditional (two cases):

$$CW_{Mode2} = (100 - SOC) * \frac{Capacity}{Base\ Capacity} * \frac{Max\ Charging\ Rate}{Base\ Power\ Rating} \quad (5.3)$$

$$DCW_{Mode2} = \begin{cases} SOC * \frac{Capacity}{Base\ Capacity} * \frac{Max\ Discharging\ Rate}{Base\ Power\ Rating}, & \text{if } SOC \geq SOC_{target} \\ 0, & \text{otherwise} \end{cases} \quad (5.4)$$

As a result of using the above equations, an EV under mode 2 would not be scheduled to deliver any power while the SOC is below the target SOC. Having a DCW of zero means it would not even be considered for scheduling during any train departure events. However, it could still be used to receive power during train arrival events. Once the EV's SOC exceeds the target, the scheduling is unrestrained.

Mode 3 ('Quick charge to full') also results in a zero value DCW, but unlike the previous mode, this is unconditional. The EV is expected to fully charge and even when full, is not allowed to be discharged. While in effect being the same as a mode 2 selection with a 100 % target SOC, the mode 3 selection removes the necessity to check SOC and target SOC while determining DCW. Charging is unconstrained and therefore CW follows the base equation.

$$CW_{Mode3} = (100 - SOC) * \frac{Capacity}{Base\ Capacity} * \frac{Max\ Charging\ Rate}{Base\ Power\ Rating} \quad (5.5)$$

$$DCW_{Mode3} = 0 \quad (5.6)$$

Finally, mode 4 'Charge by date/time' is the most challenging to implement as it is dependent on both the target SOC as well as the stated departure time. A possible approach might be to determine at which point in time this EV would have to start charging at a fixed rate in order to meet its target SOC at the target time. This time  $T$  could be updated regularly. As the time of scheduling approaches  $T$  and the target SOC is not reached, this EV may then be constrained to charging only.

Such an approach might be suitable for various V2G applications but raises two issues in the context of R2REE. First, determining  $T$  adds computational complexity, especially if done – like for all other modes - via ‘update’ SQL trigger (i.e. each time a corresponding EV dataset is updated, see section 5.4). Secondly, in the R2REE model as defined in chapter 4, the availability of a constant charging rate cannot be guaranteed at all times.

Consequently, the implementation of mode 4 follows a simpler, although not always optimal approach. Put simply, the EV is treated as if it were charging under mode 2 if the target time is close to the time of scheduling (i.e. discharging prohibited,  $DCW = 0$ ) but treated as an EV under mode 1 (unconstrained) if the target time is in the relatively distant future.

The threshold is set to be a time difference of six hours between the time of scheduling and the target time – a relatively long time to constrain EV usage by the aggregator, but one which (in most cases) ensures that a charging target is reached (see section 5.5). For the CW and DCW equations, this results in an unconditional CW following the base equation and a conditional (three cases) DCW equation:

$$CW_{Mode4} = (100 - SOC) * \frac{Capacity}{Base\ Capacity} * \frac{Max\ Charging\ Rate}{Base\ Power\ Rating} \quad (5.7)$$

$$DCW_{Mode4} = \begin{cases} SOC * \frac{Capacity}{Base\ Capacity} * \frac{Max\ Discharging\ Rate}{Base\ Power\ Rating}, & \text{if } SOC \geq SOC_{target} \\ \begin{cases} SOC * \frac{Capacity}{Base\ Capacity} * \frac{Max\ Discharging\ Rate}{Base\ Power\ Rating}, & \text{if } T_{target} \geq T_{now} + 6h \\ 0, & \text{otherwise} \end{cases} \end{cases} \quad (5.8)$$

## 5.4 SQL triggers

The scoring system previously defined to account for EV user inputs is integrated into the aggregator control using so-called SQL triggers within the database (following the same approach detailed in chapter 3; in particular subsection 3.4.1). A SQL trigger is a pre-defined stored procedure in an SQL database [220] that

is executed automatically when a relevant dataset is manipulated. Trigger conditions can be the insertion of a new data entry, the deletion of an existing entry or an update to an existing entry [221].

The procedures shown below are applied to both, data insertion and data updates. In the context of the V2G aggregator control, this means that CW and DCW are (re-)evaluated whenever the data collection module (see section 3.2) adds a new EV dataset (i.e. a new EV connects to the network) or updates an existing EV dataset (i.e. new data on an existing EV is available).

Using SQL triggers decouples the determination of CW and DCW from the data collection and the scheduling processes (both are time-sensitive processes and their execution times have a major impact on overall system responsiveness). Instead, the computational resources of the SQL database server are used (which is often idling, waiting for queries from the main processes).

The first trigger procedure, referred to as the default SQL trigger for the rest of this chapter, is a simple unconditional implementation of the base equations 3.1 and 3.2 in SQL syntax. It does not take into account any user inputs to determine CW and DCW. This procedure was used for all simulations presented in previous chapters:

```

1 SET new.CW = (100-new.SOC)*(new.Capacity)*(new.
    ↪ MaxChargingRate), new.DCW = (new.SOC)*(new.
    ↪ Capacity)*(new.MaxDischargingRate);

```

Note that parameters base capacity and base power rating were omitted from the SQL implementation of the CW/DCW equations. As these were chosen to be 1 kWh and 1 kW respectively, the resulting factors of 1 are redundant within the SQL trigger.

To account for user charging preferences the second 'enhanced' set of SQL triggers is used instead. It differentiates between the 4 charging modes presented in this chapter:

```

1 IF (new.mode = '1') THEN #Use base equations
2   SET new.CW = (100-new.SOC)*(new.Capacity)*(new.
    ↪ MaxChargingRate), new.DCW = (new.SOC)*(new.
    ↪ Capacity)*(new.MaxDischargingRate);

```

```

3
4 ELSEIF (new.mode = '2') THEN #If target SOC exceeded
    ↪ use base equations, otherwise charge only
5     IF (new.SOC > new.TargetSOC) THEN
6         SET new.CW = (100-new.SOC)*(new.Capacity)*(new
    ↪ .MaxChargingRate), new.DCW = (new.SOC)*(new.
    ↪ Capacity)*(new.MaxDischargingRate);
7     ELSE
8         SET new.CW = (100-new.SOC)*(new.Capacity)*(new
    ↪ .MaxChargingRate), new.DCW = 0;
9     END If;
10
11 ELSEIF (new.mode = '3') THEN #Charge only
12     SET new.CW = (100-new.SOC)*(new.Capacity)*(new.
    ↪ MaxChargingRate), new.DCW = 0;
13
14 ELSEIF (new.mode = '4') THEN #If target SOC exceeded
    ↪ use base equations, otherwise check time
    ↪ available until target
15     IF (new.SOC > new.TargetSOC) THEN
16         SET new.CW = (100-new.SOC)*(new.Capacity)*(new
    ↪ .MaxChargingRate), new.DCW = (new.SOC)*(new.
    ↪ Capacity)*(new.MaxDischargingRate);
17     ELSEIF (new.TargetDateTime > (NOW() + INTERVAL 6
    ↪ HOUR)) THEN #Is target datetime more than 6
    ↪ hours away? Then use base equations, otherwise
    ↪ charge only
18         SET new.CW = (100-new.SOC)*(new.Capacity)*(new
    ↪ .MaxChargingRate), new.DCW = (new.SOC)*(new.
    ↪ Capacity)*(new.MaxDischargingRate);
19     ELSE
20         SET new.CW = (100-new.SOC)*(new.Capacity)*(new
    ↪ .MaxChargingRate), new.DCW = 0;
21     END If;
22 END IF

```

If 'Mode 1' is selected, no preferences/targets are given and the CW/DCW equations used are identical to those in the default SQL trigger procedure.

In case ‘Mode 2’ is selected, any discharging is disabled while the EV’s SOC is below the user’s set target. This is done by setting DCW to zero, meaning this EV will not be considered for discharge by the scheduling module (its data will not be passed on to the scheduling process as only EVs with a non-zero CW or DCW appear in SQL queries by the scheduling module, see section 3.4).

Similarly, if ‘Mode 3’ is selected, DCW is set to zero, although this is not conditional on the EV’s SOC. Hence, this EV would not be considered for any discharging through the aggregator.

Finally, ‘Mode 4’ represents the most complex trigger condition as it depends on the EV’s SOC and the target-time by which a target SOC is to be reached. In case the EV’s current SOC already exceeds the target SOC, this EV is treated as if no constraints apply, so the base equations 3.1 and 3.2 are applied to determine CW and DCW. The same is true in cases in which the stated target time is further than six hours away (as defined in the previous section).

It is assumed that the V2G network is set up and enough power is available to ensure that any connected EV receives a net charge over time and therefore no restrictions need to be applied to the discharging of an EV under Mode 4 this long before the target time. In the final case where the target SOC is not reached and the target time is closer than six hours, discharging is disabled by setting DCW to zero.

### 5.5 *R2REE simulations with enabled EV owner charging preferences*

This section investigates the effects of enabling EV owner charging preferences on both the EV population and the V2G network’s ability to support the connected rail system. For this purpose, several simulations of 24-hour R2REE operation were undertaken with and without considering EV user inputs during scheduling. The simulations discussed below are similar to those in the previous chapter in using the same EV population model for the ‘bulk’ of simulated EVs (see section 4.3) as well as the same rail system model (see section 4.2).

*Full simulation results for every scenario discussed below can be found in appendix Appendix A6.*

Scenario	Grid Connection Limit (kW)	User inputs
I	200	enabled
II	300	enabled
III	400	enabled
IV	200	disabled
V	300	disabled
VI	400	disabled

Table 5.1: Scenario definitions

### 5.5.1 Control EV and scenario definitions

To examine the effect of EV user inputs, six different scenarios were simulated. In each scenario, the same 24-hour period with identical rail power demand and an identical EV population (up to 100 simulated EVs) was used and the aggregator control system was operating in real-time. Unlike the simulations in the previous chapter, only the grid connection limit was altered (200 kW, 300 kW or 400 kW) while the global charging limit remained constant at 50 kW between scenarios - representing the upper limit considered in the previous chapter (chosen here to highlight differences between EVs charging under different modes).

For each grid connection limit, one simulation ignored user-inputs (CW and DCW are calculated within the database using the default SQL triggers) while another one took user-inputs into account during scheduling (using the enhanced SQL triggers instead). The six resulting scenarios are defined in Table 5.1. To avoid confusion between these simulations and those from the previous chapter scenarios are numbered using Roman numerals here.

Among the simulated EVs were six control EVs - each with 40 kWh capacity and a maximum charging rate of 50 kW (the equivalent of a 2019 model Nissan Leaf). These control EVs were initialised with the user charging preferences and initial conditions shown in Table 5.2. All EVs disconnected from the network simultaneously at 18:00 in each scenario. The control EVs were monitored throughout the simulation and charging rates, as well as changes in SOC over time, were recorded.

The ‘bulk’ of the simulated EV population consists of random EV models (see Table 3.2), initialised with randomised initial conditions and user charging pref-

Control EV Name	Initial SOC	Connection Time	Charging Mode	Charging Target
EV A	50 %	08:00:00	1	-
EV B	40 %	08:00:00	2	70 % SOC
EV C	20 %	09:00:00	2	90 % SOC
EV D	40 %	09:00:00	3	-
EV E	40 %	10:00:00	4	80 % SOC at 18:00:00
EV F	20 %	10:00:00	4	90 % SOC at 13:00:00

Table 5.2: User charging preferences of Control EVs

erences (using ‘seeded’ random number generation to ensure identical EV populations between simulations, see section 3.6).

An exception to the aforementioned randomisation of user preferences is the selection of ‘target time’ and ‘target date’ (both only relevant when mode 4 is selected): the target date was set to be the date of the simulation (to avoid unrealistic circumstances where several EVs are assumed to be parked for excessive periods) and the target time was constrained to be after the EVs connection time. However, no mitigation for ‘unrealistic’ charging expectations was implemented (for example an EV requesting to charge from 20 % SOC to 80 % within a minute).

### 5.5.2 Simulation results

The first set of simulations to be considered here are scenarios I and IV. In both scenarios the grid connection limit was set to 200 kW - the lowest within the simulations discussed in this chapter (thus the least power available for EV charging). In scenario I user inputs were enabled, whereas scenario IV disregarded user inputs (thus this simulation was akin to those undertaken in chapter 4).

Comparing the SOC developments of the control EVs shows a stark contrast between the scenarios. In scenario IV all EVs are ‘treated equally’ by the aggregator (all control EVs are charged overtime at similar rates, see Figure 5.10). Recall that all control EVs are of the same model and therefore the only difference between them (when user charging preferences are ignored) is the SOC at any given moment. Thus, the EV trajectories of any two control EVs in scenario IV do not ‘cross’ or ‘overtake’ one another at any point (the order from highest to lowest SOC between control EVs never changes).



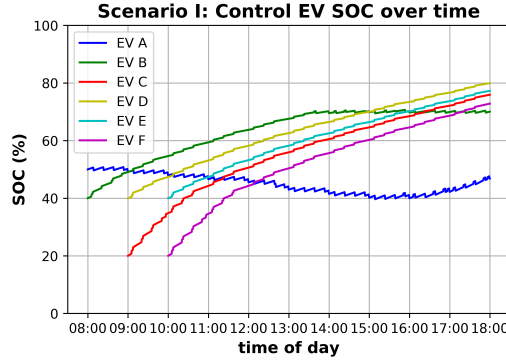


Figure 5.9: Scenario I: changes in SOC for all control EVs while connected

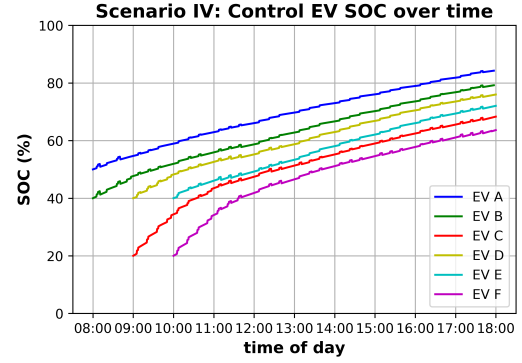


Figure 5.10: Scenario IV: changes in SOC for all control EVs while connected, user charging preferences disabled

By contrast, in scenario I two EVs immediately stand out. In Figure 5.9, EVs A and B show significantly different trajectories once the charging preferences of EV users are taken into account. All other control EVs follow similar trajectories to those in scenario IV. Comparing the final SOC for each control EV between both scenarios (see Table 5.3) reveals that EVs A and B both ‘lost’ SOC whereas other control EVs ‘gained’ SOC once user charging preferences were taken into account.

Scenario	EV A	EV B	EV C	EV D	EV E	EV F
I	46.85	70.06	75.93	79.95	77.29	72.84
IV	84.27	79.21	68.32	76.00	72.07	63.65
Change	-37.42	-9.15	7.61	3.95	5.22	9.19

Table 5.3: Comparison between scenarios I and IV, SOC (in %) of EVs at 18:00

EV A, which is using charging mode 1 (‘Free V2G’) is seen to actually lose charge over the first seven hours after connecting to the network in scenario I (see Figure 5.11). Only for about the last two hours before disconnecting the EV is gaining charge - although not enough to compensate for the previous SOC decline. Thus EV A’s SOC at 6 pm (46.85 %) is in fact below its initial SOC (50 %) - making it the only control EV to lose charge over the connection period.

EV A, as the major outlier within the control group, is arguably significantly ‘disadvantaged’ over the other EVs (which points towards the need for fair/ap-

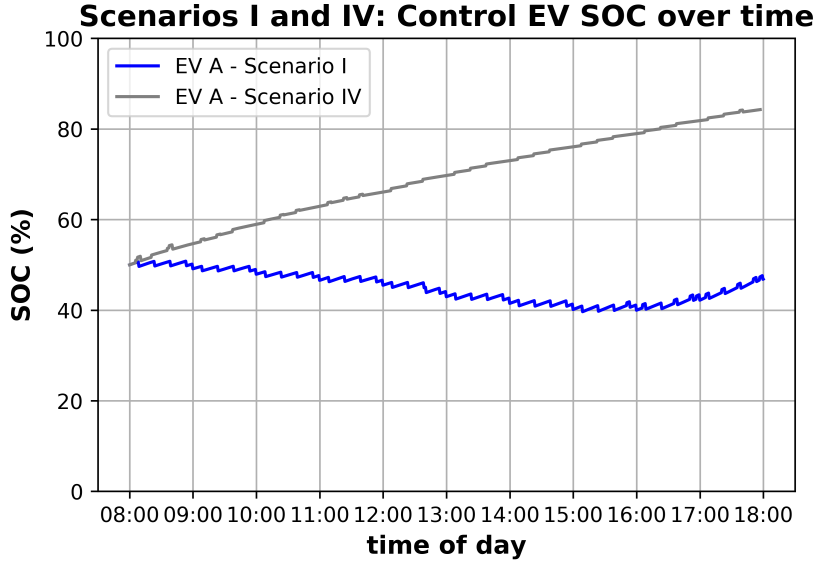


Figure 5.11: Comparison: EV A SOC over time in scenarios I and IV

appropriate compensation to EV owners choosing ‘mode 1’ to encourage V2G participation). However, mode 1 is intentionally unconstrained allowing the aggregator to make full use of an EV operating under this mode; as such, EV A is only subject to global (i.e. system-wide) scheduling rules.

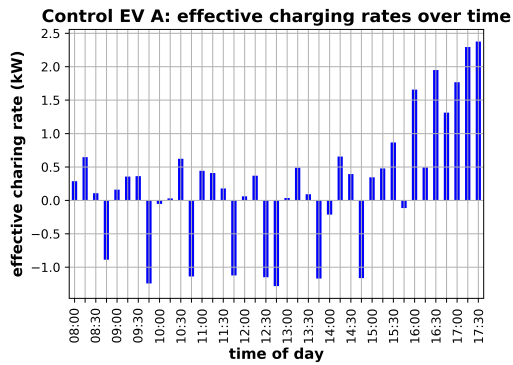


Figure 5.12: Scenario I: EV A effective charging rate over time

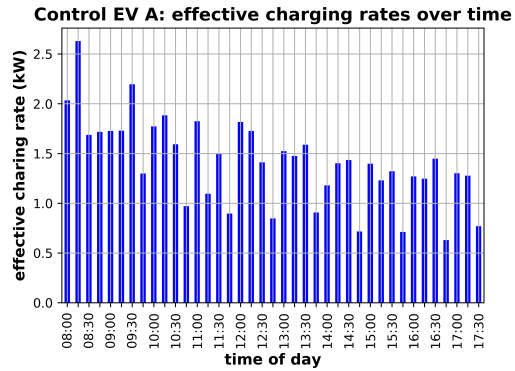


Figure 5.13: Scenario IV: EV A effective charging rate over time

To analyse how EVs were used by the aggregator over the day, the average charging rates over 15-minute timeslots throughout the day were recorded for each control EV (hereafter referred to as ‘effective charging rates’). For EV A these

effective charging rates reveal that, indeed, the aggregator made heavy use of EV A for discharging purposes in scenario I (see Figure 5.12) with several periods of negative average charging rates. In scenario IV, the effective charging rates were positive throughout the day - although slowly declining as EV A's SOC increased, see Figure 5.13.

Can the treatment of EV A be considered 'fair'? On one hand, selecting charging mode 1 (as defined in this work) implies the *unconstrained* usage of an EV through the aggregator - including the possibility of losing charge over time. On the other hand, most EV owners plugging their EV into a (bi-directional) charger for ten hours may very well expect their EV to have a higher range afterwards in any case. This could be remedied through some adjustments within the scheduling like higher minimum charging rates during smart charging periods (i.e. periods without rail traffic, see subsection 3.4.5) or some further constraints in the scheduling process (arguably defeating the purpose of the CW/DCW scoring system by adding complexity).

The author believes that V2G aggregator design and scheduling rules in any real-life implementation of V2G should ensure that even connected EVs without explicit constraints through user charging preferences should, over time, be gaining charge. However, it should be noted that scenarios I and IV were heavily constrained by the low grid connection limit of 200 kW and all control EVs have shown relatively low gains in SOC (in contrast to the scenarios discussed hereafter). Thus, the issue here lies with the global setup of these scenarios; a 200 kW grid connection limit is insufficient to serve this EV population.

Control EV B is another interesting example with regards to 'fairness' within the EV population. In scenario I, this EV was connected to the network under charging mode 2 ('Quick charge to X % SOC') and, as can be seen in Figure 5.14, reached its target SOC of 70 % at around 1:40 pm before 'plateauing' (i.e. maintaining its target SOC). While its final SOC at 6 pm was higher in scenario IV (79.21 %, see Table 5.3), the target SOC was reached later than in scenario I (70 % SOC was reached at around 2:50 pm here).

When comparing Figure 5.15 and Figure 5.16 it can be seen that while effective charging rates were positive throughout in scenario IV (although declining over time as EV B's SOC increases), rates dropped immediately in scenario I as the target SOC was reached.

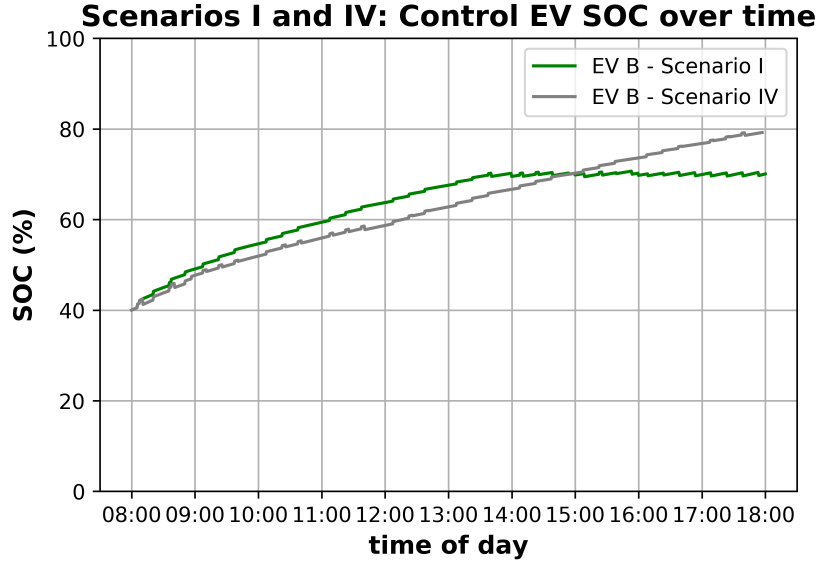


Figure 5.14: Comparison: EV B SOC over time in scenarios I and IV

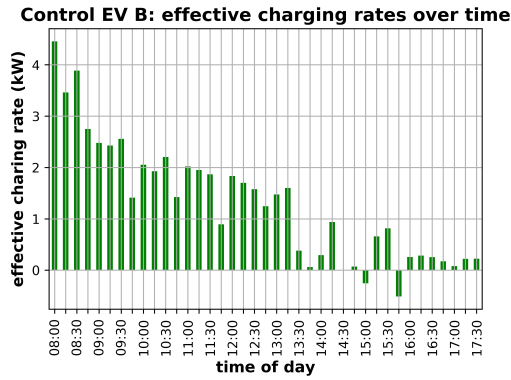


Figure 5.15: Scenario I: EV B effective charging rate over time

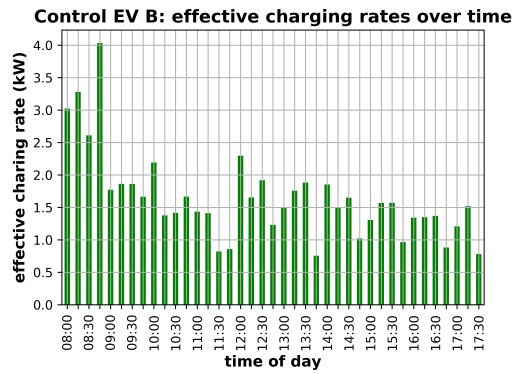


Figure 5.16: Scenario IV: EV B effective charging rate over time

The remaining four control EVs all achieved a higher final SOC under scenario I compared to scenario IV (see Table 5.3). However, none of these EV has achieved its charging target by 6 pm (again highlighting the significance of the global constraints from the low grid connection limit). While this indicates that the aggregator differentiates well between those EVs in need of charging and those less in need (and prioritises accordingly), it also underlines that setting charging targets does not guarantee for those targets to be reached. Prioritisation within the

EV population does not compensate for an overall system-wide lack of available power.

The next set of simulations increases the power made available system-wide. In scenarios II and V the grid connection limit was raised to 300 kW. The rail system power demand model is identical to the previous scenarios. Therefore, the additional power made available is used purely for EV charging. Analogous to the previous discussion, EV user charging preferences were not considered in scenario V (see Figure 5.18) whereas scenario II included user inputs (see Figure 5.17).

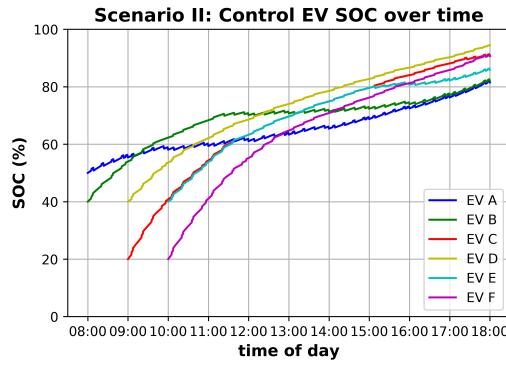


Figure 5.17: Scenario II: changes in SOC for all control EVs while connected

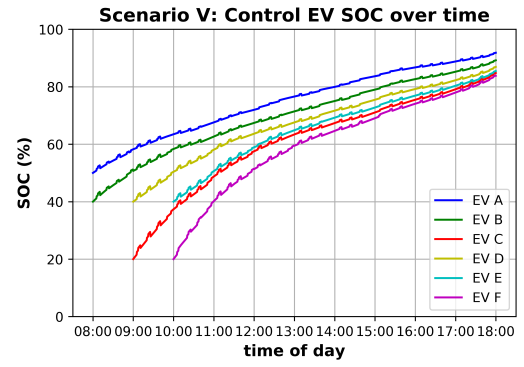


Figure 5.18: Scenario V: changes in SOC for all control EVs while connected, user charging preferences disabled

As more power is available for charging in scenario II (compared to scenario I), EV A no longer experiences an overall decline in SOC over time and EV B is now exceeding its 70 % target SOC towards the late afternoon. Comparing the final SOC for each control EV between scenarios II and V (see Table 5.4) shows the same ‘winners’ and ‘losers’ as in the previous discussion (EVs A and B receive less charge when user inputs are considered, other EVs receive more). However, the differences between enabled and disabled user inputs are not as stark before.

Within scenario II, the comparison between control EVs C and E is the most interesting (see Figure 5.19). While both EVs connect to the network an hour apart and utilise different charging modes (EV C uses mode 2 with a target SOC of 90 %, EV E uses mode 4 with a target SOC of 80 % by 6 pm), they show a very similar trajectory of SOC changes over time for most of the simulation.

Scenario	EV A	EV B	EV C	EV D	EV E	EV F
II	81.47	82.05	90.87	94.47	85.83	90.60
V	91.83	89.20	84.81	86.93	85.50	83.81
Change	-10.36	-7.15	6.06	7.54	0.33	6.79

Table 5.4: Comparison between scenarios II and V, SOC (in %) of Control EVs at 18:00

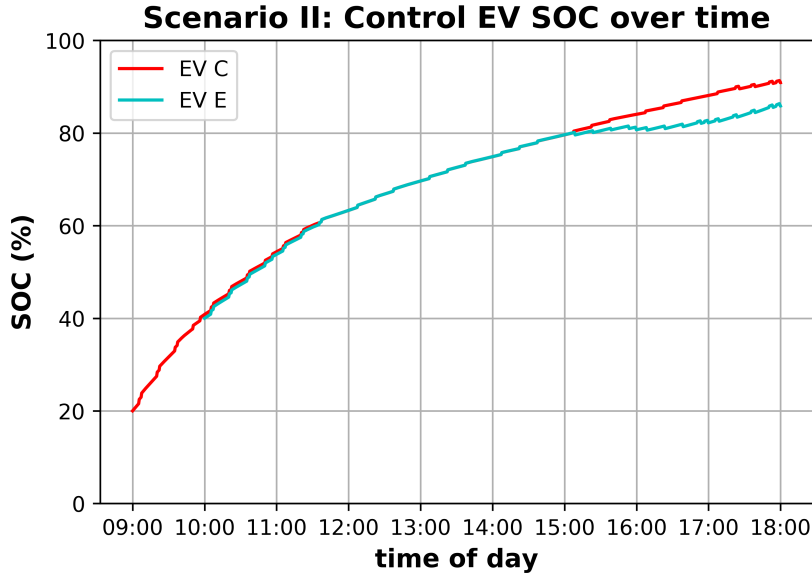


Figure 5.19: Comparison: EVs C and E, SOC over time in scenario II

Despite the different initial conditions of both EVs, a similar 'trajectory' in the early hours, by chance (i.e. not by design - it is of course the result of the underlying scheduling rules), led to both EVs reaching an identical SOC from about 11:40 am onwards. From this point EV C and EV E were practically identical for the V2G aggregator (identical CW and a DCW of zero). Thus, both EVs were treated the same until EV E reached 80 % target shortly after 3 pm (at which its DCW was no longer set to zero).

This is confirmed by the effective charging rates shown in Figure 5.20 and Figure 5.21 - from the 11:45 timeslot up to (and including) the 14:45 timeslot, the average charging rates of both EVs are identical. At 3 pm, however, the average charging rate of EV E drops to about a quarter of EV C's charging rate.

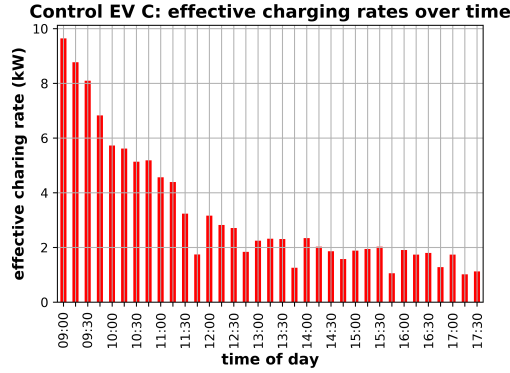


Figure 5.20: Scenario II: EV C effective charging rate over time

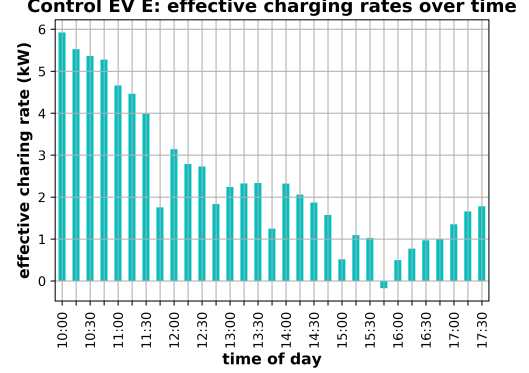


Figure 5.21: Scenario II: EV E effective charging rate over time

In the last set of scenarios to be discussed here - scenarios III and VI - the grid connection limit was raised even further to 400 kW. The predictable effect of this is that all EVs in either scenario are charged quicker than in the previous simulations. This is confirmed by comparing the SOC developments within the control population for scenario VI (see Figure 5.23) where user inputs were not taken into account with scenario III (see Figure 5.22) where user inputs were considered. It can be seen that, regardless of user inputs being considered or not, all EVs have reached a full battery before 6 pm.

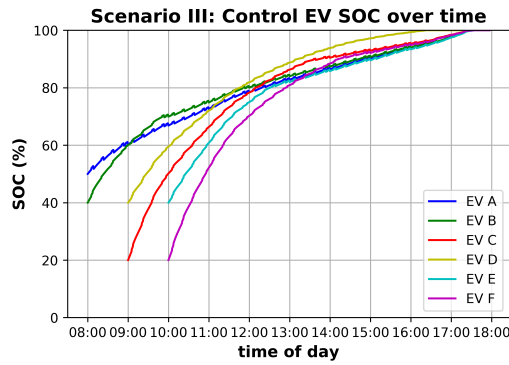


Figure 5.22: Scenario III: changes in SOC for all control EVs while connected

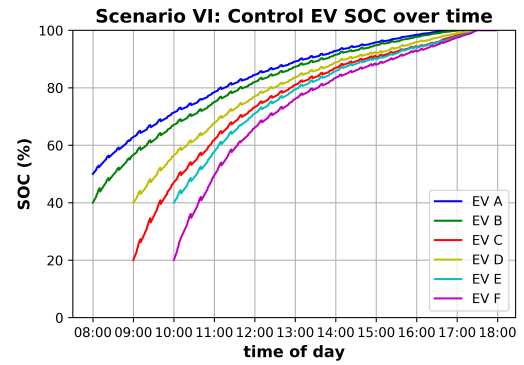


Figure 5.23: Scenario VI: changes in SOC for all control EVs while connected, user charging preferences disabled

The times at which the control EVs have first reached a full battery (they may still have been discharged for short periods afterwards) are listed in Table 5.5. It can be seen that for control EVs C, E and F there is little difference between the two scenarios (a few minutes in each case). EVs A and B have reached a full battery 44 minutes and 42 minutes later respectively when user charging preferences are considered. Only control EV D, which was connected under mode 3 ('Quick charge to full') - and therefore has never been discharged through the aggregator - has significantly gained by reaching a full battery over an hour earlier as user inputs were enabled.

Scenario	EV A	EV B	EV C	EV D	EV E	EV F
III	17:19	17:19	17:15	16:12	17:18	17:14
VI	16:35	16:37	17:17	17:15	17:20	17:20
Change	+44 min	+42 min	+2 min	-63 min	+2 min	+6 min

Table 5.5: Comparison between scenarios III and VI, time at which each EV is considered fully charged

*Note: in Table 5.5 EVs are considered fully charged when the reported SOC reached 99.9 % or more in the logged data. For reasons of sequencing within the database, data points at which SOC = 100 % may not always exist.*

### System-wide impact of enabling EV user charging preferences

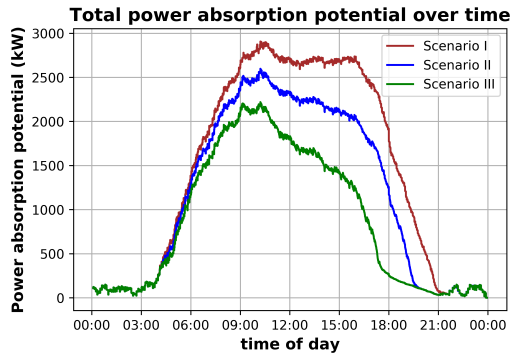


Figure 5.24: Comparison of scenarios I, II and III: total power absorption potential of the aggregated EV population over time

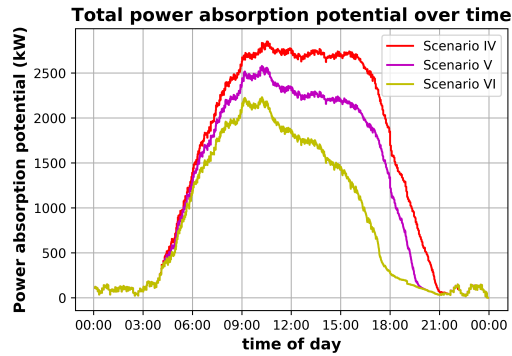


Figure 5.25: Comparison of scenarios IV, V and VI: total power absorption potential of the aggregated EV population over time



So far only the impact that including user charging preferences has on individual EVs has to be discussed. To assess how this inclusion influences the global performance of the whole V2G network, the aggregated power absorption and power provision potentials over 24 hours of V2G operation need to be considered. The power absorption potential over time for scenarios considering user inputs (i.e. scenarios I, II and III) are shown in Figure 5.24). For those scenarios disregarding user charging preferences (i.e. scenarios IV, V and VI) see Figure 5.25.

It can be observed that differences between both sets of simulations are minuscule, suggesting a very minor impact of user charging preferences on the V2G network's ability to absorb power (differences due to changing grid connection limits seen within each set are far more pronounced). Thus, when user inputs are considered, any impact of the aggregator's altered prioritisation of charging rate allocation (due to CW/DCW changes from the charging mode selection) has on the maximum charging rates of individual EVs (due to changes in their SOC) roughly 'balance out' in the aggregate.

In other words, while some EVs within the population are 'gaining' SOC due to the inclusion of charging modes (leading to a decrease in their maximum charging rate), their effect on the aggregated power absorption potential is compensated for by those EVs 'losing' SOC (thus not experiencing a decrease in maximum charging rate). Therefore, introducing user charging preferences into the scheduling had no negative effect on the network's ability to provide traction power to the rail system.

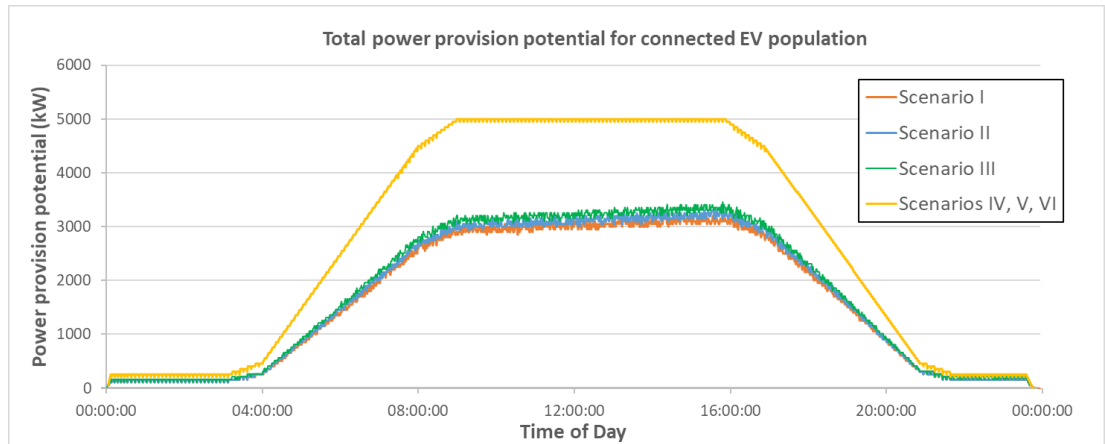


Figure 5.26: Total power provision potential of aggregated EV populations over 24 hours, Scenarios I to VI

However, the same cannot be said about the V2G network's power provision potential - i.e. its ability to provide traction power to the rail system by discharging connected EVs, see Figure 5.26. It can be seen that the power provision potential when disregarding user inputs (scenarios IV, V and VI) is significantly higher than when allowing various conditional and non-conditional opt-outs of V2G operation.

Once user inputs are considered, a fraction of the EV population immediately becomes unavailable for any discharging operation by the aggregator (in particular for 'mode 3' which prohibits discharging of an EV altogether). The power provision potential is significantly lowered and more 'noisy' (presumably as some EVs 'fluctuate' around their target SOC). Differences between scenarios I, II and III are minor, however (recall that the initial conditions of the simulated EV population are identical in each case). The power provision potential in scenario III is slightly higher than in scenario II which is slightly higher than in scenario I (as scenario III had the highest grid connection limit all EVs with charging target presumably reached these targets earlier and became available for discharging through the aggregator).

Figure 5.26, however, should only be regarded as purely indicative of how the inclusion of user charging preferences would affect a real system. As the bulk population in any simulation uses random charging preferences the behaviour of real drivers is not at all represented. Within the bulk population, all charging modes have an equal chance of being selected within the randomised population.

How EV owners would choose cannot be conclusively determined. Would most of them be 'selfish' (or suffer from irrational 'range anxiety') and always request fast charging via 'mode 3'? If so, the V2G network's power provision potential might be even more severely reduced. More insight into EV owner behaviour is required to make this assessment. A related unanswered question is if the EV population would be the same in either case (i.e. including user charging preferences or not).

The introduction of charging preferences may indirectly have a positive impact if more EV owners are willing to connect, not having to worry about range limitations resulting from participation (presumably boosting V2G acceptance). This is, however, fully speculative and further work on these social/behavioural aspects (of V2G in general, R2REE and user inputs in particular) is suggested.

## 6. CONCLUSIONS

In this project, the Road-to-Rail Energy Exchange (R2REE) concept was explored. R2REE represents a novel large-scale application of V2G in which an aggregated population of EVs supports the power demands of nearby electric rail systems. This includes the supply of traction power for accelerating trains but also the acceptance of power from the regenerative braking of decelerating trains. Major challenges of this particular V2G application are the sudden changes in power flows and power flow peaks on a megawatt-scale.

In the context of V2G aggregator control, these challenges translate to a need for a very quick system response (within seconds) while managing a large population of connected EVs (potentially thousands if one aggregator oversees multiple train stations). While the project focus is on addressing these R2REE specific challenges, many of the project's findings are equally applicable to other V2G applications – namely the methods/concepts described in chapter 3 (aggregator control structure and multi-layer event-based scheduling approach) and chapter 5 (pre-scheduling assessment of EVs including user charging preferences via charging modes).

The ongoing electrification of transport is a global trend that is virtually certain to continue well into the future - in line with a global drive to reduce emissions. This is true for both individual transport and mass transportation. Thus, not only are EVs expected to become more numerous (gradually replacing 'traditional' ICE vehicles), electric rail systems are also becoming more common.

While this can generally be regarded as a positive development, the resulting electricity demand represents a major challenge to power grids worldwide. This is not only due to the overall increase in electricity consumption but also because of the difficulty of balancing power supply and demand at any given time - a feat already becoming more difficult because of the increased power supply intermittency from the expansion of renewable energy sources. Energy storage

technologies are universally accepted to be part of the solution, with V2G being one proposed and highly debated concept.

V2G has previously been proposed for various grid services with active research largely focused on economic considerations (highly dependent on local electricity market conditions and not generally conclusive), effects on the degradation of EV batteries, power electronics design and V2G scheduling models.

Electric rail system design was also found to be an active field of research with issues of rail power demand peaks and the dissipation of energy from regenerative braking being widely discussed. Various types of energy storage technology either on-board or along track lines have been proposed to accept power from regenerative braking for later use during acceleration. Another approach is dwell time optimisation in which the departures and arrivals of multiple trains on a network are synchronised so that an accelerating train accepts power from a decelerating one (which significantly constrains train schedules).

Using the V2G concept to support an electric rail system was found to be a completely novel approach not previously discussed in existing literature. Consequently, while V2G has been widely discussed for various applications, existing aggregator control methods and scheduling models do not meet the requirements of R2REE. For most applications of V2G, the system responsiveness is not a major consideration as changes in power demand are gradual and a delay of a few seconds in making scheduling decisions would not significantly affect the system performance. Given the rapidly changing power demands on a megawatt scale within R2REE a quasi-instant system response is desirable.

Thus, while various scheduling models exist with varying degrees of computational complexity, algorithm execution times are rarely reported and additional delays due to aggregator-to-EV communication are not considered. Generally, the IT challenges associated with large scale, centrally controlled V2G applications (EV management, efficient communication and scheduling) seem to be under-appreciated and barely considered in current literature.

### *6.1 Vehicle-to-Grid Aggregator Control*

V2G aggregator control in this project was found to benefit from separating its control algorithms into several modules accessing a mutual database. For the implementation of R2REE, which requires quick system response, this separation

is significant as delays in aggregator-to-EV communication (on average found to be about 15 milliseconds per EV) make a single algorithm approach to aggregator control unviable (i.e. collect data, make charging/discharging decisions and implement decisions in sequence).

A novel modular aggregator control structure, similar to that shown in Figure 3.2 improves system responsiveness, robustness and versatility in any large-scale, centrally controlled V2G system. This modular approach involves splitting up the fundamental tasks of V2G aggregator control – data collection, scheduling and schedule implementation – into separate processes (referred to as first-order modularisation) and integrate these processes with a suitable communications and data management system.

These fundamental tasks can be split further to allow multiple separate processes per task (referred to as second-order modularisation). This structure allows for, for example, multiple scheduling processes operating simultaneously while applying different scheduling rules (a pre-requisite of the multi-layered scheduling strategy used for R2REE).

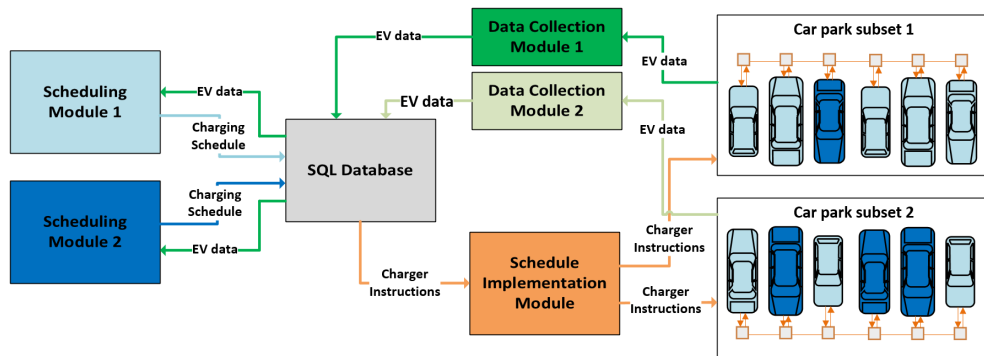


Figure 3.2: Modular aggregator control structure, multiple modules per task - second-order modularisation

Inter-compatibility between modules was achieved through indirect communication via the usage of a mutual database. A suitable database structure for a ‘mySQL’ database was presented. Aggregator-to-EV communication uses the REST API in an existing computer network (using both WiFi and Ethernet). Suitable REST calls for data collection and schedule implementation were presented.

The modular aggregator control, as well as communication and data management, have been extensively tested using a simulated EV population but also using a proof-of-concept hardware prototype of an EV-communication system. Both the chosen database structure and API are mature technologies that are commonly used in industry and compatible with a wide range of hard- and software.

The modularisation of V2G aggregator control allows for workload distribution over multiple processors and thereby increases system responsiveness. Further, it aids system robustness by decoupling scheduling processes from any delays due to faulty communication routes between the aggregator and the EV population. Second-order modularisation could also aid the versatility of a V2G network by enabling the usage of multiple scheduling modules that provide multiple grid services simultaneously – however, this was not within the scope of this project.

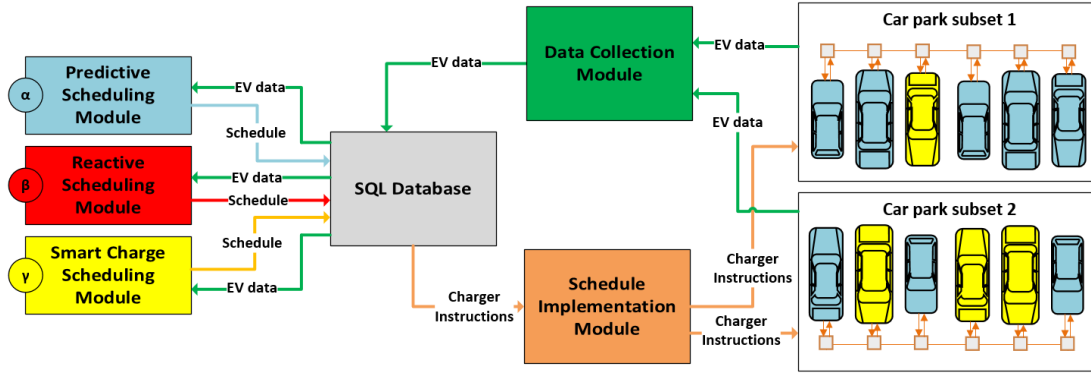


Figure 3.8: Modular aggregator control structure for Road-to-Rail Energy Exchange using multiple scheduling modules.

Instead, second-order modularisation in this project enabled the novel concept of multi-layer event-based V2G scheduling (see Figure 3.8). Novelty in this scheduling strategy lies in combining predictive and reactive scheduling approaches (thus eliminating the disadvantages of either approach) and in the exploitation of ‘events’ to enable short-term predictive capability. Generally, an event was defined as a time-limited, predictable pattern of power demand over time with known start and end time.

In the context of R2REE, events were defined as the departure or arrival of electric trains at a station resulting in a sudden surge in power demand under train acceleration or excess power under train deceleration due to regenerative

braking. This strategy mitigates the respective disadvantages of purely predictive scheduling or purely reactive scheduling. Uncertainty is a major challenge of any purely predictive scheduling approach whereas a purely reactive scheduling approach naturally leads to a lag in system response. A combined approach offers a compromise, where quick system response is achieved (through predictive scheduling) without sacrificing the reactive ability to adjust to inaccuracies (due to uncertainty in the predictive model).

For R2REE, three distinct scheduling layers are proposed. Shortly before an event occurs the predictive scheduling layer determines the V2G network's response to said event based on the predicted power demand (predictable as train arrival and departures are reoccurring patterns). The reactive scheduling continuously checks for and corrects any mismatch in power flow between the EV population, power grid and the rail system. In periods where no event occurs, a smart charging layer applies a separate set of scheduling rules to charge connected EVs (as no event occurs, no discharging of EV battery packs is required).

It was shown that the multi-layer scheduling approach can lead to a quasi-instantaneous system responsiveness as long as power demands can be accurately predicted. Lags in system response are still present if uncertainty leads to a mismatch between expected and actual power demands, but the length of such lags depends on the magnitude of the mismatch (determining how many schedule adjustments need to be made by the reactive scheduling layer).

To reduce the complexity of the scheduling processes, a method was devised to assess EVs prior to scheduling. This is done by assigning weighting factors, termed CW and DCW for charge and discharge events respectively. CW evaluates the potential of an EV to receive power from the aggregator. DCW evaluates the potential of an EV to supply power. This approach is revisited and significantly expanded upon in the chapter 5 as a tool to account for EV user charging preferences in the scheduling process.

## 6.2 Road-to-Rail Energy Exchange

The R2REE case study in this work was based on a real third-rail DC powered rail system in Merseyside, England. The train power demands and potential regenerative braking power were modelled over 24 hours based on the real train timetable for Hoylake train station. This relatively small station is served by just a single type of train, has only two tracks (trains may leave in either direction following the same speed profile) and traction power is provided by a single substation.

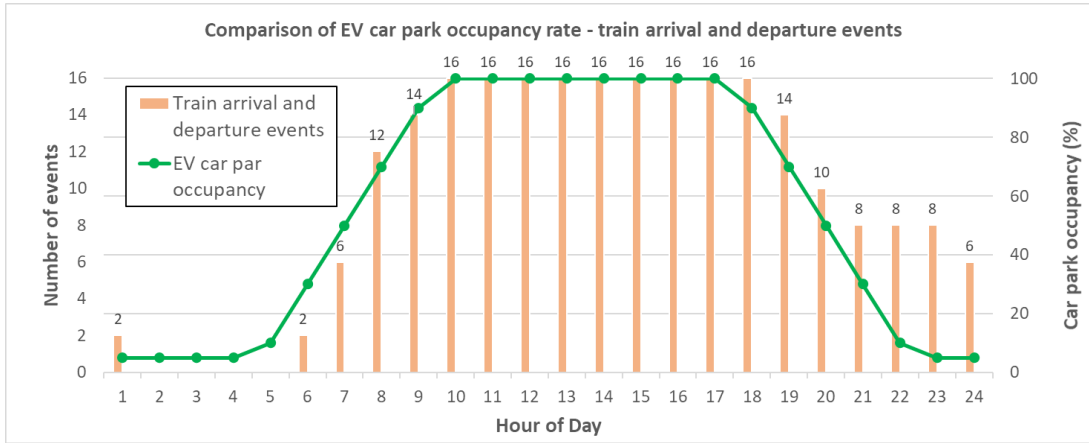


Figure 4.14: Assumed car park occupancy rate and number of train arrival/departure events over 24 simulation period

Using the author's aggregator control strategy R2REE operation was simulated in real-time using an EV population of variable size (50 to 100 EVs). The car park occupancy rate over time was modelled based on data from train station car parks in London. It was found that periods of high activity on the rail system generally coincide with periods of high availability of EVs (see Figure 4.14). Other variables between simulations were the total power available to the whole system (car park plus rail) from the shared power grid connection (see Figure 3.7) as well as the maximum charging/discharging rates of the bidirectional EV chargers.

As electric trains accelerate (causing a spike in power demand for traction) the connected EV population (or parts thereof) are discharged, feeding into the rail system and reducing the load on the local substation. As arriving trains decelerate using regenerative braking, the resulting spike in power from the rail system would be fed into the V2G network. Both these operations reduce fluctuations in the



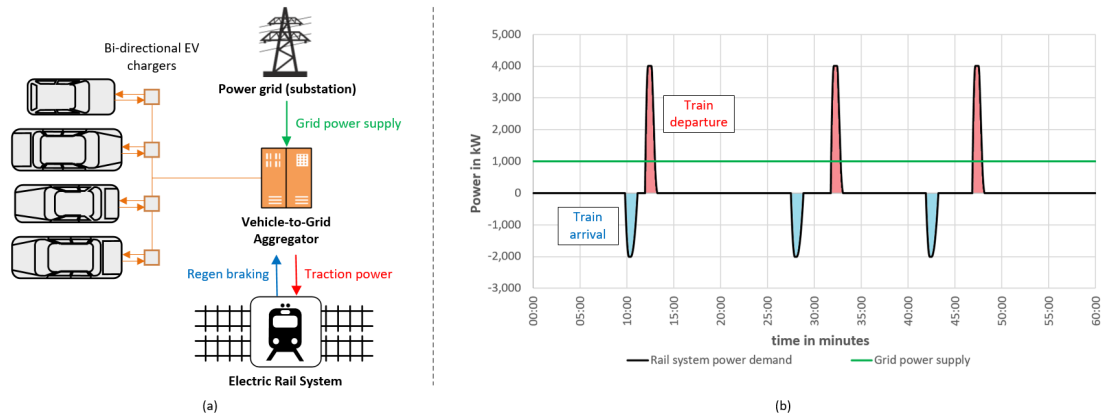


Figure 3.7: (a) V2G for support of local electric rail systems, system overview and power flows: EV population acts as buffer between the grid connection and the fluctuating rail system power demands to ensure steady power flow from the grid; (b) Rail system power demand over one hour (3 trains arriving/departing sequentially, varying dwell time): traction power drawn for train acceleration - positive/red, power supplied from regenerative braking - negative/blue.

power demand experienced by the substation (similar in effect to the concept of dwell time optimisation but without the constraints to train schedules). In periods without rail traffic, the EV population can draw power from the shared grid connection for battery charging, thereby maintaining a steady power flow from the grid.

Using the case study, it has been shown that - given a suitable EV population - R2REE would offer several advantages: R2REE would lower grid connection upgrade requirements for new rail electrification projects (support from the V2G network would lower peaks in power demand from train acceleration experienced by the grid). It would lower grid connection upgrade requirements for new EV charging infrastructure (assuming a new EV car park can share the connection with the electrified rail infrastructure). It would enable brake energy recovery in third rail systems where it has not been available before (leading to energy savings and potential cost savings due to reduced wear on the mechanical brake systems). Local peak demand stresses on the power grid arising from electrified rail traffic would be reduced.

However, all of these potential advantages are highly situational and depend heavily on the availability of EVs. It has been shown that as few as 50 connected

EVs can fully support the traction power demands of the rail system. Although the absorption of power from train brake energy recovery by the EV population was found to be more challenging than ensuring an adequate supply of traction power.

Generally, any EV population able to fully absorb power from a train arrival event was also found to be able to fully supply the traction power needed for a train departure event. In order for just 50 EVs to suffice in fully absorbing power from a train's regenerative braking, most EVs need to be at a relatively low SOC to allow for appropriately high charging rates.

As would be expected, global maximum charging/discharging rates affect the EV population's ability to support the rail application. Although this was found to be much less significant than the effects of reduced charging rates of individual EVs as their SOC increases. Connecting each EV to 50 kW bi-directional chargers instead of 35 kW led to an insignificantly higher power absorption potential of any EV population (only about 2% difference in a population of 75 Nissan Leaf equivalents).

It was also found that the total power made available from the shared power grid connection has a huge impact on the effectiveness of the R2REE system. In most scenarios, EVs were either charging 'too quickly' to be useful to the rail system or 'too slowly' to realistically satisfy any EV owner. Finding a 'goldilocks' compromise between them might be possible with a sufficiently sized EV population, although such an assessment might be rather subjective.

Another significant challenge is the low car park occupancy rate in the early and late hours. While there is a rough correlation between the 'busy' periods of the rail system and the modelled car park (i.e. most train arrivals/departures happen while the car park is relatively full), early and late trains require just as much power as those during 'rush hour'.

All of the issues outlined above are of course mitigated as the overall EV population size increases. However, while EV population size was a controlled input variable in the simulations, it could not be easily controlled in a real R2REE system. Instead it would be the result of many site-specific factors (passenger numbers, EV penetration, EV owner behaviour, etc.).

### 6.3 EV Owner Control Over V2G Scheduling

By allowing EV owners to control charging and V2G usage of their vehicles more depth was added to the V2G scheduling process. A method was proposed that allows owners to state charging preferences via an on-board user interface that informs the assessment of all EV's CW and DCW scores. The inclusion of EV user charging preferences adds further constraints on the scheduling process and increases computational complexity.

Taking these preferences into account and weighing them against the often conflicting needs of the power grid without negatively affecting system responsiveness is addressed through the novel approach of resolving user inputs and (re-)evaluating CW and DCW within the database *prior to* the actual scheduling.

This separates the analysis of user inputs from the time-sensitive scheduling process and instead utilises commonly idling computational resources of the shared database (using SQL trigger conditions). This computationally efficient method of capturing charging preference is suitable for other V2G applications than just R2REE.

Four distinct charging modes have been presented which offer an EV user a large degree of control over charging and discharging. These range from 'no preference' (no further constraints on the aggregator) to 'charging only' (effectively opting out of V2G usage). The four charging modes were implemented on a touch screen interface for the EV communication system prototype.

Several simulations similar to those presented in chapter 4 showed that under the rules presented, the four charging modes have a minimal impact on system-wide absorption potential, but can severely limit power provision (if a large fraction of the EV population opts out of V2G usage). It was also shown that, as would be expected, EVs limiting discharging operations do so at the expense of EVs without such restrictions (see Figure 5.17 and Figure 5.18, scenarios defined in section 5.5).

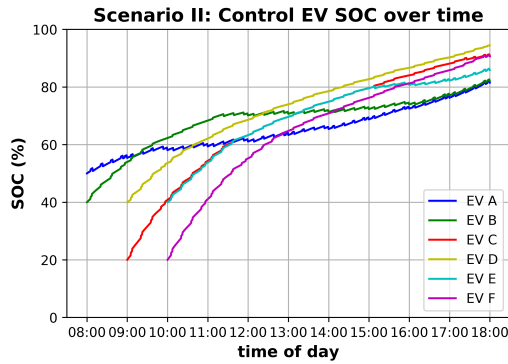


Figure 5.17: Scenario II: changes in SOC for all control EVs while connected, user charging preferences enabled

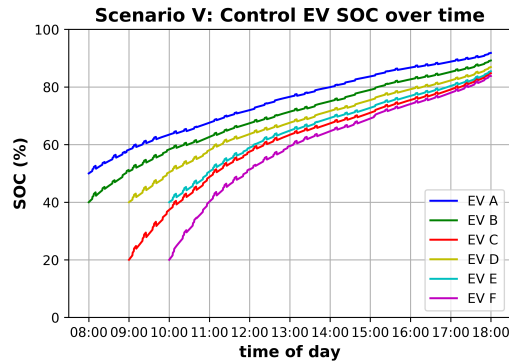


Figure 5.18: Scenario V: changes in SOC for all control EVs while connected, user charging preferences disabled

#### 6.4 Summary and further work

How realistic is the R2REE proposition? As chapter 4 has shown, the system described can be beneficial but is subject to many conditions. The main issue at hand is uncertainty on the side of the EV population. For the system to work to its full potential, it either requires a very large EV population, say hundreds of EVs, with enough redundancy to account for high SOC EVs with very limited charging rates or a moderate number of EVs under just the right circumstances (relatively low SOC, high capacity battery packs, many EVs connected in early and late hours, etc.).

The former seems implausible in non-urban areas (like Hoylake), the latter is difficult (and risky) to plan for. Even if enough EVs are theoretically available, will enough EV users connect to the system rather than charging at home? How many EV owners would even commute to a train station and stay for long periods (encouraging park and ride usage has been attempted by many cities with limited success)? Will private car ownership still be significant in the face of car-sharing and ongoing urbanisation?

Such planning uncertainty is very problematic for any rail infrastructure project where costs and usage scenarios are modelled for decades ahead. Thus, a real-life implementation of the R2REE system as described seems rather unlikely in the foreseeable future. Of course, such uncertainty is not unique to R2REE; the

research area of V2G, in general, is still shrouded with uncertainty (particularly on profitability).

There are however several routes yet to be explored that could make R2REE more viable and are well worth revisiting the concept in future research. An electric rail system may use R2REE as a supplemental system rather than fully relying on it for operation. As was shown in the chapter 4, the absorption of energy from regenerative braking within the EV population was more restricted than the supply of traction power as EVs reached high SOC.

Thus, treating regenerative braking as an optional ‘nice-to-have’ and ‘dumping’ excess energy through resistors if the available EV capacity is insufficient still maintains some of R2REE’s benefits such as shared power infrastructure. As a supplemental system, it may not completely flatten the power demands of the rail system and the charging EV population but would still reduce peak demands.

R2REE may be reconfigured to not only rely on a single central EV car park but instead also manage individually parked EVs in the vicinity. This may include EVs parked on private property and could help the system to maintain capacity in the early hours and overnight (at the expense of significantly increased system complexity).

Further, urban settings where the frequency of train arrivals/departure is higher and more EVs might be available can be expected to be more suitable for R2REE. In either case, more research is required to understand how future EV owners are likely to behave and use their EVs.

Finally, R2REE might be considered as part of a hybrid solution. The connected EV population may suffice during working hours and trackside batteries, flywheels or other energy storage technologies may take over in the interim. If R2REE will find a future application may only be clear in decades as EVs become more numerous and V2G technologies gradually mature.



## APPENDIX





## A1. SQL DATABASE TABLE DEFINITIONS

This appendix contains the table definitions for the main tables in the mySQL database needed for reproduction of the aggregator control defined in chapter 3.

Table Column	Data Type	Description
OrderID	int(10) Auto Increment	Key variable identifying individual orders; assigned within database upon creation of a new entry
ExecutionTime	datetime	Date/time at which order is due for execution
IPAddress	text	Network IP address (with port number if applicable) of connected EV/charger
PowerFlow	float	Charging rate to be assigned to EV in kW (negative value if discharging)
Status	text	Order status; if empty order awaits implementation; if 'queued' order is already passed on to schedule implementation module (and can no longer be amended)
MaxPowerFlow	float	Maximum EV charging rate (needed if order has to be amended)
PreviousPowerFlow	double	Charging rate of EV before order (needed if order has to be amended/-cancelled)

*Table A1.1:* SQL table definitions for 'Schedule' table which contains individual charging/discharging instructions to be passed onto EVs/chargers by the schedule implementation module

Table Column	Data Type	Description
EventID	smallint(6) Auto Increment	Key variable identifying event occurrence; needs to be unique; assigned within database upon creation of a new entry
time	time	Time at which event begins; no date required at each event assumed to occur 'today'
event	text	Event type as defined in predictive scheduling algorithm

Table A1.2: SQL table definitions for 'Events' table which contains the event schedule

Table Column	Data Type	Description
ID	int(10) unsigned	Key variable identifying EVs; needs to be unique; assigned by data collection module (via auto incrementation)
Name	text	Vehicle name; field can be left empty (only used for user readability)
Capacity	float unsigned	EV battery pack capacity in kWh
IPAddress	text	Network IP address (with port number if applicable) of connected EV/charger
SOC	float unsigned	Current EV battery pack SOC in %
Mode	tinyint(3) unsigned	Charging mode selected by EV user, '0' by default
TargetSOC	float unsigned	EV battery pack target SOC in %; 100 % by default
TargetDateTime	datetime	Target date/time by which the target SOC shall be reached; default value '0000-00-00 00:00:00'
Location	text	EV location information; no fixed format but typically contains latitude, longitude and altitude coordinates; can be left empty
CW	float unsigned [0]	Charge weighting (CW) assigned to EV via SQL triggers
DCW	float unsigned [0]	Discharge weighting (DCW) assigned to EV via SQL triggers
ChargeValue	float	Current EV charging rate in kW
MaxChargingRate	float	Current maximum EV charging rate in kW
MaxDischargingRate	float	Current maximum EV discharging rate in kW
InEvent	bit(1) [b'0']	Indicator used to avoid double assignment of EVs through multiple scheduling modules; '1' if EV is currently assigned to serve an event, '0' otherwise
SmartCharging	bit(1) [b'0']	'1' indicates EV is currently managed by smart charging algorithm, '0' otherwise
InEventUntil	datetime	Date/time at which the EV's assignment to serve a specific event ends (and the EV becomes available for re-assignment)

Table A1.3: SQL table definitions for 'Vehicles' table which contains all data on EVs currently connected to network

## A2. AGGREGATOR CONTROL CODE REPOSITORY

This appendix lists all code for the algorithms discussed in chapter 3. Please follow the Digital Object Identifier (DOI) below for read-only access to the file repository - doi:10.5258/SOTON/D1671.

### A2.1 *Data Collection*

**Preamble:** This script manages 'Vehicles' mySQL table, by adding new arriving vehicles ('newVehicles' table), removing leaving vehicles (orderly via 'leavingVehicles' table or disorderly by failing communication) and regularly updating info on each known vehicle already in the database.

**Filename:** ManageVehicles.py

**Type:** PY file (python)

**Libraries required:**

- pymysql (enabling database access)
- requests (enabling communication via REST API)
- time, datetime (enabling efficient handing of date and time data)

**Notes:** Only executes when linked to a SQL database as defined in Appendix A1. Change database definition (hostname, username, password, database name) in line 31 to run.

## A2.2 Schedule Implementation

**Preamble:** Implementation algorithm that loads 'Schedule' table in SQL database, parses schedule entries into charging instructions and submits instructions to EVs.

**Filename:** Implementation.py

**Type:** PY file (python)

**Libraries required:**

- pymysql (enabling database access)
- requests (enabling communication via REST API)
- time, datetime (enabling efficient handling of date and time data)

**Notes:** Only executes when linked to a SQL database as defined in Appendix A1. Change database definition (hostname, username, password, database name) in line 29 to run.

## A2.3 Predictive Scheduling

**Preamble:** V2G scheduling algorithm (predictive scheduling layer). Loads EV data from table 'vehicles' in SQL database and event schedule. Schedule entries saved in 'schedule' table.

**Filename:** Schedule.py

**Type:** PY file (python)

**Libraries required:**

- pymysql (enabling database access)
- time, datetime (enabling efficient handling of date and time data)
- sys (needed for error handling)

**Notes:** Only executes when linked to a SQL database as defined in Appendix A1. Change database definition (hostname, username, password, database name) in line 29 to run.

### A2.4 *Reactive Scheduling*

**Preamble:** V2G scheduling algorithm (reactive scheduling layer). Loads EV data from table 'vehicles' in SQL database, grid power flow from 'PowerFlowNow' and power flow goal from 'PowerAvailable'.

**Filename:** ReactiveScheduling.py

**Type:** PY file (python)

**Libraries required:**

- pymysql (enabling database access)
- requests (enabling communication via REST API)
- time, datetime (enabling efficient handing of date and time data)

**Notes:** Only executes when linked to a SQL database as defined in Appendix A1. Change database definition (hostname, username, password, database name) in line 29 to run.

### A2.5 *Smart Charging*

**Preamble:** Off-event EV charging algorithm. Loads EV data from table 'vehicles' in SQL database and power flow goal from 'PowerAvailable'.

**Filename:** SmartCharge.py

**Type:** PY file (python)

**Libraries required:**

- pymysql (enabling database access)
- requests (enabling communication via REST API)
- time, datetime (enabling efficient handing of date and time data)
- sys (needed for error handling)

**Notes:** Only executes when linked to a SQL database as defined in Appendix A1. Change database definition in line 31 to run.

## A2.6 *Arduino Mega*

**Filename:** `myMegaCode.ino`

**Type:** `.ino` (Arduino file)

**Libraries required:**

- `Nextion.h` (for communication with Nextion touch screen display)
- `Adafruit_GPS.h` (for communication with GPS module and parsing of GPS data)
- `SoftwareSerial.h` (for compatability with GPS module library)
- `Wire.h` (for synchronous serial communication with Arduino Tian)

**Notes:** Uncompiled source code. Requires Arduino IDE to view and compile.

## A2.7 *Arduino Tian*

**Filename:** `myTianCode.ino`

**Type:** `.ino` (Arduino file)

**Libraries required:**

- `Ciao.h` (for interaction with on-board Linino OS)
- `Wire.h` (for synchronous serial communication with Arduino Mega)

**Notes:** Uncompiled source code. Requires Arduino IDE to view and compile.

## A2.8 *Nextion Touchscreen Interface*

**Filename:** `Interface.HMI`

**Type:** `.hmi` (proprietary file format for Nextion touch screen interfaces)

**Notes:** Uncompiled source code for EV user interface discussed in section 5.2. Requires 'Nextion Editor' [192] to view and compile.

### A2.9 EV Simulator (randomised)

**Preamble:** EV simulator algorithm mimicking EV communication and charging behaviour. EV model, user charging preferences and initial SOC randomly selected from fixed list.

**Filename:** `CarSimulator.py`

**Type:** PY file (python)

**Libraries required:**

- socket (enabling access machine's network configurations)
- flask, flask\_restful (enabling communication via REST API)
- time, datetime (enabling efficient handing of date and time data)
- sys (needed for error handling)
- random (enabling random number generation)

**Notes:** Upon initialisation, the script displays the randomly selected EV model, all relevant EV parameters as well as the IP address and port number assigned to this EV simulator instance. IP address and port can then be used to interact (request information, send charging instructions) via REST API as outlined in section 3.2 and section 3.3.

### A2.10 EV Simulator (controlled)

**Preamble:** EV simulator algorithm mimicking EV communication and charging behaviour. EV model, user charging preferences and initial SOC defined by user. Script creates a data log 'EVlog.txt' of any charging instructions received and changes in SOC over time.

**Filename:** `CarSimulatorControlled.py`

**Type:** PY file (python)

**Libraries required:**

- socket (enabling access machine's network configurations)
- flask, flask\_restful (enabling communication via REST API)



- time, datetime (enabling efficient handing of date and time data)
- sys (needed for error handling)
- random (enabling random number generation)

**Notes:** EV parameters and user charging preferences to be defined in lines 99 and onwards. Upon initialisation, the script displays the IP address and port number assigned to this EV simulator instance. IP address and port can then be used to interact (request information, send charging instructions) via REST API as outlined in section 3.2 and section 3.3.

### A3. COMMUNICATION BENCHMARK

This benchmark assesses the performance of the data collection algorithm (see section 3.2). The time taken to update all EV information in the SQL database is recorded. This involves contacting each simulated EV exactly once via REST API and feeding the data into the SQL database. Cycle times are taken by logging the processor time of the machine running the aggregator control every time the algorithm contacts the first EV. The difference between two timestamps represents the time taken by the algorithm to update the whole 'Vehicles' table in the database.

For this test, any aggregator control algorithms are running on one desktop PC (i5-2400 processor, 4 CPUs at 3.1 GHz, 4 GB RAM) while the EVs are simulated (see section 3.6) on another (i5-4590 processor, 4 CPUs at 3.3 GHz, 16 GB RAM). Both machines are connected to the same network via an Ethernet connection. The data collection algorithm was tested for a varying number of simulated EVs (50 to 1,000). Each test ran for about 30 minutes and the average cycle times have been recorded.

It would be expected that a linear relationship exists between the time taken to update all EV information in the database and the number of EVs on the network. The results from this benchmark do confirm this although slight deviations from the linear trend can be seen (see Figure A3.0.1). These variations might be due to other network traffic (as the university's internal computer network with thousands of connected machines is used, this cannot be controlled) or other background processes on the PCs used (also under limited control due to constraints on the operating system). Using the campus' eduroam network and the mentioned hardware for aggregator control and EV simulation, it took about 15 seconds to collect and save data from 1,000 simulated EVs – or about 15 milliseconds per EV.

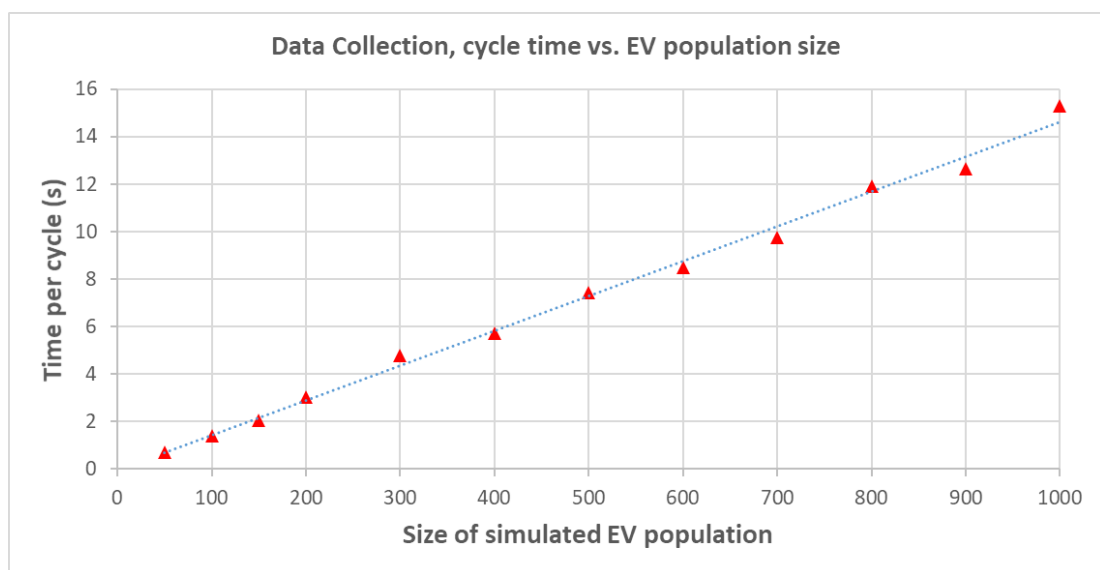


*Figure A3.0.1:* Average time taken for data collection algorithm to update all EV data in SQL database for varying EV population sizes

## A4. TRAIN SCHEDULE

Using Mon-Sat timetable for wirral-line for hoylake (15th December 2019 to 16th May 2020) [216]

Time	Destination	Platform	Time	Destination	Platform
00:02:00	West Kirby	2	14:09:00	Liverpool	1
05:54:00	Liverpool	1	14:22:00	West Kirby	2
06:24:00	Liverpool	1	14:24:00	Liverpool	1
06:52:00	West Kirby	2	14:37:00	West Kirby	2
06:54:00	Liverpool	1	14:39:00	Liverpool	1
07:09:00	Liverpool	1	14:52:00	West Kirby	2
07:22:00	West Kirby	2	14:58:00	Liverpool	1
07:24:00	Liverpool	1	15:07:00	West Kirby	2
07:39:00	Liverpool	1	15:09:00	Liverpool	1
07:52:00	West Kirby	2	15:22:00	West Kirby	2
07:58:00	Liverpool	1	15:24:00	Liverpool	1
08:07:00	West Kirby	2	15:37:00	West Kirby	2
08:09:00	Liverpool	1	15:39:00	Liverpool	1
08:22:00	West Kirby	2	15:52:00	West Kirby	2
08:37:00	West Kirby	2	15:58:00	Liverpool	1
08:39:00	Liverpool	1	16:07:00	West Kirby	2
08:52:00	West Kirby	2	16:09:00	Liverpool	1
08:58:00	Liverpool	1	16:22:00	West Kirby	2
09:07:00	West Kirby	2	16:24:00	Liverpool	1
09:09:00	Liverpool	1	16:37:00	West Kirby	2
09:22:00	West Kirby	2	16:39:00	Liverpool	1
09:24:00	Liverpool	1	16:52:00	West Kirby	2
09:37:00	West Kirby	2	16:58:00	Liverpool	1
09:39:00	Liverpool	1	17:07:00	West Kirby	2
09:52:00	West Kirby	2	17:09:00	Liverpool	1

09:58:00	Liverpool	1	17:22:00	West Kirby	2
10:07:00	West Kirby	2	17:24:00	Liverpool	1
10:09:00	Liverpool	1	17:37:00	West Kirby	2
10:22:00	West Kirby	2	17:39:00	Liverpool	1
10:24:00	Liverpool	1	17:52:00	West Kirby	2
10:37:00	West Kirby	2	17:58:00	Liverpool	1
10:39:00	Liverpool	1	18:07:00	West Kirby	2
10:52:00	West Kirby	2	18:09:00	Liverpool	1
10:58:00	Liverpool	1	18:22:00	West Kirby	2
11:07:00	West Kirby	2	18:24:00	Liverpool	1
11:09:00	Liverpool	1	18:37:00	West Kirby	2
11:22:00	West Kirby	2	18:39:00	Liverpool	1
11:24:00	Liverpool	1	18:52:00	West Kirby	2
11:37:00	West Kirby	2	19:04:00	Liverpool	1
11:39:00	Liverpool	1	19:07:00	West Kirby	2
11:52:00	West Kirby	2	19:22:00	West Kirby	2
11:58:00	Liverpool	1	19:34:00	Liverpool	1
12:07:00	West Kirby	2	19:37:00	West Kirby	2
12:09:00	Liverpool	1	20:02:00	West Kirby	2
12:22:00	West Kirby	2	20:04:00	Liverpool	1
12:24:00	Liverpool	1	20:32:00	West Kirby	2
12:37:00	West Kirby	2	20:34:00	Liverpool	1
12:39:00	Liverpool	1	21:02:00	West Kirby	2
12:52:00	West Kirby	2	21:04:00	Liverpool	1
12:58:00	Liverpool	1	21:32:00	West Kirby	2
13:07:00	West Kirby	2	21:34:00	Liverpool	1
13:09:00	Liverpool	1	22:02:00	West Kirby	2
13:22:00	West Kirby	2	22:04:00	Liverpool	1
13:24:00	Liverpool	1	22:32:00	West Kirby	2
13:37:00	West Kirby	2	22:34:00	Liverpool	1
13:39:00	Liverpool	1	23:02:00	West Kirby	2
13:52:00	West Kirby	2	23:04:00	Liverpool	1
13:58:00	Liverpool	1	23:32:00	West Kirby	2
14:07:00	West Kirby	2	-	-	-

Table A4.1: Train schedule for Hoylake train station (Using Mon-Sat timetable for Wirral-line; valid 15th December 2019 to 16th May 2020)

## A5. FULL SIMULATION RESULTS FOR CHAPTER 4

This appendix contains a catalogue of all results for the simulated scenario discussed in chapter 4.

- All simulations were run in real-time using the aggregator control algorithms outlined in chapter 3.
- The simulated EV population follows the 24-hour car park occupancy model outlined in section 4.3.
- Rail system power flows follow the power demand curves and train schedule outlined in section 4.2.
- Within the simulated EV population were three controlled/monitored EV's as outlined in section 3.6. These 'control EVs' have identical capacity (40 kWh) and maximum charging rate (50 kW), but connect to the network at different times and with different initial SOC (see Table A5.1). All control EVs were connected for 8 hours.

<b>Control EV Name</b>	<b>Initial SOC</b>	<b>Connection Time</b>
EV A	50 %	08:00:00
EV B	30 %	09:00:00
EV C	70 %	10:00:00

*Tab. A5.1:* Control EV definitions (identical for all scenarios in discussed in this chapter): initial SOC and connection time

## A5.1 Scenario A

Scenario specific parameters:

- The simulation assumes a constant grid connection limit of 200 kW
- EV user inputs are enabled and inform V2G scheduling (SQL triggers used: see section 5.4)
- The default CW and DCW equations for four charging modes are used to assess each EV (see section 5.3)

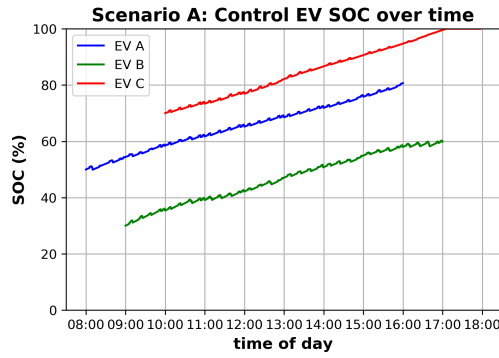


Fig. A5.1.1: All control EVs, SOC over time

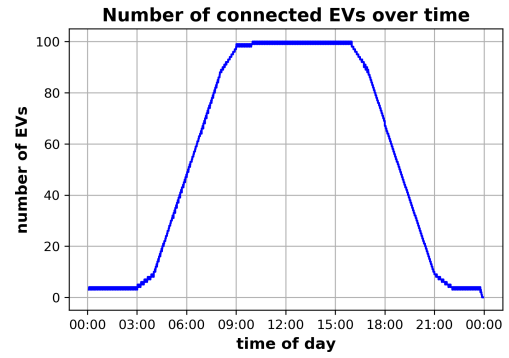


Fig. A5.1.2: Number of simulated EVs connected to V2G network over time

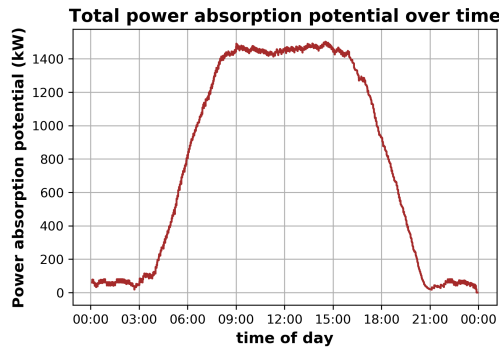


Fig. A5.1.3: Aggregated EV population, total power absorption potential

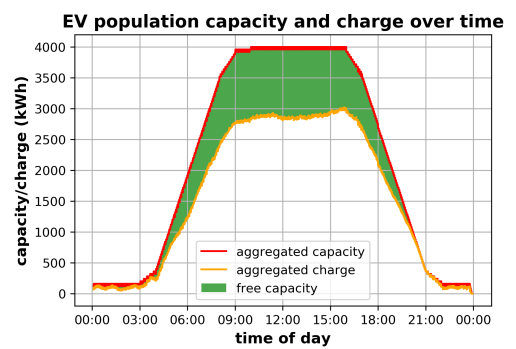


Fig. A5.1.4: Aggregated EV population, total capacity, total charge and free capacity

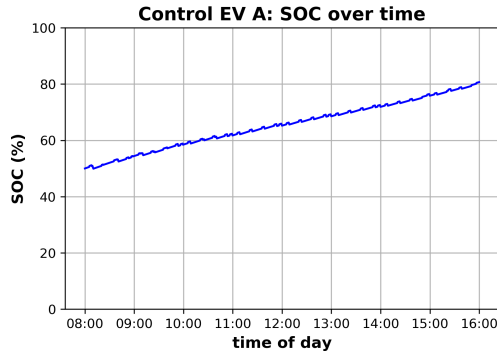


Fig. A5.1.5: Control EV A, SOC over time while connected

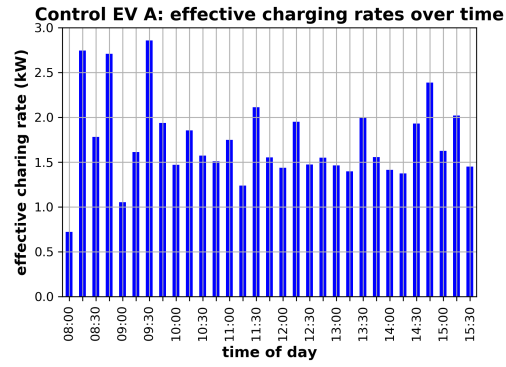


Fig. A5.1.6: Control EV A, average power flow over 15 min

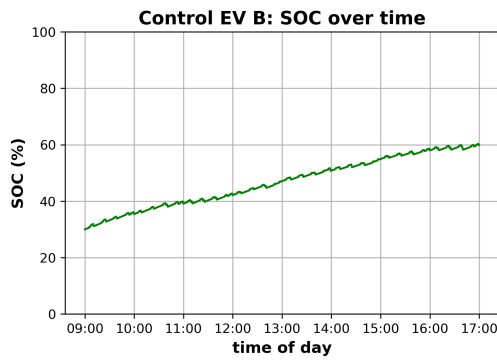


Fig. A5.1.7: Control EV B, SOC over time while connected

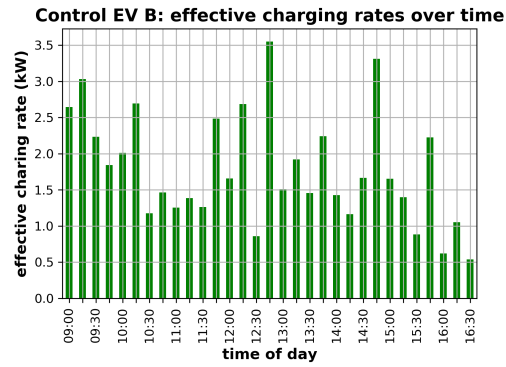


Fig. A5.1.8: Control EV B, average power flow over 15 min

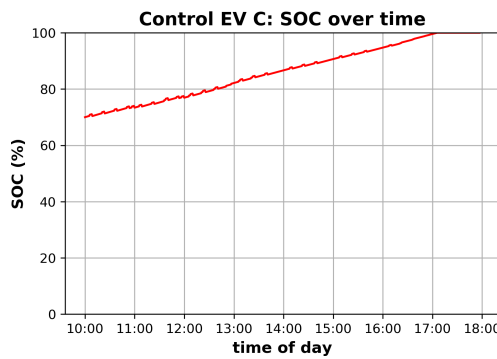


Fig. A5.1.9: Control EV C, SOC over time while connected

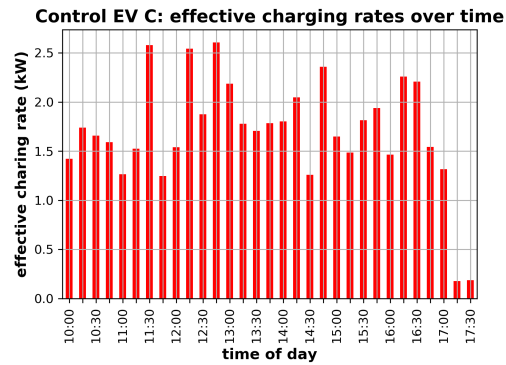


Fig. A5.1.10: Control EV C, average power flow over 15 min



## A5.2 Scenario B

Scenario specific parameters:

- The simulation assumes a constant grid connection limit of 200 kW
- EV user inputs are enabled and inform V2G scheduling (SQL triggers used: see section 5.4)
- The default CW and DCW equations for four charging modes are used to assess each EV (see section 5.3)

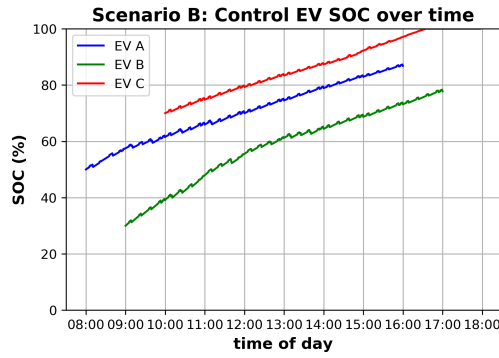


Fig. A5.2.1: All control EVs, SOC over time

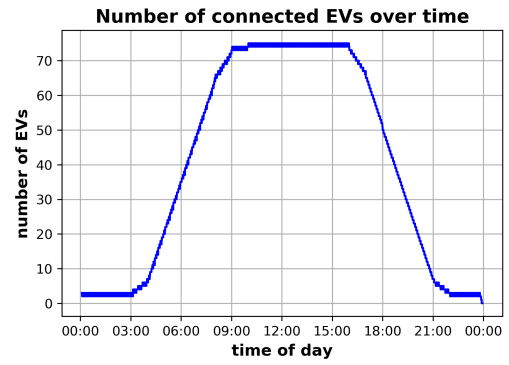


Fig. A5.2.2: Number of simulated EVs connected to V2G network over time

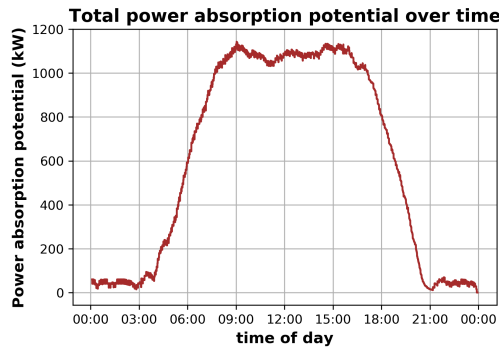


Fig. A5.2.3: Aggregated EV population, total power absorption potential

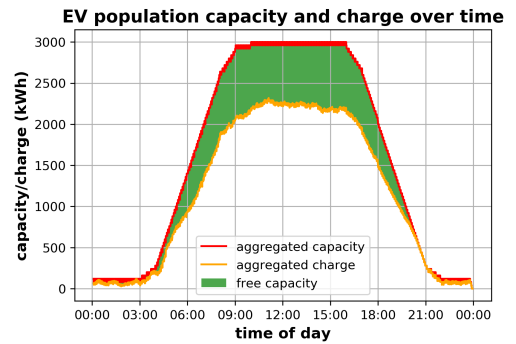


Fig. A5.2.4: Aggregated EV population, total capacity, total charge and free capacity

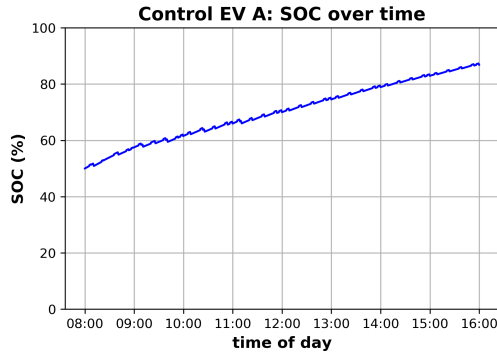


Fig. A5.2.5: Control EV A, SOC over time while connected

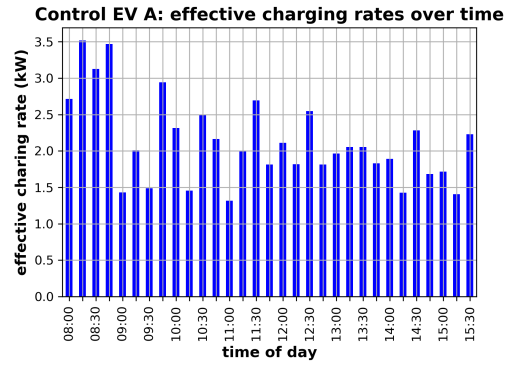


Fig. A5.2.6: Control EV A, average power flow over 15 min

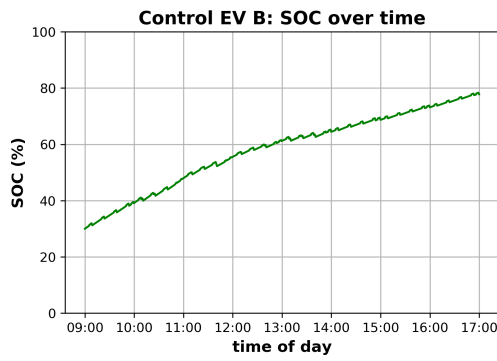


Fig. A5.2.7: Control EV B, SOC over time while connected

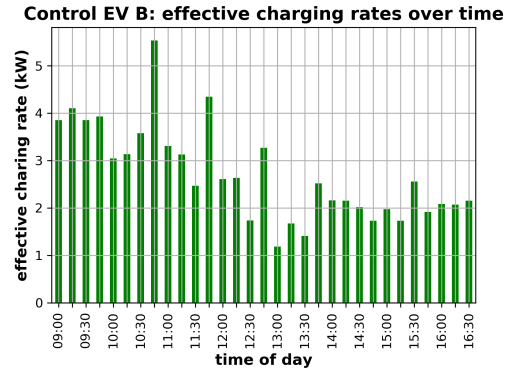


Fig. A5.2.8: Control EV B, average power flow over 15 min

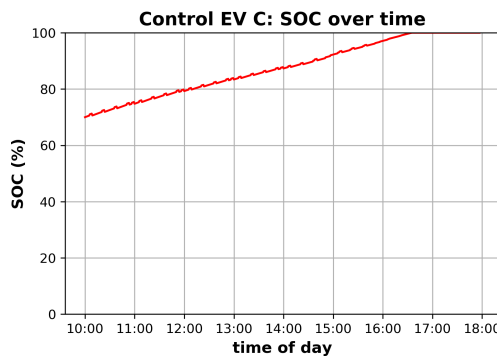


Fig. A5.2.9: Control EV C, SOC over time while connected

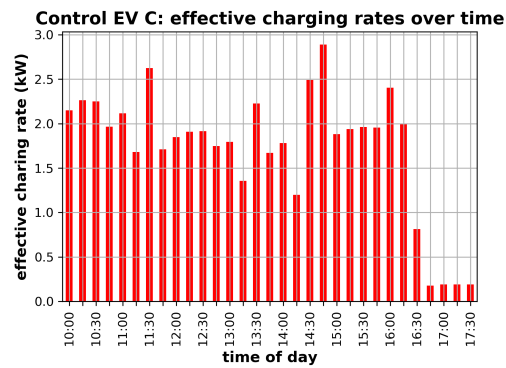


Fig. A5.2.10: Control EV C, average power flow over 15 min

## A5.3 Scenario C

Scenario specific parameters:

- The simulation assumes a constant grid connection limit of 200 kW
- EV user inputs are enabled and inform V2G scheduling (SQL triggers used: see section 5.4)
- The default CW and DCW equations for four charging modes are used to assess each EV (see section 5.3)

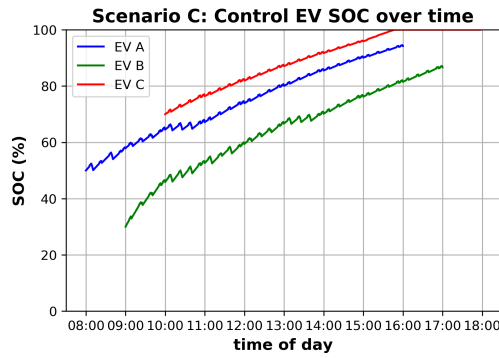


Fig. A5.3.1: All control EVs, SOC over time

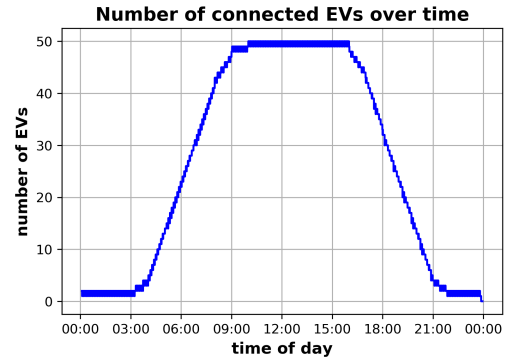


Fig. A5.3.2: Number of simulated EVs connected to V2G network over time

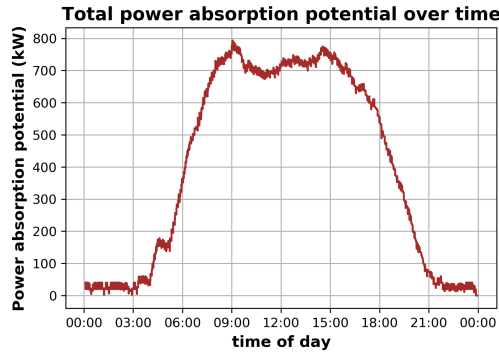


Fig. A5.3.3: Aggregated EV population, total power absorption potential

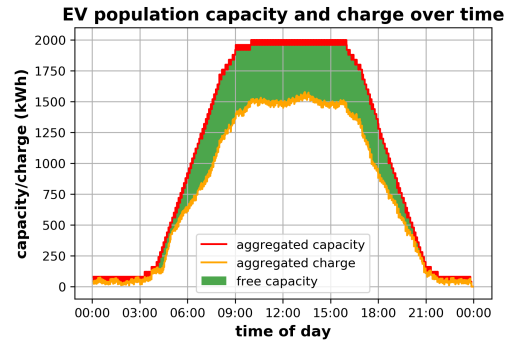


Fig. A5.3.4: Aggregated EV population, total capacity, total charge and free capacity

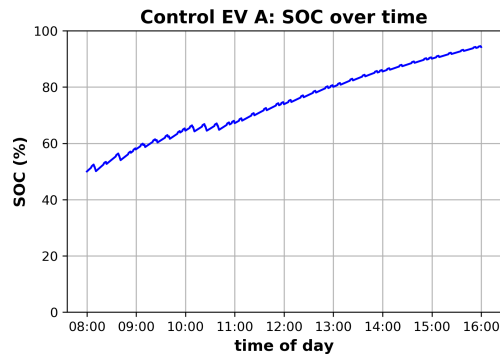


Fig. A5.3.5: Control EV A, SOC over time while connected

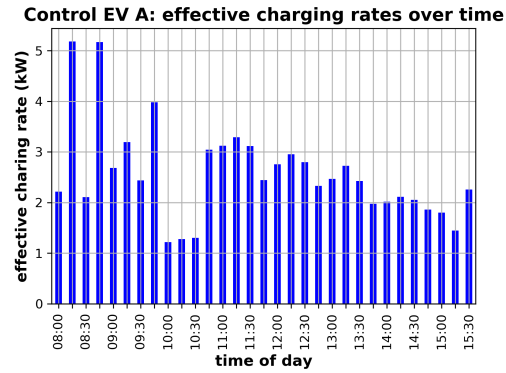


Fig. A5.3.6: Control EV A, average power flow over 15 min

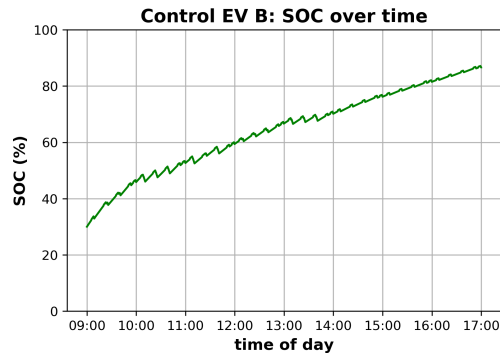


Fig. A5.3.7: Control EV B, SOC over time while connected

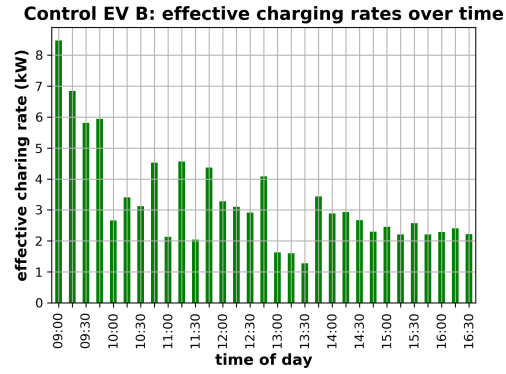


Fig. A5.3.8: Control EV B, average power flow over 15 min

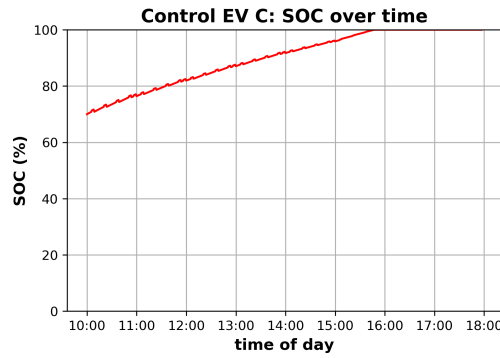


Fig. A5.3.9: Control EV C, SOC over time while connected

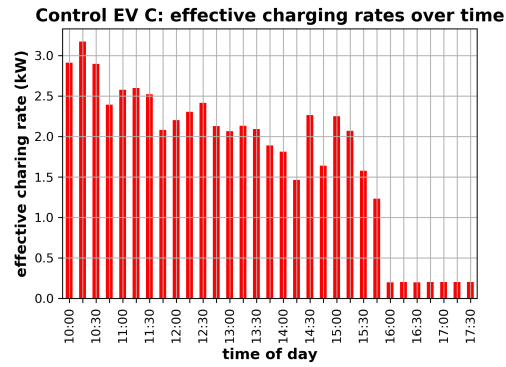


Fig. A5.3.10: Control EV C, average power flow over 15 min

## A5.4 Scenario D

Scenario specific parameters:

- The simulation assumes a constant grid connection limit of 200 kW
- EV user inputs are enabled and inform V2G scheduling (SQL triggers used: see section 5.4)
- The default CW and DCW equations for four charging modes are used to assess each EV (see section 5.3)

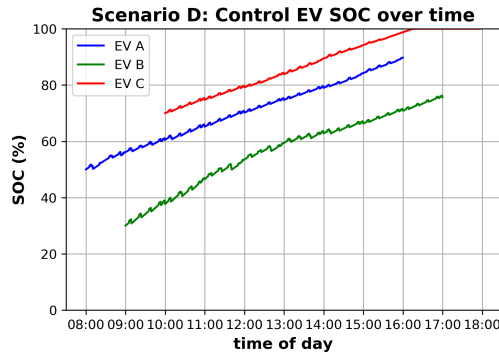


Fig. A5.4.1: All control EVs, SOC over time

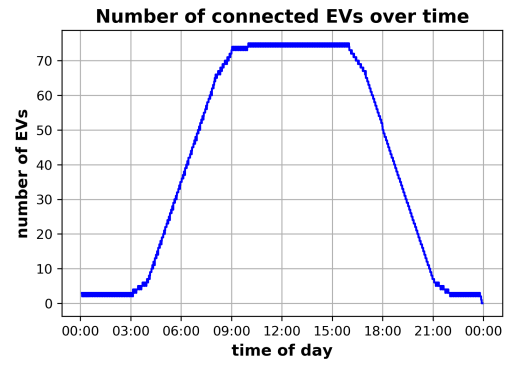


Fig. A5.4.2: Number of simulated EVs connected to V2G network over time

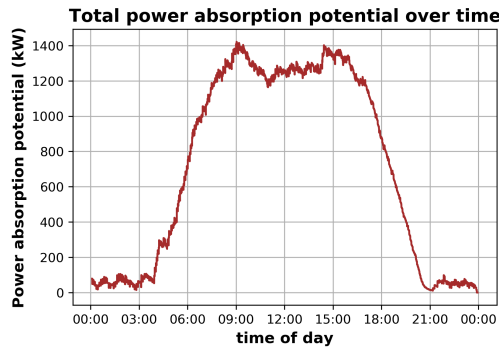


Fig. A5.4.3: Aggregated EV population, total power absorption potential

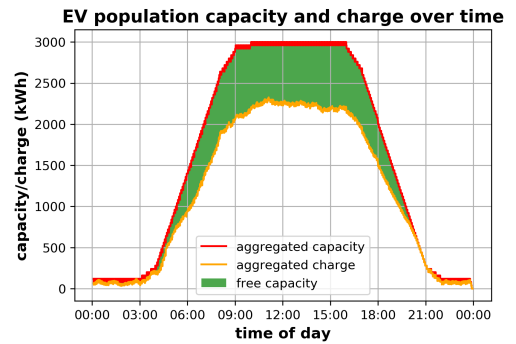


Fig. A5.4.4: Aggregated EV population, total capacity, total charge and free capacity

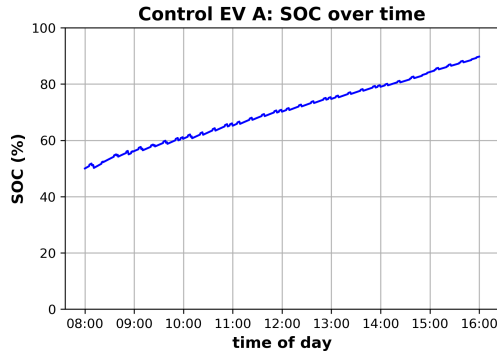


Fig. A5.4.5: Control EV A, SOC over time while connected

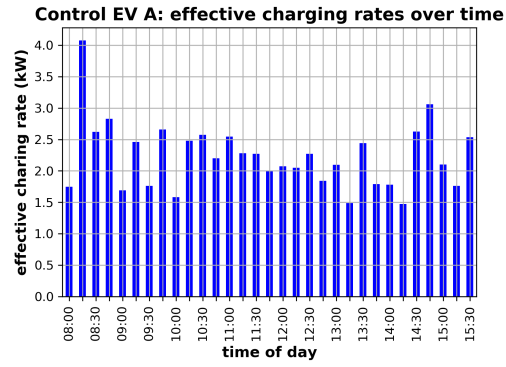


Fig. A5.4.6: Control EV A, average power flow over 15 min

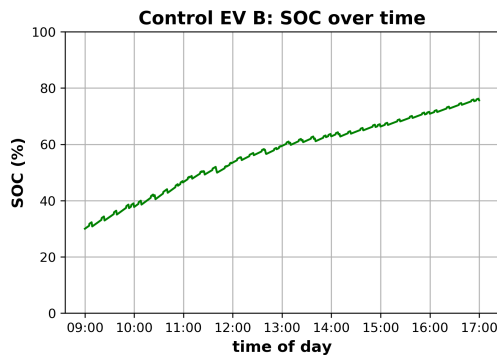


Fig. A5.4.7: Control EV B, SOC over time while connected

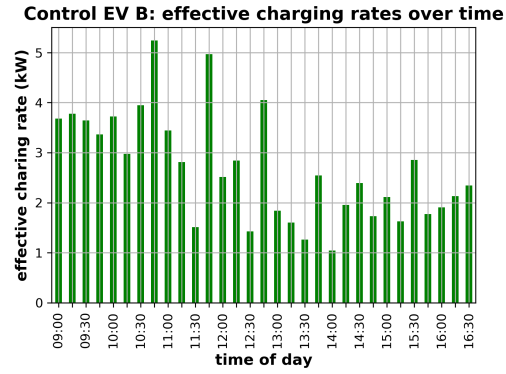


Fig. A5.4.8: Control EV B, average power flow over 15 min

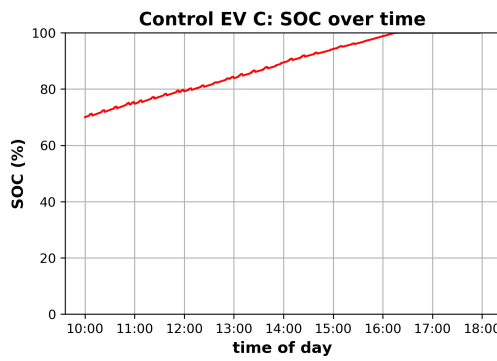


Fig. A5.4.9: Control EV C, SOC over time while connected

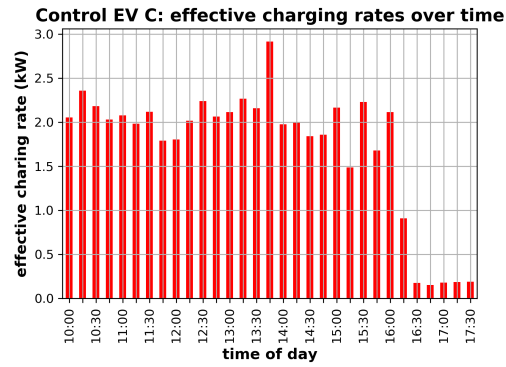


Fig. A5.4.10: Control EV C, average power flow over 15 min

## A5.5 Scenario E

Scenario specific parameters:

- The simulation assumes a constant grid connection limit of 200 kW
- EV user inputs are enabled and inform V2G scheduling (SQL triggers used: see section 5.4)
- The default CW and DCW equations for four charging modes are used to assess each EV (see section 5.3)

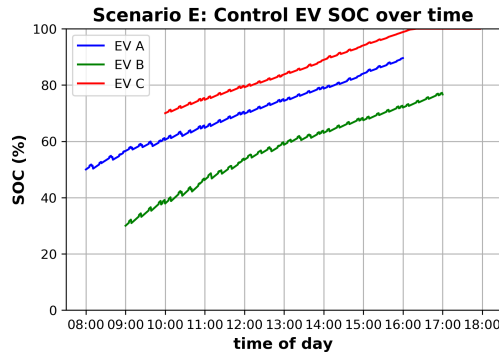


Fig. A5.5.1: All control EVs, SOC over time

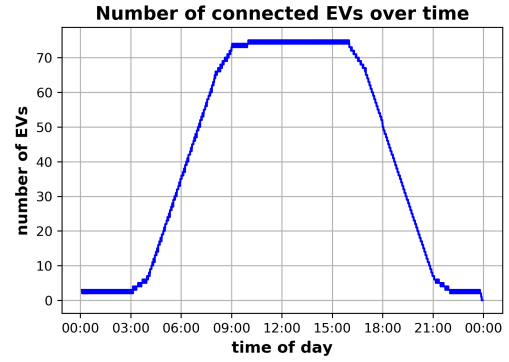


Fig. A5.5.2: Number of simulated EVs connected to V2G network over time

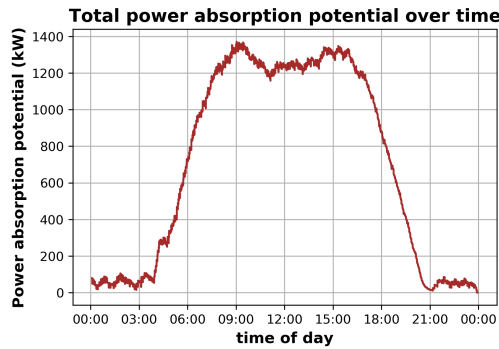


Fig. A5.5.3: Aggregated EV population, total power absorption potential

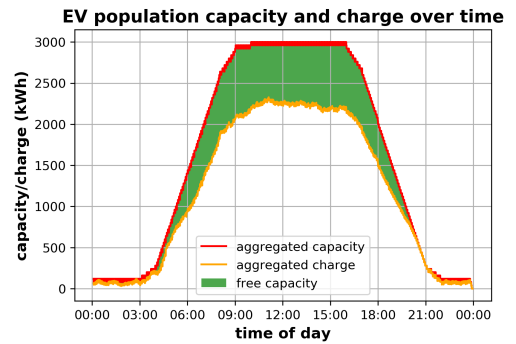


Fig. A5.5.4: Aggregated EV population, total capacity, total charge and free capacity

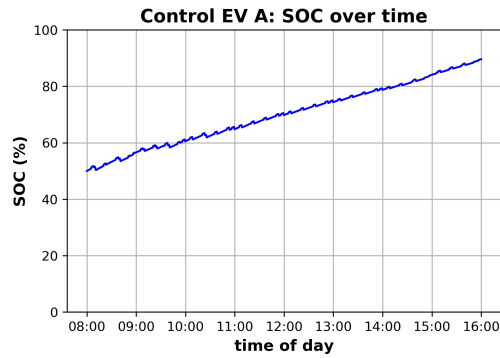


Fig. A5.5.5: Control EV A, SOC over time while connected

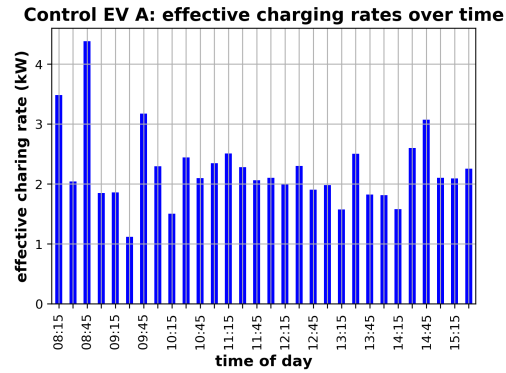


Fig. A5.5.6: Control EV A, average power flow over 15 min

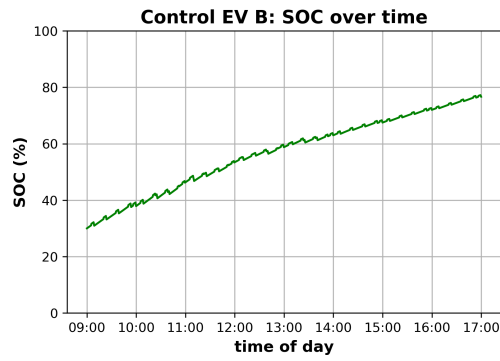


Fig. A5.5.7: Control EV B, SOC over time while connected

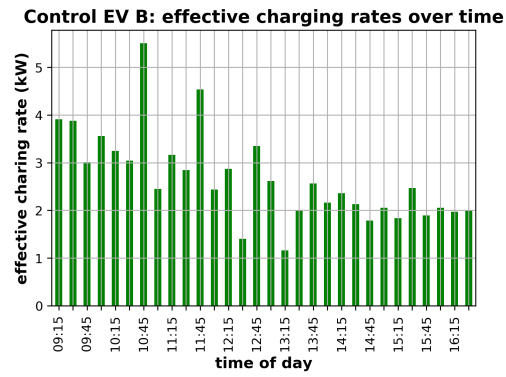


Fig. A5.5.8: Control EV B, average power flow over 15 min

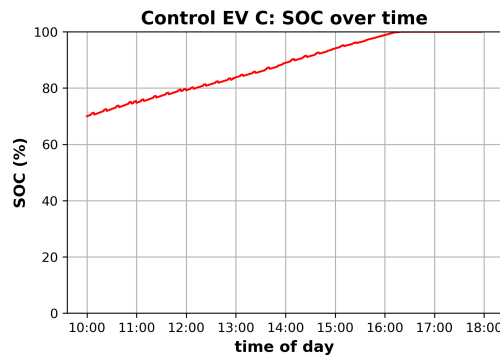


Fig. A5.5.9: Control EV C, SOC over time while connected

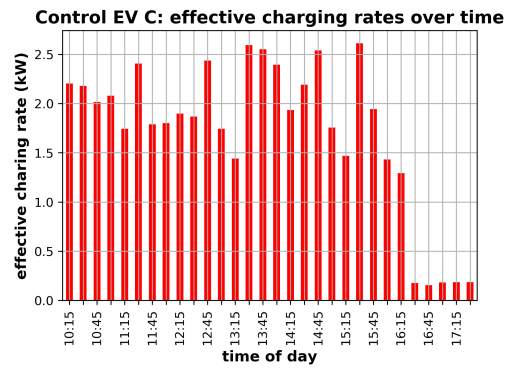


Fig. A5.5.10: Control EV C, average power flow over 15 min



## A5.6 Scenario F

Scenario specific parameters:

- The simulation assumes a constant grid connection limit of 300 kW
- EV user inputs are enabled and inform V2G scheduling (SQL triggers used: see section 5.4)
- The default CW and DCW equations for four charging modes are used to assess each EV (see section 5.3)

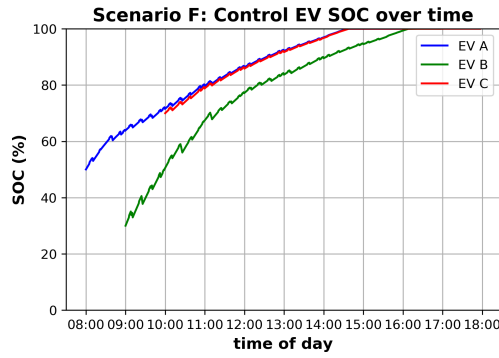


Fig. A5.6.1: All control EVs, SOC over time

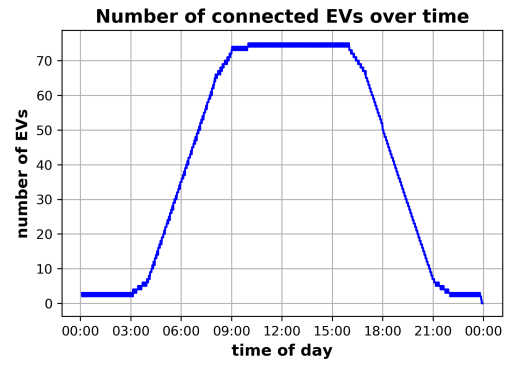


Fig. A5.6.2: Number of simulated EVs connected to V2G network over time

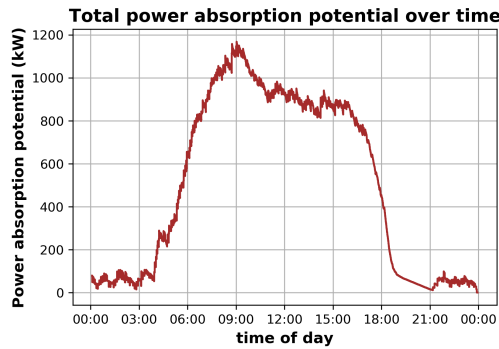


Fig. A5.6.3: Aggregated EV population, total power absorption potential

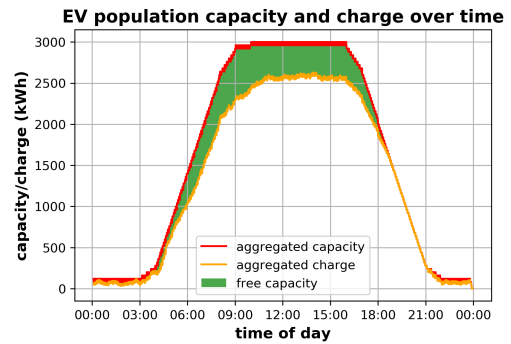


Fig. A5.6.4: Aggregated EV population, total capacity, total charge and free capacity

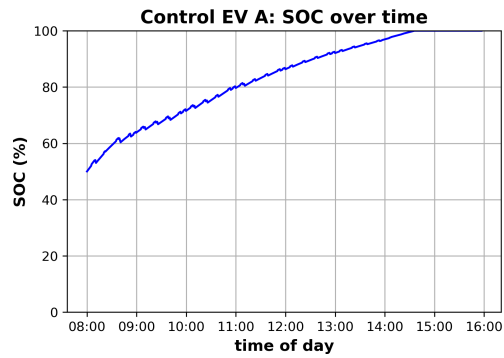


Fig. A5.6.5: Control EV A, SOC over time while connected

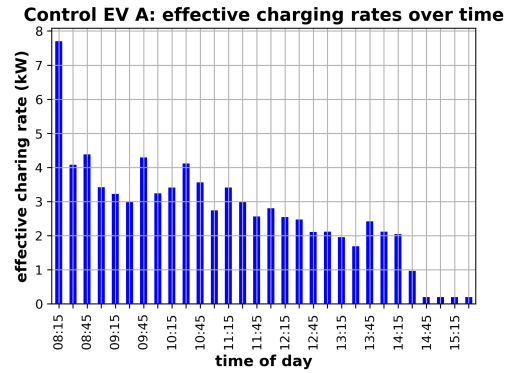


Fig. A5.6.6: Control EV A, average power flow over 15 min

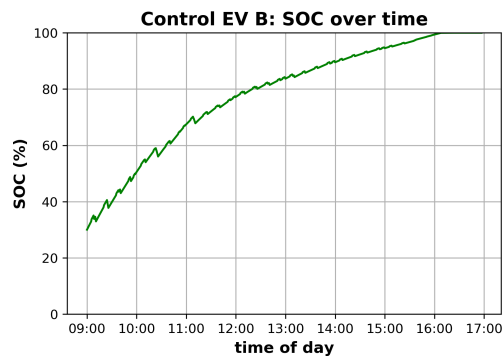


Fig. A5.6.7: Control EV B, SOC over time while connected

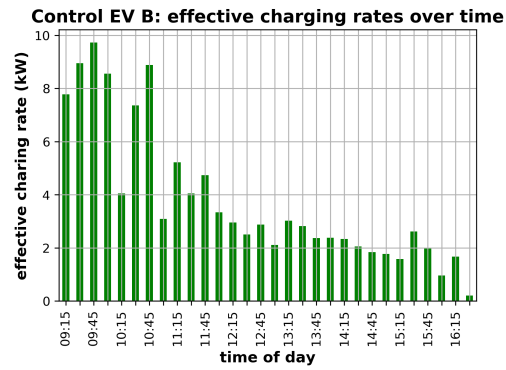


Fig. A5.6.8: Control EV B, average power flow over 15 min

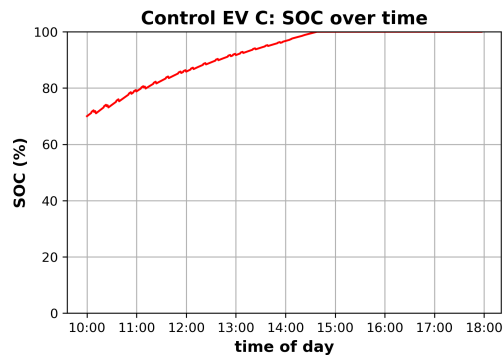


Fig. A5.6.9: Control EV C, SOC over time while connected

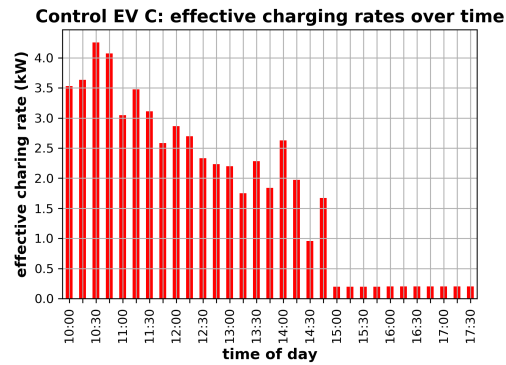


Fig. A5.6.10: Control EV C, average power flow over 15 min

## A5.7 Scenario G

Scenario specific parameters:

- The simulation assumes a constant grid connection limit of 300 kW
- EV user inputs are enabled and inform V2G scheduling (SQL triggers used: see section 5.4)
- The default CW and DCW equations for four charging modes are used to assess each EV (see section 5.3)

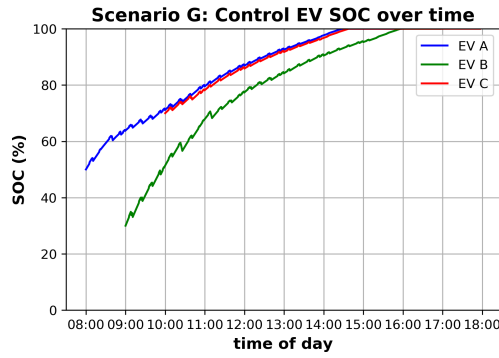


Fig. A5.7.1: All control EVs, SOC over time

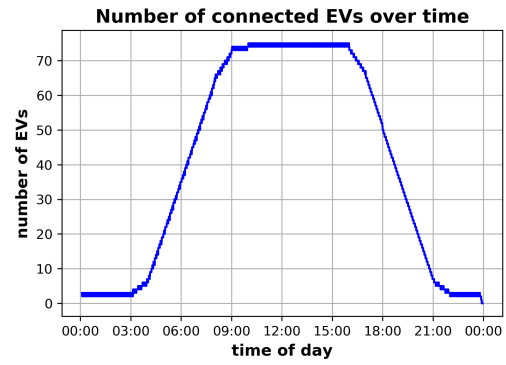


Fig. A5.7.2: Number of simulated EVs connected to V2G network over time

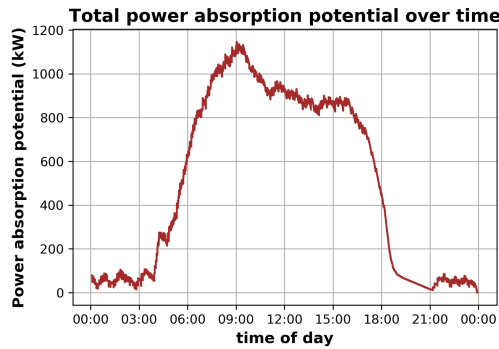


Fig. A5.7.3: Aggregated EV population, total power absorption potential

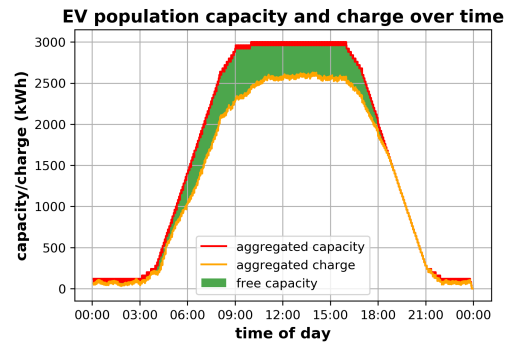


Fig. A5.7.4: Aggregated EV population, total capacity, total charge and free capacity

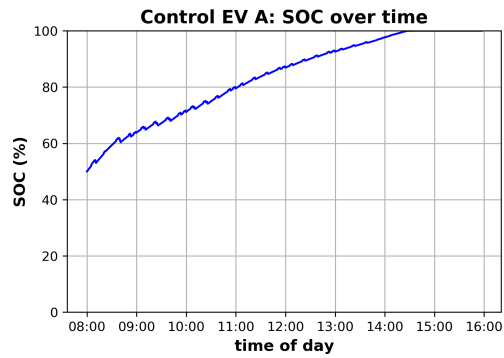


Fig. A5.7.5: Control EV A, SOC over time while connected

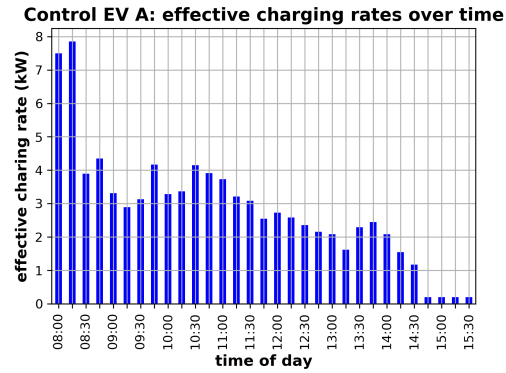


Fig. A5.7.6: Control EV A, average power flow over 15 min

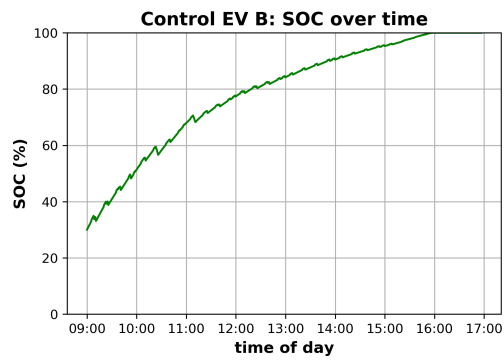


Fig. A5.7.7: Control EV B, SOC over time while connected

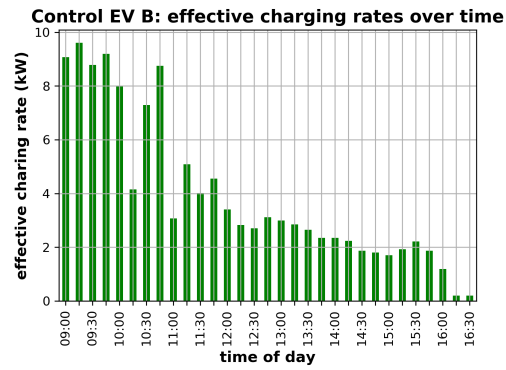


Fig. A5.7.8: Control EV B, average power flow over 15 min

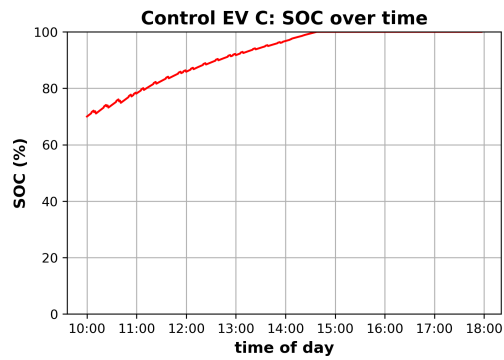


Fig. A5.7.9: Control EV C, SOC over time while connected

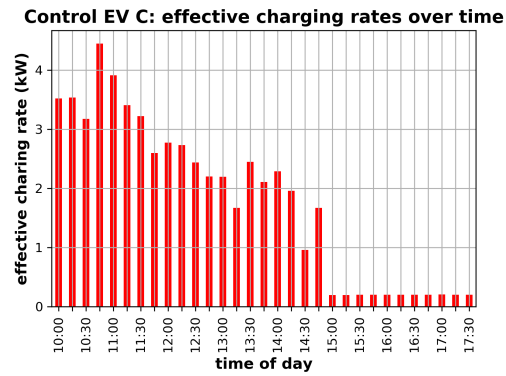


Fig. A5.7.10: Control EV C, average power flow over 15 min

## A5.8 Scenario H

Scenario specific parameters:

- The simulation assumes a constant grid connection limit of 300 kW
- EV user inputs are enabled and inform V2G scheduling (SQL triggers used: see section 5.4)
- The default CW and DCW equations for four charging modes are used to assess each EV (see section 5.3)

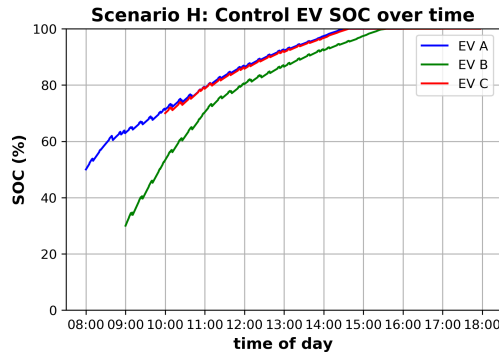


Fig. A5.8.1: All control EVs, SOC over time

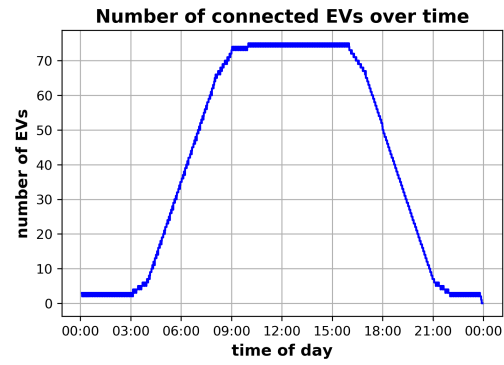


Fig. A5.8.2: Number of simulated EVs connected to V2G network over time

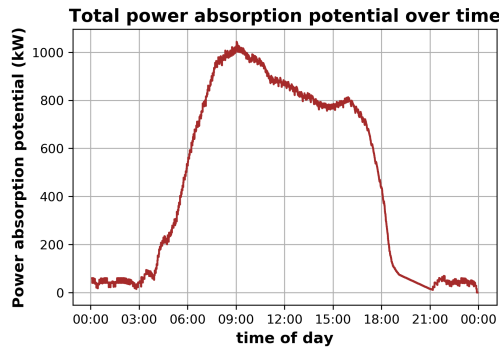


Fig. A5.8.3: Aggregated EV population, total power absorption potential

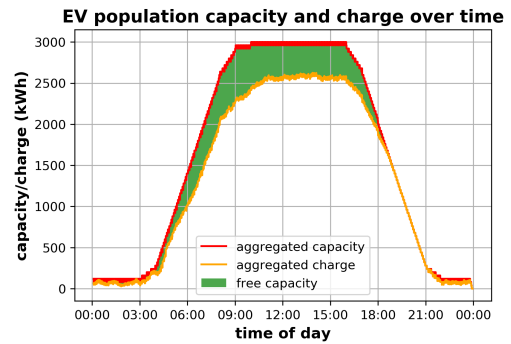


Fig. A5.8.4: Aggregated EV population, total capacity, total charge and free capacity

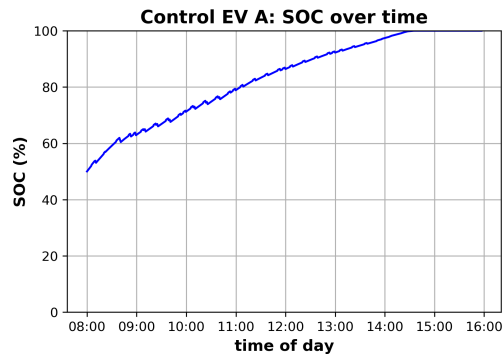


Fig. A5.8.5: Control EV A, SOC over time while connected

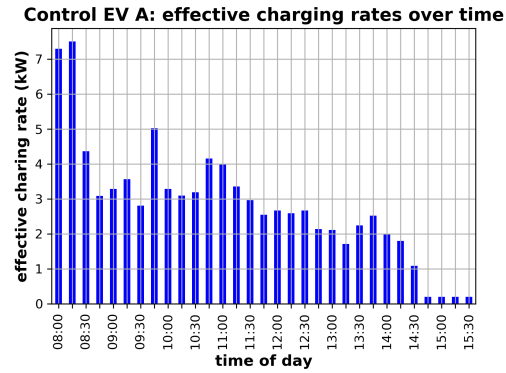


Fig. A5.8.6: Control EV A, average power flow over 15 min

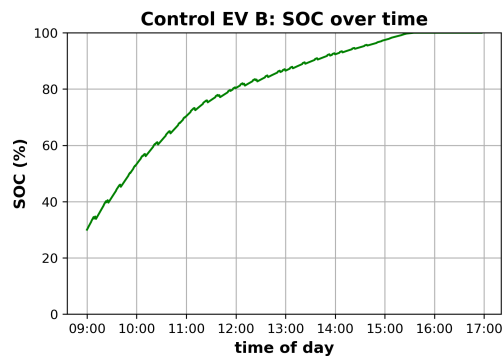


Fig. A5.8.7: Control EV B, SOC over time while connected

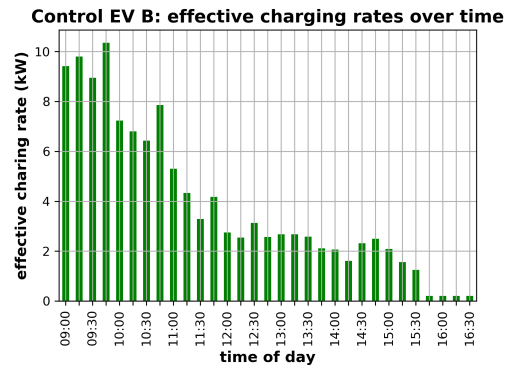


Fig. A5.8.8: Control EV B, average power flow over 15 min

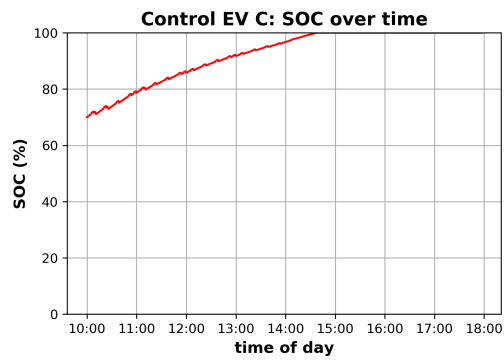


Fig. A5.8.9: Control EV C, SOC over time while connected

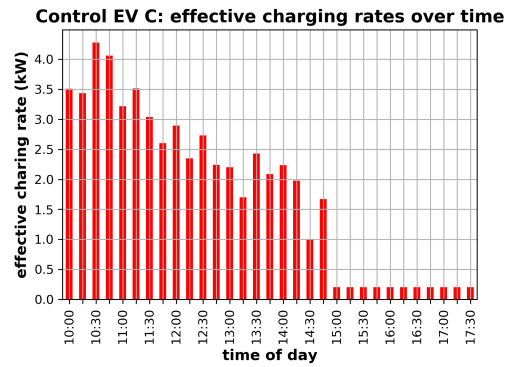


Fig. A5.8.10: Control EV C, average power flow over 15 min

## A5.9 Scenario I

Scenario specific parameters:

- The simulation assumes a constant grid connection limit of 300 kW
- EV user inputs are enabled and inform V2G scheduling (SQL triggers used: see section 5.4)
- The default CW and DCW equations for four charging modes are used to assess each EV (see section 5.3)

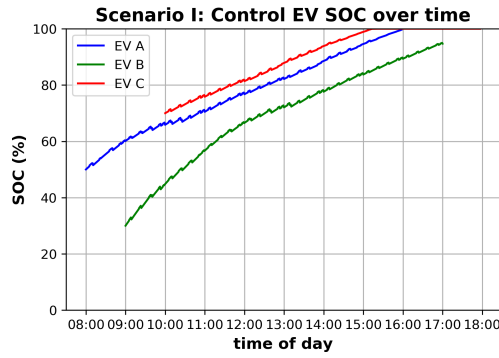


Fig. A5.9.1: All control EVs, SOC over time

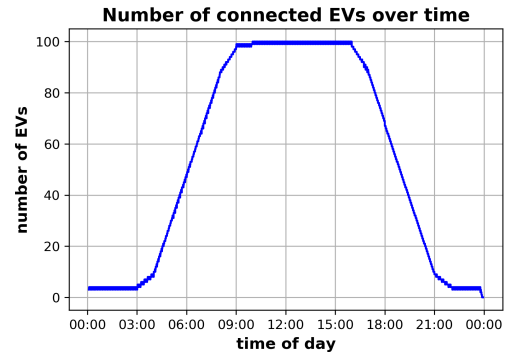


Fig. A5.9.2: Number of simulated EVs connected to V2G network over time

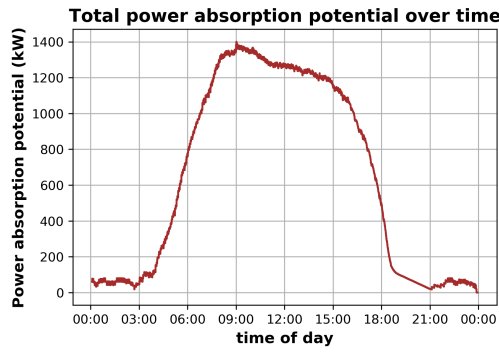


Fig. A5.9.3: Aggregated EV population, total power absorption potential

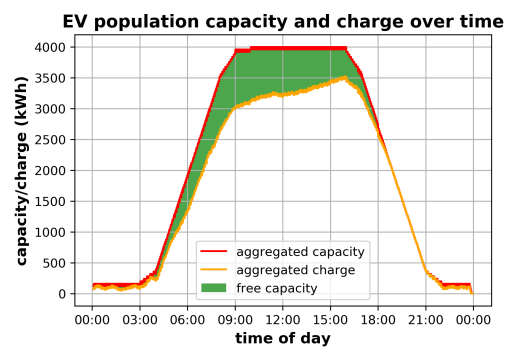


Fig. A5.9.4: Aggregated EV population, total capacity, total charge and free capacity

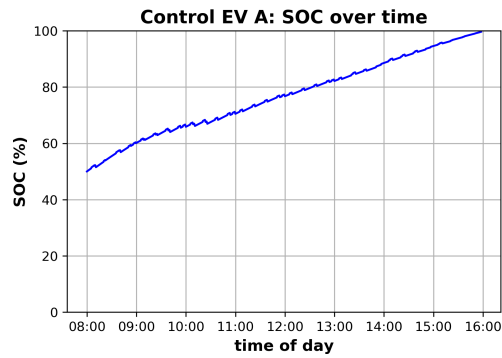


Fig. A5.9.5: Control EV A, SOC over time while connected

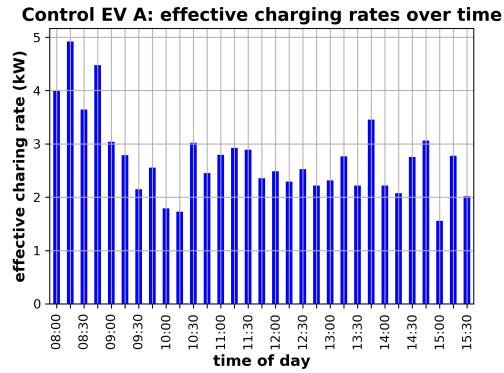


Fig. A5.9.6: Control EV A, average power flow over 15 min

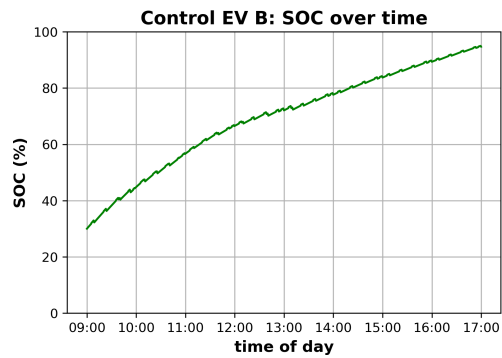


Fig. A5.9.7: Control EV B, SOC over time while connected

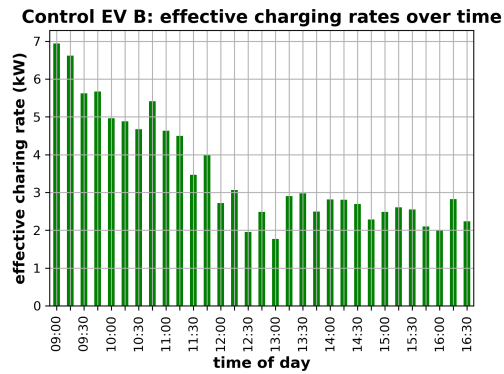


Fig. A5.9.8: Control EV B, average power flow over 15 min

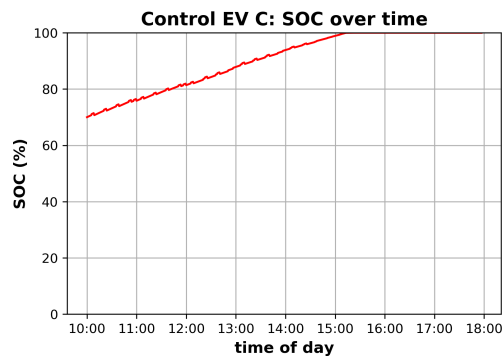


Fig. A5.9.9: Control EV C, SOC over time while connected

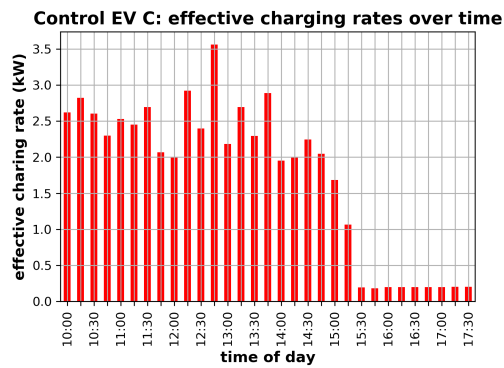


Fig. A5.9.10: Control EV C, average power flow over 15 min



## A5.10 Scenario J

Scenario specific parameters:

- The simulation assumes a constant grid connection limit of 400 kW
- EV user inputs are enabled and inform V2G scheduling (SQL triggers used: see section 5.4)
- The default CW and DCW equations for four charging modes are used to assess each EV (see section 5.3)

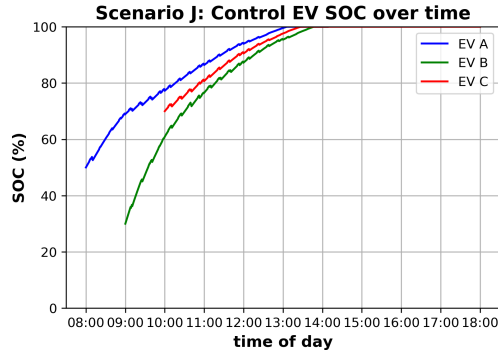


Fig. A5.10.1: All control EVs, SOC over time

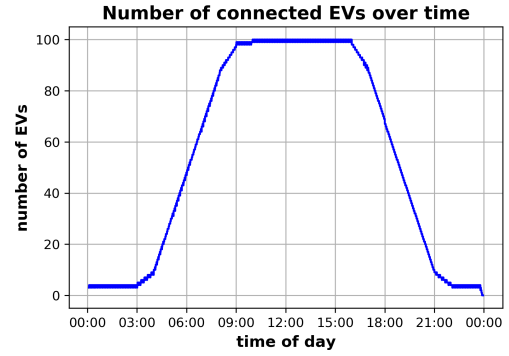


Fig. A5.10.2: Number of simulated EVs connected to V2G network over time

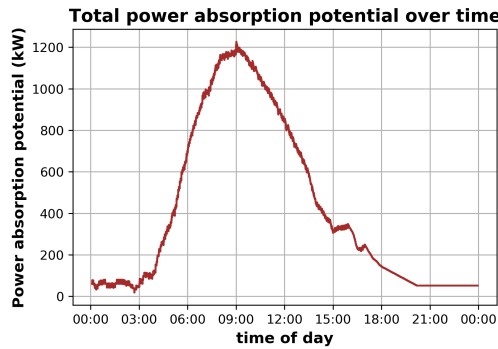


Fig. A5.10.3: Aggregated EV population, total power absorption potential

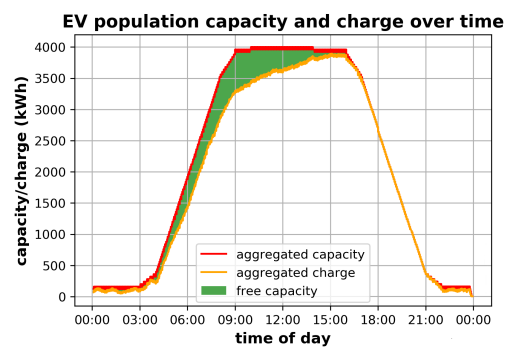


Fig. A5.10.4: Aggregated EV population, total capacity, total charge and free capacity

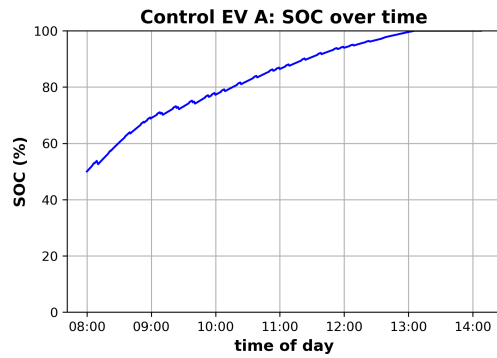


Fig. A5.10.5: Control EV A, SOC over time while connected

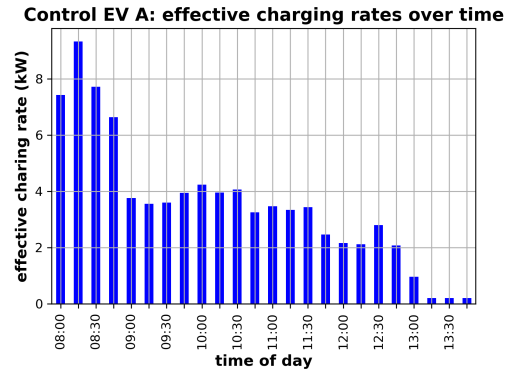


Fig. A5.10.6: Control EV A, average power flow over 15 min

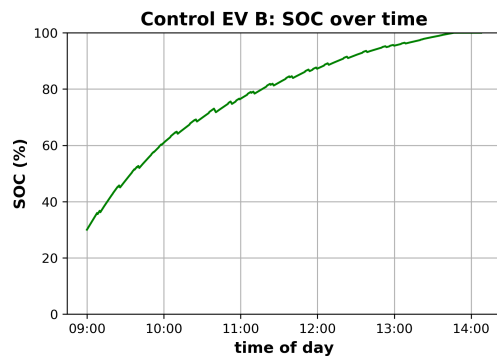


Fig. A5.10.7: Control EV B, SOC over time while connected

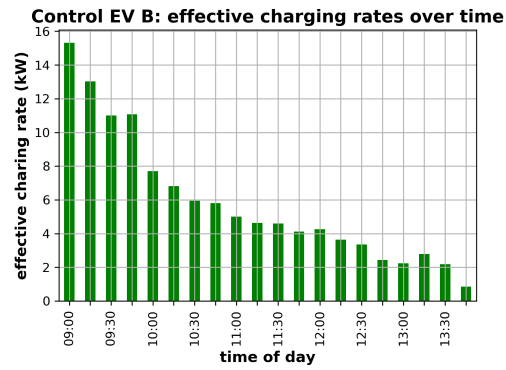


Fig. A5.10.8: Control EV B, average power flow over 15 min

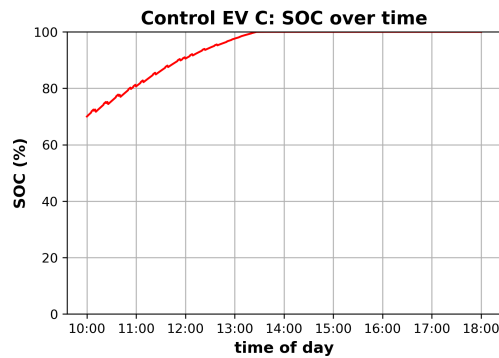


Fig. A5.10.9: Control EV C, SOC over time while connected

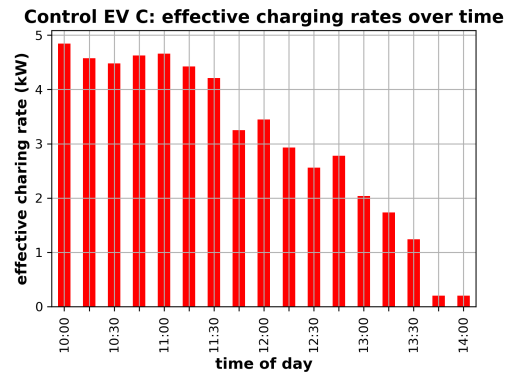


Fig. A5.10.10: Control EV C, average power flow over 15 min

## A5.11 Scenario K

Scenario specific parameters:

- The simulation assumes a constant grid connection limit of 500 kW
- EV user inputs are enabled and inform V2G scheduling (SQL triggers used: see section 5.4)
- The default CW and DCW equations for four charging modes are used to assess each EV (see section 5.3)

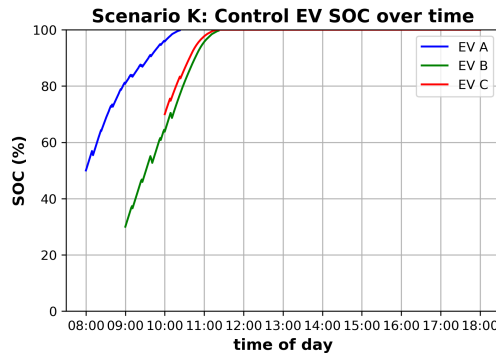


Fig. A5.11.1: All control EVs, SOC over time

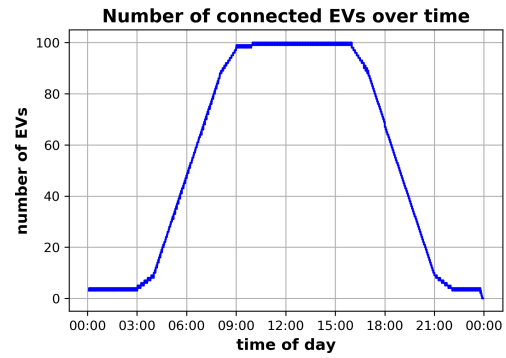


Fig. A5.11.2: Number of simulated EVs connected to V2G network over time

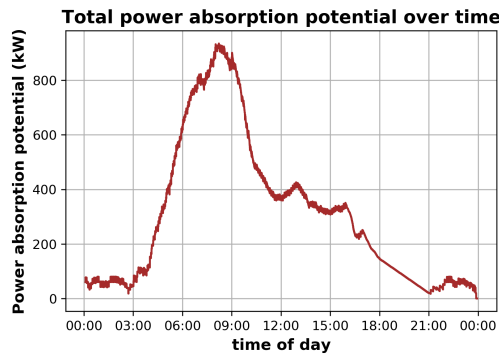


Fig. A5.11.3: Aggregated EV population, total power absorption potential

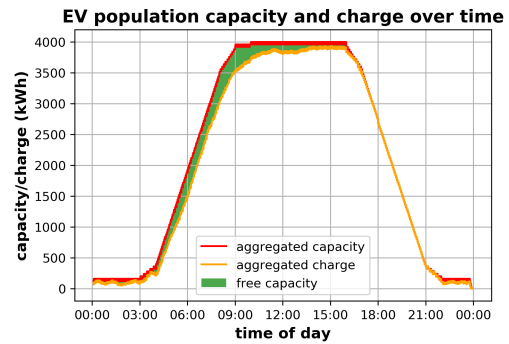


Fig. A5.11.4: Aggregated EV population, total capacity, total charge and free capacity

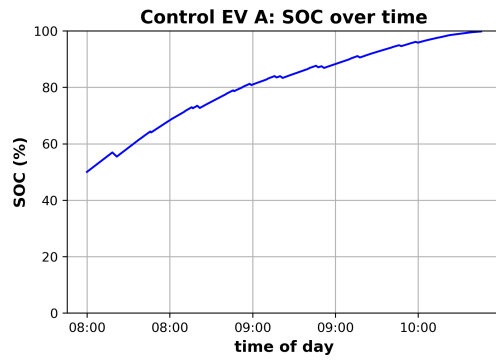


Fig. A5.11.5: Control EV A, SOC over time while connected

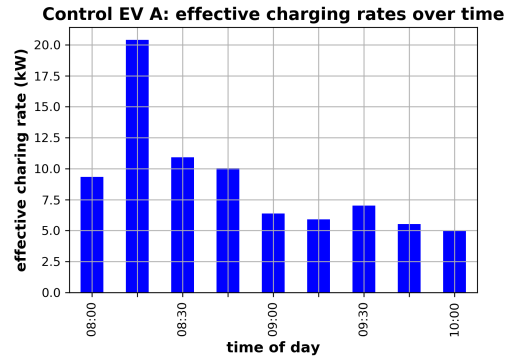


Fig. A5.11.6: Control EV A, average power flow over 15 min

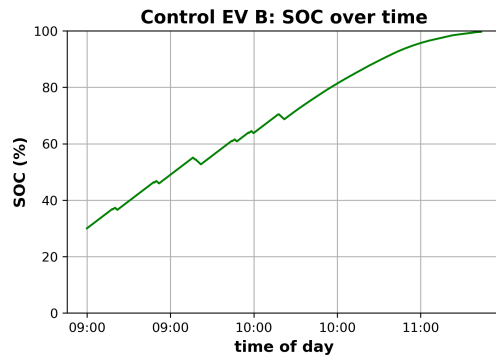


Fig. A5.11.7: Control EV B, SOC over time while connected

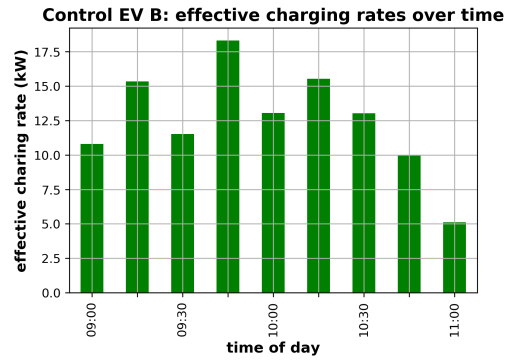


Fig. A5.11.8: Control EV B, average power flow over 15 min

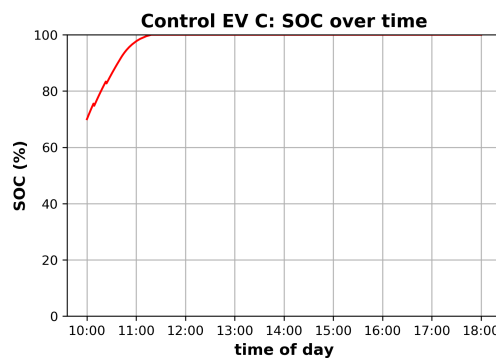


Fig. A5.11.9: Control EV C, SOC over time while connected

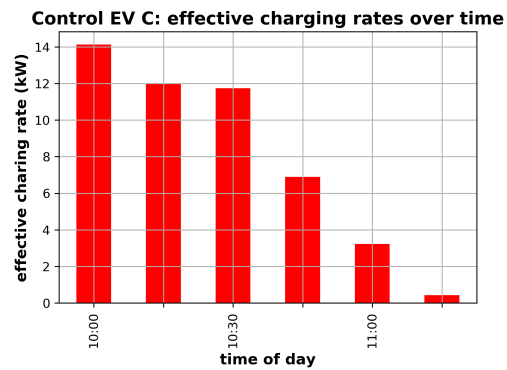


Fig. A5.11.10: Control EV C, average power flow over 15 min

## A6. FULL SIMULATION RESULTS FOR CHAPTER 5

This appendix contains a catalogue of all results for the simulated scenario discussed in chapter 5.

- All simulations were run in real-time using the aggregator control algorithms outlined in chapter 3.
- The simulated EV population of up to 100 EVs follows the 24-hour car park occupancy model outlined in section 4.3.
- Rail system power flows follow the power demand curves and train schedule outlined in section 4.2.
- Within the simulated EV population were six controlled/monitored EV's as outlined in section 3.6. These 'control EVs' have identical capacity (40 kWh) and maximum charging rate (50 kW), but connect to the network at different times and with different initial SOC (see Table A6.1). All control EVs were disconnected at 18:00.

Control EV Name	Initial SOC	Connection Time	Charging Mode	Charging Target
EV A	50 %	08:00:00	1	-
EV B	40 %	08:00:00	2	70 % SOC
EV C	20 %	09:00:00	2	90 % SOC
EV D	40 %	09:00:00	3	-
EV E	40 %	10:00:00	4	80 % SOC at 18:00:00
EV F	20 %	10:00:00	4	90 % SOC at 13:00:00

*Tab. A6.1:* Control EV definitions (identical for all scenarios in discussed in this chapter): initial SOC, connection time, charging mode (see section 5.1) and charging targets (where applicable)

### A6.1 Scenario I

Scenario specific parameters:

- The simulation assumes a constant grid connection limit of 200 kW
- EV user inputs are enabled and inform V2G scheduling (SQL triggers used: see section 5.4)
- The default CW and DCW equations for four charging modes are used to assess each EV (see section 5.3)

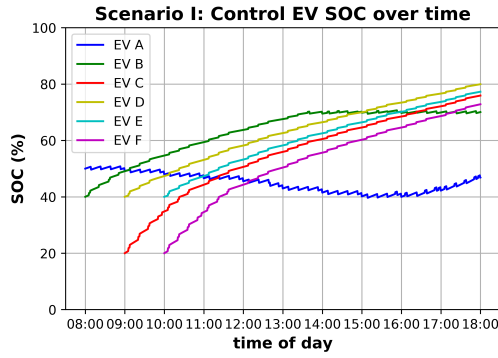


Fig. A6.1.1: All control EVs, SOC over time

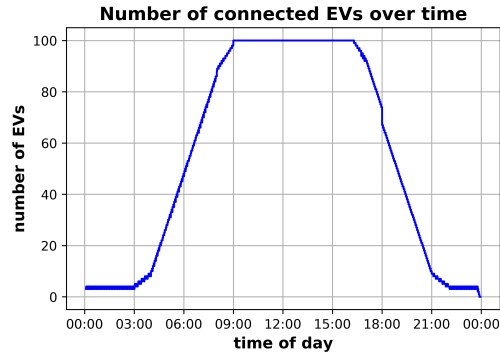


Fig. A6.1.2: Number of simulated EVs connected to V2G network over time

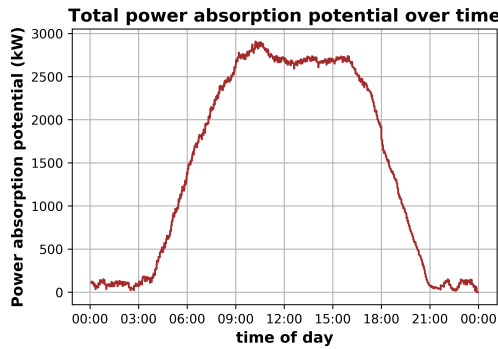


Fig. A6.1.3: Aggregated EV population, total power absorption potential

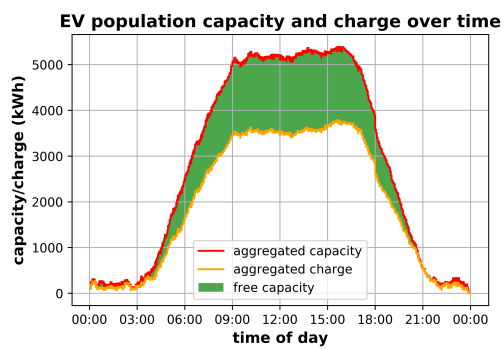


Fig. A6.1.4: Aggregated EV population, total capacity, total charge and free capacity

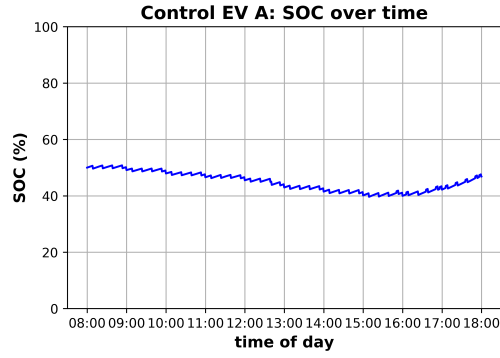


Fig. A6.1.5: Control EV A, SOC over time while connected

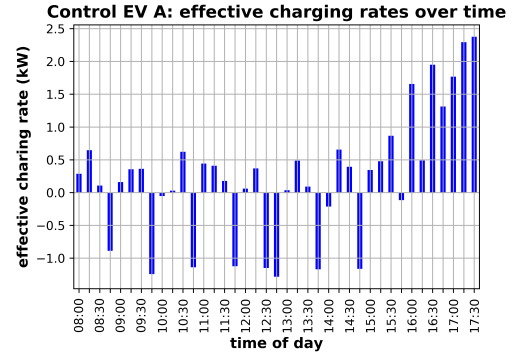


Fig. A6.1.6: Control EV A, average power flow over 15 min

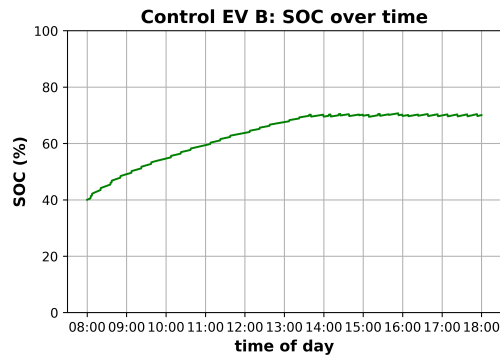


Fig. A6.1.7: Control EV B, SOC over time while connected

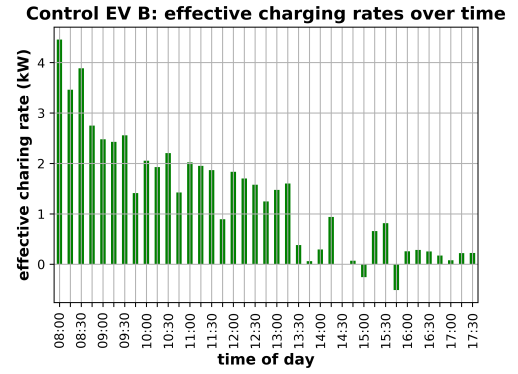


Fig. A6.1.8: Control EV B, average power flow over 15 min

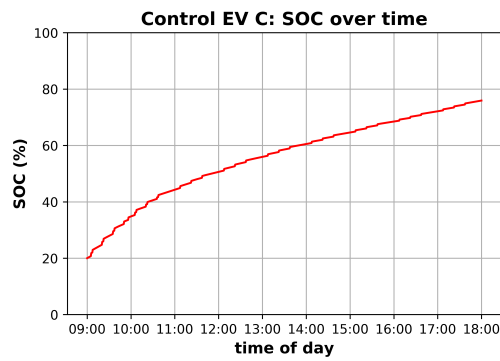


Fig. A6.1.9: Control EV C, SOC over time while connected

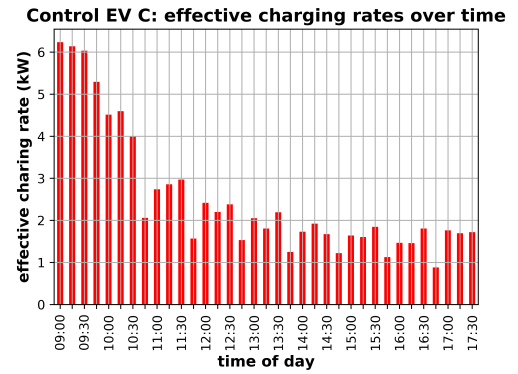


Fig. A6.1.10: Control EV C, average power flow over 15 min

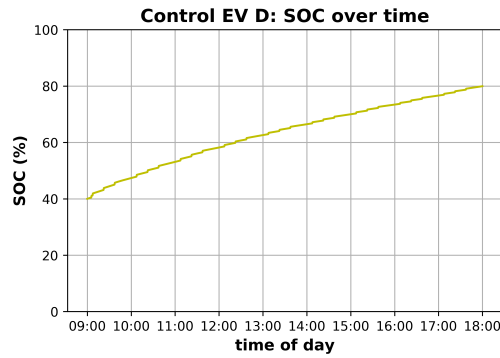


Fig. A6.1.11: Control EV D, SOC over time while connected

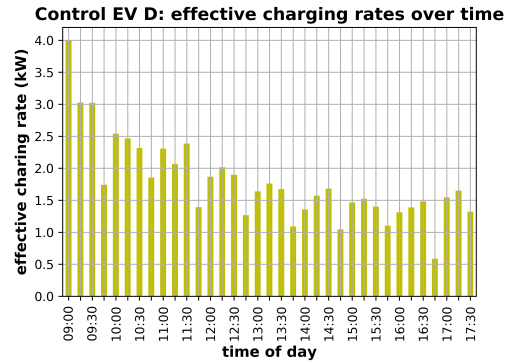


Fig. A6.1.12: Control EV D, average power flow over 15 min

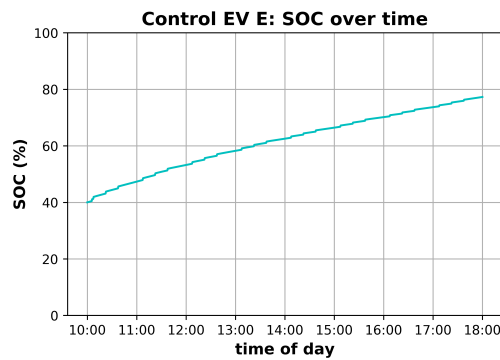


Fig. A6.1.13: Control EV E, SOC over time while connected

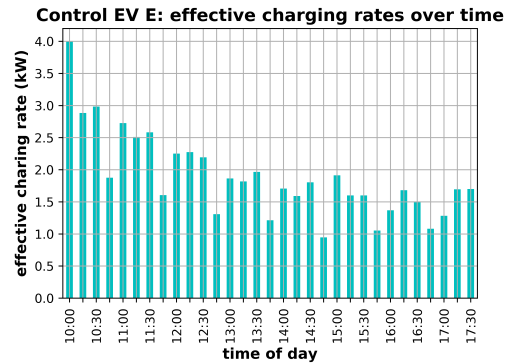


Fig. A6.1.14: Control EV E, average power flow over 15 min

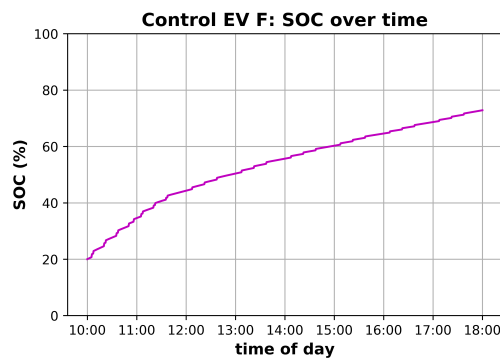


Fig. A6.1.15: Control EV F, SOC over time while connected

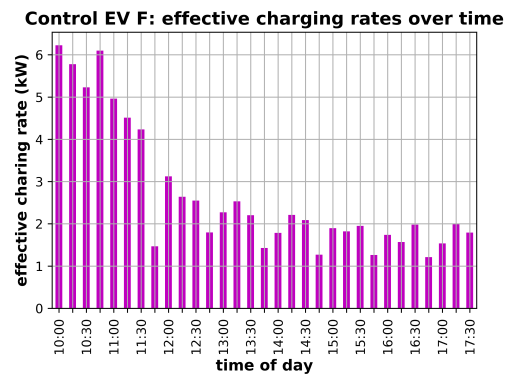


Fig. A6.1.16: Control EV F, average power flow over 15 min



## A6.2 Scenario II

Scenario specific parameters:

- The simulation assumes a constant grid connection limit of 300 kW
- EV user inputs are enabled and inform V2G scheduling (SQL triggers used: see section 5.4)
- The default CW and DCW equations for four charging modes are used to assess each EV (see section 5.3)

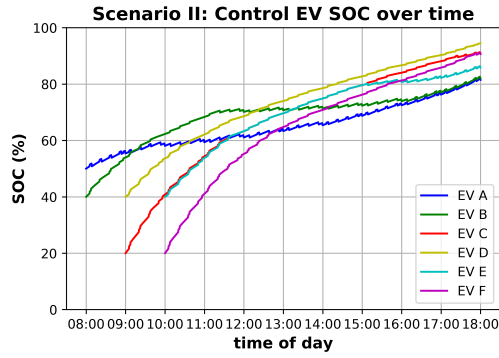


Fig. A6.2.1: All control EVs, SOC over time

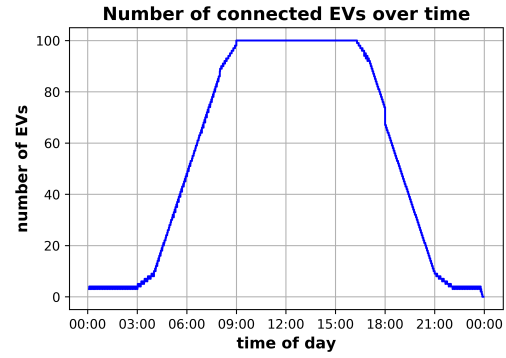


Fig. A6.2.2: Number of simulated EVs connected to V2G network over time

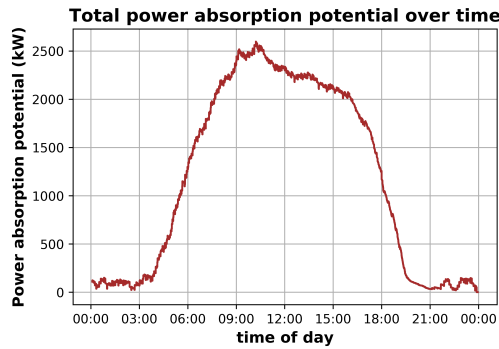


Fig. A6.2.3: Aggregated EV population, total power absorption potential

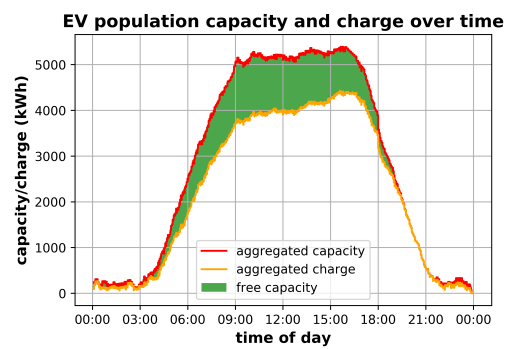


Fig. A6.2.4: Aggregated EV population, total capacity, total charge and free capacity

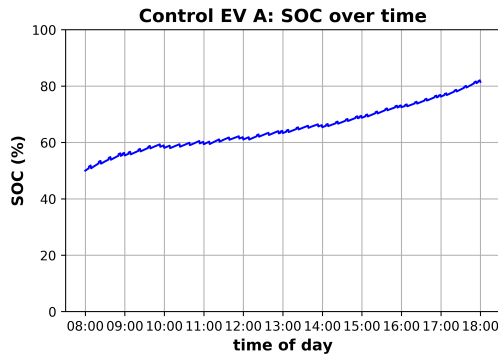


Fig. A6.2.5: Control EV A, SOC over time while connected

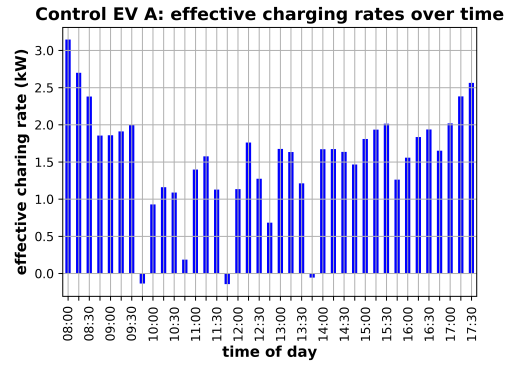


Fig. A6.2.6: Control EV A, average power flow over 15 min

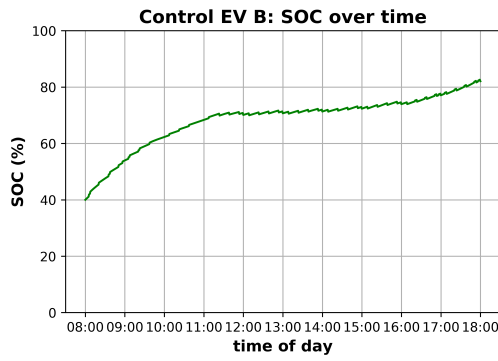


Fig. A6.2.7: Control EV B, SOC over time while connected

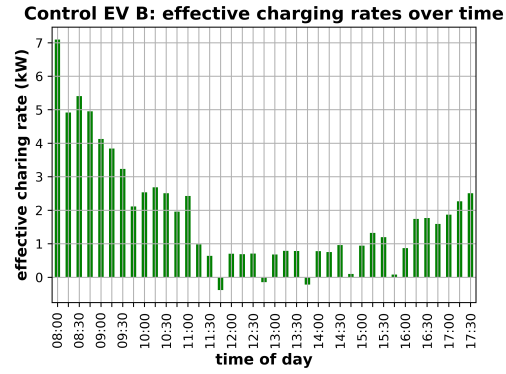


Fig. A6.2.8: Control EV B, average power flow over 15 min

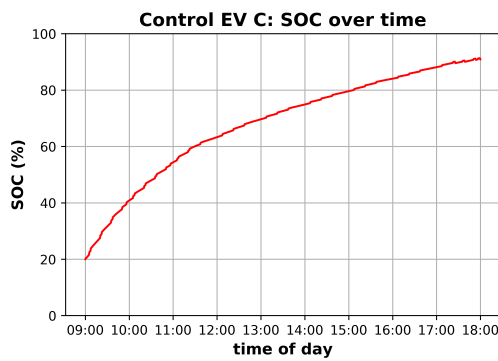


Fig. A6.2.9: Control EV C, SOC over time while connected

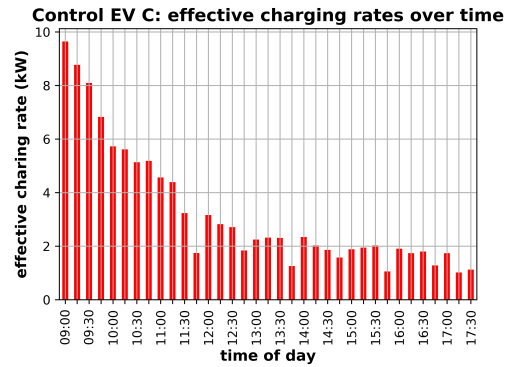


Fig. A6.2.10: Control EV C, average power flow over 15 min

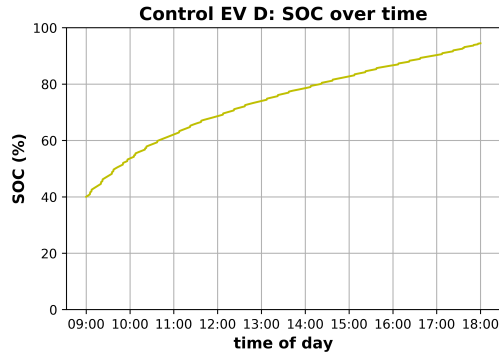


Fig. A6.2.11: Control EV D, SOC over time while connected

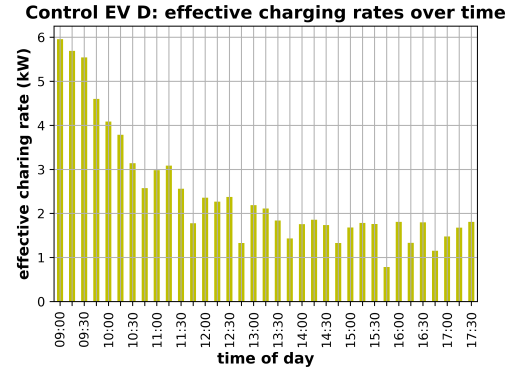


Fig. A6.2.12: Control EV D, average power flow over 15 min

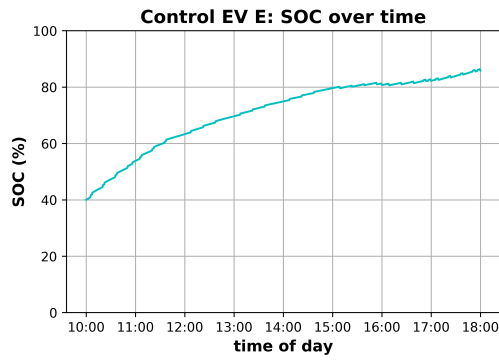


Fig. A6.2.13: Control EV E, SOC over time while connected

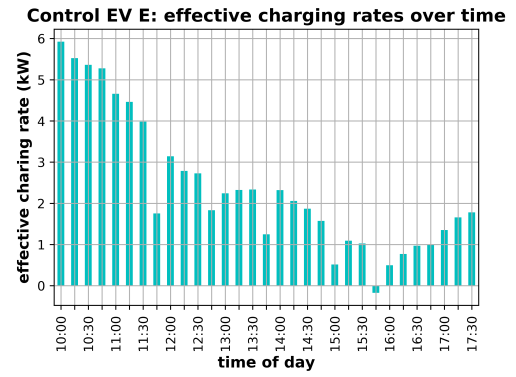


Fig. A6.2.14: Control EV E, average power flow over 15 min

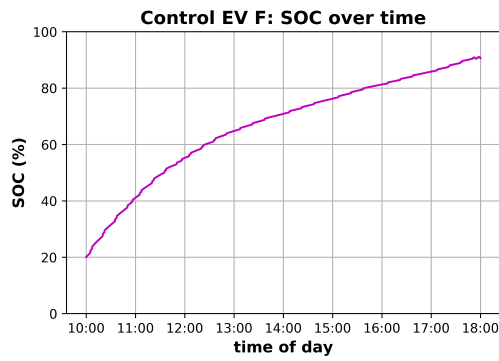


Fig. A6.2.15: Control EV F, SOC over time while connected

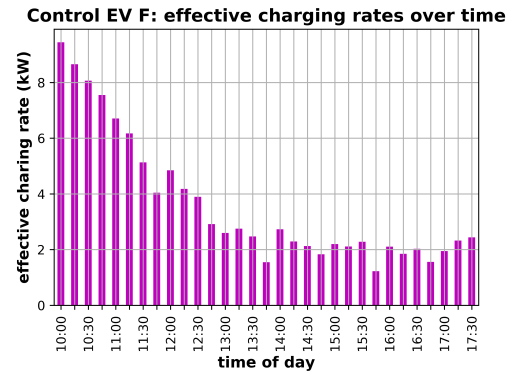


Fig. A6.2.16: Control EV F, average power flow over 15 min

### A6.3 Scenario III

Scenario specific parameters:

- The simulation assumes a constant grid connection limit of 400 kW
- EV user inputs are enabled and inform V2G scheduling (SQL triggers used: see section 5.4)
- The default CW and DCW equations for four charging modes are used to assess each EV (see section 5.3)

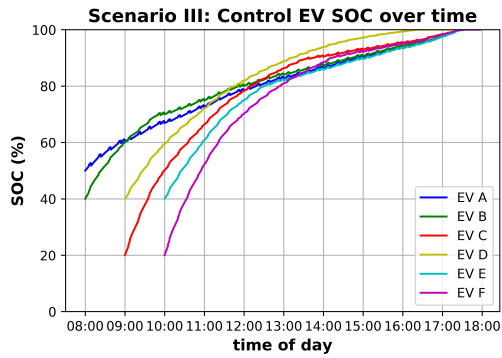


Fig. A6.3.1: All control EVs, SOC over time

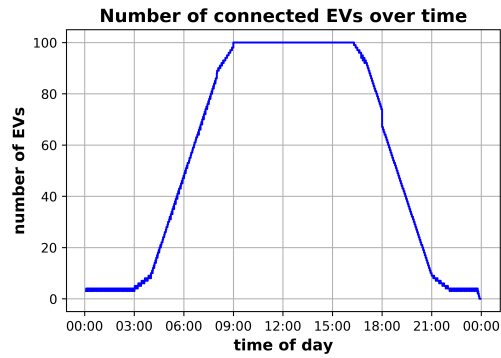


Fig. A6.3.2: Number of simulated EVs connected to V2G network over time

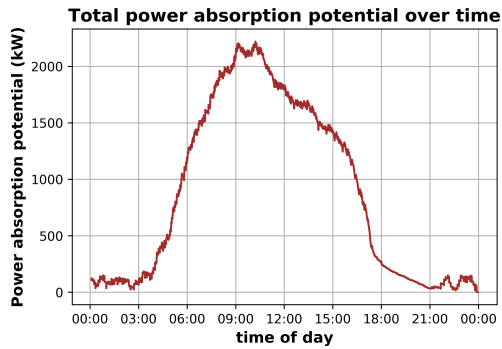


Fig. A6.3.3: Aggregated EV population, total power absorption potential

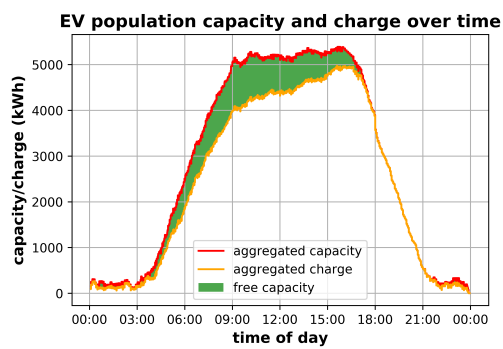


Fig. A6.3.4: Aggregated EV population, total capacity, total charge and free capacity

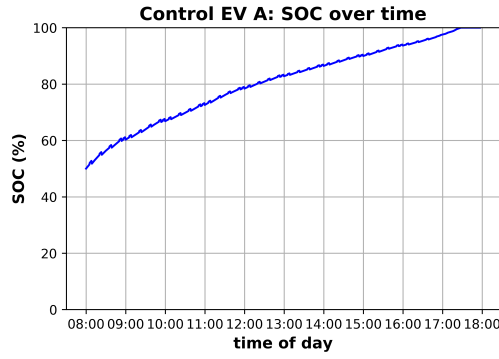


Fig. A6.3.5: Control EV A, SOC over time while connected

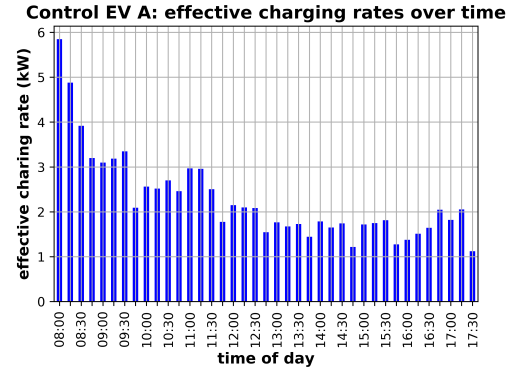


Fig. A6.3.6: Control EV A, average power flow over 15 min

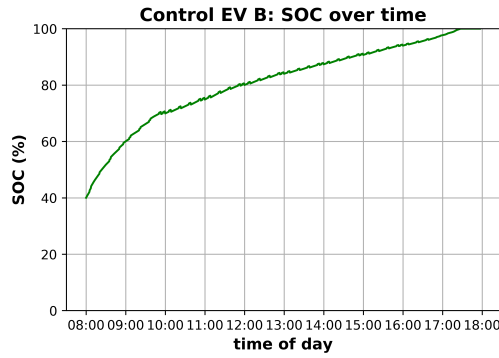


Fig. A6.3.7: Control EV B, SOC over time while connected

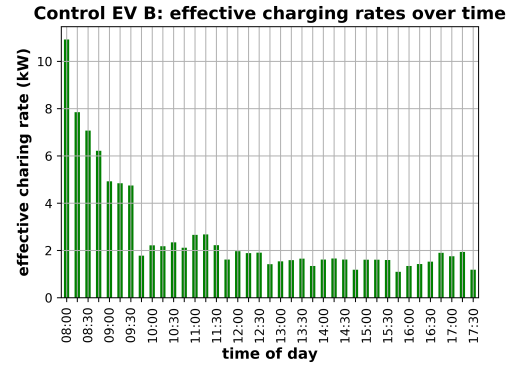


Fig. A6.3.8: Control EV B, average power flow over 15 min

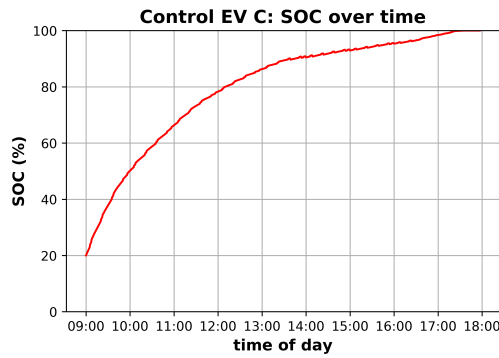


Fig. A6.3.9: Control EV C, SOC over time while connected

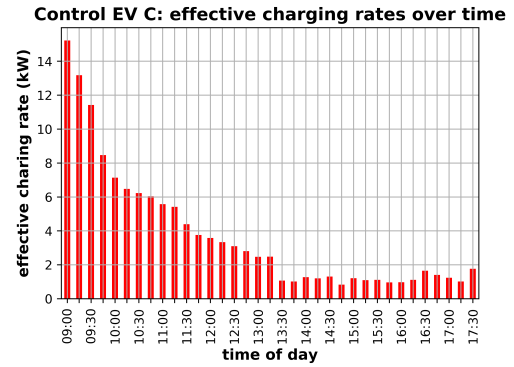


Fig. A6.3.10: Control EV C, average power flow over 15 min

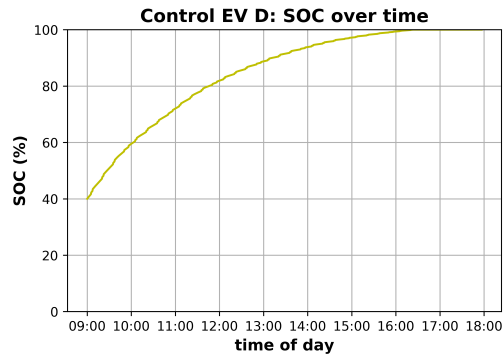


Fig. A6.3.11: Control EV D, SOC over time while connected

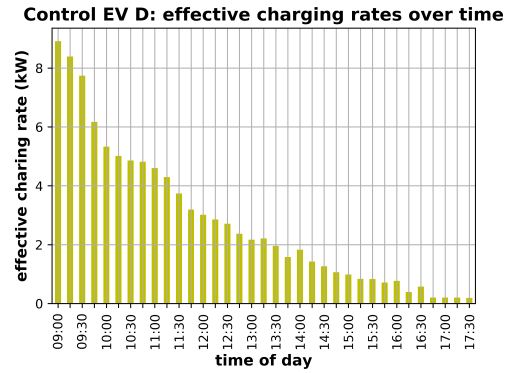


Fig. A6.3.12: Control EV D, average power flow over 15 min

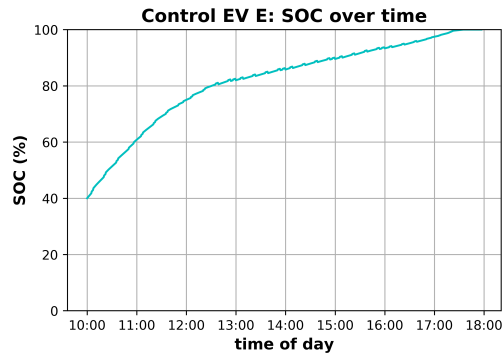


Fig. A6.3.13: Control EV E, SOC over time while connected

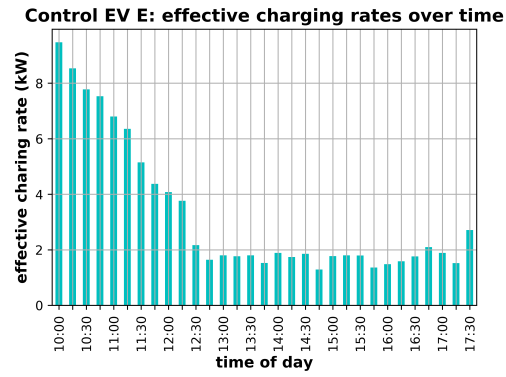


Fig. A6.3.14: Control EV E, average power flow over 15 min

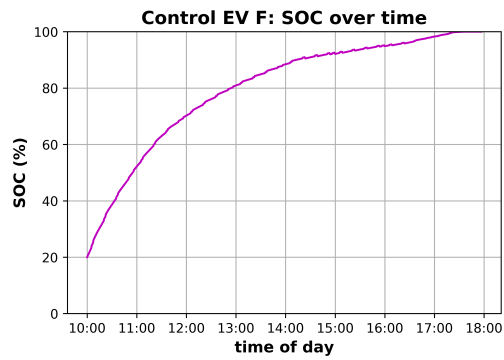


Fig. A6.3.15: Control EV F, SOC over time while connected

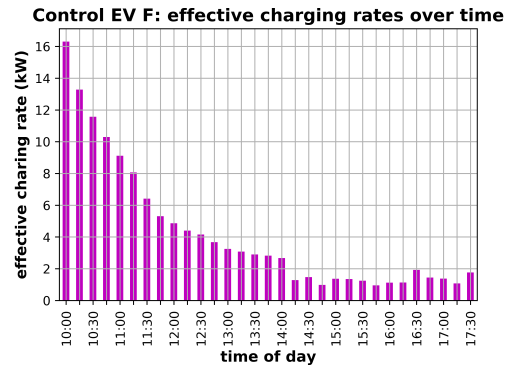


Fig. A6.3.16: Control EV F, average power flow over 15 min

## A6.4 Scenario IV

Scenario specific parameters:

- The simulation assumes a constant grid connection limit of 200 kW
- EV user inputs are disabled and do not inform V2G scheduling (SQL triggers used: see section 5.4)
- The CW and DCW equations without charging modes are used to assess each EV (see Equation 3.1 and Equation 3.2 in chapter 3)

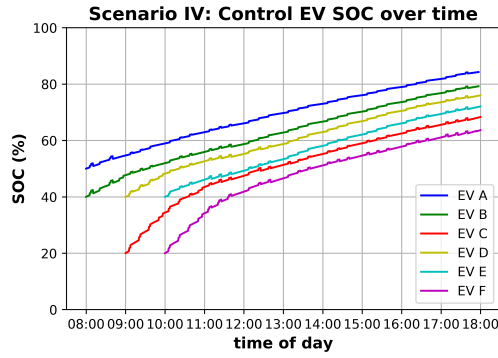


Fig. A6.4.1: All control EVs, SOC over time

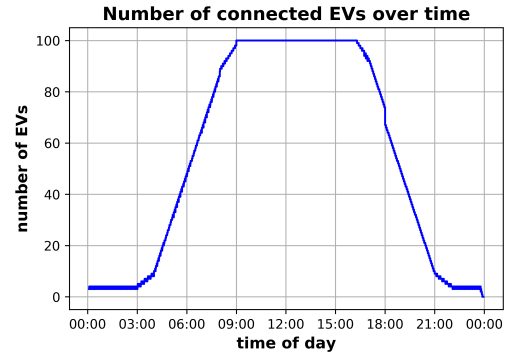


Fig. A6.4.2: Number of simulated EVs connected to V2G network over time

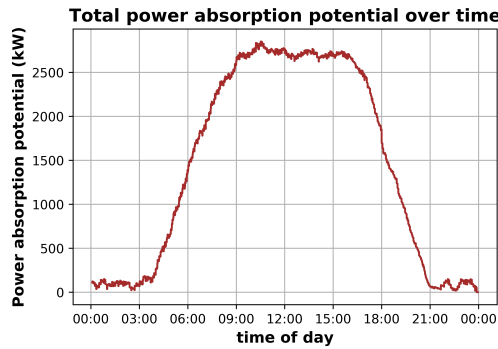


Fig. A6.4.3: Aggregated EV population, total power absorption potential

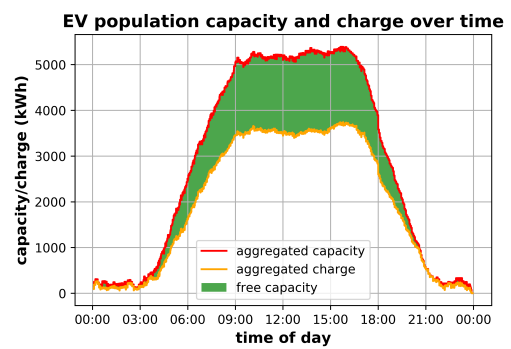


Fig. A6.4.4: Aggregated EV population, total capacity, total charge and free capacity

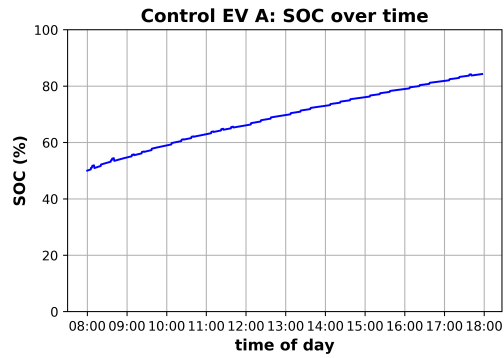


Fig. A6.4.5: Control EV A, SOC over time while connected

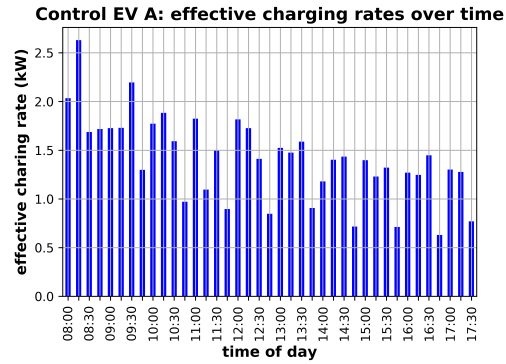


Fig. A6.4.6: Control EV A, average power flow over 15 min

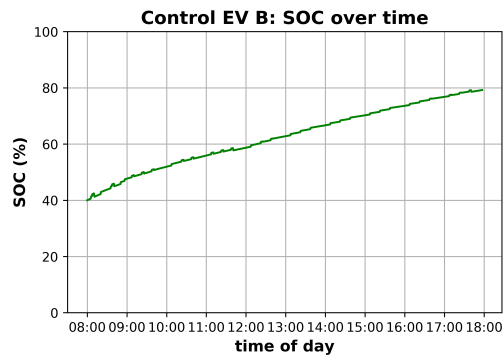


Fig. A6.4.7: Control EV B, SOC over time while connected

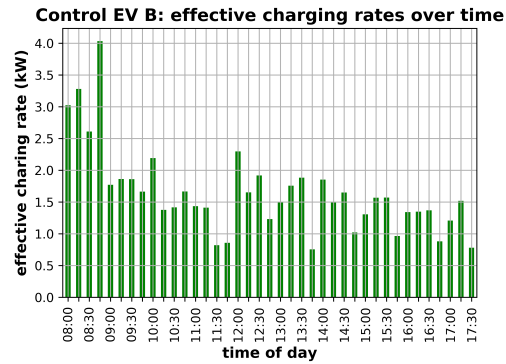


Fig. A6.4.8: Control EV B, average power flow over 15 min

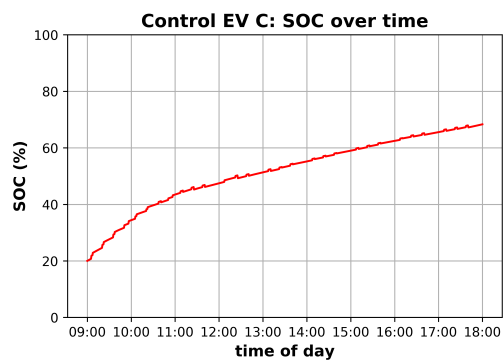


Fig. A6.4.9: Control EV C, SOC over time while connected

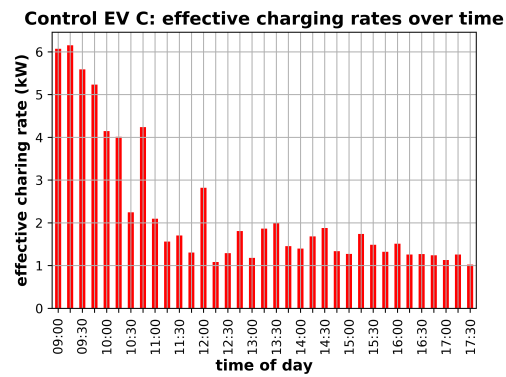


Fig. A6.4.10: Control EV C, average power flow over 15 min



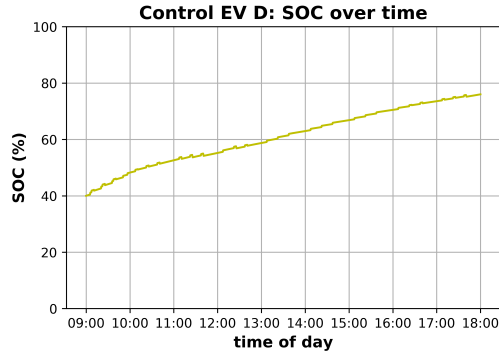


Fig. A6.4.11: Control EV D, SOC over time while connected

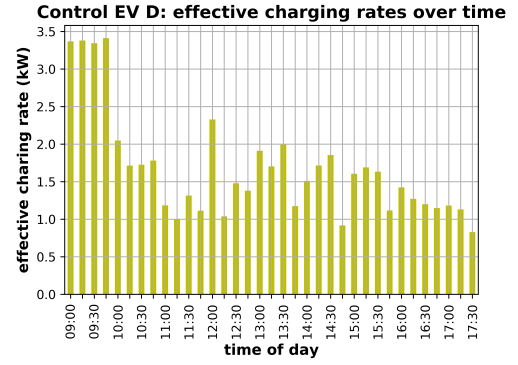


Fig. A6.4.12: Control EV D, average power flow over 15 min

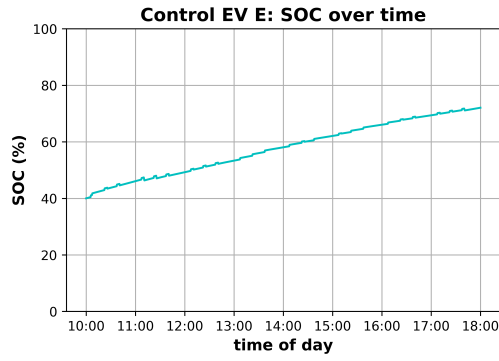


Fig. A6.4.13: Control EV E, SOC over time while connected

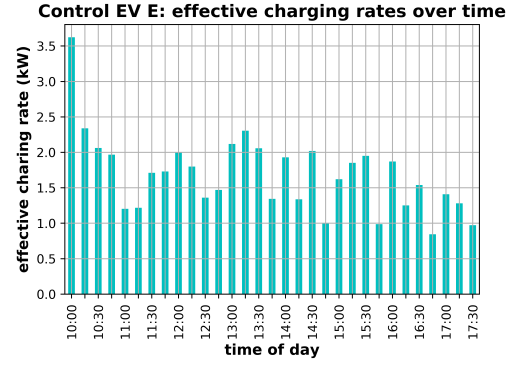


Fig. A6.4.14: Control EV E, average power flow over 15 min

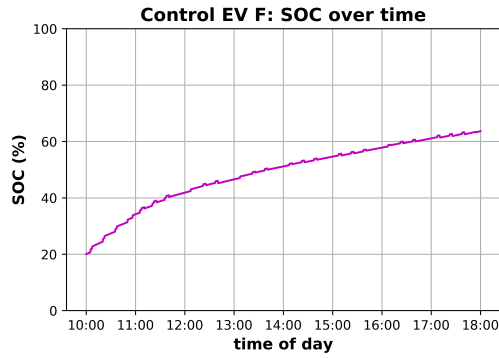


Fig. A6.4.15: Control EV F, SOC over time while connected

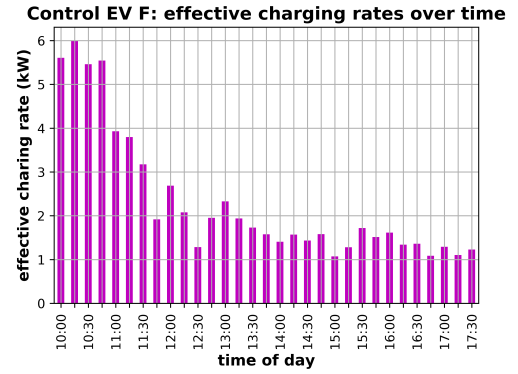


Fig. A6.4.16: Control EV F, average power flow over 15 min

### A6.5 Scenario V

Scenario specific parameters:

- The simulation assumes a constant grid connection limit of 300 kW
- EV user inputs are disabled and do not inform V2G scheduling (SQL triggers used: see section 5.4)
- The CW and DCW equations without charging modes are used to assess each EV (see Equation 3.1 and Equation 3.2 in chapter 3)

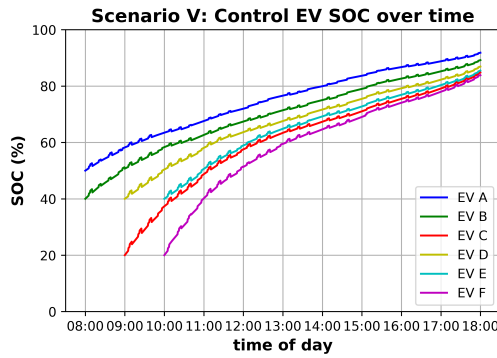


Fig. A6.5.1: All control EVs, SOC over time

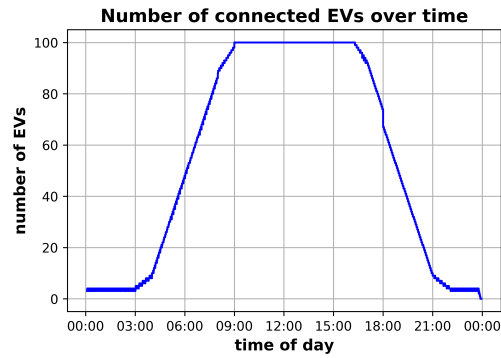


Fig. A6.5.2: Number of simulated EVs connected to V2G network over time

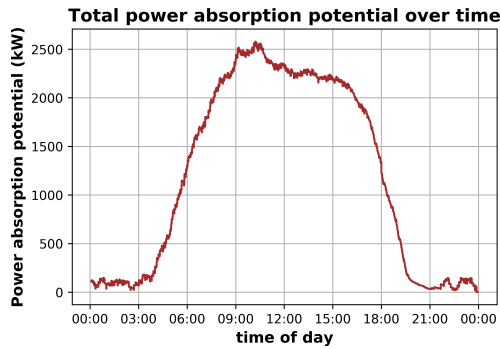


Fig. A6.5.3: Aggregated EV population, total power absorption potential

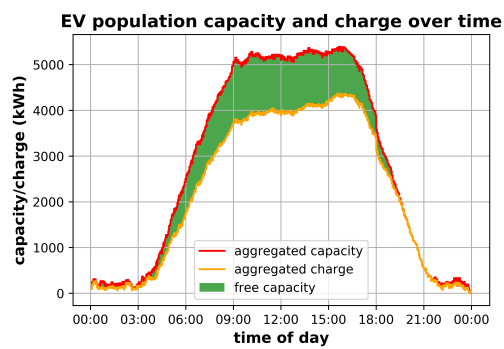


Fig. A6.5.4: Aggregated EV population, total capacity, total charge and free capacity

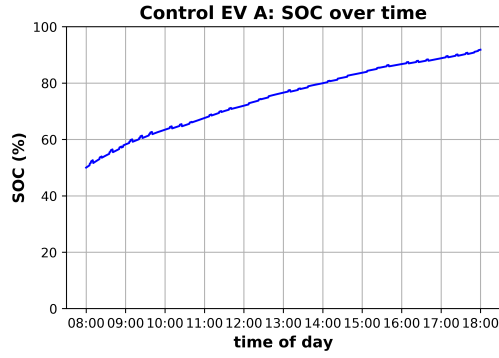


Fig. A6.5.5: Control EV A, SOC over time while connected

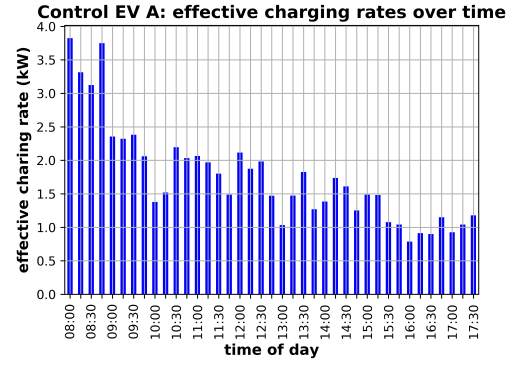


Fig. A6.5.6: Control EV A, average power flow over 15 min

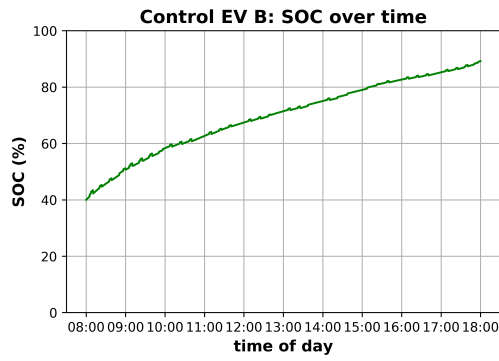


Fig. A6.5.7: Control EV B, SOC over time while connected

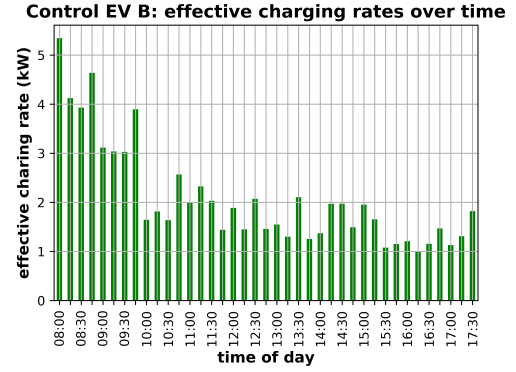


Fig. A6.5.8: Control EV B, average power flow over 15 min

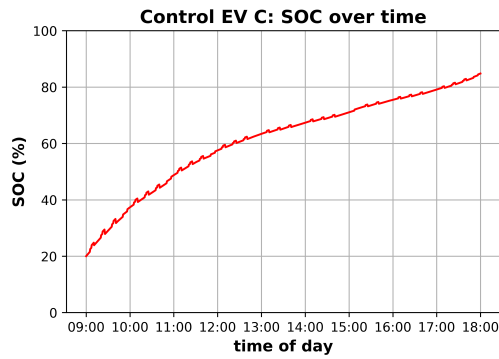


Fig. A6.5.9: Control EV C, SOC over time while connected

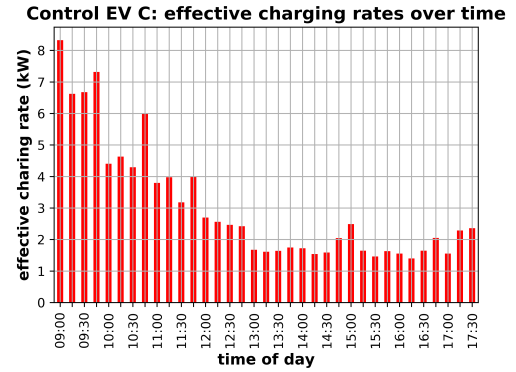


Fig. A6.5.10: Control EV C, average power flow over 15 min

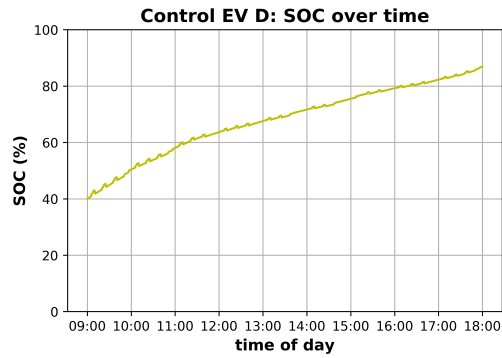


Fig. A6.5.11: Control EV D, SOC over time while connected

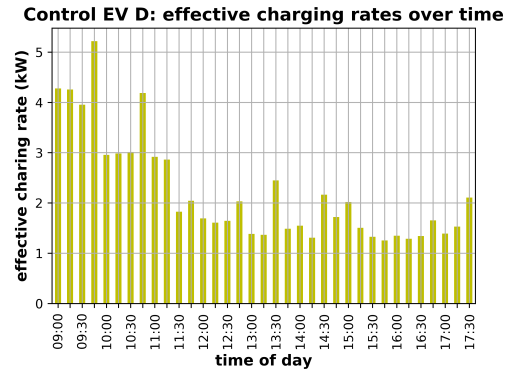


Fig. A6.5.12: Control EV D, average power flow over 15 min

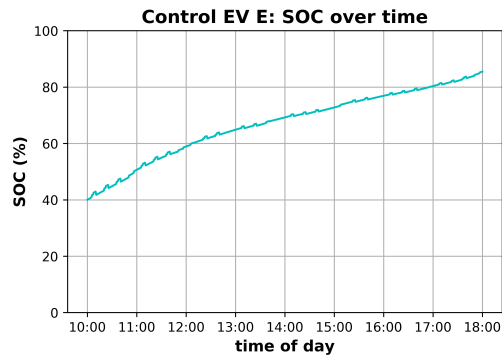


Fig. A6.5.13: Control EV E, SOC over time while connected

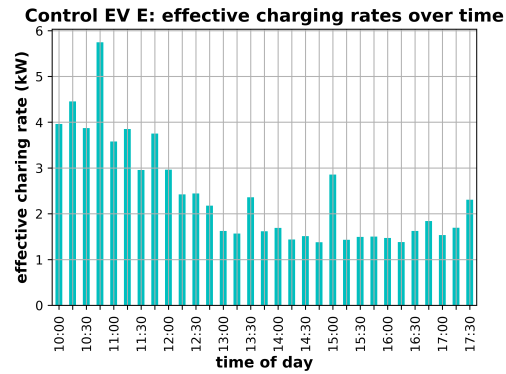


Fig. A6.5.14: Control EV E, average power flow over 15 min

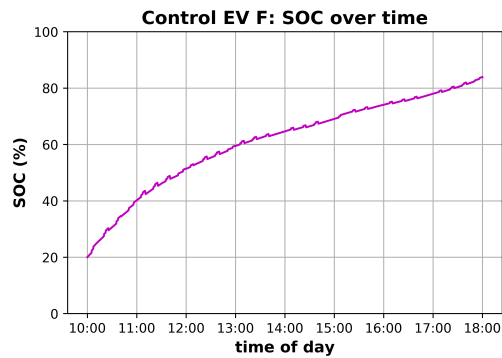


Fig. A6.5.15: Control EV F, SOC over time while connected

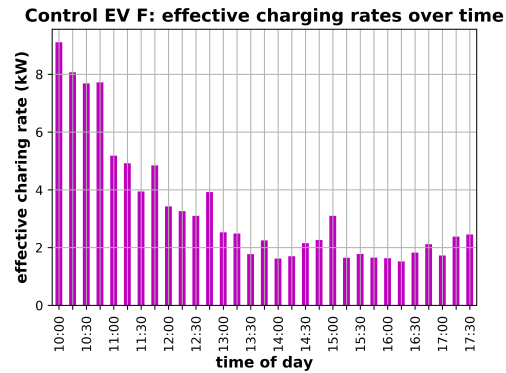


Fig. A6.5.16: Control EV F, average power flow over 15 min

## A6.6 Scenario VI

Scenario specific parameters:

- The simulation assumes a constant grid connection limit of 400 kW
- EV user inputs are disabled and do not inform V2G scheduling (SQL triggers used: see section 5.4)
- The CW and DCW equations without charging modes are used to assess each EV (see Equation 3.1 and Equation 3.2 in chapter 3)

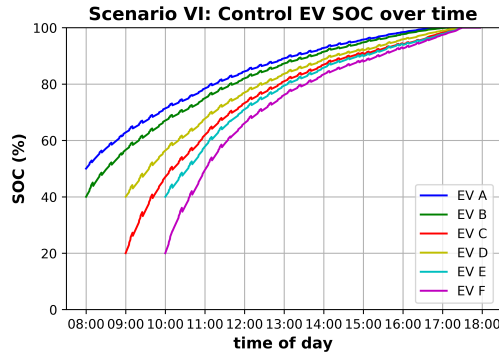


Fig. A6.6.1: All control EVs, SOC over time

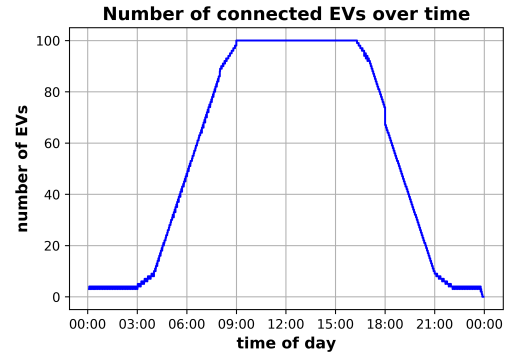


Fig. A6.6.2: Number of simulated EVs connected to V2G network over time

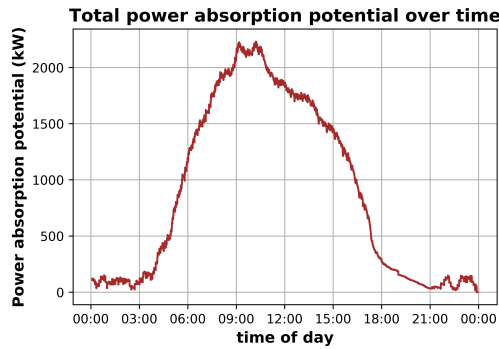


Fig. A6.6.3: Aggregated EV population, total power absorption potential

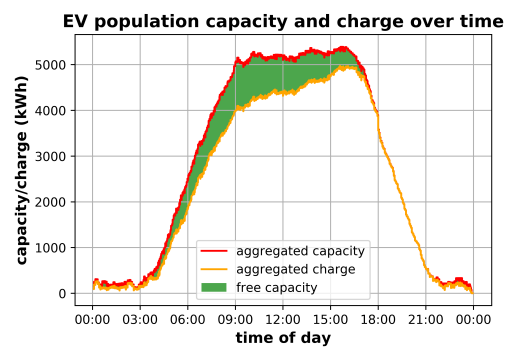


Fig. A6.6.4: Aggregated EV population, total capacity, total charge and free capacity

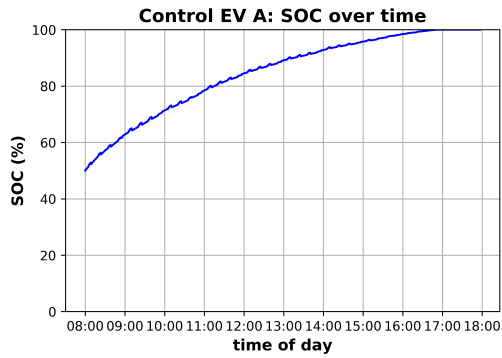


Fig. A6.6.5: Control EV A, SOC over time while connected

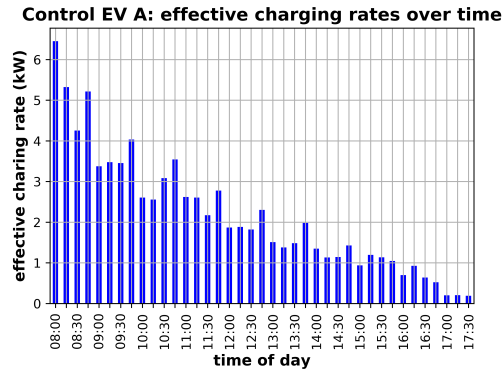


Fig. A6.6.6: Control EV A, average power flow over 15 min

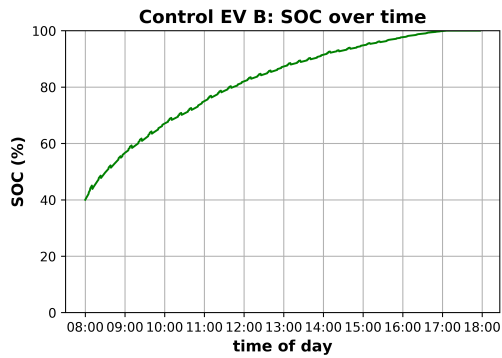


Fig. A6.6.7: Control EV B, SOC over time while connected

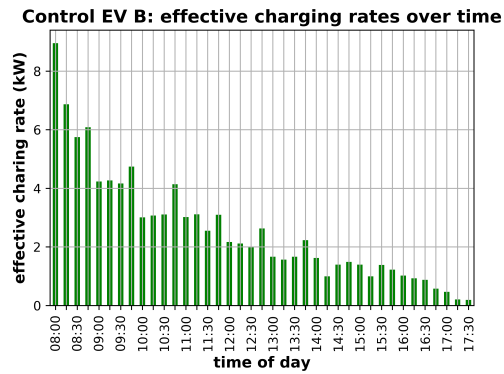


Fig. A6.6.8: Control EV B, average power flow over 15 min

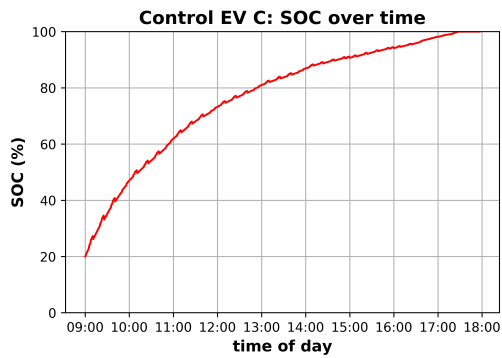


Fig. A6.6.9: Control EV C, SOC over time while connected

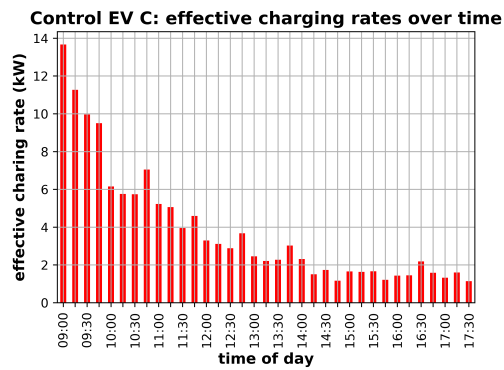


Fig. A6.6.10: Control EV C, average power flow over 15 min

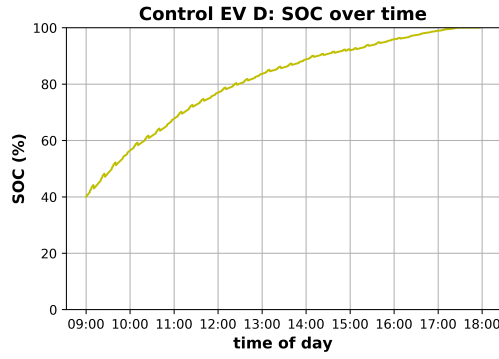


Fig. A6.6.11: Control EV D, SOC over time while connected

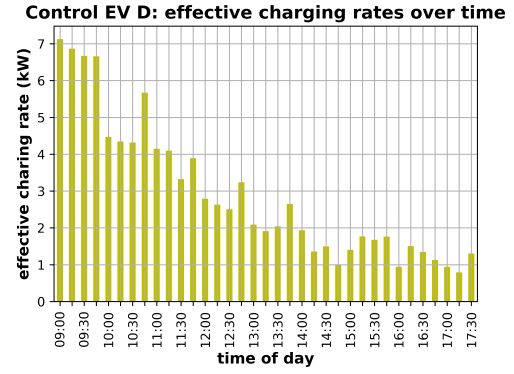


Fig. A6.6.12: Control EV D, average power flow over 15 min

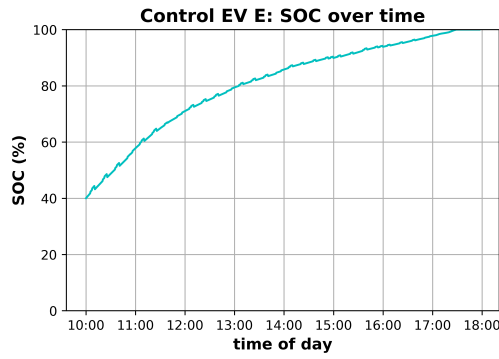


Fig. A6.6.13: Control EV E, SOC over time while connected

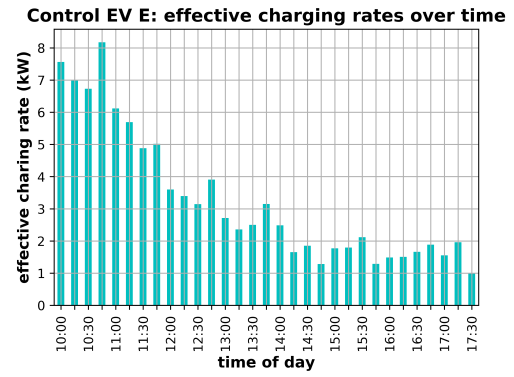


Fig. A6.6.14: Control EV E, average power flow over 15 min

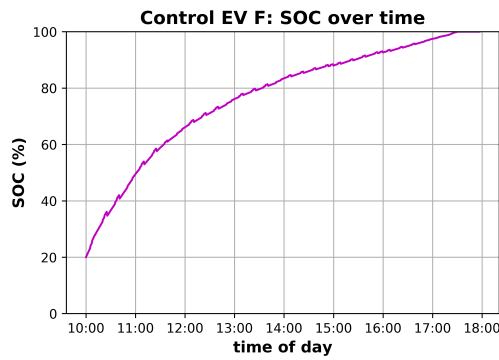


Fig. A6.6.15: Control EV F, SOC over time while connected

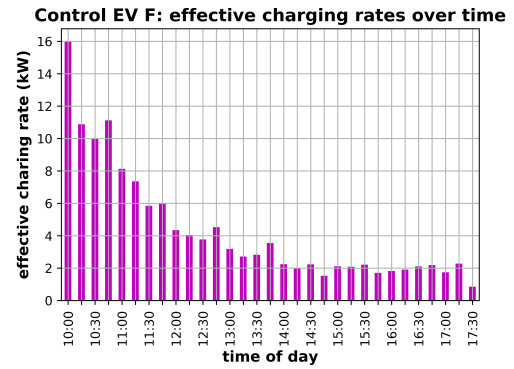


Fig. A6.6.16: Control EV F, average power flow over 15 min

## BIBLIOGRAPHY

- [1] H. Krueger and A. Cruden, “Modular strategy for aggregator control and data exchange in large scale vehicle-to-grid (V2G) applications,” *Energy Procedia*, vol. 151, pp. 7 – 11, 2018. 3rd Annual Conference in Energy Storage and Its Applications, 3rd CDT-ESA-AC, 11–12 September 2018, The University of Sheffield, UK, doi:10.1016/j.egypro.2018.09.019.
- [2] H. Krueger and A. Cruden, “Multi-layer event-based vehicle-to-grid (V2G) scheduling with short term predictive capability within a modular aggregator control structure,” *IEEE Transactions on Vehicular Technology*, vol. 69, no. 5, pp. 4727–4739, 2020. doi:10.1109/TVT.2020.2976035.
- [3] H. Krueger and A. Cruden, “Integration of electric vehicle user charging preferences into vehicle-to-grid aggregator controls,” *Energy Reports*, vol. 6, pp. 86 – 95, 2020. 4th Annual CDT Conference in Energy Storage & Its Applications, doi:10.1016/j.egyr.2020.02.031.
- [4] International Energy Agency, “Energy efficiency indicators 2019,” *IEA publications*, pp. 05–08, 2019. <https://www.iea.org/reports/energy-efficiency-indicators-2019>, accessed on 03.05.2020.
- [5] R. Zhang and S. Fujimori, “The role of transport electrification in global climate change mitigation scenarios,” *Environmental Research Letters*, vol. 15, p. 034019, feb 2020. doi:10.1088/1748-9326/ab6658.
- [6] P. Fox-Penner, W. Gorman, and J. Hatch, “Long-term u.s transportation electricity use considering the effect of autonomous-vehicles: Estimates & policy observations,” *Energy Policy*, vol. 122, pp. 203 – 213, 2018. doi:10.1016/j.enpol.2018.07.033.
- [7] V. Keller, J. English, J. Fernandez, C. Wade, M. Fowler, S. Scholtysik, K. Palmer-Wilson, J. Donald, B. Robertson, P. Wild, C. Crawford, and A. Rowe, “Electrification of road transportation with utility controlled



- charging: A case study for british columbia with a 93 *Applied Energy*, vol. 253, p. 113536, 2019. doi:10.1016/j.apenergy.2019.113536.
- [8] A. Soret, M. Guevara, and J. Baldasano, “The potential impacts of electric vehicles on air quality in the urban areas of barcelona and madrid (spain),” *Atmospheric Environment*, vol. 99, pp. 51 – 63, 2014. doi:10.1016/j.atmosenv.2014.09.048.
- [9] Y. Li and Y. Chang, “Road transport electrification and energy security in the association of southeast asian nations: Quantitative analysis and policy implications,” *Energy Policy*, vol. 129, pp. 805 – 815, 2019. doi:10.1016/j.enpol.2019.02.048.
- [10] M. Glotz-Richter and H. Koch, “Electrification of public transport in cities (horizon 2020 eliptic project),” *Transportation Research Procedia*, vol. 14, pp. 2614 – 2619, 2016. Transport Research Arena TRA2016, doi:10.1016/j.trpro.2016.05.416.
- [11] J. Quiros-Tortos, L. Victor-Gallardo, and L. Ochoa, “Electric vehicles in latin america: Slowly but surely toward a clean transport,” *IEEE Electrification Magazine*, vol. 7, pp. 22–32, 06 2019. doi:10.1109/MELE.2019.2908791.
- [12] K. Hill, “Is sub-saharan africa ready for the electric vehicle revolution?,” *World Economic Forum online resources*, 2018. <https://www.weforum.org/agenda/2018/07/sub-saharan-africa-electric-vehicle-revolution-evs/>, accessed on 02.05.2020.
- [13] Clean Energy Ministerial, “Ev30@30 - increasing uptake of electric vehicles - a campaign of the clean energy ministerial,” *online resource*, 2020. <http://www.cleanenergyministerial.org/campaign-clean-energy-ministerial/ev3030-campaign>, accessed on 08.04.2020.
- [14] International Energy Agency, “Uk and seven major companies join campaign for vehicle electrification,” *online resource*, 2018. <https://www.iea.org/news/uk-and-seven-major-companies-join-campaign-for-vehicle-electrification>, accessed on 08.04.2020.
- [15] P. Campbell, “Electric car subsidies extended in £1.3bn green vehicles drive,” *Financial Times*, 11 Mar 2020. <https://www.ft.com/content/1d2c1450-63ad-11ea-b3f3-fe4680ea68b5>, accessed on 10.08.2020.

- 
- [16] International Energy Agency, “Global ev outlook 2019,” *IEA publications*, pp. 09–10, 2019. <https://www.iea.org/reports/global-ev-outlook-2019>, accessed on 05.06.2020.
- [17] International Energy Agency, “Electric car deployment in selected countries, 2013-2018,” *online resource*, 2019. <https://www.iea.org/data-and-statistics/charts/electric-car-deployment-in-selected-countries-2013-2018>, accessed on 12.05.2020.
- [18] R. Irle, “Global bev & phev sales for 2019,” *online resource*, 2020. <https://www.ev-volumes.com/country/total-world-plug-in-vehicle-volumes/>, accessed on 12.05.2020.
- [19] Statista Research Department, “Number of cars sold worldwide between 2010 and 2020 (in million units),” *online resource*, 2020. <https://www.statista.com/statistics/200002/international-car-sales-since-1990/>, accessed on 15.08.2020.
- [20] International Energy Agency, “World energy model - scenario analysis of future energy trends,” *online resource*, 2019. <https://www.iea.org/reports/world-energy-model/sustainable-development-scenario>, accessed on 12.05.2020.
- [21] International Energy Agency, “Tracking transport,” *online resource*, 2019. <https://www.iea.org/reports/tracking-transport-2019#>, accessed on 12.05.2020.
- [22] International Energy Agency, “Electric car market share in the sustainable development scenario, 2000-2030,” *online resource*, 2019. <https://www.iea.org/data-and-statistics/charts/electric-car-market-share-in-the-sustainable-development-scenario-2000-2030>, accessed on 12.05.2020.
- [23] P. Lienert, “Global carmakers to invest at least \$90 billion in electric vehicles,” *Reuters Business News*, 15 Jan 2018. <https://www.reuters.com/article/us-autoshow-detroit-electric/global-carmakers-to-invest-at-least-90-billion-in-electric-vehicles-idUSKBN1F42NW>, accessed on 10.08.2020.
- [24] P. Campbell, “Jaguar land rover and bmw to collaborate on electric ve-

- hicles,” *Financial Times*, 5 Jun 2019. <https://www.ft.com/content/e098456c-870d-11e9-a028-86cea8523dc2>, accessed on 10.08.2020.
- [25] M. Rocco, “Volkswagen to invest \$800m in us electric vehicle production,” *Financial Times*, 14 Jan 2019. <https://www.ft.com/content/3e4e2f98-1817-11e9-9e64-d150b3105d21>, accessed on 10.08.2020.
- [26] J. Jolly, “Bmw aims to double electric and hybrid sales in next two years,” *The Guardian*, 25 Jun 2019. <https://www.theguardian.com/business/2019/jun/25/bmw-electric-hybrid-sales-eu-rules>, accessed on 10.08.2020.
- [27] P. McGee, “Porsche accelerates race for electric market share,” *Financial Times*, 22 Feb 2019. <https://www.ft.com/content/e1bc42ca-36ba-11e9-bd3a-8b2a211d90d5>, accessed on 10.08.2020.
- [28] H. Sanderson, “Coronavirus puts electric carmakers on alert over lithium supplies,” *Financial Times*, 10 Mar 2020. <https://www.ft.com/content/d539c20a-5fc4-11ea-8033-fa40a0d65a98>, accessed on 10.08.2020.
- [29] P. Campbell, “Carmakers face more than \$100bn hit to revenues,” *Financial Times*, 6 Apr 2020. <https://www.ft.com/content/f1cf0689-2825-447d-9d9a-ed99da520d05>, accessed on 10.08.2020.
- [30] Global Sustainable Electricity Partnership, “Electrification of transportation infrastructure in china improves efficiency,” *online resource*, 2019. <https://www.globalelectricity.org/case-studies/electrification-of-transportation-infrastructure-in-china-improves-efficiency/>, accessed on 23.03.2020.
- [31] R. Nunno, “Electrification of u.s. railways: Pie in the sky, or realistic goal?,” *EESI - online resource*, 2018. <https://www.eesi.org/articles/view/electrification-of-u.s.-railways-pie-in-the-sky-or-realistic-goal>, accessed on 23.03.2020.
- [32] D. Briginshaw, “Europe leads the charge to replace diesel traction,” *International Railway Journal - online resource*, 2019. <https://www.railjournal.com/opinion/europe-leads-charge-replace-diesel-traction>, accessed on 23.03.2020.
- [33] L. Kirkwood, L. Giuntini, E. Shehab, and P. Baguley, “Development of a whole life cycle cost model for electrification options on the uk rail system,”

- Procedia CIRP*, vol. 47, pp. 1 – 5, 2016. Product-Service Systems across Life Cycle, doi:10.1016/j.procir.2016.03.067.
- [34] D. Burroughs, “Gospel oak – barking line services fully electric,” *International Railway Journal - online resource*, 2019. <https://www.railjournal.com/passenger/commuter-rail/gospel-oak-barking-line-services-fully-electric/>, accessed on 23.03.2020.
- [35] J. J. Mwambeleko and T. Kulworawanichpong, “Battery electric multiple units to replace diesel commuter trains serving short and idle routes,” *Journal of Energy Storage*, vol. 11, pp. 7 – 15, 2017. doi:10.1016/j.est.2017.01.004.
- [36] ea technology, “My electric avenue - summary report,” *online resource*, 2018. <http://myelectricavenue.info/sites/default/files/Summary%20report.pdf>, accessed on 21.09.2019.
- [37] A. Grenier and S. Page, “The impact of electrified transport on local grid infrastructure: A comparison between electric cars and light rail,” *Energy Policy*, vol. 49, pp. 355 – 364, 2012. Special Section: Fuel Poverty Comes of Age: Commemorating 21 Years of Research and Policy, doi:10.1016/j.enpol.2012.06.033.
- [38] J. Kim, Y. Suharto, and T. U. Daim, “Evaluation of electrical energy storage (ees) technologies for renewable energy: A case from the us pacific northwest,” *Journal of Energy Storage*, vol. 11, pp. 25 – 54, 2017. doi:10.1016/j.est.2017.01.003.
- [39] S. Falahati, S. A. Taher, and M. Shahidehpour, “A new smart charging method for evs for frequency control of smart grid,” *International Journal of Electrical Power & Energy Systems*, vol. 83, pp. 458 – 469, 2016. doi:10.1016/j.ijepes.2016.04.039.
- [40] B. Yagcitekin and M. Uzunoglu, “A double-layer smart charging strategy of electric vehicles taking routing and charge scheduling into account,” *Applied Energy*, vol. 167, pp. 407 – 419, 2016. doi:10.1016/j.apenergy.2015.09.040.
- [41] C. O. Adika and L. Wang, “Smart charging and appliance scheduling approaches to demand side management,” *International Journal of Electrical Power & Energy Systems*, vol. 57, pp. 232 – 240, 2014. doi:10.1016/j.ijepes.2013.12.004.

- 
- [42] D. Morris, "Today's cars are parked 95% of the time," *Fortune (Transportation)*, 2016. <http://fortune.com/2016/03/13/cars-parked-95-percent-of-time/>, accessed on 29.07.2016.
- [43] J. Tomić and W. Kempton, "Using fleets of electric-drive vehicles for grid support," *Journal of Power Sources*, vol. 168, no. 2, pp. 459 – 468, 2007. doi:10.1016/j.jpowsour.2007.03.010.
- [44] A. Saber and G. Venayagamoorthy, "V2G scheduling - a modern approach to unit commitment with vehicle-to-grid using particle swarm optimization a cost-benefit analysis of alternatively fuelled buses with special considerations for V2G technology," *IFAC Proceedings*, vol. 42, pp. 261–266, 2009. doi:10.3182/20090705-4-SF-2005.00047.
- [45] IEEE Communications Society, "Vehicle-to-grid networks," *IEEE Network - The magazine of global internetworking*, 2016. url: <http://www.comsoc.org/netmag/cfp/vehicle-grid-networks>, accessed on 22.08.2016.
- [46] E. Sortomme and M. El-Sharkawi, "Optimal charging strategies for unidirectional vehicle-to-grid," *IEEE transactions on smart grid*, vol. 2, pp. 131–138, March 2011. doi:10.1109/TSG.2010.2090910.
- [47] California ISO, "California vehicle-grid integration (vgi) roadmap: Enabling vehicle-based grid services," *online resource*, 2014. <http://www.caiso.com/documents/vehicle-gridintegrationroadmap.pdf>, accessed on 15.05.2020.
- [48] C. Cleveland and C. Morris, *Dictionary of Energy*, ch. 1, p. 631. Elsevier, 2 ed., October 2014. ISBN: 9780080968117.
- [49] A. Briones, J. Francfort, P. Heitmann, M. Schey, S. Schey, and J. Smart, "Vehicle-to-grid (V2G) power flow regulations and building codes review by the AVTA." Idaho National Laboratory, September 2012. url: [https://www.energy.gov/sites/prod/files/2014/02/f8/v2g\\_power\\_flow\\_rpt.pdf](https://www.energy.gov/sites/prod/files/2014/02/f8/v2g_power_flow_rpt.pdf), accessed on 23.09.2019.
- [50] W. Kempton and J. Tomić, "Vehicle-to-grid power fundamentals: Calculating capacity and net revenue," *Journal of Power Sources*, vol. 144, no. 1, pp. 268 – 279, 2005. doi:10.1016/j.jpowsour.2004.12.025.
- [51] G. M. Freeman, T. E. Drennen, and A. D. White, "Can parked cars and carbon taxes create a profit? the economics of vehicle-to-grid energy stor-

- age for peak reduction,” *Energy Policy*, vol. 106, pp. 183 – 190, 2017. doi:10.1016/j.enpol.2017.03.052.
- [52] S. Habib, M. Kamran, and U. Rashid, “Impact analysis of vehicle-to-grid technology and charging strategies of electric vehicles on distribution networks - a review,” *Journal of Power Sources*, vol. 277, pp. 205–214, 2015. doi:10.1016/j.jpowsour.2014.12.020.
- [53] I. Pavić, T. Capuder, and I. Kuzle, “Value of flexible electric vehicles in providing spinning reserve services,” *Applied Energy*, vol. 157, p. 60–74, November 2015. doi:10.1016/j.apenergy.2015.07.070.
- [54] I. Pavić, T. Capuder, and I. Kuzle, “Value of flexible electric vehicles in providing spinning reserve services,” *Applied Energy*, vol. 157, pp. 60–74, 2015. doi:10.1016/j.apenergy.2015.07.070.
- [55] H. N. de Melo, J. P. F. Trovão, P. G. Pereirinha, H. M. Jorge, and C. H. Antunes, “A controllable bidirectional battery charger for electric vehicles with vehicle-to-grid capability,” *IEEE Transactions on Vehicular Technology*, vol. 67, pp. 114–123, Jan 2018. doi:10.1109/TVT.2017.2774189.
- [56] Z. Yuan and M. R. Hesamzadeh, “Hierarchical coordination of tso-dso economic dispatch considering large-scale integration of distributed energy resources,” *Applied Energy*, vol. 195, pp. 600 – 615, 2017. doi:10.1016/j.apenergy.2017.03.042.
- [57] Z. Xu, Z. Hu, Y. Song, W. Zhao, and Y. Zhang, “Coordination of pevs charging across multiple aggregators,” *Applied Energy*, vol. 136, p. 582–589, December 2014. doi:10.1016/j.apenergy.2014.08.116.
- [58] M. Alirezai, M. Noori, and O. Tatari, “Getting to net zero energy building: investigating the role of vehicle to home technology,” *Energy and Buildings (accepted manuscript)*, August 2016. doi:10.1016/j.enbuild.2016.08.044.
- [59] Y. Zhao and O. Tatari, “A hybrid life cycle assessment of the vehicle-to-grid application in light duty commercial fleet,” *Energy*, vol. 93, p. 1277–1286, December 2015. doi:10.1016/j.energy.2015.10.019.
- [60] W. Kempton and J. Tomić, “Vehicle-to-grid power fundamentals: Calculating capacity and net revenue,” *Journal of Power Sources*, vol. 144, pp. 268–279, 2005. doi:10.1016/j.jpowsour.2004.12.025.

- 
- [61] C. Peng, J. Zou, L. Lian, and L. Li, “An optimal dispatching strategy for v2g aggregator participating in supplementary frequency regulation considering ev driving demand and aggregator’s benefits,” *Applied Energy*, vol. 190, pp. 591 – 599, 2017. doi:10.1016/j.apenergy.2016.12.065.
- [62] R. Kurtus, “List of worldwide ac voltages and frequencies,” *Ron Kurtus’ School of Champions*, February 2016. url: [http://www.school-for-champions.com/science/ac\\_world\\_volt\\_freq\\_list.htm#.V-05JDXCBrI](http://www.school-for-champions.com/science/ac_world_volt_freq_list.htm#.V-05JDXCBrI), accessed on 19.09.2016.
- [63] H. Dorotić, B. Doračić, V. Dobravec, T. Pukšec, G. Krajačić, and N. Duić, “Integration of transport and energy sectors in island communities with 100% intermittent renewable energy sources,” *Renewable and Sustainable Energy Reviews*, vol. 99, pp. 109 – 124, 2019. doi:10.1016/j.rser.2018.09.033.
- [64] R. Gough, C. Dickerson, P. Rowley, and C. Walsh, “Vehicle-to-grid feasibility: A techno-economic analysis of ev-based energy storage,” *Applied Energy*, vol. 192, pp. 12 – 23, 2017. doi:10.1016/j.apenergy.2017.01.102.
- [65] J. Manning, “Vehicle-to-grid pilot schemes gather pace,” *online resource*, 2020. <https://www.fleeteurope.com/en/new-energies/europe/analysis/vehicle-grid-pilot-schemes-gather-pace?>, accessed on 15.03.2020.
- [66] National Grid, “Introduction to triads,” *online resource*, 2015. <https://www.nationalgrideso.com/sites/eso/files/documents/44940-Triads%20Information.pdf>, accessed on 15.03.2020.
- [67] M. Ware, “Is national grid’s triad system past its peak?,” *Green Giraffe Energy Blog*, 2019. <https://green-giraffe.eu/blog/national-grids-triad-system-past-its-peak>, accessed on 15.03.2020.
- [68] K. Darcovich, S. Recoskie, H. Ribberink, F. Pincet, and A. Foissac, “Effect on battery life of vehicle-to-home electric power provision under canadian residential electrical demand,” *Applied Thermal Engineering (corrected proof)*, July 2016. doi:10.1016/j.applthermaleng.2016.07.002.
- [69] Nissan Motor Corporation, ““vehicle to home” electricity supply system,” *Nissan global website*, 2012. [http://www.nissan-global.com/EN/TECHNOLOGY/OVERVIEW/vehicle\\_to\\_home.html](http://www.nissan-global.com/EN/TECHNOLOGY/OVERVIEW/vehicle_to_home.html), accessed on 05.09.2020.

- 
- [70] University of Nottingham, “Ev-elocity - about us,” *online resource*, 2020. <https://www.ev-elocity.com/>, accessed on 12.03.2020.
- [71] J. Gordon, “Could your car help power heathrow?,” *Raconteur*, 2019. <https://www.raconteur.net/business-innovation/V2G-technology>, accessed on 08.05.2020.
- [72] UKRI - UK Research and Innovation, “Integrated energy systems for commercial vehicles,” *UKRI Gateway - Innovate UK Projects*, 2018. <https://gtr.ukri.org/projects?ref=104222>, accessed on 03.05.2020.
- [73] SSE Enterprise Utilities, “Bus2grid - a first of its kind multi-megawatt demonstration of the technical and commercial potential of e-buses to support the electricity system via active bi-directional charging.,” *online resource*, 2020. <https://www.sseutilitiesolutions.co.uk/products/bus2grid-2/>, accessed on 30.04.2020.
- [74] Sustainable Bus, “Go-ahead london rolls out the 100th enviro200ev. it’s the first time for the 9.6-meter,” *online resource*, 2020. <https://www.sustainable-bus.com/news/go-ahead-london-rolls-out-the-100th-enviro200ev-its-the-first-time-for-the-9-6-meter/>, accessed on 20.04.2020.
- [75] N. Manthey, “22 more byd-adl electric buses for london,” *online resource*, 2019. <https://www.electrive.com/2019/10/14/22-more-byd-adl-electric-buses-for-london/>, accessed on 20.04.2020.
- [76] BYD ADL partnership, “Datasheet - byd adl enviro200ev,” *online resource*, 2020. <https://www.evbus.co.uk/wp-content/uploads/2019/12/BYD-ADL-Enviro200EV.pdf>, accessed on 20.04.2020.
- [77] BYD ADL partnership, “Datasheet - byd adl enviro400ev,” *online resource*, 2020. <https://www.evbus.co.uk/wp-content/uploads/2020/01/BYD-ADL-Enviro400EV.pdf>, accessed on 20.04.2020.
- [78] J. Geske and D. Schumann, “Willing to participate in vehicle-to-grid (V2G)? why not!,” *Energy Policy*, vol. 120, pp. 392 – 401, 2018. doi:10.1016/j.enpol.2018.05.004.
- [79] B. K. Sovacool, L. Noel, J. Axsen, and W. Kempton, “The neglected social dimensions to a vehicle-to-grid (V2G) transition: a critical and system-



- atic review,” *Environmental Research Letters*, vol. 13, p. 013001, jan 2018. doi:10.1088/1748-9326/aa9c6d.
- [80] H. Bonges and A. Lusk, “Addressing electric vehicle (ev) sales and range anxiety through parking layout, policy and regulation,” *Transportation Research Part A: Policy and Practice*, vol. 83, p. 63–73, January 2016. doi:10.1016/j.tra.2015.09.011.
- [81] L. Noel, G. Z. de Rubens], B. K. Sovacool, and J. Kester, “Fear and loathing of electric vehicles: The reactionary rhetoric of range anxiety,” *Energy Research & Social Science*, vol. 48, pp. 96 – 107, 2019. doi:10.1016/j.erss.2018.10.001.
- [82] O. Egbue and S. Long, “Barriers to widespread adoption of electric vehicles: An analysis of consumer attitudes and perceptions,” *Energy Policy*, vol. 48, pp. 717 – 729, 2012. Special Section: Frontiers of Sustainability, doi:10.1016/j.enpol.2012.06.009.
- [83] D. Carrington, “Electric cars are already cheaper to own and run, says study,” *The Guardian*, February 2019. <https://www.theguardian.com/environment/2019/feb/12/electric-cars-already-cheaper-own-run-study>, accessed on 12.02.2019.
- [84] J. Kester, L. Noel, G. Z. de Rubens], and B. K. Sovacool, “Promoting vehicle to grid (V2G) in the nordic region: Expert advice on policy mechanisms for accelerated diffusion,” *Energy Policy*, vol. 116, pp. 422 – 432, 2018. doi:10.1016/j.enpol.2018.02.024.
- [85] Energy Systems Catapult, “Pioneering electric vehicle study shows up to 95of consumers happy to use ‘smart charging’,” *online resource*, 2019. <https://es.catapult.org.uk/news/pioneering-electric-vehicle-study-shows-up-to-95-of-consumers-happy-to-use-smart-charging/>, accessed on 20.04.2020.
- [86] G. R. Parsons, M. K. Hidrue, W. Kempton, and M. P. Gardner, “Willingness to pay for vehicle-to-grid (V2G) electric vehicles and their contract terms,” *Energy Economics*, vol. 42, pp. 313 – 324, 2014. doi:10.1016/j.eneco.2013.12.018.
- [87] A. Mourad, S. Muhammad, M. O. A. Kalaa], H. H. Refai, and P. A. Hoehner, “On the performance of wlan and bluetooth for in-car infotain-

- ment systems,” *Vehicular Communications*, vol. 10, pp. 1 – 12, 2017. doi:10.1016/j.vehcom.2017.08.001.
- [88] UKRI - UK Research and Innovation, “Gendrive : Gamification for consumer engagement in V2G services,” *UKRI Gateway - Innovate UK Projects*, 2018. <https://gtr.ukri.org/projects?ref=104225>, accessed on 03.05.2020.
- [89] Newcastle University, “Gendrive - gamification for consumer engagement in V2G services,” *Newcastle University Website - research projects*, 2020. <https://www.ncl.ac.uk/engineering/research/eee/projects/gendrive.html>, accessed on 05.05.2020.
- [90] J. Bishop, C. Axon, D. Bonilla, M. Tran, D. Banister, and M. McCulloch, “Evaluating the impact of V2G services on the degradation of batteries in phev and ev,” *Applied Energy*, vol. 111, pp. 206–218, 2013. doi:10.1016/j.apenergy.2013.04.094.
- [91] C. Cleveland and C. Morris, *Dictionary of Energy*, ch. 1, p. 10. Elsevier Science, 1 ed., August 2009. eBook ISBN: 9780080965178.
- [92] M. Shafie-khah, M. Moghaddam, M. Sheikh-El-Eslami, and J. Catalão, “Optimised performance of a plug-in electric vehicle aggregator in energy and reserve markets,” *Energy Conversion and Management*, vol. 97, p. 393–408, June 2015. doi:10.1016/j.enconman.2015.03.074.
- [93] D. Hill, A. Agarwal, and F. Ayello, “Fleet operator risks for using fleets for V2G regulation,” *Energy Policy*, vol. 41, p. 221–231, 2012. doi:10.1016/j.enpol.2011.10.040.
- [94] A. Ghosh and V. Aggarwal, “Menu-based pricing for charging of electric vehicles with vehicle-to-grid service,” *IEEE Transactions on Vehicular Technology*, vol. 67, pp. 10268–10280, Nov 2018. doi:10.1109/TVT.2018.2865706.
- [95] L. Noel, G. Z. de Rubens, J. Kester, and B. K. Sovacool, *Vehicle-to-Grid: A Sociotechnical Transition Beyond Electric Mobility*. Springer, 2019. doi:10.1007/978-3-030-04864-8.
- [96] D. Richardson, “Encouraging vehicle-to-grid (V2G) participation through premium tariff rates,” *Journal of Power Sources*, vol. 243, pp. 219–224, 2013. doi:10.1016/j.jpowsour.2013.06.024.

- 
- [97] elementenergy, “V2Gb - vehicle to grid britain - project report,” *online resource*, 2019. <https://es.catapult.org.uk/wp-content/uploads/2019/06/V2GB-Public-Report.pdf>, accessed on 09.03.2020.
- [98] Upside Energy Ltd, “Haven: Home as a virtual energy network public summary,” *online resource*, 2019. <https://upside.energy/wp-content/uploads/2019/11/haven-public-summary.pdf>, accessed on 05.05.2020.
- [99] Y. Shirazi, E. Carr, and L. Knapp, “A cost-benefit analysis of alternatively fuelled buses with special considerations for V2G technology,” *Energy Policy*, vol. 87, pp. 591–603, 2015. doi:10.1016/j.enpol.2015.09.038.
- [100] Y. Zhao, M. Noori, and O. Tatari, “Vehicle to grid regulation services of electric delivery trucks: Economic and environmental benefit analysis,” *Applied Energy*, vol. 170, pp. 161–175, 2016. doi:10.1016/j.apenergy.2016.02.097.
- [101] M. MacLeod and Cenex, “V2G market study - answering the preliminary questions for V2G: What, where and how much?,” *online resource*, 2018. <https://www.seev4-city.eu/wp-content/uploads/2018/08/V2G-Market-Study-2018.pdf>, accessed on 02.03.2020.
- [102] CleanCar.io, “Vehicle to grid oxford V2Go - innovate uk funded project,” *online resource*, 2019. <https://www.v2go.org/>, accessed on 30.04.2020.
- [103] Transport Studies Unit, University of Oxford, “Research project V2Go (vehicle-to-grid oxford),” *online resource*, 2020. <https://epg.eng.ox.ac.uk/our-research/V2Go/>, accessed on 30.04.2020.
- [104] E-Flex, “E-flex report - moving towards more sustainable fleet management with vehicle-to-grid systems,” *online resource*, 2020. <https://www.e-flex.co.uk/report>, accessed on 08.05.2020.
- [105] G. Payne and Cenex, “Understanding the true value of V2G - an analysis of the customers and value streams for V2G in the uk,” *online resource*, 2019. <https://es.catapult.org.uk/wp-content/uploads/2019/06/Cenex-WP-2-True-Value-of-V2G-Report.pdf>, accessed on 02.05.2020.
- [106] National Grid, “Nets security and quality of supply standard,” *National Grid Industry Information*, 2012. <http://www2.nationalgrid.com/UK/Industry-information/Electricity-codes/SQSS/The-SQSS/>, accessed on 03.09.2016.

- 
- [107] European Distribution System Operators for Smart Grids, “Coordination of transmission and distribution system operators: a key step for the energy union,” *EDSO for smart grids publications*, 2015. <http://www.edsoforsmartgrids.eu/wp-content/uploads/public/Coordination-of-transmission-and-distribution-system-operators-May-2015.pdf>, accessed on 03.09.2016.
- [108] T. Turc, “Scada systems management based on web services,” *Procedia Economics and Finance*, vol. 32, pp. 464–470, 2015. doi:10.1016/S2212-5671(15)01419-7.
- [109] S.-C. Hui and S. Foo, “A dynamic ip addressing system for internet telephony applications,” *Computer Communications*, pp. 254–266, 1998. doi:10.1016/S0140-3664(97)00181-3.
- [110] AutoCheck, “What is a vehicle identification number (vin)?,” *AutoCheck website*, 2016. <http://www.autocheck.com/vehiclehistory/autocheck/en/vinbasics>, accessed on 07.09.2016.
- [111] H. Nicanfar, P. Talebifard, S. Hosseinienezhad, V. Leung, and M. Damm, “Security and privacy of electric vehicles in the smart grid context: problem and solution,” *Proceedings of the third ACM international symposium on Design and analysis of intelligent vehicular networks and applications*, pp. 45–54, 2013. doi:10.1145/2512921.2512926.
- [112] Nissan, “Nissanconnect services,” *online resource*, 2020. <https://www.nissan.co.uk/ownership/nissan-infotainment-system/nissanconnect-services.html>, accessed on 26.03.2020.
- [113] M. Ross, “Bmw updates i3 and i3s battery capacity and range,” *electricityhybridvehicletechnology.com*, 2018. <https://www.electricityhybridvehicletechnology.com/news/battery-technology/bmw-updates-i3-and-i3s-battery-capacity-and-range.html>, accessed on 12.02.2019.
- [114] M. Rouse, “Definition telematics,” *TechTarget SearchNetworking*, 2007. url: <http://searchnetworking.techtarget.com/definition/telematics>, accessed on 3.09.2016.
- [115] C.-L. Lin, M.-S. Hsieh, and G.-H. Tzeng, “Evaluating vehicle telematics system by using a novel mcdm techniques with dependence and feed-

- back,” *Expert Systems with Applications*, vol. 37, p. 6723–6736, 2010. doi:10.1016/j.eswa.2010.01.014.
- [116] S. Husnjak, D. Peraković, I. Forenbacher, and M. Mumdziev, “Telematics system in usage based motor insurance,” *Procedia Engineering*, vol. 100, pp. 816–825, 2015. doi:10.1016/j.proeng.2015.01.436.
- [117] E. Hossain, G. Chow, V. Leung, R. McLeod, J. Mišić, V. Wong, and O. Yang, “Vehicular telematics over heterogeneous wireless networks: A survey,” *Computer Communications*, vol. 33, p. 775–793, 2010. doi:10.1016/j.comcom.2009.12.010.
- [118] Electric Vehicle Wiki, “Leafspypro - overview,” *Category: Nissan Leaf*, 2016. url: [http://www.electricvehiclewiki.com/Leaf\\_Spy\\_Pro](http://www.electricvehiclewiki.com/Leaf_Spy_Pro), accessed on 7.09.2016.
- [119] Jesimpki - AxleAddict, “Torque diagnostic display on a toyota prius using an elm327 adapter,” *AxleAddict.com category Maintenance*, 2016. url: <https://axleaddict.com/auto-repair/Using-Torque-With-A-Toyota-Prius-Using-An-ELM327-Adapter-ScanGauge-Alternative>, accessed on 7.09.2016.
- [120] Electric Auto Association, “Prius phev techinfo,” *EAA-PHEV.org Wiki*, 2012. url: [http://www.eaa-phev.org/wiki/Prius\\_PHEV\\_TechInfo](http://www.eaa-phev.org/wiki/Prius_PHEV_TechInfo), accessed on 7.09.2016.
- [121] Rob M. - TeslaRati, “Hacking the model s on-board diagnostics (obd-ii) connector,” *TeslaRati category DIY*, 2015. url: <http://www.teslarati.com/how-to-tap-constant-12v-power-tesla-model-s/>, accessed on 7.09.2016.
- [122] EVTV LLC, “Evtv due can multicontroller adapter,” *SavvyCAN Adapter for Tesla Model S – User Manual*, 2015. url: <http://media3.ev-tv.me/TeslaModelSCANDueUserManual.pdf>, accessed on 7.09.2016.
- [123] L.-W. Chen, Y.-C. Tseng, and K.-Z. Syue, “Surveillance on-the-road: Vehicular tracking and reporting by v2v communications,” *Computer Networks*, vol. 67, pp. 154–163, 2014. doi:10.1016/j.comnet.2014.03.031.
- [124] A. Bazzi, A. Zanella, and B. Masini, “A distributed virtual traffic light algorithm exploiting short range v2v communications,” *Ad Hoc Networks*, vol. 49, pp. 42–57, 2016. doi:10.1016/j.adhoc.2016.06.006.

- 
- [125] J. Anaya, E. Talavera, F. Jiménez, F. Serradilla, and J. Naranjo, “Vehicle to vehicle geonetworking using wireless sensor networks,” *Ad Hoc Networks*, vol. 27, pp. 133–146, 2015. doi:10.1016/j.adhoc.2014.12.003.
- [126] A. Pfitzmann and M. Hansen, “A terminology for talking about privacy by data minimization: Anonymity, unlinkability, undetectability, unobservability, pseudonymity, and identity management,” *Archive TU Dresden*, 2010. [https://dud.inf.tu-dresden.de/literatur/Anon\\_Terminology\\_v0.34.pdf](https://dud.inf.tu-dresden.de/literatur/Anon_Terminology_v0.34.pdf), accessed on 07.09.2016.
- [127] W. Han and Y. Xiao, “Privacy preservation for V2G networks in smart grid: A survey,” *Computer Communications*, vol. 91, pp. 17–28, 2016. doi:10.1016/j.comcom.2016.06.006.
- [128] Techopedia, “Communication protocol,” *Dictionary - Tag Networking*, 2016. url: <https://www.techopedia.com/definition/25705/communication-protocol>, accessed on 3.09.2016.
- [129] G. Fairhurst, “Communication protocols,” *Electronics Research Group publications*, 2001. url: <http://www.erg.abdn.ac.uk/users/gorry/course/intro-pages/protocols.html>, accessed on 3.09.2016.
- [130] International Electrotechnical Commission, “Iec 61850: Power utility automation,” *Core IEC Standards*, 2003. url: <http://www.iec.ch/smartgrid/standards/>, accessed on 6.09.2016.
- [131] R. Falk and S. Fries, “Securely connecting electric vehicles to the smart grid,” *Siemens AG Publications*, 2013. url: <http://www.fi-ppp-finseny.eu/wp-content/uploads/2013/05/Securely-connecting-Electric-Vehicles-to-the-Smart-Grid.pdf>, accessed on 6.09.2016.
- [132] C. Jouvray, G. Pellischek, and M. Tiguercha, “Impact of a smart grid to the electric vehicle ecosystem from a privacy and security perspective,” *Electric Vehicle Symposium and Exhibition*, November 2013. doi:10.1109/EVS.2013.6914733.
- [133] Siemens AG, “Efficient energy automation with the iec 61850 standard application examples,” *Siemens Publications*, 2010. url: [http://m.energy.siemens.com/hq/pool/hq/energy-topics/standards/iec-61850/Application\\_examples\\_en.pdf](http://m.energy.siemens.com/hq/pool/hq/energy-topics/standards/iec-61850/Application_examples_en.pdf), accessed on 9.09.2016.

- 
- [134] IEEE Standards association, "Ieee 802.11: Wireless lans," *IEEE Publications*, 2012. url: <http://standards.ieee.org/about/get/802/802.11.html>, accessed on 6.09.2016.
- [135] P. Leupp and C. Rytoft, "Special report iec 61850," *ABB review - The corporate technical journal*, 2010. url: [https://library.e.abb.com/public/a56430e1e7c06fdcf12577a00043ab8b/3BSE063756\\_en\\_ABB\\_Review\\_Special\\_Report\\_IEC\\_61850.pdf](https://library.e.abb.com/public/a56430e1e7c06fdcf12577a00043ab8b/3BSE063756_en_ABB_Review_Special_Report_IEC_61850.pdf), accessed on 9.09.2016.
- [136] Fraunhofer ESK, "Fraunhofer esk demonstrating vehicle-to-grid communications based on iso/iec 15118 and iec 61850 standards," *Green Car Congress, Online Resources*, 2014. url: <http://www.greencarcongress.com/2014/02/20140213-esk.html>, accessed on 6.09.2016.
- [137] International Organisation for Standardization, "Iso 15118-1:2019 road vehicles — vehicle to grid communication interface — part 1: General information and use-case definition," *ISO standards catalogue*, 2019. url: <https://www.iso.org/standard/69113.html>, accessed on 6.09.2016.
- [138] J. Kester, L. Noel, X. Lin, G. Z. de Rubens], and B. K. Sovacool, "The coproduction of electric mobility: Selectivity, conformity and fragmentation in the sociotechnical acceptance of vehicle-to-grid (v2g) standards," *Journal of Cleaner Production*, vol. 207, pp. 400 – 410, 2019. doi:10.1016/j.jclepro.2018.10.018.
- [139] International Organisation for Standardization, "Iso 15118-1:2013 road vehicles – vehicle to grid communication interface," *ISO standards catalogue*, 2013. url: [http://www.iso.org/iso/catalogue\\_detail.htm?csnumber=55365](http://www.iso.org/iso/catalogue_detail.htm?csnumber=55365), accessed on 6.09.2016.
- [140] Fraunhofer ESK, "Communication for e-car energy management," *Fraunhofer ESK, Online Resources*, 2016. url: <http://www.esk.fraunhofer.de/en/research/projects/SMARTV2G.html>, accessed on 6.09.2016.
- [141] S. Voit, "Introduction to iso 15118 vehicle-to-grid communication interface," *RWE publications - Begleitforschung "Schaufenster Elektromobilität"*, 2015. url: [http://schaufenster-elektromobilitaet.org/media/media/documents/dokumente\\_steckbriefe\\_oder\\_news/ISO\\_15118\\_Workshop\\_20151001\\_Stephan\\_Voit.pdf](http://schaufenster-elektromobilitaet.org/media/media/documents/dokumente_steckbriefe_oder_news/ISO_15118_Workshop_20151001_Stephan_Voit.pdf), accessed on 9.09.2016.

- 
- [142] V2G-clarity, “What is iso 15118? - get to know one of the world’s leading international electric vehicle standards,” *online resource*, 2019. <https://v2g-clarity.com/knowledgebase/what-is-iso-15118/>, accessed on 09.05.2020.
- [143] D. Wellisch, J. Lenz, A. Faschingbauer, R. Pöschl, and S. Kunze, “Vehicle-to-grid ac charging station: An approach for smart charging development,” *IFAC-PapersOnLine*, vol. 48, no. 4, pp. 55 – 60, 2015. 13th IFAC and IEEE Conference on Programmable Devices and Embedded Systems, doi:10.1016/j.ifacol.2015.07.007.
- [144] A. Krainyukov, A. Krivchenkov, and R. Saltanovs, “Performance analysis of wireless communications for v2g applications using wpt technology in energy transfer,” *Procedia Engineering*, vol. 178, pp. 172 – 181, 2017. RelStat-2016: Proceedings of the 16th International Scientific Conference Reliability and Statistics in Transportation and Communication October 19-22, 2016. Transport and Telecommunication Institute, Riga, Latvia, doi:10.1016/j.proeng.2017.01.085.
- [145] M. Rouse, “Ieee 802 wireless standards: Fast reference,” *TechTarget Search-Networking*, 2015. url: <http://searchmobilecomputing.techtarget.com/definition/IEEE-802-Wireless-Standards-Fast-Reference>, accessed on 5.09.2016.
- [146] I. Al-Anbagi and H. Mouftah, “Wave 4 V2G: Wireless access in vehicular environments for vehicle-to-grid applications,” *Vehicular Communications*, vol. 3, pp. 31–42, 2016. doi:10.1016/j.vehcom.2015.12.002.
- [147] Z. Wan, W.-T. Zhu, and G. Wang, “Prac: Efficient privacy protection for vehicle-to-grid communications in the smart grid,” *Computers & Security*, vol. 62, p. 246–256, 2016. doi:10.1016/j.cose.2016.07.004.
- [148] C. Hoehne and M. Chester, “Optimizing plug-in electric vehicle and vehicle-to-grid charge scheduling to minimize carbon emissions,” *Energy*, vol. 115, p. 646–657, 2016. doi:10.1016/j.energy.2016.09.057.
- [149] J. Yu, V. Li, and A. Lam, “Optimal V2G scheduling of electric vehicles and unit commitment using chemical reaction optimization,” *IEEE Congress on Evolutionary Computation*, 2013. doi:10.1109/CEC.2013.6557596.
- [150] M. Nourinejad, J. Chow, and M. Roorda, “Equilibrium scheduling of



- vehicle-to-grid technology using activity based modelling,” *Transportation Research Part C: Emerging Technologies*, vol. 65, p. 79–96, 2016. doi:10.1016/j.trc.2016.02.001.
- [151] G. Reddy, V. Ganesh, and C. Rao, “Implementation of clustering based unit commitment employing imperialistic competition algorithm,” *International Journal of Electrical Power & Energy Systems*, p. 621–628, 2016. doi:10.1016/j.ijepes.2016.04.043.
- [152] M. López, S. Martín, S. Aguado, and J. de la Torre, “V2G strategies for congestion management in microgrids with high penetration of electric vehicles,” *Electric Power Systems Research*, vol. 104, pp. 28–34, 2013. doi:10.1016/j.epsr.2013.06.005.
- [153] R. Shi, Y. Yang, L. Shi, and K. Y. Lee, “Bi-level day ahead optimization of V2G dispatch strategy based on the dynamic discharging electricity price,” *IFAC-PapersOnLine*, vol. 51, no. 28, pp. 462 – 467, 2018. 10th IFAC Symposium on Control of Power and Energy Systems CPES 2018, doi:10.1016/j.ifacol.2018.11.746.
- [154] L. Wang, S. Sharkh, A. Chipperfield, and A. Cruden, “Dispatch of vehicle-to-grid battery storage using an analytic hierarchy process,” *IEEE Transactions on Vehicular Technology*, vol. 66, pp. 2952–2965, April 2017. doi:10.1109/TVT.2016.2591559.
- [155] E. Sortomme and M. A. El-Sharkawi, “Optimal scheduling of vehicle-to-grid energy and ancillary services,” *IEEE Transactions on Smart Grid*, vol. 3, pp. 351–359, March 2012. doi:10.1109/TSG.2011.2164099.
- [156] S. Faddel, A. Aldeek, A. T. Al-Awami, E. Sortomme, and Z. Al-Hamouz, “Ancillary services bidding for uncertain bidirectional V2G using fuzzy linear programming,” *Energy*, vol. 160, pp. 986 – 995, 2018. doi:10.1016/j.energy.2018.07.091.
- [157] Y. He, B. Venkatesh, and L. Guan, “Optimal scheduling for charging and discharging of electric vehicles,” *IEEE Transactions on Smart Grid*, vol. 3, pp. 1095–1105, Sep. 2012. doi:10.1109/TSG.2011.2173507.
- [158] H. Turker and S. Bacha, “Optimal minimization of plug-in electric vehicle charging cost with vehicle-to-home and vehicle-to-grid concepts,” *IEEE*

- Transactions on Vehicular Technology*, vol. 67, pp. 10281–10292, Nov 2018. doi:10.1109/TVT.2018.2867428.
- [159] F. Grée, V. Laznikova, B. Kim, G. Garcia, T. Kigezi, and B. Gao, “Cloud-based big data platform for vehicle-to-grid (V2G),” *World Electric Vehicle Journal*, vol. 11, p. 30, 03 2020. doi:10.3390/wevj11020030.
- [160] Upside Energy Ltd, “Upside energy - company website,” *online resource*, 2019. <https://upside.energy/>, accessed on 03.05.2020.
- [161] UKRI - UK Research and Innovation, “V2street,” *UKRI Gateway - Innovate UK Projects*, 2018. <https://gtr.ukri.org/projects?ref=104224>, accessed on 03.05.2020.
- [162] UKRI - UK Research and Innovation, “Vehicle-to-grid intelligent control (vigil),” *UKRI Gateway - Innovate UK Projects*, 2018. <https://gtr.ukri.org/projects?ref=104222>, accessed on 03.05.2020.
- [163] BusinessGreen, “Vigil hails successful electric vehicle-to-grid trial in birmingham,” *online resource*, 2020. <https://www.businessgreen.com/news/4014681/vigil-hails-successful-electric-vehicle-grid-trial-birmingham>, accessed on 03.05.2020.
- [164] Electronic Engineering Journal, “Vigil V2G project successfully completed,” *online resource*, 2020. [https://www.eejournal.com/industry\\_news/vigil-V2G-project-successfully-completed/](https://www.eejournal.com/industry_news/vigil-V2G-project-successfully-completed/), accessed on 03.05.2020.
- [165] edie, “Government-funded vehicle-to-grid project completes grid balancing trials,” *online resource*, 2020. <https://www.edie.net/news/8/Government-funded-Vehicle-to-Grid-project-completes-grid-balancing-trials/>, accessed on 03.05.2020.
- [166] S. Gao, K. T. Chau, C. Liu, D. Wu, and C. C. Chan, “Integrated energy management of plug-in electric vehicles in power grid with renewables,” *IEEE Transactions on Vehicular Technology*, vol. 63, pp. 3019–3027, Sep. 2014. doi:10.1109/TVT.2014.2316153.
- [167] J. J. Escudero-Garzas, A. Garcia-Armada, and G. Seco-Granados, “Fair design of plug-in electric vehicles aggregator for V2G regulation,” *IEEE Transactions on Vehicular Technology*, vol. 61, pp. 3406–3419, Oct 2012. doi:10.1109/TVT.2012.2212218.

- 
- [168] Energy Storage Association, “Frequency regulation - executive summary,” *Energy Storage Association, Online Resources*, 2019. <http://energystorage.org/energy-storage/technology-applications/frequency-regulation>, accessed on 04.03.2019.
- [169] D. Greenwood, K. Lim, C. Patsios, P. Lyons, Y. Lim, and P. Taylor, “Frequency response services designed for energy storage,” *Applied Energy*, vol. 203, pp. 115 – 127, 2017. doi:10.1016/j.apenergy.2017.06.046.
- [170] A. Abdallah and X. S. Shen, “Lightweight authentication and privacy-preserving scheme for V2G connections,” *IEEE Transactions on Vehicular Technology*, vol. 66, pp. 2615–2629, March 2017. doi:10.1109/TVT.2016.2577018.
- [171] octopusev, “Powerloop - introducing the octopus vehicle-to-grid bundle,” *online resource*, 2020. <https://www.octopusev.com/powerloop>, accessed on 02.05.2020.
- [172] M. Neaimeh, “e4future V2G - the e4future project proposes a large-scale demonstrator of up to 1,000 battery electric vehicles (bevs) and novel bidirectional chargers (V2G).,” *online resource*, 2020. <https://www.ncl.ac.uk/cesi/research/additionalresearch/e4futureV2G/>, accessed on 30.04.2020.
- [173] V2GHub, “e4future summary,” *online resource*, 2020. <https://www.V2G-hub.com/projects/e4future/>, accessed on 30.04.2020.
- [174] Kaluza, “Kaluza leading the way with domestic vehicle-to-grid (V2G) optimisation,” *online resource*, 2019. <https://www.kaluza.com/case-studies/project-sciurus/>, accessed on 15.04.2020.
- [175] Cenex, “Project sciurus - project brief,” *online resource*, 2020. <https://www.cenex.co.uk/projects-case-studies/sciurus/>, accessed on 15.04.2020.
- [176] Oracle Corporation, “Mysql,” *MySQL website*, 2018. <https://www.mysql.com/>, accessed on 27.02.2018.
- [177] M. Paredes-Valverde, G. Alor-Hernández, A. Rodr’guez-González, and G. Hernández-Chan, “Developing social networks mashups: An overview of rest-based apis,” *Procedia Technology*, vol. 3, p. 205–213, 12 2012. doi:10.1016/j.protcy.2012.03.022.

- 
- [178] R. Battle and E. Benson, “Bridging the semantic web and web 2.0 with representational state transfer (rest),” *Web Semantics: Science, Services and Agents on the World Wide Web*, vol. 6, pp. 61–69, 02 2008. doi:10.1016/j.websem.2007.11.002.
- [179] C. Q. Adamsen, A. Møller, R. Karim, M. Sridharan, F. Tip, and K. Sen, “Repairing event race errors by controlling nondeterminism,” *Proceedings of the 39th International Conference on Software Engineering*, pp. 289–299, 2017. doi:10.1109/ICSE.2017.34.
- [180] F. Lin, S. Liu, Z. Yang, Y. Zhao, and Z. Y. H. Sun, “Multi-train energy saving for maximum usage of regenerative energy by dwell time optimization in urban rail transit using genetic algorithm,” *Energies*, vol. 9, March 2016. doi:10.3390/en9030208.
- [181] Z. Zhang, X. Liu, and K. Holt, “Positive train control (ptc) for railway safety in the united states: Policy developments and critical issues,” *Utilities Policy*, vol. 51, pp. 33 – 40, 2018. doi:10.1016/j.jup.2018.03.002.
- [182] V. Behrends, M. Haunschild, and N. Galonske, “Smart telematics enabling efficient rail transport – development of the viwas research and development project,” *Transportation Research Procedia*, vol. 14, pp. 4430 – 4439, 2016. Transport Research Arena TRA2016, doi:10.1016/j.trpro.2016.05.365.
- [183] R. I. Rajkumar, P. E. Sankaranarayanan, and G. Sundari, “Gps and ethernet based real time train tracking system,” in *2013 International Conference on Advanced Electronic Systems (ICAES)*, pp. 282–286, Sep. 2013. doi:10.1109/ICAES.2013.6659409.
- [184] A. González-Gil, R. Palacin, P. Batty, and J. Powell, “A systems approach to reduce urban rail energy consumption,” *Energy Conversion and Management*, vol. 80, pp. 509–524, 2014. doi:10.1016/j.enconman.2014.01.060.
- [185] Laird, “Wpa2 enterprise vs. personal,” *wireless connectivity blog*, 2014. <http://www.summitdata.com/blog/wpa2-enterprise-vs-wpa2-personal/>, accessed on 23.11.2016.
- [186] TechTarget, “Peap (protected extensible authentication protocol),” *Network Security - Definitions*, 2008. <http://searchsecurity.techtarget.com/definition/PEAP-Protected-Extensible-Authentication-Protocol>, accessed on 23.11.2016.

- 
- [187] Arduino, “Arduino mega,” *Arduino Product Overview*, 2017. <https://www.arduino.cc/en/Main/arduinoBoardMega>, accessed on 26.06.2017.
  - [188] Arduino, “Arduino tian,” *Arduino Product Overview*, 2017. <http://www.arduino.org/products/boards/arduino-tian>, accessed on 26.06.2017.
  - [189] Linino.org, “Internet of everything,” *Linino website*, 2017. <http://www.linino.org>, accessed on 26.06.2017.
  - [190] Adafruit, “Adafruit ultimate gps breakout - 66 channel w/10 hz updates - version 3,” *Adafruit Online Store*, 2017. <https://www.adafruit.com/product/746>, accessed on 26.06.2017.
  - [191] iTead Online Resources, “Nextion enhanced nx8048k070 overview,” *itead.cc wiki*, 2017. <https://www.itead.cc/wiki/N15048K070>, accessed on 26.06.2017.
  - [192] iTead Online Resources, “Nextion editor – make gui easier,” *itead.cc wiki*, 2017. <https://nextion.itead.cc/>, accessed on 26.06.2017.
  - [193] Pivotal Software, “Understanding rest,” *spring.io website*, 2018. <https://spring.io/understanding/REST>, accessed on 13.03.2018.
  - [194] Analog Devices, “Evaluation board for the ad7280a lithium ion battery monitoring system,” *Evaluation Board User Guide UG-252*, 2011. <http://www.analog.com/media/en/technical-documentation/user-guides/UG-252.pdf>, accessed on 26.06.2017.
  - [195] Electric Vehicle Database, “Ev data sheets,” *ev-database.uk*, 2019. <https://ev-database.uk/>, accessed on 12.02.2019.
  - [196] Audi United Kingdom, “The reveal, electric goes audi,” *audi.co.uk*, 2019. <https://beta.audi.co.uk/electric-car/e-tron.html>, accessed on 12.02.2019.
  - [197] Hyundai Motor UK, “Ioniq electric,” *hyundai.co.uk*, 2019. <https://www.hyundai.co.uk/new-cars/ioniq/electric>, accessed on 12.02.2019.
  - [198] Jaguar Land Rover Limited, “Jaguar i-pace,” *jaguar.co.uk*, 2019. <https://www.jaguar.co.uk/jaguar-range/i-pace/electric-vehicles/index.html>, accessed on 12.02.2019.
  - [199] Nissan Motor (GB) Limited, “e-nv200,” *nissan.co.uk*, 2019. <https://>

- [www.nissan.co.uk/vehicles/new-vehicles/e-nv200.html](http://www.nissan.co.uk/vehicles/new-vehicles/e-nv200.html), accessed on 12.02.2019.
- [200] Nissan Motor (GB) Limited, “Nissan leaf,” *nissan.co.uk*, 2019. <https://www.nissan.co.uk/vehicles/new-vehicles/leaf/range-charging.html>, accessed on 12.02.2019.
- [201] Volkswagen UK, “e-golf specs & pricing,” *volkswagen.co.uk*, 2019. <https://www.volkswagen.co.uk/new/golf-vii-pa/which-model-compare/details/3183#tech-spec>, accessed on 12.02.2019.
- [202] D. Kar, S. Panigrahi, and S. Sundararajan, “Sqligot: Detecting sql injection attacks using graph of tokens and svm,” *Computers & Security*, vol. 60, pp. 206 – 225, 2016. doi:10.1016/j.cose.2016.04.005.
- [203] P. Tang, W. Qiu, Z. Huang, H. Lian, and G. Liu, “Detection of sql injection based on artificial neural network,” *Knowledge-Based Systems*, vol. 190, p. 105528, 2020. doi:10.1016/j.knosys.2020.105528.
- [204] P. R. McWhirter, K. Kifayat, Q. Shi, and B. Askwith, “Sql injection attack classification through the feature extraction of sql query strings using a gap-weighted string subsequence kernel,” *Journal of Information Security and Applications*, vol. 40, pp. 199 – 216, 2018. doi:10.1016/j.jisa.2018.04.001.
- [205] S. Prowell, R. Kraus, and M. Borkin, “Chapter 1 - denial of service,” *Seven Deadliest Network Attacks*, pp. 1 – 21, 2010. doi:10.1016/B978-1-59749-549-3.00001-8.
- [206] T. S. Bryden, A. J. Cruden, G. Hilton, B. H. Dimitrov, C. P. de León, and A. Mortimer, “Off-vehicle energy store selection for high rate ev charging station,” *6th Hybrid and Electric Vehicles Conference (HEVC 2016)*, pp. 1–9, Nov 2016. doi:10.1049/cp.2016.0986.
- [207] G. Rempel, “Vehicle-to-railway (v2r) technology development: Issues & considerations,” *online resource*, 2018. [https://www.itscanada.ca/files/ACGM18/3\\_RempelV2R%20technologies%20FINAL%20for%20distribution.pdf](https://www.itscanada.ca/files/ACGM18/3_RempelV2R%20technologies%20FINAL%20for%20distribution.pdf), accessed on 12.06.2020.
- [208] R. Aquino-Santos, “Wireless technologies in vehicular ad hoc networks: Present and future challenges: Present and future challenges,” *Premier Reference Source*, p. 212, 2012. <https://books.google.de/books?id=j6hqPmTWELMC>, accessed on 12.06.2020.

- 
- [209] M. Ceraolo, G. Lutzemberger, E. Meli, L. Pugi, A. Rindi, and G. Pancari, “Energy storage systems to exploit regenerative braking in dc railway systems: Different approaches to improve efficiency of modern high-speed trains,” *Journal of Energy Storage*, vol. 16, pp. 269 – 279, 2018. doi:10.1016/j.est.2018.01.017.
- [210] S. Morant, “Flywheel technology generates energy efficiencies for metros,” *International Railway Journal - online resource*, 2017. [https://www.railjournal.com/in\\_depth/flywheel-technology-generates-energy-efficiencies-for-metros](https://www.railjournal.com/in_depth/flywheel-technology-generates-energy-efficiencies-for-metros), accessed on 13.09.2020.
- [211] Network Rail, “Section 11, network capability,” *2003 Business plan, Technical Plan*, 2003. url: [www.networkrail.co.uk/documents3177BusinessPlan2003NetworkCapability.pdf](http://www.networkrail.co.uk/documents3177BusinessPlan2003NetworkCapability.pdf), accessed on 28.08.2016.
- [212] Network Rail, “Our challenges, opportunities and approach to technology,” *2013 Technical Strategy*, pp. 9, 54, 2013. url: <https://www.networkrail.co.uk/publications/technical-strategy/>, accessed on 28.08.2016.
- [213] D. I. Fletcher, R. F. Harrison, and S. Nallaperuma, “Transenergy – a tool for energy storage optimization, peak power and energy consumption reduction in dc electric railway systems,” *Journal of Energy Storage*, vol. 30, p. 101425, 2020. doi:10.1016/j.est.2020.101425.
- [214] Google Maps, Bluesky, Infoterra Ltd, Getmapping plc, Maxar Technologies, The GeoInformation Group, “Composite satellite imagery and data,” *Google Maps*, 2020. <https://www.google.com/maps/@53.3893231,-3.1789543,265m/data=!3m1!1e3>, accessed on 22.08.2020.
- [215] E. Stewart, P. Weston, S. Hillmanssen, and C. Roberts, “The merseyrail energy monitoring project,” *9th World Congress on Railway Research*, May 2011. [http://www.railway-research.org/IMG/pdf/a4\\_weston\\_paul.pdf](http://www.railway-research.org/IMG/pdf/a4_weston_paul.pdf), accessed on 03.09.2019.
- [216] Merseyrail, “Train times wirral line,” *online resource*, 2019. <https://www.merseyrail.org/media/1295978/wirral-line-from-15th-december-2019-to-16th-may-2020-website.pdf>, accessed on 17.03.2020.
- [217] Department for Business, Energy & Industrial Strategy, “Sub-national

- electricity and gas consumption summary report 2018,” *online resource*, 2019. <https://www.gov.uk/government/collections/sub-national-electricity-consumption-data>, accessed on 22.04.2020.
- [218] Transport for London, “Car park usage at london underground,” *TfL publications*, April 2010. <http://content.tfl.gov.uk/car-park-usage-at-london-underground-report.pdf>, accessed on 31.05.2019.
- [219] J. Dedek, T. Docekal, S. Ozana, and T. Sikora, “Bev remaining range estimation based on modern control theory - initial study,” *IFAC-PapersOnLine*, vol. 52, no. 27, pp. 86 – 91, 2019. 16th IFAC Conference on Programmable Devices and Embedded Systems PDES 2019, doi:10.1016/j.ifacol.2019.12.738.
- [220] SQLSvertutorial.net, “Sql server triggers,” *online resource*, 2019. <http://www.sqlsvertutorial.net/sql-server-triggers/>, accessed on 31.05.2019.
- [221] MySQLtutorial.org, “Introduction to sql trigger,” *online resource*, 2019. <http://www.mysqltutorial.org/sql-triggers.aspx>, accessed on 31.05.2019.